NEW CONSTRUCTION TECHNIQUES OF GREEN ROOFS BY USING LIGHTWEIGHT CELLULAR CONCRETE MATERIAL

HANNY CHANDRA PRATAMA

A Thesis Submitted in Partial Fulfillment of the Requirements for the Degree of Doctor of Philosophy in Civil, Transportation and Geo-resources Engineering
Suranaree University of Technology
Academic Year 2023

เทคนิคการก่อสร้างหลังคาเขียวแบบใหม่
โดยใช้วัสดุคอนกรีตมวลเบา

นายฮานนี่ ชานดร้า ปราทามา

วิทยานิพนธ์นี้เป็นส่วนหนึ่งของการศึกษาตามหลักสูตรปริญญาวิศวกรรมศาสตรดุษฎีบัณฑิต
สาขาวิชาวิศวกรรมโยธา ขนส่ง และทรัพยากรธรณี
มหาวิทยาลัยเทคโนโลยีสุรนารี
ปีการศึกษา 2566

NEW CONSTRUCTION TECHNIQUES OF GREEN ROOFS BY USING LIGHTWEIGHT CELLULAR CONCRETE MATERIAL

Suranaree University of Technology has approved this thesis submitted in partial fulfillment of the requirements for the Degree of Doctor of Philosophy.

Thesis Examining Committee

Vanchai Sata.
....
(Prof. Dr. Vanchai Sata)
Chairperson

theerawat Sin
....
(Assist. Prof. Dr. Theerawat Sinsiri)
Member (Thesis Advisor)

Aphai Chapirom
....
(Dr. Aphai Chapirom)
Member (Thesis Co-advisor)

....
(Asst. Prof. Dr. Griengsak Kaewkulchai)
Member

....
(Assist. Prof. Dr. Akawut Siriruk)
Member

Yupaporn
....
(Assoc. Prof. Dr. Yupaporn Ruksakulpiwat)
Vice Rector for Academic Affairs
and Quality Assurance

....
(Assoc. Prof. Dr. Ponsiri Jongkol)
Dean of Institute of Engineering

นายฮานนี่ ชานดร้า ปราทามา: เทคนิคการก่อสร้างหลังคาเขียวแบบใหม่โดยใช้วัสดุคอนกรีตมวลเบา (NEW CONSTRUCTION TECHNIQUES OF GREEN ROOFS BY USING LIGHTWEIGHT CELLULAR CONCRETE MATERIAL)
อาจารย์ที่ปรึกษา: ผู้ช่วยศาสตราจารย์ ดร.ธีรวัฒน์ สินศิริ, 212 หน้า.

คำสำคัญ : หลังคาเขียว คอนกรีตมวลเบา ความยั่งยืน วัสดุก่อสร้าง

หลังคาเขียว (Green Roofs: GR) ยังไม่เป็นที่แพร่หลายในประเทศไทย เนื่องจากขั้นตอนการก่อสร้างที่ซับซ้อน และส่วนใหญ่ชั้นฐานรองรับวัสดุหลังคาเขียว ใช้คอนกรีตทั่วไป (Normal Concrete: NC) เป็น โครงสร้างรับน้ำหนัก ส่งผลให้โครงสร้างหลังคาเขียวมี น้ำหนักและค่าสัมประสิทธิ์การนำความร้อน ที่สูง จากผลงานวิจัยนี้ได้นำเสนอเทคนิคการก่อสร้างหลังคาเขียวแบบใหม่ โดยใช้ คอนกรีตมวลเบาแบบเติมฟองอากาศ (Lightweight Cellular Concrete: LCC) เป็นฐานรองรับวัสดุหลังคาเขียว คอนกรีตมวลเบานี้เป็นชนิดแบบไม่รับน้ำหนัก

ได้ทำการศึกษาคุณสมบัติทางกล คอนกรีตมวลเบาแบบเติมฟองอากาศ ความหนาแน่น 1200 (LCC 12) และ LCC 1400 (LCC 14) กิโลกรัมต่อลูกบาศก์เมตร มีผลการทดสอบสอดคล้องตามมาตรฐาน ACI และค่าสัมประสิทธิ์ในการนำความร้อน (Thermal Conductivity: k) เท่ากับ 0.40 และ 0.65 วัตต์ต่อเมตร เคลวิน ตามลำดับ และมีค่าต่ำกว่า NC จากผลการทดสอบ LCC มาใช้เป็นฐานรองรับวัสดุหลังคาเขียว (Green Roof Lightweight Cellular Concrete: GR-LCC) ของ GR-LCC 12 มีประสิทธิภาพที่ช่วยลดอุณหภูมิภายนอกและภายในแตกต่างกันในช่วง 4.62 - 11.34 °C และการถ่ายเทความร้อน (Thermal Transfer Value: Q) ต่ำที่สุด เท่ากับ 0.69 วัตต์ต่อตารางเมตร เมื่อเปรียบเทียบกับหลังคาเขียวที่ใช้ฐานรองรับ LCC 14 และ NC

ค่าสัมประสิทธิ์ในการนำความร้อน LCC 12 ได้รับอิทธิพลจากปริมาตรฟองอากาศ LCC ทำให้เกิด รูพรุนอากาศภายในเนื้อวัสดุ ได้ทำการวิเคราะห์ด้วยวิธี Synchrotron Radiation X-ray Tomography Microscopy (SRXTM) พบว่าปริมาตรฟองอากาศ LCC 12 เท่ากับ ร้อยละ 39.74 ของปริมาตร สูงกว่า LCC 14 คุณลักษณะ รูพรุนอากาศ มีรูปร่างค่อนข้างกลม ไม่ต่อเนื่องกัน (Close Cell) และกระจายตัว รูพรุนอากาศ ทำให้มีความเป็นฉนวนภายใน LCC ช่วยขัดขวางการแผ่ความร้อน จากการออกแบบสัดส่วนผสม (Mix Design) LCC 12 กำหนดปริมาตรฟองอากาศ ไว้ที่ ร้อยละ 45 ของปริมาตร จากการวิเคราะห์ด้วยวิธี SRXTM และโปรแกรม OCTOPUS พบว่า ปริมาณรูพรุนอากาศมีค่าเท่ากับ ร้อยละ 39.74 และมีฟองอากาศ ขนาดเส้นผ่านศูนย์กลาง 147 – 264 μm (ช่วง D50 ถึง D90) สอดคล้องกับมาตรฐาน ACI ที่กำหนดไว้ จากงานวิจัยดังกล่าวได้นำ LCC 12 ไปทดสอบในสถานที่ก่อสร้างจริง พบว่าสามารถนำมาประยุกต์ใช้เป็นเทคนิคในหลังคาเขียวได้ ช่วยลดขั้นตอน น้ำหนัก และมีคุณสมบัติสัมประสิทธิ์การนำความร้อนต่ำ มีความแข็งแรง ดูดซึมน้ำต่ำ แต่การนำ LCC มาใช้ ต้องพิจารณา ความหนาแน่นแห้ง , ขนาดเส้นผ่านศูนย์กลางฟองอากาศ , ปริมาตร

ฟองอากาศ และลักษณะฟองอากาศ ให้สอดคล้องกับงานวิจัยนี้ เพื่อเป็นแนวทางในการนำเทคนิคก่อสร้างดังกล่าวไปใช้งานต่อไป

สาขาวิชา วิศวกรรมโยธา

ปีการศึกษา 2566

ลายมือชื่อนักศึกษา ....

ลายมือชื่ออาจารย์ที่ปรึกษา ....

ลายมือชื่ออาจารย์ที่ปรึกษาร่วม ....

HANNY CHANDRA PRATAMA: NEW CONSTRUCTION TECHNIQUES OF GREEN ROOFS BY USING LIGHTWEIGHT CELLULAR CONCRETE MATERIAL. THESIS ADVISOR: ASST. PROF. THEERAWAT SINSIRI, Ph.D., 212 PP.

Keywords: Green roofs, Lightweight Cellular Concrete, Sustainability, Construction Materials

Green Roofs (GR) are still not widely known in Thailand due to their complex construction process. Typically, the base layer supporting green roof materials uses normal concrete (NC) as the load-bearing structure, resulting in green roofs having heavy weight and high thermal conductivity. This research presents a new construction technique for green roofs using Lightweight Cellular Concrete (LCC) as the base support for green roof materials. LCC is a type of non-load-bearing concrete.

The study examined the physical properties of Lightweight Cellular Concrete with densities of 1200 kg/m³ (LCC 12) and 1400 kg/m³ (LCC 14). The test results confirmed to ACI standards, with thermal conductivity (k) values of 0.40 and 0.65 W/mK, respectively, lower than NC's. The use of LCC as a base support for green roof materials (GR-LCC) in GR-LCC 12 effectively reduced the temperature difference between the outside and inside by 4.62 - 11.34 °C and had the lowest thermal transfer value (Q) of 0.69 W/m² when compared to LCC 14 and NC.

The thermal conductivity of LCC 12 is influenced by the volume of air voids, creating air pores within the material. Analysis using Synchrotron Radiation X-ray Tomography Microscopy (SRXTM) revealed that the air void volume of LCC 12 was 39.74% of the total volume, higher than that of LCC 14. The air pores were relatively spherical, non-continuous (closed cell), and well-distributed, enhancing the insulating properties of LCC by hindering heat radiation. The mix design of LCC 12 set the air void volume at 45% of the total volume. Analysis using SRXTM and the OCTOPUS program found that the air pore volume was 39.74%, with pore diameters ranging from 147 to 264 μm (from D50 to D90), in accordance with ACI standards.

Field experiments using LCC 12 in actual construction sites confirmed its applicability as a green roof technique. It helps reduce construction steps, weight, low thermal conductivity, strong, and has low water absorption. However, the use of LCC 12 in green roofs requires consideration of dry density, pore diameter, air void volume,

and pore characteristics to align with this research, providing guidance for the future application of this construction technique.

School of Civil Engineering
Academic Year 2023

Student's Signature Chandra P.
Advisor's Signature thuwawat Sim
Co-advisor's Signature Aphai Chapirom

ACKNOWLEDGEMENT

I would like to express my deepest gratitude to all those who have supported and guided me throughout the journey of completing this dissertation.

First and foremost, I am profoundly indebted to my advisor, Assist. Prof. Dr. Theerawat Sinsiri, and my co-advisor, Dr. Aphai Chapirom, whose expertise, patience, and continuous encouragement have been invaluable. Your insightful feedback and unwavering support have significantly shaped the direction and quality of this research.

I extend my sincere thanks to the members of my dissertation committee, Prof. Vanchai Sata, Asst. Prof. Dr. Griengsak Kaewkulchai], and Assist. Prof. Dr. Akawut Siriruk, for their constructive critiques, and suggestions, for generously giving their time and knowledge.

I would like to acknowledge the financial support received from One Research One Grant (OROG) from Suranaree University of Technology, SCG Roofing, Co. Ltd, and SIECON SUT research centre which made this research possible.

A special acknowledgement goes to my colleagues and friends at Suranaree University of Technology whose camaraderie and stimulating discussions have enriched my academic experience. I am also grateful to the administrative and technical staff for their assistance and support.

Lastly, my heartfelt appreciation goes to my family. To my parents, for their unconditional love and belief in me; to my partner, Ms. Mutyarsih Oryza, for your constant encouragement and understanding; for helping to give new insight, and for being a source of joy and balance in my life. This accomplishment would not have been possible without all of you. Thank you.

HANNY CHANDRA PRATAMA

TABLE OF CONTENTS

Page

TABLE OF CONTENTS (Continued)

Page

TABLE OF CONTENTS (Continued)

Page

LIST OF FIGURES

Figure **Page**

LIST OF FIGURES (Continued)

Figure **Page**

LIST OF FIGURES (Continued)

Figure **Page**

LIST OF TABLES

LIST OF TABLES (Continued)

Table **Page**

LIST OF ABBREVIATIONS

LCC = Lightweight Cellular Concrete
NC = Normal Concrete
GR = Green Roof
Non GR= Non-Green Roof
GR-NC = Green Roof Based Normal Concrete
GR-LCC = Green Roof Based Lightweight Cellular Concrete
k = Thermal Conductivity Value
Q = Thermal Transfer Value
SRXTM = Synchrotron Radiation X-ray Tomographic Microscopy
ACI = American Concrete Institute
ASTM = American Society for Testing and Material
TIS = Thai Industrial Standard
MPa = Mega Pascal
GPa = Giga Pascal
BEC = Building Energy Code
OTTV = Overall Thermal Transfer Value
RTTV = Roof Thermal Transfer Value

CHAPTER I
INTRODUCTION

1.1 Background and Rationale

The global temperature has risen yearly, contributing to significant climatic changes worldwide (IPCC, 2014). Thailand, for example, reached the second-highest temperature in Asia in 2024, with a peak of 44.6°C, as reported by crisis24 (in press). Consequently, Beckstead et al. (2023) reported that Thailand's energy consumption increases by 10% annually.

Green building solutions are needed to avoid more severe impacts. As highlighted by B. J. He (2022), it offers a multifaceted approach to urban heat mitigation by energy conservation, which can avoid extreme heat conditions and improve indoor quality. The Ministry of Energy's Notification emphasizes the importance of such measures in reducing overall energy consumption as stated in the recommendation code of the Building Energy Code (BEC), the energy-saving rating code for buildings in Thailand (Department of Alternative Energy Development and Efficiency, 2009). These conservation energy practices for well-being goals align with the United Nations Sustainable Development Goals (SDGs) (Wen et al., 2020).

The building facade is crucial in shielding the interior from external thermal transfer to prevent heat gain in a building. The roof, in particular, is responsible for the most significant portion of heat transfer, accounting for approximately 25–35% of the total facade. The phenomenon is due to its direct exposure to sunlight for over 12 hours each day. Therefore, utilizing roofing materials with low thermal transfer values is highly recommended to minimize heat absorption in the building (Shandilya et al., 2020).

Green roofs in developed countries are commonly used and recommended as an energy-efficient roof material. However, using green roofs in Thailand is still limited and not growing due to several factors, such as high installation cost, heavy structure load, complicated installation, and lack of expertise and knowledge (Pratama et al., 2023). Therefore, developing material innovation to promote green roofs in Southeast Asia, especially Thailand, is essential.

Chica and Alzate (2019) described lightweight cellular concrete (LCC) as lightweight concrete with a density ranging from 300 – 1,800 kg/m^3, which can be applied in various construction works. LCC has many benefits, such as being lightweight, heat resistant, water resistant, and porous stable, which has the potential to be used as an alternative to using a concrete roof deck on a green roof layer. So, it can add value to the green roof and increase its thermal resistance performance from good to very good. Research on the use of LCC in green roofs is still very limited. This research aims to study the potential for using LCC in green roof systems to improve temperature and energy performance and use it as a new efficient green roof construction technique.

1.2 Research Questions

1.2.1 Do Green Roof LCC properties have a beneficial impact on reducing temperature and improving energy performance?

1.2.2 How is the LCC microstructure impacting the green roof LCC performance?

1.3 Research Hypothesis

1.3.1 Different layer properties in green roof material layers are associated with changes in green roof performance, which can lead to temperature and energy performance variations.

1.3.2 A stable foam porosity of LCC optimizes physical property performance and is beneficial for use as a construction material.

1.4 Research Objectives

1.4.1 To study the properties of LCC materials to use in green roofs

1.4.2 To compare the thermal performance of green roofs LCC and other selected roofs using a green roof experimental box in an open-air space.

1.4.3 To study the microstructure of porosity in LCC, which can influence the behavior of green roofs

1.4.4 To compare the energy performance of green roofs LCC and other selected roofs by RTTV calculation.

1.5 Scope of Research

1.5.1 This study covers the following topic:

1) Obtaining physical properties data of LCC and its correlation as a potential to be used for roof deck layer on green roof
2) An open-air experiment of green roof boxes to obtain thermal data for temperature and energy performance analysis.
3) Microstructure LCC studies are needed to validate the foam stabilize quality as a potential use for the roof deck layer on green roofs.

1.5.2 The research used the LCC in various densities range 1000 – 1800 kg/m^3, consisting of:

1) LCC density 1000 kg/m^3 (LCC 10)
2) LCC density 1200 kg/m^3 (LCC 12)
3) LCC density 1400 kg/m^3 (LCC 14)
4) LCC density 1600 kg/m^3 (LCC 16)
5) LCC density 1800 kg/m^3 (LCC 18)

1.5.3 The LCC is used from the innovation LCC product developed by the Center of Excellence on Sustainable Innovative and Energy-efficient Construction Material (SIECON-SUT), Suranaree University of Technology. The latest version of the LCC SUT mix incorporates fibers to prevent cracking.

1.5.4 The test of physical properties LCC:

1) Compressive Strength
2) Dry Density
3) Water Absorption
4) Thermal Conductivity
5) Flexural Strength
6) Tensile Strength
7) Elastic Modulus

1.5.5 The microstructure analysis was conducted using Synchrotron Radiation X-ray Tomographic Microscopy (SRXTM). The test is located at Synchrotron Light Research Institute (SLRI), Suranaree University of Technology. The microscopic test examined the LCC 1200 and LCC

1400, which will be utilized for GR-LCC to evaluate the pore structure and the stability of porosity.

1.5.6 LCC 12 and LCC 14 were used in the open-air experiment. The data on thermal temperature were collected for three consecutive days. The open-air experiment was conducted in Nakhon Ratchasima, Thailand, during summer weather (no rain). The research carried out consisted of four variations of roof samples, including:

1) Normal Concrete Roof (Non GR)
2) Green Roof Concrete (GR-NC)
3) Green Roof LCC 1200 (GR-LCC 12)
4) Green Roof LCC 1400 (GR-LCC 14)

1.6 Anticipated Outcomes

The expected benefit of this study lies in providing valuable performance that can enhance green roofs in the construction industry. The findings serve as a new knowledge base, particularly in understanding the advantages of LCC in green roof systems. By utilizing the microstructure-level parameters as indicators, this research offers practical guidelines for implementing and optimizing green roof systems using LCC.

1.7 Structure of Dissertation

This thesis consists of three main chapters and is divided according to the following outlines:

Chapter I is the introduction part that presents the objective and scope of the study.

Chapter II presents the literature review of the recent research papers on green roof types and benefits, an overview of lightweight cellular concrete, energy efficiency in buildings, and the microstructure porosity in lightweight cellular concrete.

Chapter III presents the methodology of the research.

Chapter IV presents the results and discussion of the performance of various roof variables, the microstructure analysis, and the carbon footprint impacts of GR-LCC.

Chapter V shows the recent project that has been done by applying GR-LCC. This chapter also shows the potential of GR-LCC to be commercialized on real construction sites.

Chapter IV concludes the research work and presents the innovative prediction equation useful for the green building assessment of roofs, as well as provides suggestions and recommendations on the development of GR-LCC.

CHAPTER II
LITERATURE REVIEW

2.1 Green Roofs: Concepts and Benefits

2.1.1 Definition and Types of Green Roofs

Green roofs, also known as vegetated or living roofs, are innovative roofing systems that consist of a vegetation layer and growing medium placed on top of roof deck structures. These systems serve multiple functions, offering environmental, economic, and social benefits. Green roofs have become increasingly popular as a sustainable solution for urban development. (Castleton et al., 2010). Green roofs are classified into three primary types: extensive, semi-intensive, and intensive, as illustrated in Figure 2.1.

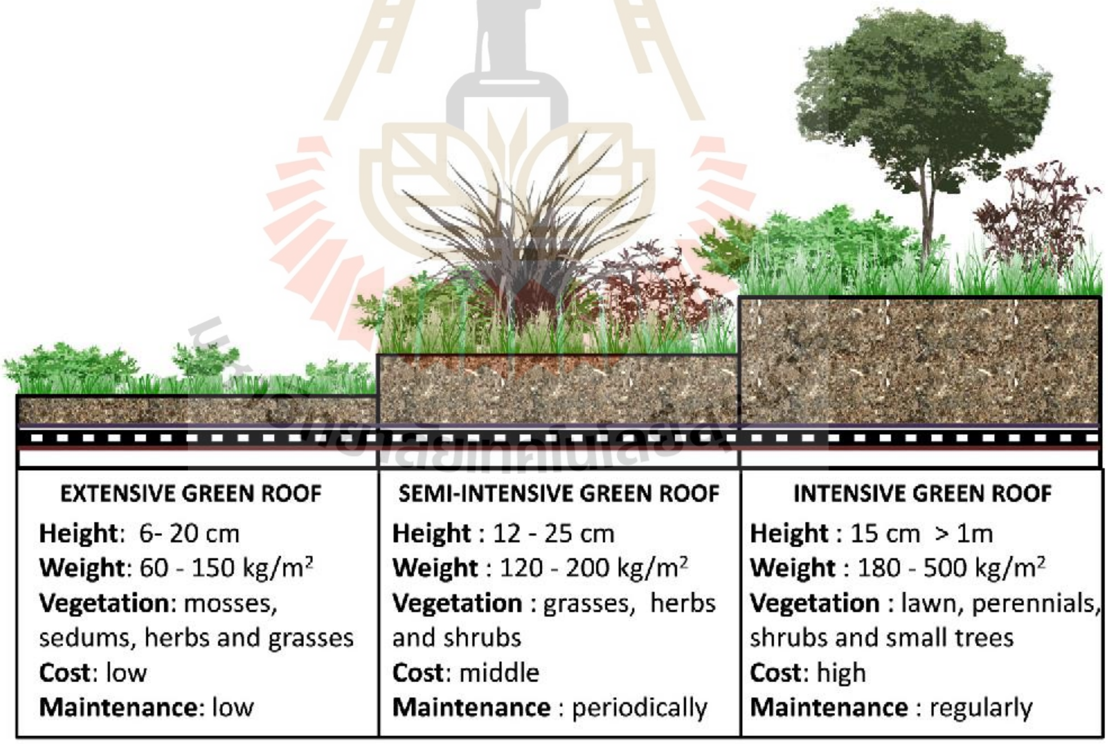

Figure 2.1 The various green roof types (Fernandez-Cañero et al., 2013)

Extensive green roofs are characterized by their lightweight construction, typically consisting of a thin growing medium layer measuring between 6 and 20 cm. This type of green roof supports resilient, low-maintenance vegetation, such as grasses, sedums, and mosses, which are well-adapted to the challenging rooftop environment, requiring minimal watering and maintenance. Extensive green roofs are primarily designed to offer environmental benefits, including enhanced stormwater management through rainfall absorption, improved thermal insulation, reduced energy consumption for heating and cooling, and the creation of habitats for urban wildlife. Their lower installation and maintenance costs make them a cost-effective option for retrofitting existing buildings

Semi-intensive green roofs represent a middle ground between extensive and intensive systems, with a growing medium depth typically ranging from 12 to 25 cm. Compared to extensive green roofs, this type allows for a greater variety of plant species, including perennials, grasses, and small shrubs, promoting increased biodiversity and aesthetic appeal. Semi-intensive green roofs require moderate maintenance and watering while offering balanced benefits, such as enhanced stormwater management, improved thermal performance, and opportunities for urban greening and recreational use. These roofs are suitable for both new constructions and retrofitting projects, providing a versatile option for a wide range of building types.

Intensive green roofs are distinguished by their complexity and resemblance to traditional gardens or parks. They feature deeper soil layers, typically ranging from 25 cm to 100 cm, allowing for the growth of a diverse range of plant species, including shrubs, trees, and even small water features. These roofs have a significantly higher weight and require additional structural reinforcement, leading to increased installation and maintenance costs. However, intensive green roofs offer substantial aesthetic and recreational benefits by creating vibrant green spaces that can be enjoyed by building occupants and the general public. They can serve as communal spaces, enhance property values, and provide opportunities for urban farming and community gardening

Each of the three categories of green roofs—extensive, semi-intensive, and intensive—contributes to urban biodiversity by providing habitats for various species. Additionally, they help mitigate the urban heat island effect by cooling the surrounding air and improving air quality by filtering pollutants. Furthermore, green roofs can extend the lifespan of the underlying roof membrane by offering protection against UV radiation, extreme temperatures, and physical damage. The economic feasibility of green roofs is further enhanced by energy savings resulting from improved insulation and reduced cooling demands.

In summary, green roofs offer a versatile and multifaceted solution to various urban challenges. Whether through low-maintenance, environmentally friendly extensive systems, balanced semi-intensive designs, or complex and aesthetically pleasing intensive green roofs, these systems provide a sustainable approach to enhancing urban environments, improving building performance, and fostering healthier, more resilient cities.

2.1.2 Material Used in Green Roofs

Green roofs are complex systems that require a variety of materials to function effectively and sustainably. They help mitigate the urban heat island effect by replacing heat-absorbing surfaces with vegetation and specialized supporting layers, resulting in cooler urban environments.

Niachou et al. (2001) stated that the benefits of green roofs in retrofitting existing buildings demonstrate significant energy savings. In buildings without insulation (U-value up to 1.99 W/m²K) or with moderate insulation (U-value up to 0.8 W/m²K), green roofs can reduce annual energy consumption by up to 48% and 7%, respectively. The combination of each green roof layer contributes to improving the U-value, resulting in a roof with higher thermal resistance.

Figure 2.2 Green roof layers (Vijayaraghavan, 2016)

Pianella et al. (2017) described four key components of a green roof system are the vegetation layer, growth substrate, irrigation system, and protection layer, as shown in Figure 2.2 and described below:

1) Vegetation

The choice of vegetation is crucial for successfully implementing a green roof. Hardy and water-efficient plants such as sedums, grasses, and mosses are typically selected for extensive green roofs due to their minimal maintenance requirements. In contrast, intensive green roofs, with their deeper soil layers, can support a broader range of plant species, including shrubs, trees, and flowering plants

2) Growth substrate

The growing substrate is a carefully formulated soil mixture designed to support plant growth. It is lightweight and provides adequate drainage. Typical components include mineral aggregates such as expanded clay and pumice, along with organic materials like compost. An optimal growing medium must strike a balance between water retention and drainage to promote plant health while preventing waterlogging.

3) Irrigation

The irrigation system of a green roof is composed of multiple layers, including filter fabric geotextile, a drainage layer, and a root barrier, each serving a specific function. The filtration fabric, typically made of non-woven geotextile, prevents the erosion of the growing medium into the drainage layer by allowing water to pass through while retaining soil particles. The drainage layer is essential for managing excess water, ensuring proper drainage, and preventing root rot and structural damage. It may be constructed using materials such as plastic or polystyrene panels, gravel, or specialized drainage mats, which help channel water toward drainage outlets and prevent water accumulation in the growing medium. The root barrier, made from durable and non-porous materials like thick plastic or rubber sheets, is installed to protect the roof membrane by preventing root infiltration, thus extending the roof's lifespan.

4) Protection layer

The structure of a green roof includes two critical layers: the waterproof membrane and insulation. These layers are installed on the roof deck to prevent leaks and enhance the roof's thermal resistance. Common materials for roof decks include concrete, wood, metal, and structural panels, all of which require both layers to ensure the long-term durability of the green roof system. The waterproof membrane is a key element that prevents water infiltration into the roof deck. Typically constructed from materials such as bitumen, PVC, EPDM rubber, or modified asphalts, the membrane must be strong enough to resist root penetration and support the weight of the green roof system.

The addition of insulation improves the building's thermal regulation. Extruded polystyrene (XPS) and expanded polystyrene (EPS) are commonly used insulation materials for green roofs, offering thermal resistance and contributing to energy efficiency. Each component is crucial to a green roof's overall performance and long-term viability. Careful planning is essential to selecting and integrating materials that align with the building's specific requirements, local climate, and the intended use of the green roof.

As research and technology continue to advance, it is important to further enhance the performance of green roofs by developing new materials and methods. These improvements will increase their value for sustainable urban development. Table 2.1 outlines the typical layers of green roofs and their respective properties.

Table 2.1 Typical layers in green roofs (D'Orazio, Di perna and Di giuseppe, 2012)

Layer	Thickness [m]	Material	Density [kg/m^3]	Thermal Conductivity [W/mK]
Vegetation and soil substrate	0.150	Grass and compost	582	0.170 (dry) 0.330 (saturated)
Filter sheet	0.001	Polypropylene	910	0.220
Drainage, storage, and ventilation element	0.002	Polyethylene	950	0.380
Air (inside the drainage system)	0.023	Air	-	0.160
Insulation	0.120	EPS	25	0.035
Roof slab	0.100	Concrete	2400	2.25

2.1.3 Benefits of Green Roof

Green roofs offer numerous advantages, contributing to various direct and indirect environmental benefits. The following sections provide a detailed description of these benefits:

1) Stormwater Management

Green roofs effectively mitigate stormwater runoff by absorbing and retaining rainwater. This approach helps alleviate urban flooding, reduces the burden on municipal drainage systems, and improves water quality by filtering out contaminants. According to Talebi et al. (2019), implementing a green roof can result in an average runoff retention rate of 40-80%.

2) Urban Heat Island Mitigation

Green roofs incorporating vegetation on traditional rooftops help mitigate the urban heat island effect and reduce surface temperatures. This cooling effect can lower ambient temperatures in metropolitan areas, creating a more comfortable environment and reducing energy demands for air conditioning. Santamouris (2014) compared several mitigation strategies to minimize the impact of urban heat islands (UHI). It was proposed that the widespread implementation of green roofs could reduce ambient temperatures ranging from 0.3 to 3 °C.

3) Air Quality Improvement

The vegetation on green roofs captures airborne pollutants and particulate matter, thereby improving air quality. Additionally, plants absorb carbon dioxide and release oxygen, further enhancing urban air quality. Lei et al. (2018) conducted a study in Zhengzhou, China, revealing that trees absorb 87.0% of airborne dust, while shrubs account for 11.3%, and grass contributes 1.7%. Additionally, it has been demonstrated that the vegetation on green roofs can effectively purify air contaminants.

4) Biodiversity and Habitat Creation

Green roofs support a wide variety of plant and animal species, thereby enhancing urban biodiversity. They serve as sanctuaries for birds, insects, and other fauna, promoting ecological balance in urban areas. Numerous studies have demonstrated the effectiveness of green roofs in mitigating habitat loss in densely built environments. Additionally, green roofs increase opportunities for recreational activities in urban settings and contribute to wildlife conservation by providing animals with access to green spaces (Lei et al., 2018).

5) Energy Efficiency

The insulating properties of green roofs reduce energy consumption for both heating and cooling. Green roofs help keep buildings cooler in summer by providing shade and reducing heat transfer.

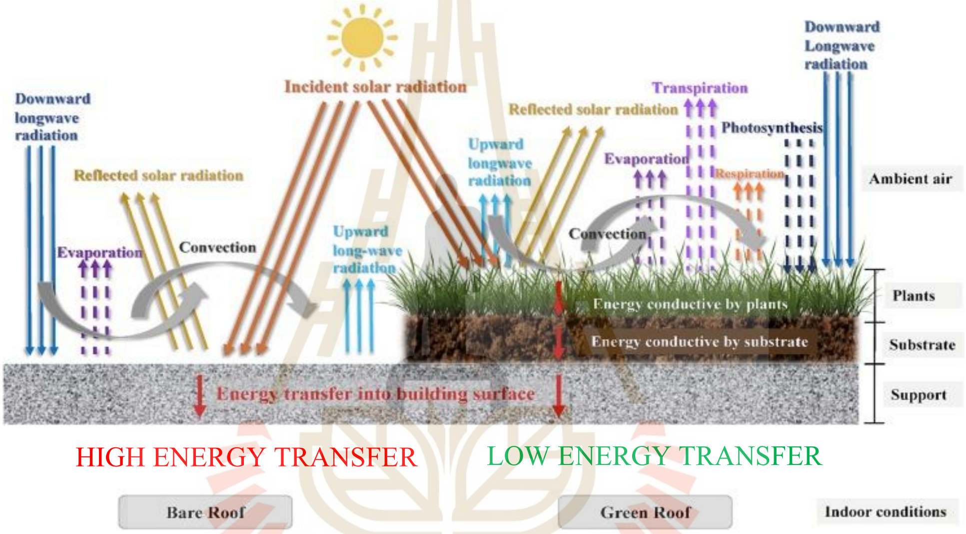

Figure 2.3 The role of energy efficiency in green roofs compared to bare roof (Lei et al., 2018)

Figure 2.3 illustrates one of the key advantages of green roofs, specifically the energy efficiency benefits they provide compared to bare roofs. The layers of vegetation in the green roof system help minimize energy transfer from the exterior. Niachou et al. (2001) conducted a study in Greece, which found that green roofs can significantly reduce energy consumption for cooling by 2% to 48%, depending on the extent of green roof coverage. Additionally, these roofs can lower indoor temperatures by up to 4°C. The improvement in thermal efficiency is primarily attributed to increased shading, enhanced insulation, and the greater thermal mass provided by the roof system.

6) Carbon Sequestration

Green roofs contribute to climate change mitigation by sequestering carbon dioxide through photosynthesis. Vegetation absorbs carbon dioxide (CO_2) and stores carbon in plant biomass and soil. The presence of plants on green roofs has been shown to reduce a building's CO_2 emissions by approximately 28.16 kg/m², primarily through the absorption of carbon dioxide via photosynthesis. (Niachou et al., 2001).

7) Economic Benefits

Green roofs shield the underlying roof membrane against UV radiation, severe temperatures, and physical harm. This significantly prolongs the roof's durability by up to 40 years, minimizing the need for frequent replacements and the accompanying expenses. Furthermore, by enhancing thermal insulation, green roofs effectively reduce energy expenses associated with heating and cooling. Buildings that use green roofs can substantially decrease energy expenses, leading to long-term financial savings. Green roofs offer both aesthetic and environmental advantages that can increase home prices. Buildings featuring green roofs are more visually appealing to potential purchasers or renters, increasing market prices and rental incomes. The alternative roofs' Net Present Value (NPV) is around 30-40% lower than traditional roofs (Niu et al., 2010).

8) Mental Health and Well-being

Creating a well-being world is one of the Sustainable Development Goals (SDGs) objectives. Evidence shows that access to green areas enhances mental health and general well-being. Green roofs help with this by connecting city people to the natural world, lowering stress levels, and enhancing wellbeing (Niu et al., 2010). As shown in Table 2.2, Pratama, Sinsiri, and Chapirom (2023) described green roofs in tropical areas such as ASEAN countries can significantly improve building performance. Green roofs have numerous advantages beyond their immediate use. To promote healthier, more sustainable urban environments, green roof adoption must be developed as cities grow and face environmental difficulties. Development can be carried out to enhance benefit value by improving the green roof function.

Table 2.2 Green roof performance in tropical countries (Pratama et al., 2023)

Parameter	Green Roof Performance	Remarks
Energy consumption savings	11 – 21%	Singapore, Extensive Green Roof, Comparison of rooftop garden with turfing, shrubs, and tree
Outdoor surface temperature	10 – 24 °C	Malaysia, Extensive Green Roof, Green roof improving public environment
Indoor temperature	24 – 38 °C	Thailand, EGR, Local material Thailand (Green Mat) on green roofs
Temperature reduction	Up to 10.2 °C	Aceh, Indonesia, Extensive Green Roof, Precast foamed concrete, Combination of lightweight foamed concrete and green roof

.

2.1.4 Development of Green Roofs Construction

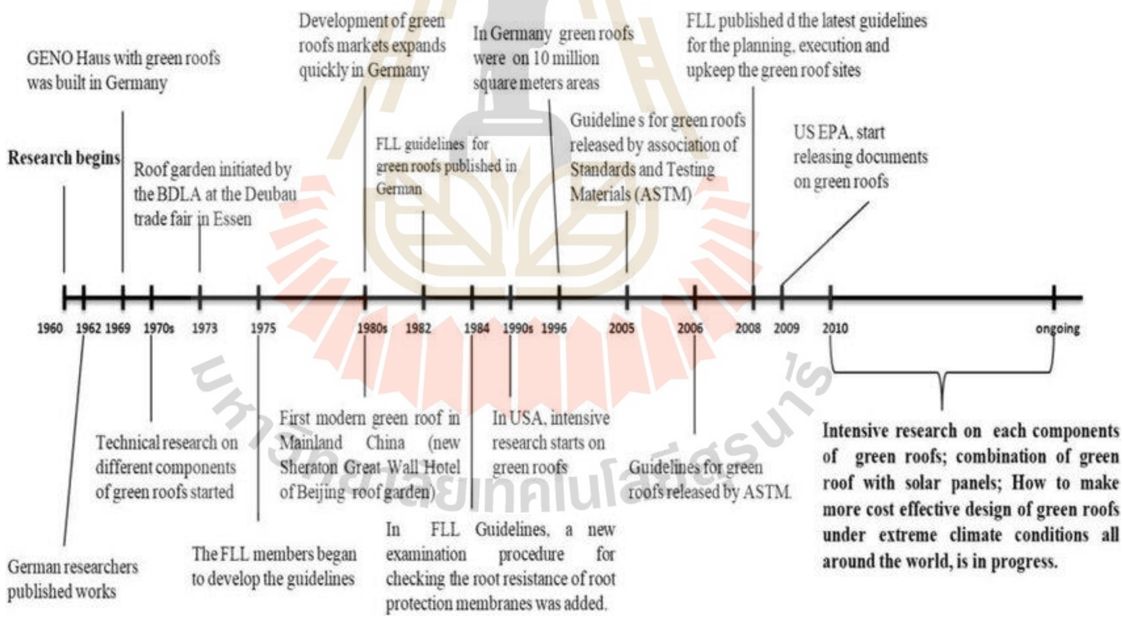

Figure 2.4 The history of green roof research (Cascone, 2019)

The development of green roof construction has evolved significantly over the past few decades, driven by technological advances, increasing environmental awareness, and the growing need for sustainable urban solutions. Figure 2.4 depicts the progression of research on green roofs, which commenced in 1960 and continues to develop until the present moment. This section outlines the historical progression and technological innovations in green roof construction.

1) Historical Progression

Green roofs have been used on building rooftops for many centuries. In ancient times, people created rooftop gardens for their insulating properties. One of the most renowned ancient green roofs was the Hanging Gardens of Babylon, built around 500 BCE (Abass et al., 2020). The application of green roofs on modern buildings is becoming increasingly common. Figure 2.5 illustrates the difference between green roofs in ancient and present times.

Figure 2.5 The Hanging Garden of Babylon in the Ancient and The Meera Sky Garden House of Singapore in the present (Abass et al., 2020)

During an energy crisis, modern green roofs originated in Germany in the early 1960s. By the early 1980s, the green roof market expanded rapidly, and many green roofs were constructed in Germany following the Forschungsgesellschaft Landschaftsentwicklung Landschaftsbau (FLL) guidelines, also known as the Guidelines for the Planning, Construction, and Maintenance of Green Roofs (Landscape Development and Landscaping Research Society, 2018). Due to their numerous benefits, green roofs have gained popularity worldwide. Furthermore, ongoing research into green roof guidelines, implementation, and maintenance continues to improve the quality of green roofs for the future.

2) Technological Innovations

A study investigated green roofs' guidelines, implementation, and maintenance to promote their use worldwide. Countries like the United States, Canada, Singapore, Australia, Japan, China, Hong Kong, and South Korea actively strive to implement green roofs on new and existing structures to attain various advantages. Niu studied the literature on green roofs and discovered that the United States accounted for 34% of the overall papers, while Europe and Asia contributed 33% and 20% of the total publications, respectively (Niu et al., 2010). Nevertheless, the progress of green roof development in Asia lags far behind that of the United States and Europe. Adopting green roofs in Asia offers numerous advantages, mainly due to their predominant location in tropical temperature regions, which receive more daylight than temperate countries.

Nevertheless, as Figure 2.6 depicts, a comprehensive and efficient strategy is a substantial barrier to developing green roofs in Thailand.

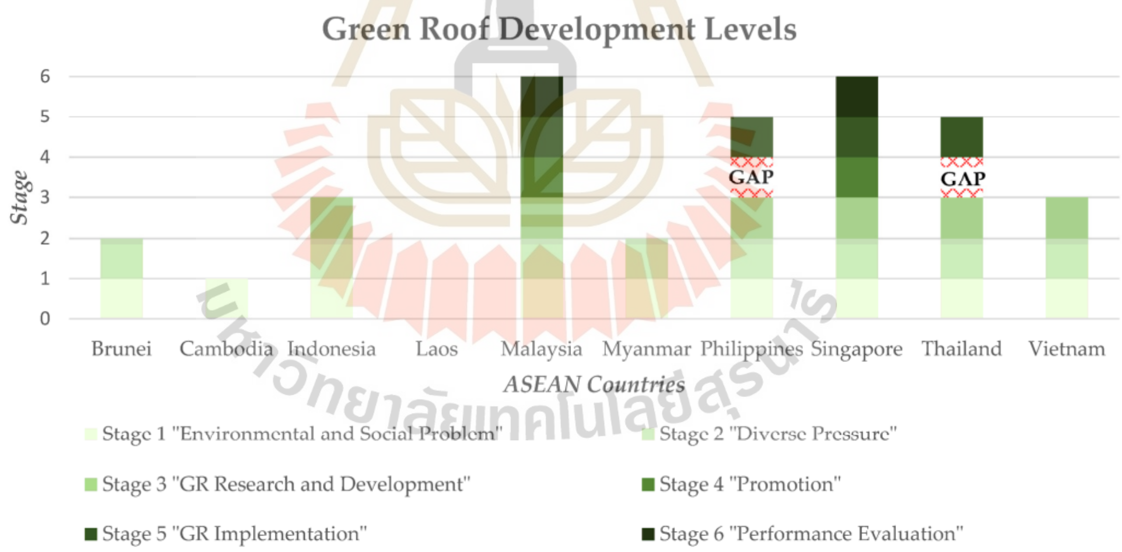

Figure 2.6 The Green Roof Development Levels in ASEAN Countries (Pratama et al., 2023)

Upon closer analysis, it becomes evident that research in Asia has predominantly originated from a select few countries: China, Japan, South Korea, India, Taiwan, and Iran. Despite the dominance of ASEAN countries in the tropical region of Asia, published literature on green roofs has been scarce. Among the approximately ten member states of ASEAN, Singapore stands out as the sole leader in green building technologies, including implementing green roofs (Pratama et al., 2023). Singapore has enacted rules to encourage the adoption of green roofs and urban greenery, shown by programs such as the Skyrise Greenery Incentive Scheme. Green roofs have become increasingly popular in Malaysia, particularly in urban areas such as Kuala Lumpur. The government has implemented criteria to encourage the adoption of environmentally friendly construction methods, which include the certification known as the Green Building Index (GBI). Pilot projects for green roofs are currently being implemented in Bangkok, the capital of Thailand, as well as other cities. These projects aim to showcase the advantages and viability of green roofs in urban environments.

A comprehensive analysis of data on the progress of green roofs in ASEAN identified four key challenges hindering their development in the region:

1) High Initial Costs: The initial costs of building green roofs might be substantial, hindering their wider adoption.
2) Increased Weight: Green roofs provide a substantial amount of weight to structures due to the multiple layers of soil, vegetation, and water retention systems they include. The added weight can vary between 50 and 300 kg/m² for extensive green roofs and maybe even greater for intensive green roofs.
3) High Maintenance: Green roofs require regular maintenance to ensure the vegetation's health and the roof's structural integrity.
4) Lack of Technical Expertise: Specialised knowledge and skills are required to design, install, and maintain green roofs.

To successfully adopt green roofs in the ASEAN region, it is necessary to tackle the structural obstacles related to significant weight. These difficulties can be efficiently addressed using material innovations, engineering techniques, design analytic approaches, and favorable legislation.

Lightweight cellular concrete (LCC), a type of concrete that is lighter in weight, provides a valuable chance to address the structural issues related to green roof systems, especially in reducing weight and improving insulation. Through harnessing its distinctive characteristics, including it in green roof designs, and addressing practical problems, LCC has the potential to contribute significantly to the progress of sustainable urban development in the ASEAN region. By consistently innovating and conducting research, utilizing LCC in green roofs can enhance their value as an exceptional insulating material and effectively address the issue of excessive weight. The following section will provide a more detailed description of LCC.

2.2 Lightweight Cellular Concrete (LCC)

This section overviews lightweight cellular concrete (LCC), detailing its characteristics and potential applications in various construction projects. Additionally, it examines the key factors driving the advancement of LCC technologies, with particular emphasis on its use as an alternative roof deck material in green roof systems, enhancing overall green roof performance.

2.2.1 Overview of LCC

Lightweight cellular concrete (LCC), commonly called foamed concrete, is a lighter concrete type that contains random air spaces created by incorporating foam agents into the mortar. This foam is produced by utilizing a foaming agent, which can either be pre-formed and combined with the base material or created on-site during the mixing process. Figure 2.7 shows the material used in LCC. The outcome is a type of concrete significantly lighter than conventional concrete, with densities varying between 800 and 1800 kg/m³ (Chica and Alzate, 2019).

Figure 2.7 Material of LCC (Raj et al., 2019)

The utilization of LCC has significantly increased in the construction field, as it has many advantages, such as being easy to add the foam directly and pump, workability, and self-leveling. Moreover, LCC can adjust the weight depending on its non-load-bearing or load-bearing function, enhance heat insulation by its low thermal conductivity, and improve water and sound absorption.

LCC's decreased weight and enhanced workability make it a highly suitable material for various building purposes, including void filling, thermal insulation layers, precasting wall panels, slabs, and lightweight blocks. Table 2.3 explains several uses of LCC in construction based on density.

Table 2.3 Summary of LCC applications based on density (Sari and Sani, 2017)

Density (kg/m^3)	Application
300 - 600	Replacement of existing soil, soil stabilization, geotechnical rehabilitation, raft foundation
600 - 800	Widely used in void filling as an alternative to granular fill, some such applications include filling old sewerage pipes, wells, basements, and subways.
800 - 900	They are primarily used in producing blocks and other non-load bearing building elements such as balcony railings, partitions, parapets, etc.
1100 - 1600	Used in prefabrication and cast-in-place wall, either load bearing or non-load bearing, and floor screeds house applications
1600 - 1800	Recommended for slabs and other load-bearing building elements where higher strength is required

2.2.2 Materials of LCC

Lightweight Cellular Concrete (LCC) is a versatile construction material composed of Portland cement, water, and a foaming agent that produces air bubbles within the mixture, resulting in a lightweight and highly workable material. Additionally, the porous nature of foamed concrete bestows it with excellent thermal insulation properties, making it a suitable choice for energy-efficient building envelopes (Zhou et al., 2022). The details below describe the materials used in LCC.

1) Portland Cement

As its leading binding agent, LCC is frequently utilized in Portland cement type 1, also known as Ordinary Portland Cement (OPC). They use Portland cement outcomes of compressive strength progression for 3 to 5 days. During this period, LCC undergoes frequent curing. To initiate the hydration reaction and will have an impact on physical properties. Excessive use of cement can lead to thermal accumulation in the concrete and will affect the air void, can fracture, and incur elevated production expenses. Guidelines for utilizing cement are contingent upon the intended density.

2) Fine Aggregates

Fine aggregate refers to the granular material used in the concrete mixing process. The generally used range of particle sizes for sand includes river sand, land sand, or sand, with sizes ranging from 0.075 millimeters to 4.75 millimeters, and it should be free of any dust particles. The primary component utilized in the blending of cellular concrete is predominantly sand. Concrete aggregates should conform to ASTM. Specifications C 33, C 144, C 332, or C 330 with the provision that aggregates fail to meet these specifications. Using foam in a stable blend of cement and sand can enhance the uniformity of the mortar. Less dense foam will exhibit upward buoyancy, causing air spaces to rise, whereas denser materials will experience downward gravitational forces, causing them to sink. Thoroughly combining the ingredients can stabilize the position of the air bubble, ensuring that it is equally distributed. Uniformly distributed space helps optimize the characteristics of LCC, particularly its ability to withstand high temperatures. Lighter substances (fillers) will probably substitute the empty spaces, resulting in a smoother foam surface. The strength of concrete has diminished.

3) Water and Plasticizers

The water requirement in foamed concrete depends upon the constituents and the use of admixtures. The desired mix's uniformity, consistency, and stability also govern water content. Generally, the water-to-cement ratio range was suggested to be from 0.4 to 1.25 or 6.5% to 14% of the target density. The amount of water must be appropriate to guarantee that the workability of the premixed paste or mortar is acceptable for foamed concrete fresh design mix. Otherwise, the cement would absorb water from the foam and cause rapid degeneration of the foam. ASTM standards suggest that the optimum water/cement ratio should be limited between 0.5 and 0.6 (ASTM C869, 1999). The plasticizers significantly improve workability and stabilize foamed concrete's compatibility. They are practically defined as waterreducers used to increase the performance of fresh concrete by easing its mobility and plasticity; however, no significant effects on concrete segregation were observed. The plasticizer content is approximately 0.45% and 5% of foam agent volume.

4) Foam agent

Foam agents control the concrete density through a rate of air bubbles created in the cement paste mixture. Foam bubbles are defined as enclosed air voids formed by adding foam agents. The most common foam agents are synthetic and protein-based. The protein-based foam agents result in a more robust and closed-cell bubble structure, which permits the inclusion of more significant amounts of air and provides a more stable air void network. In contrast, the synthetic ones yield more significant expansion and thus lower density. It is reported that the excessive foam volume results in a drop in flow. However, the flow is significantly affected by mixing time. Chapirom et al. (2019) Reported that the greater the mixing time, the more entrained air there is, albeit prolonged mixing may cause the loss of entrained air by dropping the air content. The mixing rotation speed of the concrete mixer at 45 rpm reported a higher compressive strength and water absorption in which the foam size and spread are more even in the concrete than at all the other speeds. The air voids range between 6% and 35% of the total volume of the final mix in most foamed concrete applications. The foam introduced by ACI 523.3R-93 is produced by blending the foam agent, water, and compressed air (generated by an air compressor) in pre-calculated proportion ratios in a foam generator calibrated for a discharge rate. The foam quality was vital because it represented the stability of foamed concrete and affected the strength and stiffness of the resultant foamed concrete.

5) Fibers

Fibers used in the foamed concrete are synthetic or natural: alkali-resistant glass, kenaf, steel, oil palm fiber, and polypropylene fiber. The volumetric fraction of these fibers ranges between 0.25% and 0.4% of the total volume of mix design constituents. Previously, it was reported that a significant improvement in mechanical and impact properties was observed when the foamed concrete was reinforced with polypropylene fibers.

2.2.3 Typical Properties of LCC

The properties of LCC are subject to changes based on variations in mix design. Every property possesses distinct features that are influenced by both the production process and the level of performance. The following are the essential properties of LCC:

1) Compressive strength

The compressive strength is directly proportional to the density, meaning that a decrease in density will harm it. Compressive strength is generally influenced by various factors, including the foam agent rate, water-to-cement ratio, type of sand particles, ratio of cement to sand, and properties of other components and their distribution. Jones and McCarthy (2005) They reported that the LCC, with a density range of 280 – 1800 kg/m3, has compressive strengths at 28 days at 0.6 – 43 MPa. Applying the curing process and incorporating fiber also contribute to achieving a high compressive strength. The unmolded LCC must be cured in a room with 100% relative humidity (RH) for at least three days. The compressive strength of foamed concrete can be improved by including fibers as they prevent micro-crack formation and raise the energy absorption rate (Wan Ibrahim et al., 2014). Table 2.4 below shows the standard compressive strength in the Thai industry following TIS 2601-2556.

Table 2.4 Compressive strength of LCC (Thai Industrial Standard, 2018)

Density (kg/m^3)	Minimum of compressive strength (MPa)
600 - 800	2.0
900 - 1200	2.5
1400 - 1600	5.0

2) Dry density

The density of the mixture can be assessed in two distinct phases: wet density and dry density. Wet density is measured during the mixing process to calibrate the target density of the mortar. Meanwhile, dry density is measured when the sample from LCC is dehydrated through oven drying. The allowable tolerance for wet and dry density is limited to ±50 kg/m^3. However, for high-density foamed concrete mixes (i.e., 1600 kg/m^3 above), the variance may go up to ±100 kg/m^3 following the TIS 2601-2556 (Thai Industrial Standard, 2018). Determining the wet density establishes the precise design mix and casting control volume. In contrast, dry density effectively regulates hardened foamed concrete's mechanical, physical, and durability characteristics.

3) Water absorption

Water absorption is a precise measurement of a substance's capacity to soak up a liquid into a capillary of LCC. This critical component, which affects the longevity of LCC, is primarily affected by various parameters, including the foaming agent, type of mineral admixtures, density, permeability characteristics, and curing conditions. These properties influence the likelihood of water movement concerning the size of bubbles (pore size), the degree of winding or twisting, and the consistency of distribution and connection.

Several studies have investigated water absorption characteristics in LCC and indicated that water flow into LCC is not just determined by porosity but is influenced by factors such as pore distribution, diameter, continuity, and tortuosity. As a result, the behavior of LCC is more intricate due to a greater volume of air voids. At increased density, the ability of LCC to absorb declines, and this is also followed by a decrease in the volume of air-void. The water absorption standard set by LCC complies with the TIS 2601-2556 standard.

Table 2.5 Water absorption of LCC (Thai Industrial Standard, 2018)

Density (kg/m^3)	Maximum of water absorption (%)
600 - 800	25
900 - 1200	23
1400 - 1600	20

4) Thermal conductivity

The LCC is composed of a closed-cell structure with lower heat conductivity than regular concrete. The thermal conductivity is directly related to the density, and the thermal insulation diminishes as the volume density increases. Ganesan et al. (2015) investigated the normal concrete exhibits a heat conductivity of 1.6 W/mK at a 2200 kg/m^3 density, 59% more efficient than the LCC. The low thermal conductivity of LCC provides substantial advantages, especially in actual construction. It offers superb insulation, which boosts energy efficiency by lowering heating and cooling expenses and enhances thermal comfort for inhabitants. The thermal conductivity of LCC, with a density ranging from 800 to 1800 kg/m3, falls within the range of 0.2 to 0.75 W/mK, as specified in detail below following the ACI 523.3R-93 (American Concrete Institute, 2014).

Table 2.6 Thermal conductivity of LCC (American Concrete Institute, 2014)

Density (kg/m^3)	Guideline of thermal conductivity (W/mK)
800	0.20
920	0.24
1120	0.30
1280	0.36
1340	0.43
1600	0.51
1760	0.61

5) Flexural strength

Flexural strength, sometimes referred to as modulus of rupture, bend strength, or transverse rupture strength, is the capacity of a material to withstand deformation when subjected to stress. Fracture stress is the highest level of stress that a material can withstand at the point of breaking during a bending test. Narayanan and Ramamurthy (2000) LCC's flexural and tensile strength is within 15% to 35% of its compressive strength.

6) Tensile strength

The tensile strength can be defined as the maximum stress a material can bear before breaking when it can be stretched or pulled. In foamed concrete, the tensile strength is lower than that of normal concrete. In general, the ratio of tensile strength to compressive strength of foamed concrete ranges between 0.2 and 0.4, which is higher than that of normal concrete. Since low-density cellular concretes have very low tensile strengths, adding fiber can increase the splitting tensile strength by about 31.7% compared to non-PP fiber foamed concrete.

7) Modulus of Elasticity

Its density and compressive strength determine LCC's modulus of elasticity (E-value). (Yu et al., 2020). The E-values of LCC are four times lower than normal concrete's, possibly due to the absence of coarse material in the mix. The British Concrete Association (BCA) states that the modulus of elasticity of LCC ranges from 1 to 12 GPa. (Sari and Sani, 2017). Polypropylene fibers can be incorporated into the mixture to enhance the E-value.

2.2.4 The potential of LCC to use as a roof deck for green roof

Lightweight cellular concrete (LCC) offers numerous advantages in construction due to its adjustable density based on specific requirements. Leo A. (1960) outlined four key applications of this material: floor fill, roof deck, engineered infill, and precast elements. Using the right mix selection of the roof deck function, LCC can be used as a sub-base for green roof construction. The roof deck is used for casting over galvanized steel decking, which can be corrugated or fluted. This application offers benefits such as fire ratings, enhanced seismic protection, thermal insulation, and a sloped roof deck for efficient drainage. In previous research, a roof deck on a green roof was carried out on LCC with a density of 1400 kg/m^3 by applying a precast system with dimensions of 400 x 1800 mm. The maximum moment for all panel specimens with the green roof load is assumed to be 60 - 150 kg/m^2 for an extensive green roof, and the live load that works on the roof is 100 kg (the maximum moment at mid-span). The test showed that the LCC roof deck has the maximum moment of the green roof load, which is only 5% of the ultimate moment (Munir et al., 2020).

Apart from that, LCC is also often used because of its excellent properties, which can reduce thermal transfer. The incorporation of LCC leads to a decrease in the direct cost of an apartment by about 8.2%–13.9%, compared to one built with conventional (Pan et al., 2007). Previous studies using an LCC density of 1400 kg/m^3 were carried out to improve thermal performance. Using LCC on a green roof can reduce the room temperature by 10 °C cooler than the outdoor temperature (Munir et al., 2020). However, deeper learning about using LCC on green roofs is still limited, especially concerning LCC's quality microstructure, which impacts thermal performance. The alternative use of LCC on the roof deck on a green roof is needed because using normal concrete poses various obstacles that may prevent the successful installation of green roofs. An important concern is the substantial weight of the roof, which could cause tremendous pressure on the structure of the building. The structure frequently requires significant and expensive strengthening, especially in retrofitting projects where the original buildings were not intended to bear such loads. In addition, concrete does not possess the necessary thermal insulating qualities for achieving ideal energy efficiency, resulting in increased expenses for heating and cooling.

As shown in Figure 2.8, an insulating layer is typically placed on top of the concrete deck to enhance its thermal resistance. Nevertheless, including an insulating layer will increase the weight and cost of the green roof.

Figure 2.8 The insulation layer placed above the roof deck (Abass et al., 2020)

These issues emphasize the necessity for advanced and flexible materials, such as using LCC material to substitute the concrete deck, to address the constraints of conventional concrete in green roof installations. LCC can be used as a roof deck material in green roof systems. It can help overcome structural issues and offers improved thermal performance and durability. The low density of LCC, which varies from 800 to 1800 kg/m^3, effectively minimizes the extra burden caused by green roofs. This characteristic makes it suitable for both new constructions and the process of upgrading existing buildings. Table 2.7 explains several comparative reviews of normal concrete and LCC properties.

The FLL Green Roof Guidelines are globally acknowledged benchmarks for designing and constructing green roofs. These guidelines highlight the significance of temperature reduction as a primary advantage of green roofs (Landscape

Development and Landscaping Research Society, 2018). LCC plays a vital role in this area by offering exceptional thermal insulation characteristics, decreasing the artificial heating and cooling requirement.

Table 2.7 Comparative of properties of normal concrete and LCC (Ahmad et al., 2017; American Concrete Institute, 2014; Chica and Alzate, 2019; Thai Industrial Standard, 2018)

Properties	Normal Concrete	LCC
Density	2400 kg/m^3	800 – 1920 kg/m^3
Compressive strength	31.2 MPa	1.7 – 24.7 MPa
Thermal conductivity	2.25 W/mK	0.2 – 1.3 W/mK
Water absorption	7.93%	7 – 25%
Tensile strength	2.07 MPa	0.34 – 4.94 MPa
Flexural strength	2.7 – 4.8 MPa	0.51 – 7.41 MPa
Modulus of elasticity	26300 MPa	4800 MPa
Total porosity	25.42%	62.50%*
Opened porosity	15.09%	20.40%*
Closed porosity	10.62%	42.10%*

*Porosity in LCC density 1000 kg/m^3

The air-void composition of LCC traps air, generating an insulating stratum that aids in preserving consistent indoor temperatures irrespective of external climatic circumstances. LCC improves the energy efficiency of buildings by efficiently controlling heat transfer, resulting in decreased energy usage. LCC's properties make it a highly suitable material for green roofs. The following part will provide a more comprehensive analysis of exploring the air void of LCC by microstructure analysis and its relation to enhancing energy efficiency while applying it on green roofs.

2.3 Microstructure Porosity of LCC

Lightweight cellular concrete (LCC) is a porous material with numerous pores inside it. The pore structure inside the material strongly affects the cell (solid) structure and its characteristics and properties. Like other types of concrete, the material properties of LCC are significantly affected by the pore characteristics, and many studies have been reported about the pore characteristics of foamed concrete over the past few years. Ramamurthy et al. (2009) found that concrete with uniform air-void sizes, circular air voids, and optimal spacing between voids can produce LCC with good mechanical properties. Further, durability studies showed that the foam cell structure and possible porosity do not make it less resistant to penetration of aggressive ions than densely compacted normal-weight concrete. The ratio of connected pores to total pores, which determines the durability, is lower in LCC. Hence, it has good resistance to freeze and thaw, fire, thermal conductivity, and lower sorptivity.

2.3.1 Fundamental Observations of Foamed Concrete Stability

Porosity results from the use of injection foam into mortar, with pore volumes reaching up to 62.5% at a LCC density of 1000 kg/m³, as presented in Table 2.7. As the density of LCC decreases, the volume of porosity increases, and each change in density yields distinct property values. Therefore, the application of LCC in construction must be carefully assessed for its structural strength, while also optimizing other essential properties, such as thermal insulation and potential water resistance.

The pore structure properties of cementitious materials are commonly assessed using various methods such as digital image processing, mercury intrusion porosimetry, or scanning electron microscopy. However, most of these techniques rely on the assumption of pore shape when interpreting results and are either invasive or restricted to two-dimensional (2D) data. The use of 3D data-based analysis has been very popular in recent decades. The method commonly used is using X-ray computed tomography (XCT). The following are some explanations of imaging analysis techniques of cementitious material:

1) Digital Image Processing (DIP)

Digital camera imaging involves capturing digital images of objects to analyze their surface properties. A digital image is composed of pixels, and the image's quality depends on the camera sensor's resolution. Digital image processing (DIP) techniques extract meaningful information from these images, which can be subdivided into homogeneous regions to identify objects of interest. Digital cameras are widely used due to their simplicity, availability, and ability to produce high-quality images cheaply. However, the DIP cameras capture 2D images, which do not provide information about the sample's internal structure. The use of DIP limits the analysis to surface characteristics (Douglass et al., 2017).

2) Mercury Intrusion Porosimetry (MIP)

Mercury Intrusion Porosimetry (MIP) is a widely utilized technique in concrete technology for investigating the pore structure of cement-based materials such as mortar and concrete. MIP works by intruding mercury into the pores of a sample under controlled pressure, allowing for the measurement of pore size distribution, porosity, and other related parameters. The technique relies on the Washburn equation, which assumes cylindrical pore shapes to calculate pore sizes based on the applied pressure and the known properties of mercury, such as surface tension and contact angle. However, the results of MIP are highly sensitive to sample preparation methods, such as drying techniques, sampling methods, and sample size. Variations in these factors can lead to discrepancies in the results (Ma, 2014).

3) Scanning Electron Microscopy (SEM)

Scanning Electron Microscopy (SEM) is a powerful imaging technique used to observe and analyze the microstructure of materials at a very high resolution, ranging from micrometers to nanometers. SEM utilizes a focused beam of electrons to scan the surface of a sample. The interaction of the electrons with the sample produces various signals, such as secondary electrons (SEs) and backscattered electrons (BSEs), which are collected to form detailed images of the sample's surface and provide information about its composition. SEM requires the sample to be conductive or coated with a conductive material, and it is usually conducted in a high-vacuum environment. However, the sample can be altered or damaged because SEM requires coated samples. SEM can only analyze a sample's surface or near-surface regions, as the electron beam cannot penetrate deeply into the material.

4) X-Ray Computed Tomography (XCT) Scan

X-ray Computed Tomography (XCT) scanning is a non-destructive imaging technique that uses X-rays to create detailed cross-sectional images of an object, which can be reconstructed into three-dimensional (3D) models. It is widely used in medical imaging, material science, and engineering to analyze the internal structures of objects without altering or damaging them. XCT scanning involves rotating an X-ray source around the object while detectors measure the intensity of X-rays that pass through it. The collected data is processed using reconstruction algorithms to produce a series of cross-sectional images (slices) of the object. These slices can be stacked to create a detailed 3D model, providing insights into the internal features and composition of the sample.

There are two primary methods to produce X-rays used to obtain data using X-ray CT: X-ray tubes or synchrotron radiation. X-ray tube-based CT systems use an electron beam directed onto a metal target to produce X-rays and are known for their flexibility, high resolution, and cost-effectiveness. These systems are widely used in industrial applications, quality control, and laboratory environments due to their accessibility and ability to handle various sample types and sizes. However, they have lower photon flux and beam collimation than synchrotron sources. In contrast, synchrotron radiation-based CT, known as Synchrotron Radiation X-ray Tomographic Microscopy (SRXTM) systems, generates X-rays by deflecting high-speed electrons with magnetic fields, producing highly collimated and monochromatic beams. These systems offer superior spatial resolution and higher photon flux, making them ideal for detailed internal structure analysis in scientific research fields such as materials science. Synchrotron microtomography can attain resolutions of about 1 μm to cement-based materials (Gallucci et al., 2007). According to Cebeci (1981), air-entraining agents introduce large air voids without appreciably altering the characteristics of the fine pore structure of hardened cement paste. Therefore, by knowing the solid density of matrix paste (without foam), one can easily predict the porosity of LCC of any other density using the following equation:

$$P = \frac{(Wsat - Wdry)}{(Wsat - Wwat)} \text{ x } 100$$

Where,

P = vacuum saturation porosity (%);

W_{sat} = weight in air of saturated sample

W_{wat} = weight in water of saturated sample

W_{dry} = weight of oven-dried sample.

Prior research has mostly employed 2D image analysis techniques such as optical and scanning electron microscopy (SEM) to characterize the pore structure parameter. The optical microscopy observed a wider distribution of air voids and lower strength for higher foam volume (Nambiar and Ramamurthy, 2007). For the detailed observation of microstructure and volume, the x-ray observation is necessary. Synchrotron X-ray sources outperform conventional X-ray tubes in several significant aspects. The superior collimation and parallelism of synchrotron beams, combined with their higher photon flux, allow monochromators to achieve monochromatic radiation at desired energy levels, reducing beam hardening artifacts and enhancing contrast resolution, resulting in exceptional spatial resolution and high-quality imaging. The synchrotron-based CT is ideal for applications requiring optimal contrast resolution and artifact-free data, particularly in research projects where precision is paramount (Brunke, 2010). Figures 2.9 - 2.11 demonstrate the different results of output images between the X-ray CT and Synchrotron X-ray.

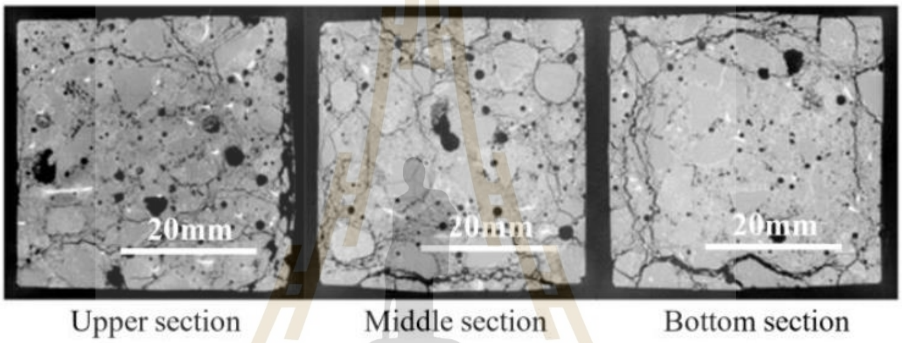

Figure 2.9 2D output image sample using X-ray CT (Kim et al., 2013)

Figure 2.9 shows the previous study, using X-ray CT to investigate how high temperatures affect the discontinuity of pore structures and the formation and spread of cracks in cement-based materials through the 2D output images. The X-EYE System was employed for this test with a scanning voltage and current of 150 kV and 100 μA, allowing imaging at a resolution of 6.18 μm. The experiment validated the use of CT technology for examining changes in pore structure and the propagation of cracks in cement-based materials under high-temperature conditions.

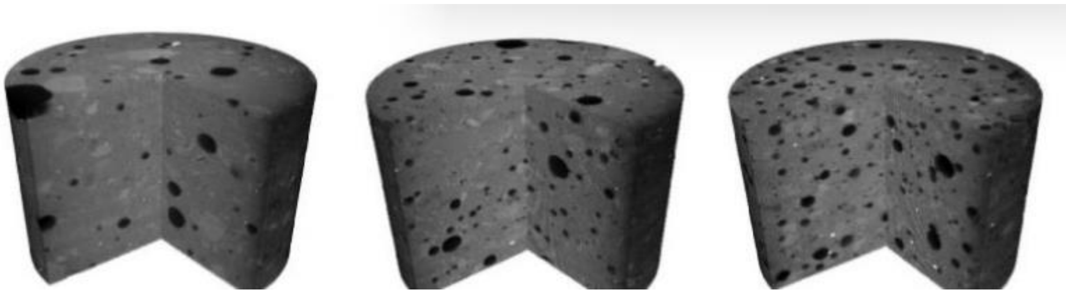

Figure 2.10 3D output image sample using X-ray CT (Kim et al., 2012)

Figure 2.10 shows CT images used to determine the air content in hardened concrete. They quantified air content and void frequency to evaluate the engineering properties of cement-based materials. The sample size was Φ12 mm × 10 mm. The CT equipment used in the study was the X-EYE CT, featuring an X-ray source of 150 kV and 100 μA. A total of 1024 images were scanned longitudinally at 8.7 μm intervals, with each image measuring 1024 × 1024 pixels and a resolution of 10.8 μm.

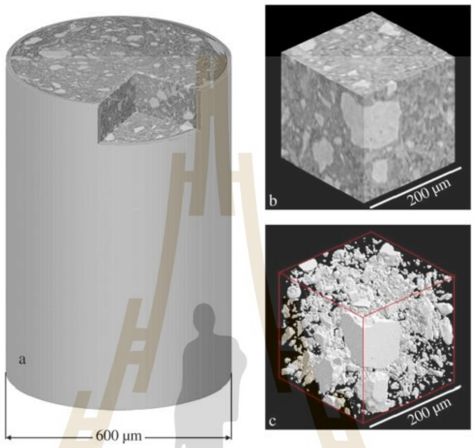

Figure 2.11 Output images of research using synchrotron X-ray microtomography (Gallucci et al., 2007)

Figure 2.11 illustrates the study of cementitious materials' microstructural evolution and pore structure. Tomographic scans were conducted at the Swiss Light Source (SLS) in Villigen, Switzerland, on the MS-X04SA-Tomo beamline. Depending on the sample age, the beam energy ranged from 12.3 to 15 keV, with the intensity maintained at 200 mA. One thousand projections were captured with an angular step of 0.18° and an exposure time of 3 seconds each, using a 2048px CCD camera with a 1400 mm field of view and a 10× magnification optical objective. Under these conditions, the pixel resolution was 0.6835 μm. As the capabilities of microtomography systems in synchrotron radiation facilities have improved, it is now possible to achieve a complete three-dimensional representation with a resolution better than 1 μm. As a result, Synchrotron X-ray is gaining popularity because it offers greater accuracy than X-ray tube analysis. Table 2.8 summarizes the comparison features of imaging analysis techniques of cementitious material.

Table 2.8 Comparative features of imaging analysis techniques (Gallucci et al., 2007; Brunke, 2010; Ma, 2014; Douglass et al., 2017,)

Imaging Techniques	DIP	MIP	SEM	XCT	SRXTM
Sample size	Destructive sample, ± 50 mm	Destructive sample, ± 50 mm	Destructive sample, ± 10-50 mm	Non-destructive sample, ± 50–100 mm	Non-destructive sample, ± 3 – 5 mm
Sample penetration	Cannot penetrate the sample	Cannot penetrate the sample	Can penetrate up to 3 μm	Can penetrate the internal surface	Can penetrate the internal surface
Type of output image	2D image	2D image	2D image	2D & 3D image	2D & 3D image
Source	Light	Liquid Mercury	Electron beam	X-ray beam	Synchrotron beamline
Imaging Tools	A Digital camera with image processing software/code	-	SEM or ESEM; Image processing software	X-ray CT scanning machine; Image processing software	Multipole wiggler, 2.18 Tesla, Image processing software
Image Resolution	up to 50.6 megapixels (4 μm)	-	up to 1 nm	Up to 100–200 μm	Up to 1 μm
Produced Data	- aggregate gradation, size, and distribution. Volumetric properties of air voids Cracks and changes due to F–T cycles	- size and distribution - Air void volumes	5) Aggregate gradation, size, and distribution 6) Air void volumes 7) Cracks and changes due to F–T cycles	8) 3D simulation 9) Aggregate gradation, size, and distribution 10) The volume of air voids 11) Surface texture 12) Cracks and changes due to F–T cycles	13) 3D simulation 14) Aggregate gradation, size, and distribution 15) The volume of air voids 16) Surface texture 17) Cracks and changes due to F–T cycles

2.3.2 Microstructure Analysis Using Synchrotron Radiation X-ray Tomographic Microscopy (SRXTM)

Synchrotron Radiation X-ray Tomographic Microscopy (SRXTM) is a powerful, non-destructive imaging technique that utilizes the highly intense and tunable X-ray beam generated by a synchrotron light source. A synchrotron is a type of particle accelerator that uses a combination of magnetic and electric fields to accelerate electrons to nearly the speed of light. These electrons travel in a circular path and emit a powerful beam of electromagnetic radiation, including X-rays when magnetic fields bend their path. This synchrotron radiation is millions of times brighter than conventional X-ray sources, making it highly valuable for detailed imaging and analysis. Synchrotron-based X-ray microtomography offers several benefits over traditional X-ray systems, including higher resolution down to the micro- or nanometer scale, rapid acquisition times, and using monochromatic light for optimal contrast. These capabilities are crucial for various applications, such as studying multiphase flow in porous media and characterizing biofilm architecture. The high photon flux and tunable energy range of synchrotron radiation allow researchers to quickly capture detailed, high-quality images, facilitating advanced research in soil science, hydrology, environmental engineering, and beyond.

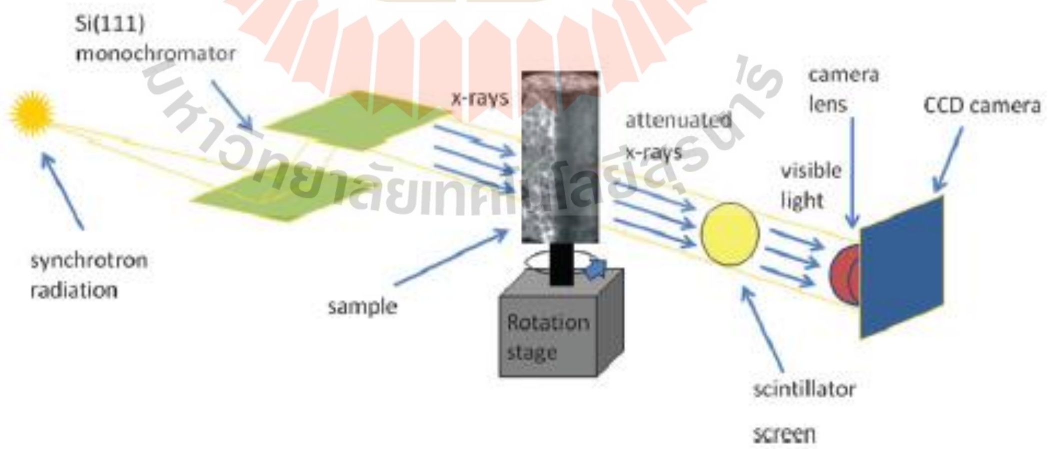

Figure 2.12 Workflow of Synchrotron Radiation X-Ray Tomographic Microscopy (Wildenschild et al., 2015)

As shown in Figure 2.12, CT images were used to determine the air content in hardened concrete. They quantified air content and void frequency to evaluate the engineering properties of cement-based materials. The sample size was Φ12 mm × 10 mm. The CT equipment used in the study was the X-EYE CT, featuring an X-ray source of 150 kV and 100 μA. A total of 1024 images were scanned longitudinally at 8.7 μm intervals, with each image measuring 1024 × 1024 pixels and a resolution of 10.8 μm. A sequence of calibration procedures follows the acquisition of an image. Flat-field correction eliminates artifacts from optical path distortions and camera sensitivity variations by employing bright and dark current photos. To optimize image quality, noise reduction and beam intensity normalization are frequently implemented during preprocessing.

Over the past few years, these methods for characterizing air voids in lightweight concrete have been widely utilized using X-ray micro-computed tomography (micro-CT). Several works focused on quantifying total macro porosity and examined the physical measurements of capillary water absorption in concretes and thermal characteristics of foamed concrete (Lu et al., 2017). However, The microstructure of LCC can be analyzed using micro-CT; however, its level of detail is inferior to that of SRXTM. Consequently, to accurately assess the volume and distribution of void water, microstructure research of LCC utilizing SRXTM is required, thereby supplying critical data for subsequent research. In this research, the SRXTM method was used to analyze the microstructure of LCC, which is applied to green roofs as an alternative to new green roof construction using LCC material.

2.3.3 Relation of Microstructure LCC and Thermal Performance

Porous materials have found essential applications as filters, catalyst support, and thermal insulators. With present-day concerns of energy saving in high temperature in industrial processes and buildings, developing new thermal insulators has become the object of much recent research. Given the lower value of the thermal conductivity of air compared with a solid phase, the incorporation of porosity into a material significantly decreases its effective conductivity. The thermal conductivity of lightweight cellular concrete (LCC) is closely related to its microstructure, particularly its porosity and the distribution of air voids. The amount and distribution of pores within the solid matrix affect thermal conductivity. Higher porosity generally reduces thermal conductivity because air within the pores is a poor conductor of heat. However, the connectivity and size of the pores also play a role.

Before thermal conductivity measurement, pore volume fraction and morphology of closed pores are essential parameters that must be carefully determined. The information can be obtained through image analysis, such as MIP or SEM. However, advanced analysis technology provides valuable information on the morphology of pores using two- or three-dimensional images to determine the accurate size and porosity of distribution. The study of air void correlation on cement-based with thermal conductivity shows that the increase in median diameter value (D50) reduces thermal conductivity. The study also proclaimed that the smaller pores of 90th percentiles (D90) for thermal conductivity showed that smaller pores substantially influence the conductivity. The mixes with a narrower range of air-void size distribution showed higher conductivity at lower density, larger voids, and wider distribution of voids, resulting in reduced conductivity. The performance of LCC is controlled by their microstructure, especially the pores structure. Figure 2.13 shows two types of pores that can occur in LCC: open and closed pores.

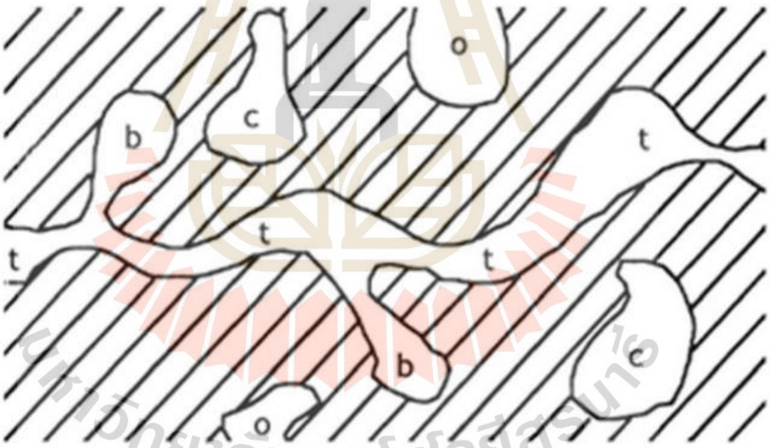

Figure 2.13 Types of pores in LCC:
o – open, c – close, t – transportation, b - blind (Kurpinska and Ferenc, 2017)

Open pores are connected to the material surface and, thus, permeable to liquids and gases. Closed pores are isolated and not connected. LCC containing only closed pores is impermeable to liquids and gases and is thus commonly used as thermal and acoustic insulation. The microstructure and porosity of LCC play a crucial role in determining its stability, mechanical properties, and overall performance.

The stability of LCC is significantly influenced by the uniformity and nature of its pore structure. Stable foam concrete microstructure has the following characteristics:

1) Uniform Pore Distribution: Stable foam concrete has a highly uniform pore distribution, which means that the pores are evenly spread throughout the matrix. This uniformity ensures consistent mechanical properties and strength.
2) Cell Structure: The pores are mostly closed cells, contributing to the material's lower permeability and higher strength. Closed cells trap air, providing good insulation properties and making the material more resistant to water absorption.
3) Consistent Pore Size: The pores are consistent, which helps maintain the uniformity of the material's density and strength. This consistency minimizes weak points within the structure, enhancing overall durability.

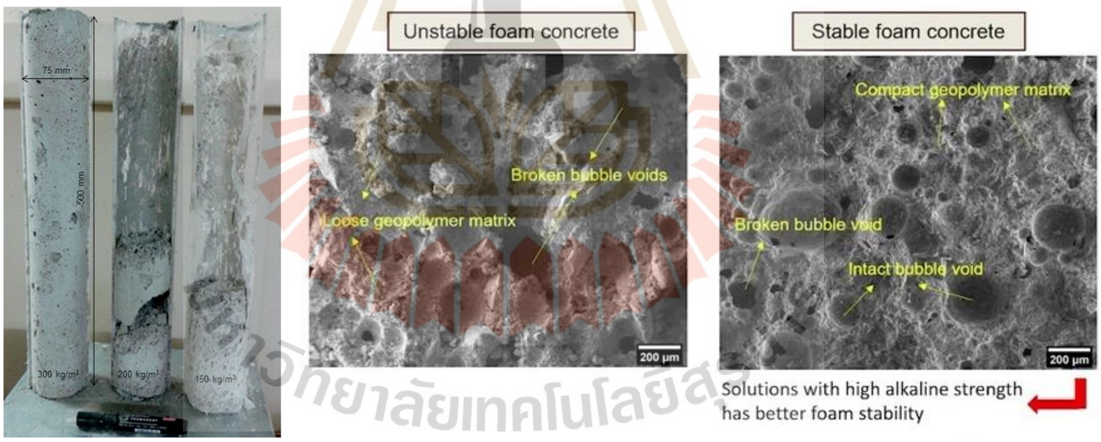

Figure 2.14 Unstable and stable air void of LCC (Jones et al., 2016)

The consistent pore size further contributes to the material's uniform density and strength, reducing weak points and enhancing durability. Consequently, stable foam concrete exhibits higher mechanical strength, excellent thermal insulation, and resistance to environmental factors such as moisture and temperature variations, making it suitable for structural applications. Figure 2.14 shows the difference between the unstable and stable LCC.

This study will use SRXTM to investigate the microstructure of LCC, including the volume, distribution, and stability of air voids. High-quality and stable air voids in LCC are expected to provide excellent thermal insulation, thereby enhancing the performance of green roofs. The next section will discuss the energy efficiency of green roofs in buildings.

2.4 Energy Efficiency in Buildings

Energy efficiency in buildings is essential as it decreases energy consumption, resulting in substantial financial savings, reduced emissions of greenhouse gases, and enhanced indoor comfort. Efficient buildings have a direct impact on reducing utility bills and operational expenses, resulting in economic advantages. Energy-efficient buildings improve occupant comfort by providing superior temperature regulation and air quality.

With the growing significance of sustainability, energy-efficient buildings can better meet requirements and obtain green certifications, leading to a rise in interest in green buildings in the future. This section will provide an overview of building energy efficiency rules, explicitly focusing on the Building Energy Code (BEC) regulations. These regulations are established by the Ministry of Energy in Thailand and serve as standards for assessing the energy efficiency of buildings. Furthermore, this text will explain the function of the LCC roof deck inside a green roof system to enhance energy efficiency.

2.4.1 Standard of Energy Efficiency: Building Energy Code (BEC)

Thailand's commitment to sustainable development and energy efficiency has motivated the establishment of legislation governing energy consumption in buildings. These regulations aim to decrease energy use in residential and commercial buildings in response to the increasing worries about energy usage and its environmental impact.

The Building Energy Code (BEC) is a set of regulations that establish the minimum energy efficiency requirements for buildings seeking approval for construction or renovation with the Department of Alternative Energy Development and Efficiency (DEDE), as outlined in the Ministerial Regulation B.E. 2552 (Department of Alternative Energy Development and Efficiency, 2009). The BEC is a crucial instrument that ensures the design of a building focuses on conserving the highest amount of energy, enhancing energy efficiency in both new and refurbished structures, and minimizing energy usage and greenhouse gas emissions.

As shown in Figure 2.15, the evaluation certificate of energy conservation building design, as required by the Ministry of Energy's Notification B.E. 2564, must comply with four main components under the BEC standard as follows:

1) Overall Thermal Transfer Value (OTTV): The value of thermal transfer from the external wall of the building entering inside the building.
2) Roof Thermal Transfer Value (RTTV): The value of thermal transfer from the roof passes into the inside of the building.
3) Lighting Power Density (LPD): Maximum value of lighting power density for its average value per area
4) Coefficient of Performance (COP): Calculation of the coefficient of performance shall focus only on the heating value

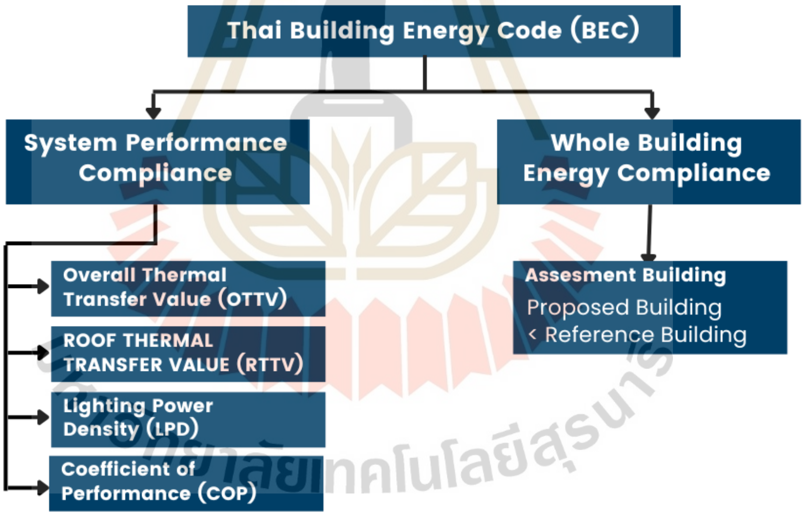

Figure 2.15 The assessment of the Thai Building Energy Code (BEC) (Sudprasert and Klinsmith, 2014)

Figure 2.16 shows every building energy criterion's benchmark energy standard value in BEC. Details of the BEC standard requirement and the calculation method are specified in the Ministry of Energy’s Notification B.E. 2564. Moreover, the benchmark standard indicates that it will improve in the future years up to the Economic Building level (ECON)

ปีที่บังคับ (B.C.)	Reference Building Ref. 2009	Building Energy Code BEC 2019	High Performance Standards HEPS 2025	Economic Building ECON 2031
OTTV (W/m²)	50	50	40	30
RTTV (W/m²)	15	10	8	6
LPD (W/m²) *Group 1 Academy and office	14	10	8	4
Split Type (EER)	Reference : Number 5's label of EGAT*			
Air-cooled Chiller (kW/ton)	1.33	1.12	0.8	0.6
Water-cooled Chiller (kW/ton)	1.24	0.88	0.6	0.4
Efficiency (%)	80	80	85	90

*EGAT = Electricity Generating Authority of Thailand

Figure 2.16 The benchmark of the Thai Building Energy Code (BEC) (Department of Alternative Energy Development and Efficiency, 2009)

2.4.2 Analysis of heat transfer of construction material

Lightweight Cellular Concrete (LCC) plays a significant role in enhancing the energy efficiency of green roofs. The heat transfer mechanism is shown in Figure 2.17.

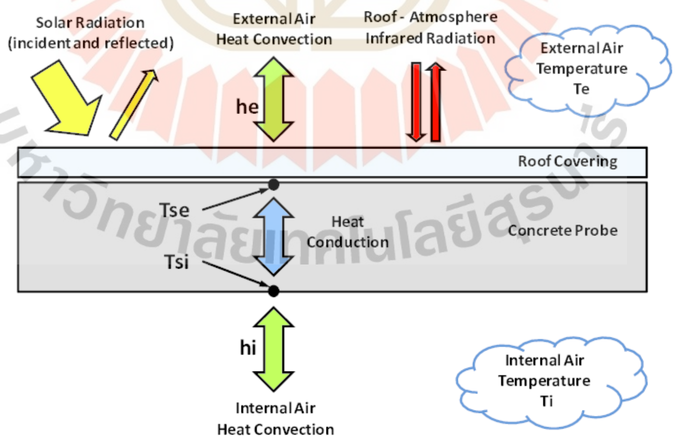

Figure 2.17 Heat Transfer Mechanism in Building Roofs (Jones et al., 2016)

1) Solar Radiation: Electromagnetic energy from the sun, including solar light, ultraviolet light, and infrared radiation.
2) Heat Convection: Heat transfer through the movement of fluids (liquids or gases), driven by temperature differences.

3) Heat Conduction: Direct contact transfers heat through a material, moving energy from warmer to cooler areas.

The main cause of thermal transfer is conduction, as it involves direct contact between the material and the sun's rays, transmitting heat energy to the material's layers. Materials possessing lower thermal conductivity may reduce the transfer of heat energy into the structure. Prior research on LCC has demonstrated its primary benefit is its exceptional thermal resistance, a crucial factor in reducing heat transfer from the exterior to the interior of buildings. When LCC is utilized as a roofing material, it reduces heat conduction due to its low thermal conductivity, improving the thermal resistance and the ability to prevent heat across its thickness. Ganesan et al. (2015) observed that the low thermal conductivity results from its lightweight density, which falls between 700 and 1400 kg/m^3, and its thermal conductivity, which ranges from 0.24 to 0.74 W/mK. This indicates that LCC has high thermal resistance due to low thermal conductivity.

The thermal performance of normal concrete and LCC under different climatic conditions has been investigated by studying temperature differences in outdoor trials. A study has indicated that normal concrete has a greater capacity to absorb and retain heat than LCC, resulting in higher maximum temperatures during the day and slower cooling at night. LCC, in contrast, exhibits reduced temperature fluctuations and maintains a more consistent thermal performance due to its lower thermal conductivity (Yang et al., 2023). Due to its numerous advantages, LCC is widely utilized in various construction projects.

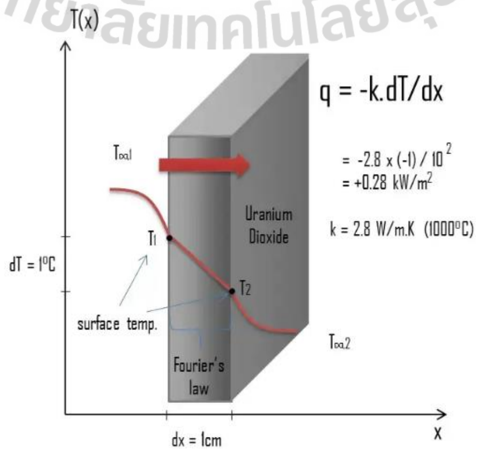

Figure 2.18 The role of heat transfer in a material (Koenders et al., 2018)

Heat transfer by conduction occurs when heat is generated within a material that serves as an opaque medium. The rate of heat transfer by conduction, denoted as (Q), is directly proportional to the temperature gradient (dT/dx) and the material's thickness, as illustrated in Figure 2.18. The actual rate of heat transfer can be calculated by knowing the thermal conductivity (k), a material-specific property that describes how efficiently heat moves through the substance. This calculation follows Fourier's law of heat conduction, as represented by the equation below:

$$Q = -kA\,\frac{\mathrm{dT}}{\mathrm{dx}}$$

In recent years, there has been an increasing interest in utilizing multi-layered materials to improve heat barriers in structural components. As shown in Figure 2.19, a multi-layered composite typically consists of multiple layers of different materials with varying physical properties. The jointed composite combination results in an increase in features that differ from those of the individual components. Altering the layers' components or thicknesses can create unique characteristics for composite materials or structures.

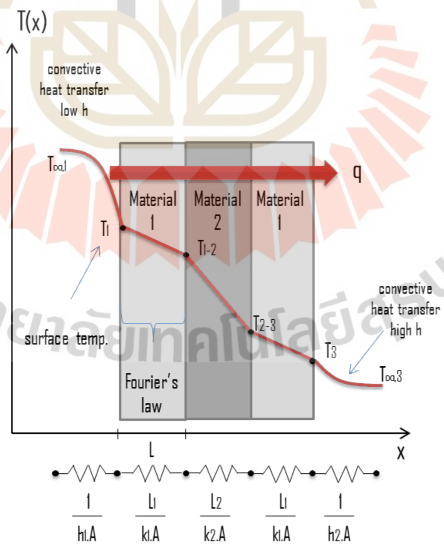

Figure 2.19 The effectiveness of multi-layered material in preventing heat transfer (Koenders et al., 2018)

Based on the graphical concept of multi-layered heat transfer, the reduction of thermal transfer is affected by the thermal resistance. Thermal resistance is defined as a heat property and a temperature difference measurement by which an object or material resists a heat flow. The thermal resistance for conduction in a plane wall is defined as:

$$\mathrm{R}_t = \left(\frac{\mathrm{L}}{k\mathrm{A}}\right)_1 + \left(\frac{\mathrm{L}}{k\mathrm{A}}\right)_2 + \left(\frac{\mathrm{L}}{k\mathrm{A}}\right)_3$$

Where,
R_t is the thermal resistance (m^2k/W)
k is the material conductivity (W/mK)
L is the plane thickness (m)
A is the plane area (m^2)

Consider a plane wall of thickness (L) and average thermal conductivity (k). As shown in Figure 2.19, the wall's three-layer material is maintained at constant temperatures of T_1 and T_3. For one-dimensional steady heat conduction through the wall, we have T(x). Then Fourier's law of heat conduction for the wall can be expressed as:

$$Q = \frac{\mathrm{dT}}{R_t} = \frac{\mathrm{T}_1 - \mathrm{T}_3}{(\mathrm{L}/k\mathrm{A})_1 + (\mathrm{L}/k\mathrm{A})_2 + (\mathrm{L}/k\mathrm{A})_3}$$

Where,
Q is the heat flux through plane (W)
k is the materials conductivity (W/mK)
T_1 is the most outside temperature surface (°C)
T_3 is the most inside temperature surface (°C)
L is the plane thickness (m)
A is the plane area (m^2)

The calculation does not account for the plane area to determine the heat transfer value per unit area (W/m²) for a multi-layered system. Based on this consideration of the multilayer concept, green roofs significantly enhance thermal resistance through their multi-layered structure, which optimizes their thermal conductivity. The various layers, including vegetation, soil, drainage, and thermal insulation above the concrete roof deck, reduce heat transfer into buildings. Numerous investigations have demonstrated that concrete roofs have a thermal conductivity of

0.8 W/mK compared to green roofs of 0.66 W/mK. The maximum daily temperature compares up to 10 °C (Yang et al., 2023). Further research indicates differences in temperature across different layers. Specifically, the temperature in the vegetation layer is measured at 33.8 °C, followed by a decrease to 25.8 °C in the substrate layer and further dropping to 20.8 °C in the roof layer. The terminology employed for multi-layered elements that enhance heat conduction is pivotal. Implementing the green roof approach aims to only slightly reduce the roof thermal transfer value (RTTV), aligning with the standards set forth by the Thai Building Energy Code (BEC).

2.5 Case Studies

From reviewing research related to the use of lightweight cellular concrete on green roofs, it was found that there is research both in the country and abroad who have studied the LCC for use on green roof systems, RTTV performance on green roofs, and air void characterization, which can be a guideline for research are reasonable as follows.

2.5.1 Lightweight cellular concrete for use on green roof systems

Munir et al. (2020) explore the application of precast LCC panels for the structural deck of green roof systems, aiming to address urban heat island (UHI) effects and high energy consumption in buildings. LCC, known for its low density and good thermal insulation, is proposed to reduce the structural load and enhance the thermal performance of buildings.

Figure 2.20 Roof box model with and without green roof system (Munir et al., 2020)

The study involved testing three U-shaped LCC panels with a density of 1,400 kg/m^3 and different widths under load until failure. The mixtures with a density of 1,400 kg/m^3 had a compressive strength lower than 17 MPa, the minimum requirement for compressive strength for structurally used concrete. The research is continuously conducted to assess the thermal performance of green roofs using foamed concrete decks.

Munir and Afifuddin (2020), The study involved constructing two prototype rooms with precast foamed concrete panels as roofs—one with a green roof and the other without. Over three days, the prototypes were exposed to direct sunlight, and various thermal parameters were continuously measured. Results indicated that green roofs significantly reduce heat gain from solar radiation during the day, thus lowering the cooling load for air conditioning systems. Using lightweight foamed concrete, with its low density and thermal conductivity, further benefits the structural load and thermal performance when integrated with green roofs.

Table 2.9 Peak temperature of green roof and non-green roof (Munir et al., 2020)

Temperature	Non-green roof			Green roof			Diff.
	Day 1	Day 2	Day 3	Day 1	Day 2	Day 3	
External surface	58.4	54.8	47.0	35.4	34.1	33.4	19.2
Internal surface	57.7	53.9	46.7	36.3	34.7	34.0	17.8
Indoor air	50.4	47.3	42.2	37.9	36.3	35.2	10.2

2.5.2 Green roof performance calculated by RTTV

Y. He et al. (2021) developed a model to predict the Roof Thermal Transfer Value (RTTV) for green roofs in tropical climates. The RTTV metric estimates the annual average heat gain through a building's roof, which is crucial for evaluating the energy performance of green roofs. Figure 2.20 shows a field experiment that validated the hygrothermal transfer model of green roofs against real-time data. Using this model, the study simulated annual heat gain through four types of green roofs and calculated their RTTV values, which ranged from 2.29 to 2.49 W/m^2, showed in Figure 2.21, significantly lower than those of bare roofs.

The study also calculated the equivalent thermal resistance of the plant layer using the RTTV model and compared it with other simplified methods, discussing the reasons for the differences. The RTTV model provides a reliable method for evaluating green roofs' energy performance, highlighting their cooling effects and potential to reduce building energy consumption.

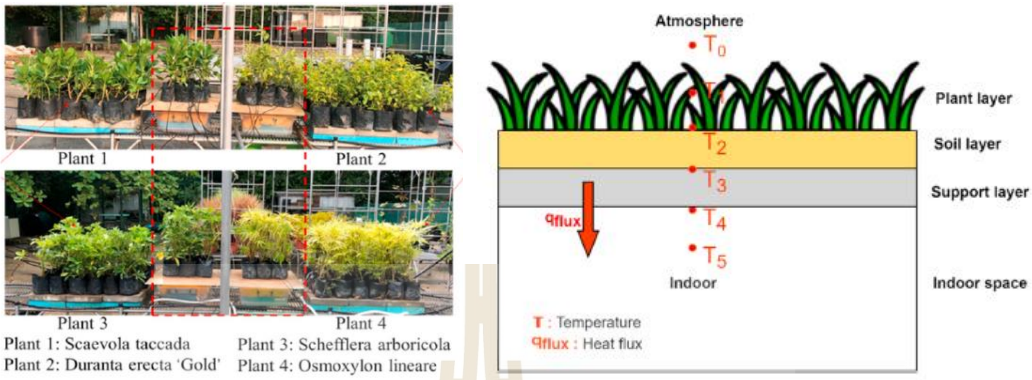

Figure 2.21 Field experiment and sensor layout on green roofs (Y. He et al., 2021)

Furthermore, the study calculated the equivalent thermal resistance of the plant layer using the RTTV. The research provides a methodology for quick thermal performance evaluation of green roofs during the early design stages, facilitating better design decisions for energy efficiency in tropical regions.

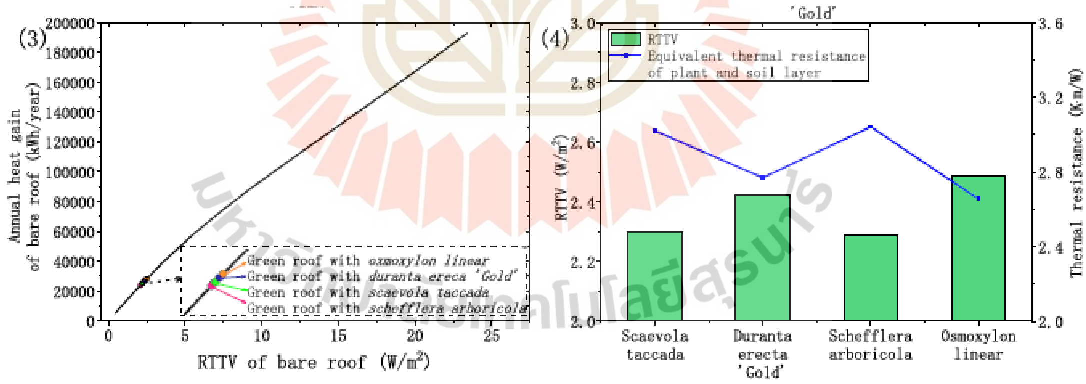

Figure 2.22 Thermal performance of green roof calculated using RTTV (Y. He et al., 2021)

2.5.3 X-ray Microtomography on LCC Microstructure Analysis

Chung et al. (2017) conducted a study to investigate the microstructure of LCC using X-ray microtomography (micro-CT). In this study, foamed concrete specimens with varying densities were prepared using a pre-foaming method. The micro-CT images were processed into binary and 3D models, with enhanced quality achieved through watershed segmentation. Figure 2.22 shows the image output of X-ray microtomography. Probabilistic functions like two-point correlation and lineal-path functions were employed to describe pore distribution and connectivity, while quantitative methods assessed local porosity and pore sphericity.

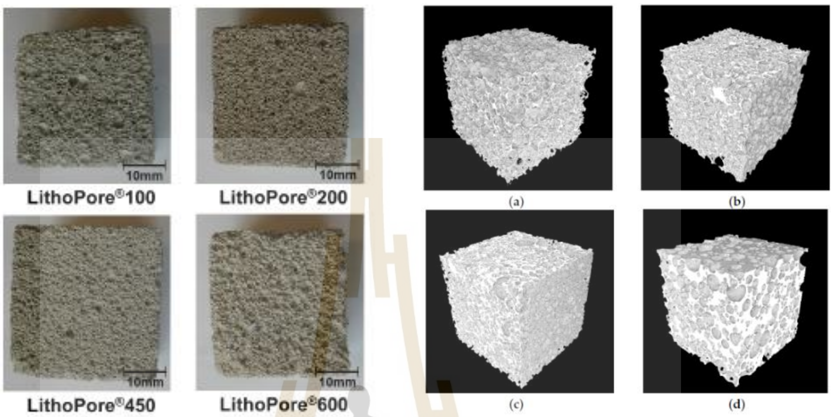

Figure 2.23 3D micro-CT images of foamed concrete specimens (Chung et al., 2017)

This detailed analysis of pore characteristics is crucial for understanding and predicting the thermal performance of foamed concrete. Larger and more clustered pores, which increase air voids, tend to reduce thermal conductivity. By combining micro-CT imaging with finite element (FE) simulations, researchers can accurately compute thermal properties and validate these findings through experimental measurements using tools like the Hot Disk instrument. This integrated approach helps optimize the thermal performance of foamed concrete, supporting the development of more efficient and sustainable building materials

CHAPTER III
RESEARCH METHODOLOGY

The study of the literature and relevant research in Chapter 2 related to the potentiality to integrate lightweight cellular concrete (LCC) and green roofs (GR). It was found that LCC has properties that can potentially support the green roof system, including its lightweight material and good thermal insulation, which is related to energy efficiency. This chapter's research methodology is structured into three sections as follows:

1) LCC properties test: to study and develop the lightweight cellular concrete mixture in the green roof system.
2) LCC microstructure analysis: to study the microstructure of porosity in LCC using Synchrotron radiation X-ray tomographic microscopy (SRXTM)
3) Green roof experimental in open air: To validate the efficiency of using LCC on green roof systems regarding thermal and energy performance, a green roof experimental box in an open-air space and RTTV calculations were used.

This research project aims to add value to green roofs by applying LCC as a roof deck. It also encourages the promotion of green roofs with LCC for commercial use, which has numerous advantages for customers.

3.1 Sample and Method 1: LCC Properties Test

3.1.1 Materials

Figure 3.1 illustrates the schematic representation of the LCC mixing process. The components utilized in the mixing process of LCC include the following materials:

1) Portland Cement Type-I, SG = 3.15
2) Fine Sand, SG = 2.60
3) Water

4) Foam Agent SUT V2.1 foam agent (Suranaree University of Technology foam agent version 2.1), made by a natural protein pH of 8.55, SG of 1 -1.05, and foam density of 40 - 60 kg/m^3, tested following the ASTM C 796 standards.
5) Polypropylene Fiber (PPF) is used to improve the LCC strength, length 12 mm, diameter 60 μm, SG = 0.91. The mixture using the PPF is the latest development of LCC SUT (LCC SUT Ver. 2)

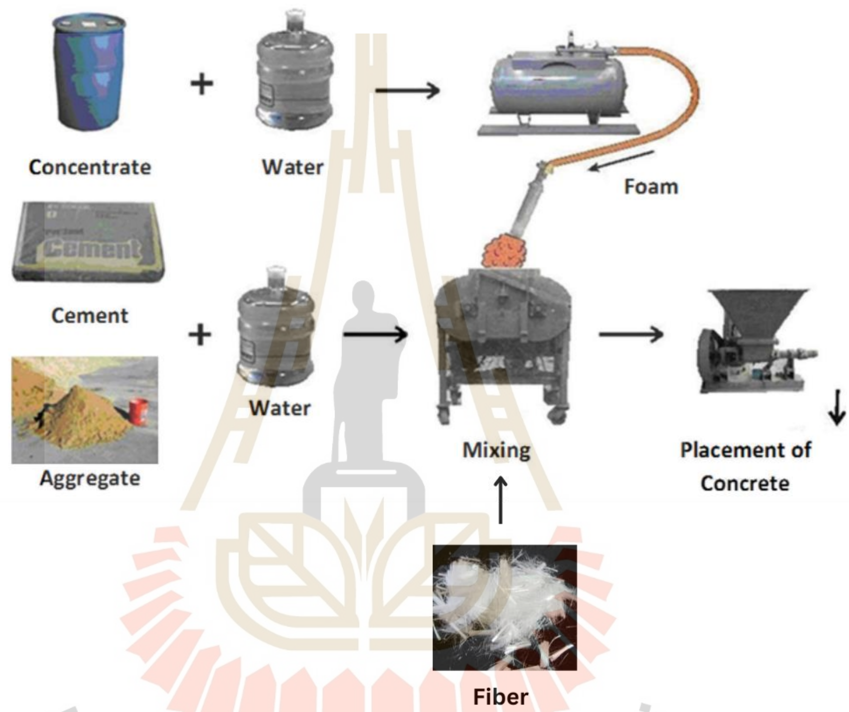

Figure 3.1 The production process of LCC

3.1.2 Equipment

The equipment utilized in the mixing process of LCC include the following materials:

1) Horizontal lightweight cellular concrete mixer: The lightweight concrete mixer is a horizontally rotating shaft type with a screw-type agitator. It has a maximum mixing capacity of 0.8 m^3 and is driven by a 5-horsepower electric motor. The agitator rotates at a pace of 45 rpm developed by Chapirom (2017) through the patent in Thailand industrial number 14175, as shown in Figure 3.2.

Figure 3.2 Horizontal LCC mixer machine and stirring blades agitator type

2) Time-controlled cellular concrete foam foaming machine: The foam generator, also known as a foam generator, is a device that operates on a timed mechanism and uses a pressure pump in conjunction with an air compressor. Apply pressure to the air compressor regulator to sustain a consistent pressure of 0.6 MPa. A device combining liquid foam with air and water generates significant bubbles. Stir and gently mix the air-foaming solution until it reaches a weight ratio 1:40, as shown in Figure 3.3.

Figure 3.3 Time-controlled air bubble generator LCC lightweight concrete

3) Air compressor: When employed alongside a pressure pump-type bubble generator, an air compressor introduces air into the foam generator. The pressure is regulated within the 1–1.2 MPa range with a tolerance of ± 0.007 MPa.

4) Foam weighing container: Conducting a test to determine the density of air bubbles can be accomplished by introducing air foam into a container of a predetermined volume. The density of liquid foam in

lightweight concrete mixtures is determined by the ratio of the weight of the foam in the tank to the volume of the tank. The density of foam must range from 40 – 60 kg/m^3.

5) Mix Design: All concrete should be mechanically mixed to produce a uniform distribution of the materials with a suitable consistency and the required wet unit weight. The mixing calculation refers to American Concrete Institute (ACI) Guide 523.3R-14 guidelines. These guidelines help determine the correct proportions of different components to be used. The composition of the mix can be adjusted to meet the LCC's specific density and weight requirements.

This study on LCC uses LCC with a density range between 1000 – 1800 kg/m^3. The density range is based on using LCC in slab concrete construction with a minimum density of 1000 kg/m^3. The list of mix designs for the LCC experimental is shown in Table 3.1. Moreover, the normal concrete mix will also be added as a reference mix while testing the green roof comparison.

Table 3.1 Composition of normal concrete (control) and LCC (treatments)

Sample Name	Target Density (kg/m^3)	W/C ratio = 0.5, Volume = 1 m^3							
		Cement (kg)	Sand (kg)	Gravel (kg)	Water (kg)	Foam Agent (kg)	Admix ture (kg)	Fiber (kg)	Measured foam volume (%)
NC	2400	320	480	960	144	-	-	-	-
LCC 10	1000	410	400	-	171	24	1.2	0.4	52
LCC 12	1200	400	620	-	164	21	1.6	0.4	45
LCC 14	1400	390	840	-	160	17	1.9	0.4	38
LCC 16	1600	385	1050	-	155	14	2.7	0.4	32
LCC 18	1800	380	1258	-	151	11	2.9	0.4	24

Test properties on normal concrete were taken from secondary studies because they are general properties carried out in many previous studies. The process of LCC sample preparation is shown in Figure 3.4.

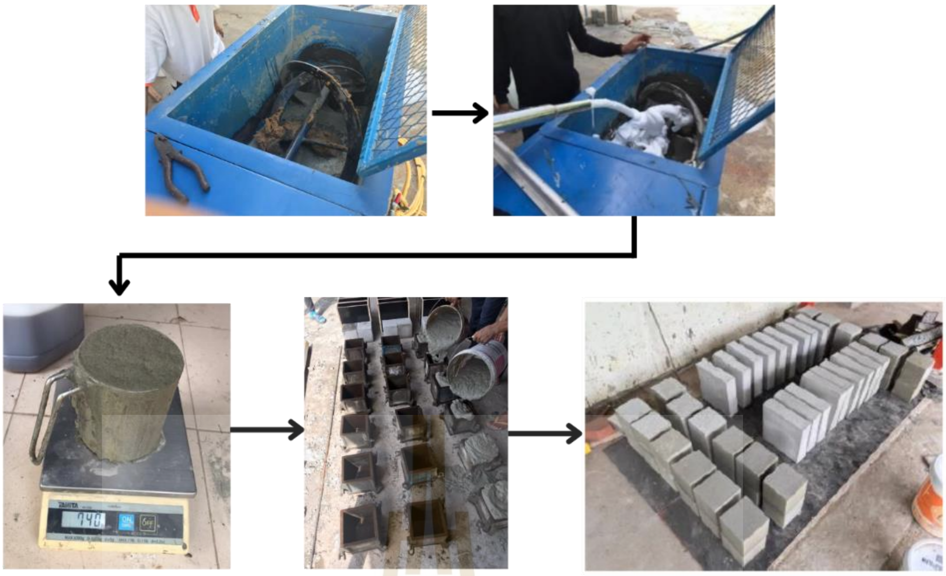

Figure 3.4 LCC sample preparation

3.1.3 Experimental Methods

Test properties for each LCC density and the number of test samples are described in Table 3.2.

Table 3.2 List of test samples for each variable density (LCC 10, LCC 12, LCC 14, LCC 16, LCC 18)

No.	Sample LCC	Sample Size (cm)	Number of samples/test age (samples/days)			
			3	7	14	28
1	Compressive strength	15 x 15 x 15	3	3	3	3
2	Dry density	15 x 15 x 15	3	3	3	3
3	Water absorption	15 x 15 x 15	-	-	-	3
4	Thermal conductivity	30 x 30 x 7.5	-	-	-	3
5	Flexural strength	50 x 15 x 15	-	-	-	3
6	Tensile strength	d=15, h= 30	-	-	-	3
7	Modulus of elasticity	d=15, h= 30	-	-	-	3

1) Compressive strength test

Compressive strength test of LCC by casting a sample block of size 15×15×15 cm. The process begins with preparing LCC samples, which can cure for a specified age of 3, 7, 14, and 28 days. After curing, the samples are placed in a compression testing machine, which gradually applies an increasing load until the concrete fails. The maximum load applied before failure is recorded, and the compressive strength is calculated by dividing this load by the cross-sectional area of the sample. This value, expressed in pressure units such as megapascals (MPa), indicates the concrete's ability to resist compressive forces. The result of the test must pass the TIS 2601-2013 requirements.

2) Dry Density Test

The test was conducted to gauge the dry density of LCC by using standard cube-shaped sample blocks, each measuring 15 x 15 x 15 cm. The samples will be cured for 3, 7, 14, and 28 days. The test sample is dried in the oven for at least 24 hours at 105 ± 5 °C until an even mass is achieved. Afterwards, allow it to cool to ambient temperature for at least 4 hours. After that, measure the object's weight and dimensions to determine its size. Volume is the amount of space an object occupies and is measured in kg/m^3, where density is mass per unit volume. The result of the test must pass the TIS 2601-2013 requirements.

3) Water Absorption Test

A water absorption test on LCC was conducted on cubes measuring 15×15×15 cm cured to a 28-day aging process. The sample LCC were immersed in water for 24 hours. After a day of immersion, remove them from the water and use a cloth to soak up any remaining water on their surface. The samples are weighed within 30 seconds, ensuring the recorded result is the wet weight. Afterward, place the sample cubes in an oven set at 105 ± 5 °C for 24 hours. Remove the sample from the oven and let the substance reach a lower temperature in its surrounding environment. Finally, meticulously measure and document the precise numerical value. The result value represents the weight of the sample after all moisture has been removed. The result of the test must pass the TIS 2601-2013 requirements.

4) Thermal Conductivity Test

A thermal conductivity test of LCC measures the material's ability to conduct heat. The process begins with preparing and curing LCC samples to the desired specifications. These samples are placed in a thermal conductivity testing apparatus between a heat source and a heat sink. A known and steady temperature gradient is established across the sample, and sensors measure the rate of heat flow through it. The thermal conductivity is calculated using the formula,

$$k = \frac{Q\,.\,d}{\mathrm{A}\,.\,\Delta T}$$

Where (k) represents thermal conductivity, (Q) is the heat flow, (d) is the sample thickness, (A) is the cross-sectional area, and (ΔT) is the temperature difference across the sample. This test is essential for understanding the concrete's heat conduction properties, crucial for applications requiring effective temperature regulation and insulation. The result value of thermal conductivity will be examined to pass the ACI 523.3R-14

5) Flexural Strength Test

The flexural strength test, also known as the modulus of rupture test, measures the tensile strength of concrete to determine its ability to withstand bending. During this experiment, a specific type of beam specimen made of concrete, with dimensions typically measuring 50 x 15 x 15 cm, is positioned in a testing apparatus and subjected to a gradual increase in force until it ultimately fractures. The test can utilize either third-point or centre-point loading arrangements. Using established methods, the greatest load applied at the point of failure is measured and used to compute the flexural strength. This test is crucial for assessing the performance of concrete in structural components such as beams and slabs, guaranteeing its ability to endure bending stresses.

6) Tensile strength test

The tensile strength test evaluates the LCC’s capacity to withstand direct tensile forces. The split cylinder test is commonly used to execute this procedure. It involves placing a cylindrical specimen horizontally in a testing machine, typically with a diameter of 150 mm and a height of 300 mm. A vertical compressive load is exerted on the cylinder's diameter, causing it to fracture and generate tensile tension. Tensile strength is determined by measuring the highest load applied at the failure point. This test is crucial for comprehending the behaviour of concrete when subjected to tensile loads and is indispensable for designing structures that experience such forces.

7) Modulus of Elasticity

The modulus of elasticity of LCC, also known as elastic modulus, measures the concrete's ability to deform elastically (i.e., non-permanently) under load. It quantifies the relationship between stress (force per unit area) and strain (deformation per unit length) in the linear elastic range of the concrete's stress-strain curve. To determine this, a cylindrical concrete sample is subjected to a compressive load in a testing machine. The stress and corresponding strain are recorded, and the modulus of elasticity is calculated as the ratio of stress to strain in the initial, linear portion of the curve.

3.2 Sample and Method 2: LCC Microstructure Analysis

3.2.1 Materials

The LCCs selected for application in the upcoming green roof research are LCC 12 and LCC 14. Further analysis is required to examine the air-void characteristics of LCC. Data on air voids will be utilized to validate the correlation between physical properties and microstructure and their impact on enhancing the thermal performance of the LCC green roof. The sample of LCC 12 and LCC 14 with a 2-3 mm diameter and a section thickness of 20 mm, were analyzed using Synchrotron Radiation X-ray Tomographic Microscopy (SRXTM). The sampling of LCC 12 and LCC 14 is based on the same mortar used for the physical properties test. The samples must then be affixed to the sample holder using various tools, as depicted in Figure 3.5.

Figure 3.5 LCC sample for SRXTM testing

Other tools used to tidy up the sample and install the sample in the holder are as follows:

1) Sample holder

2) Sharpening equipment

3) Capillary wax

4) Wax soldering pen

3.3.2 Equipment

The beamline at BL1.2W serves as a specialized facility at the Siam Photon Source (SPS) for X-ray Tomographic Microscopy experiments. Utilizing the high-intensity X-ray beam from a 2.2-Tesla multipole wiggler with X-ray energy 5 – 20 keV provides researchers with advanced microtomography capabilities. This method allows for the reconstruction of cross-sectional details and the creation of 3D visualizations of diverse samples, with resolutions as fine as 1 μm (corresponding to a pixel size of 0.72 μm). Table 3.3 describes the details of SRXTM. The experimental station is designed using microtomography geometry principles.

Table 3.3 Synchrotron Radiation X-ray Tomographic Microscopy (SRXTM) specification

BL1.2W: X-ray Tomographic Microscopy	
Source	Multipole wiggler, 2.18 Tesla
X-ray Energy	5 – 20 keV
Operations	1. Monochromatic beam: Ge (111), approx. 1012 ph/s/0.1% BW @8 keV 2. (Filtered) White beam
Beam Size	Unfocused, (H) 10 mm x (V) 4 mm
Detection	Scintillator-coupled X-ray microscope (Optique Peter, France) PCO edge camera, 2560x2160 pixels
Resolution	1.5 μm spatial resolution 0.72 μm pixel size
Imaging	1. Absorption-contrast microtomography 2. Propagation-based phase contrast microtomography 3. Laminography

The XTM beamline machine is shown in Figure 3.6. As the X-ray beam exits the transfer tube, it projects onto the rotating sample, and the detection system captures the X-ray images. Following the sample, the detection system captures the X-ray images, consisting of a YAG-Ce scintillator, a lens-coupled microscope, and a PCO.edge 5.5 scientific CMOS camera (2560 x 2160 pixels chipset). Using a sliding guide, the detector system can be adjusted along the Y-axis to fine-tune the distance between the sample and detector from 0 to 100 cm. The experiment can be monitored externally from the enclosure with two observation cameras.

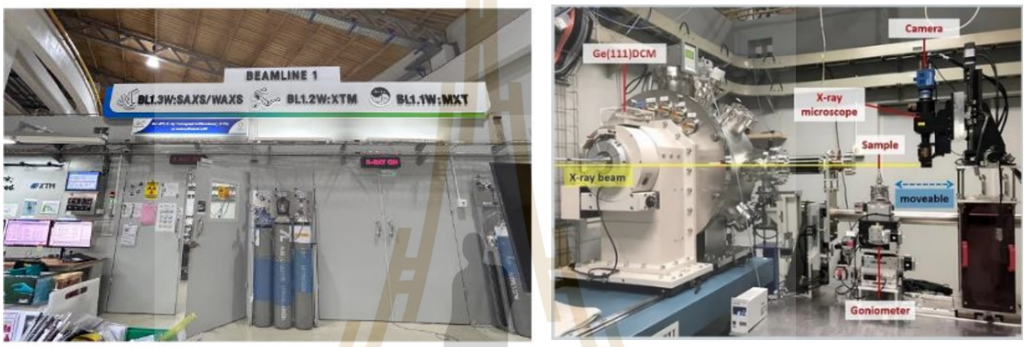

Figure 3.6 Beamline of Synchrotron Radiation X-ray Tomographic Microscopy (SRXTM)

Afterward, the outcomes of capturing photos will be analyzed. The tomographic quantitative analysis utilizes binary pictures. A threshold is determined by applying a threshold to the histogram of reconstructed slices. The process of converting photos into binary format results in a binary image. Several purposes are employed for the analysis of XTM:

Figure 3.7 Quantitative analysis software

1) Octopus Reconstruction Manual: This function involves the detailed procedures and guidelines for reconstructing data using the Octopus software. It provides step-by-step instructions for processing raw data into a usable format, often focusing on creating 3D models from imaging data.
2) Octopus Analysis Manual: This function outlines the methods and techniques for analyzing data within the Octopus software. It covers various analytical tools and approaches to interpret and quantify the data, helping users to derive meaningful insights from the reconstructed models.
3) Octopus Visualization: This function pertains to the visualization capabilities of the Octopus software, enabling users to render and display 3D models. It allows for exploring and examining complex structures, facilitating a deeper understanding of the data through visual representation.
4) Drishti 3D Software: Drishti is a 3D visualization software designed for rendering and analyzing volumetric data. It provides tools for viewing, manipulating, and interpreting 3D datasets, making it suitable for applications in fields such as medical imaging, geology, and materials science.

3.3.3 Experimental Methods

Figure 3.8 describes the experimental LCC flow using the SRXTM testing method. The sample is mounted on a high-precision rotation stage, which allows it to be rotated through a series of angles, typically 180 or 360 degrees. The stage's movements are controlled with sub-micron precision to ensure accurate positioning during image acquisition.

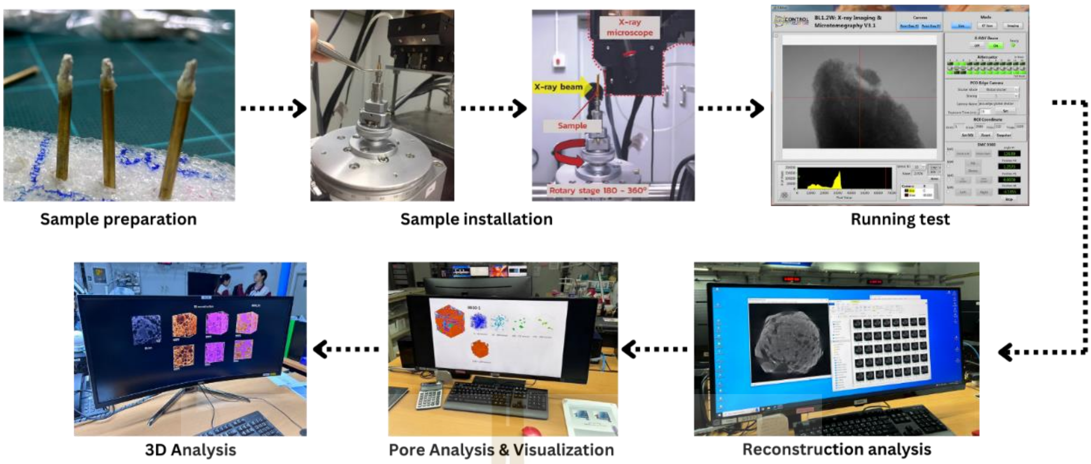

Figure 3.8 Workflow SRXTM testing

A high-resolution detector system captures the X-rays that pass through the sample. The detector converts X-rays into visible light, which is then recorded by a high-resolution camera. The setup may use scintillators, lenses, and CCD or CMOS cameras for optimal image capture. The acquired 2D projections are processed using specialized software to reconstruct a 3D volumetric image of the sample. Algorithms such as filtered back-projection or iterative reconstruction techniques are commonly used. The 3D image data is analyzed to extract quantitative information about the sample's internal features. SRXTM testing on LCC aims to investigate the porosity stability in LCC.

3.3 Sample and Method 3: Open-air experiment of green roofs

3.3.1 Materials

The open-air experiments by implementing LCC as a roof base on the extensive green roof are conducted to evaluate the green roof performance in an outdoor atmospheric setting. LCC 12 and LCC 14 were selected based on their recommendations for use as a structural slab. The dimensions of the experimental roof box were 1.00 x 1.00 x 1.00 m with a roof area of 1 m^2. The box experimental section is shown in Figure 3.9.

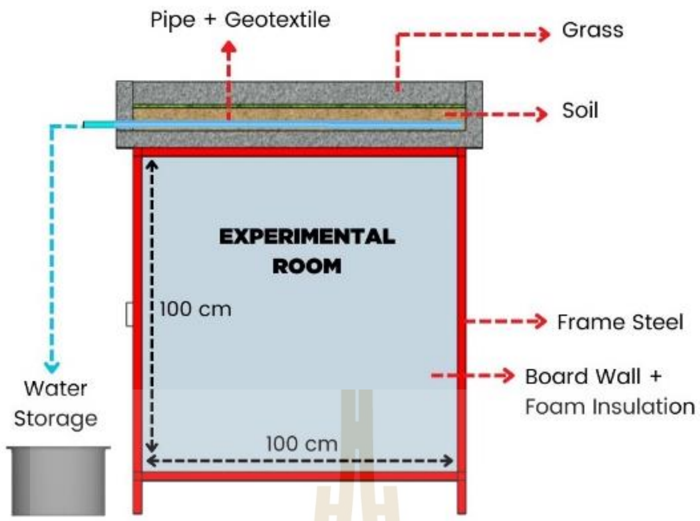

Figure 3.9 Roof box experimental section

The study evaluated the performance of green roofs by testing four different types of roof decks, as follows:

1) Normal concrete roof (Non-GR)

2) Green roof with normal concrete base (GR-NC)

3) Green roof with LCC 12 base (GR-LCC 12)

4) Green roof with LCC 14 base (GR-LCC 14)

Table 3.4 provides detailed information about the layer arrangement of each open-air experimental green roof variable.

Table 3.4 Characteristics layer of the open-air experiment green roofs

Layer Green Roof	**Non-GR** Normal Concrete Roof	**GR-NC** Green Roof Normal Concrete	**GR-LCC 12** Green Roof LCC 1200	**GR-LCC 14** Green Roof LCC 1400
Extension Vegetation	-	**General grass Zoysia matrella** 2.5 cm thick		
Substrate layer	-	**Sandy loam soil** 5.0 cm thick		
Roof deck	**Normal concrete** 7.5 cm	**Normal concrete** 7.5 cm	**LCC 12** 7.5 cm	**LCC 14** 7.5 cm
Interior room	**Hardwood board wall 5 mm with structure frame** Room size 1 x 1 x 1 m			

Figure 3.10 The view of the open-air experiment and green roof models

As explained in Section 2.1, conventional green roofs (GR-NR) consist of various layers. In this green roof experiment, only the concrete deck is used as a parameter for the green roof layer. Therefore, the study will not include other supporting layers.

3.2.2 Equipment

The environmental factors (i.e., air temperature and air humidity) were measured using the outdoor temperature and humidity sensor Modela AM2306 (RH accuracy ± 2%, temperature accuracy ± 0.3 °C). The soil temperature and humidity were measured using a needle probe sensor, Model SFP001 (RH accuracy ± 2%, temperature accuracy ± 0.5 °C). At each of the depths, the probes were placed horizontally. The outdoor and indoor roof deck surfaces were measured using a thermal type (T) sensor from National Instruments. Indoor temperatures and humidity were measured using a hanging temperature and humidity sensor, Model AM2305 (RH accuracy ± 2%, temperature accuracy ± 0.3 °C). Figure 3.11 summarises the details of the measurement points, and describes the sensor items used for the green roof experiment.

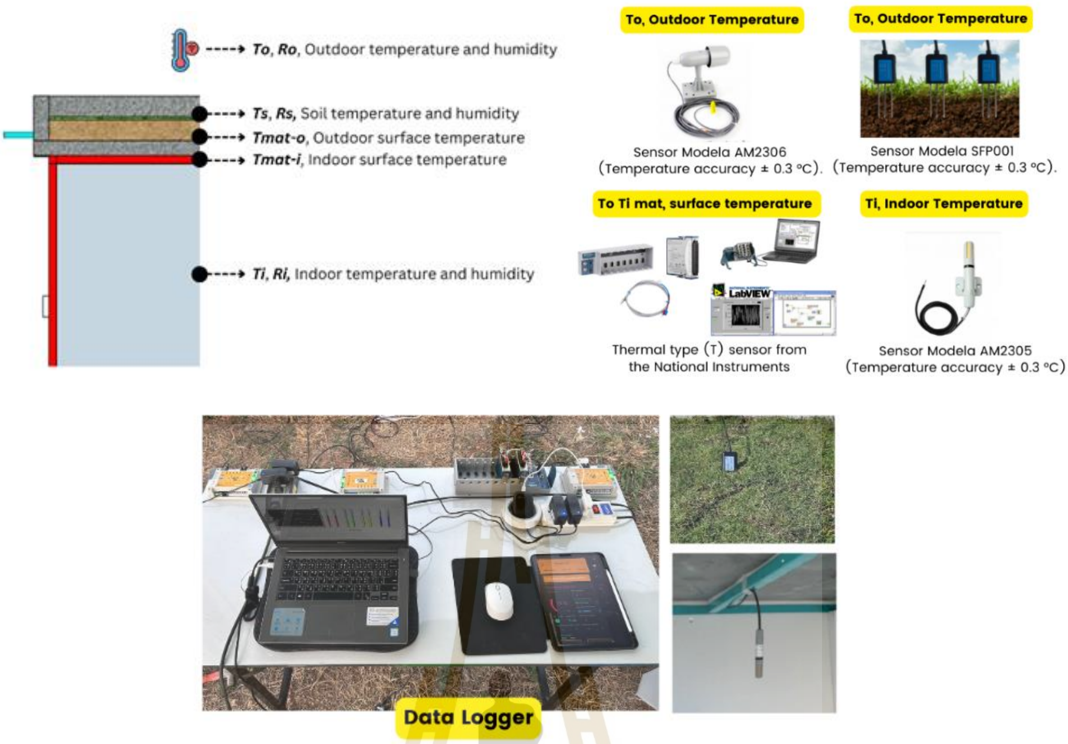

Figure 3.11 Section of sensor items and location

3.2.3 Experimental Methods

The study will compare the temperature profiles between the four roof types performed during February 2024 for three days. The test boxes are located at Suranaree University of Technology in Thailand (33° 55' 56.028'' S, 18° 38' 23.46'' E). In these open-air experiments, the study will be divided into two parts. The first part will be conducted to obtain the temperature data from every installed sensor, which will be analyzed as a temperature profile. The second part, the temperature data, will continue to calculate the thermal transfer value (Q-value) following the Thailand Building Energy Code (BEC).

CHAPTER IV
RESULTS AND DISCUSSIONS

This research focuses on studying the characteristics of lightweight cellular concrete (LCC) to develop a database that can be used for various building purposes, particularly for green roofs. Compressive strength, dry density, water absorption, thermal conductivity, and other properties are evaluated following industry standards. The analysis of the findings in this chapter will be divided into three sections:

The initial part (Section 4.1) presents the test outcomes of the LCC properties across various density variations. The collected results will be used to determine the two LCC densities to apply to the green roof.

The second part (Section 4.2) presents the results of LCC microscopy observations applied to the green roof. Data and 3D images of porosity in LCC will be presented to ensure the stability and quality of air voids in the LCC.

The last part (Section 4.3) involves conducting open-air experiments on several green roof decks to compare their thermal qualities. The thermal characteristics data will be examined and used to calculate the roof thermal transfer value (RTTV) in compliance with BEC requirements. This value serves as an indicator of the energy efficiency of roof materials.

4.1 Result and Discussion 1: LCC Properties Test

The physical property test of LCC was conducted to understand the properties of various types of LCC. The samples of LCC 10, LCC 12, LCC 14, LCC 16, and LCC 18 were chosen to be investigated. The following section presents a detailed discussion of the physical property of LCC.

4.1.1 Compressive strength

Figure 4.1 illustrates the compressive strength (MPa) of different lightweight cellular concrete (LCC) densities over different curing periods (3, 7, 14, and

28 days). The LCC mixes are categorized by their densities from 1000 - 1800 kg/m^3: LCC 10, LCC 12, LCC 14, LCC 16, and LCC 18.

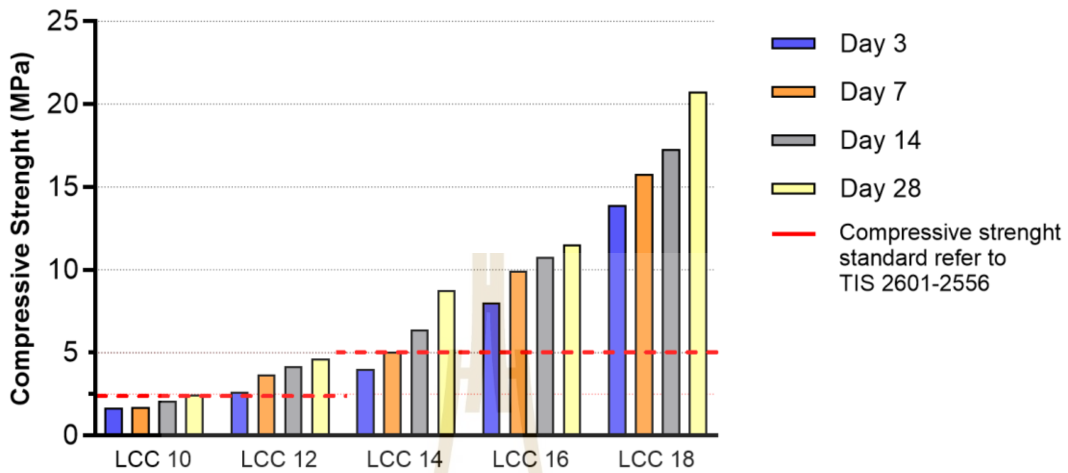

Figure 4.1 Compressive strength results of LCC

Table 4.1 Compressive strength results of LCC

Age	Compressive Strength (MPa)				
	LCC 10	LCC 12	LCC 14	LCC 16	LCC 18
Day-3	1.68	2.64	4.02	8.06	13.90
Day-7	1.74	3.69	5.07	9.97	15.78
Day-14	2.12	4.19	6.41	10.78	17.31
Day-28	2.47	4.63	8.80	11.56	20.78

The compressive strength continues to rise for all mixes at the highest values by day 28. As reported in Table 4.1, the compressive strength of LCC 10 – 18 ranges between 2.47 – 20.78 MPa. As it compared to the standard, all LCC mixes reported higher than the requirements of the Thailand industrial standard (Thai Industrial Standard, 2018), where the standards require a minimum compressive strength at LCC below 1,200 kg/m^3 must be below 2.5 MPa, and LCC below 1,600 kg/m^3 must no lower than 5.0 MPa. The results indicate that all types of LCC met the standard requirements by the 28th day.

Likewise, a previous study by Othman et al. (2022) reported similar trends in compressive strength development for LCC 16 at 10 MPa, while this current study resulted better at 11.56 MPa. The findings corroborate the current study, showing the quality of compressive strength of LCC. That can applied to the construction work. Moreover, mixing and curing time is also important in determining the compressive strength of LCC to achieve the industrial standard.

In this newly developed mix, referred to as development mix LCC SUT ver. 2, the inclusion of fiber enhances the compressive strength of the LCC mix by 10% compared to the previous formulation, which did not incorporate fiber (Pratama et al., 2022). Although normal concrete (NC) exhibits a higher compressive strength, ranging from approximately 17 MPa to 24 MPa, LCC 10 - 16 demonstrates adequate compressive strength and reduced weight, making it suitable for special use in both non-bearing and load-bearing building constructions. Based on guidelines for using LCC in construction, LCC 10 - 16 shows potential for application as a roof deck base in green roof systems (Mohd Sari and Mohammed Sani, 2017).

4.1.2 Dry density

Figure 4.2 illustrates the dry density of different LCC mixes at various curing periods (3, 7, 14, and 28 days). The result shows that the dry densities of all LCC mixes showed stability over time, with only minor fluctuations no more than ± 50 kg/m³ observed aligned with the target density.

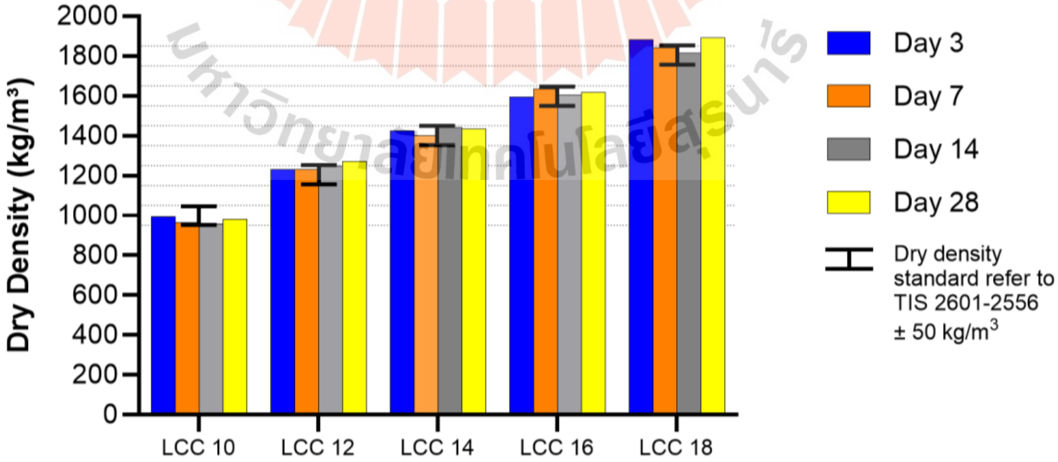

Figure 4.2 Dry density results of LCC

Table 4.2 Dry density results of LCC

Age	Dry density (kg/m^3)				
	LCC 10	LCC 12	LCC 14	LCC 16	LCC 18
3-Day	996	1232	1427	1596	1882
7-Day	964	1232	1405	1637	1844
14-Day	959	1250	1444	1606	1818
28-Day	980	1274	1436	1619	1894

A tolerance of ± 50 kg/m^3 on target density was adopted, aligning with standard practices in the LCC production industry (Thai Industrial Standard, 2018). The proportional relationship between the target density and dry density can be observed. As shown in the previous result on the compressive strength test, the compressive strength increases with the increasing density.

To achieve optimal LCC properties, deviations from the dry density must align with the target density. Previous studies by Othman et al. (2021) have shown that the compressive strength will not reach its maximum potential if the target density does not achieve the appropriate dry density. With this minor tolerance range, the stability of properties within the specified density category in LCC is anticipated to be maintained.

Compared to normal concrete (NC), which has a density ranging from 2200 to 2400 kg/m^3, LCC offers numerous advantages, particularly in reducing structural dead load, thereby lowering construction costs. An analysis of the feasibility of using LCC as a substitute for NC is necessary, particularly regarding strength and other specialized properties required to enhance building performance.

4.1.3 Water absorption

The water absorption properties of LCC at varying densities were assessed to gauge their suitability for green roof applications. Figure 4.3 summarises the results: as LCC density increases, water absorption percentage decreases.

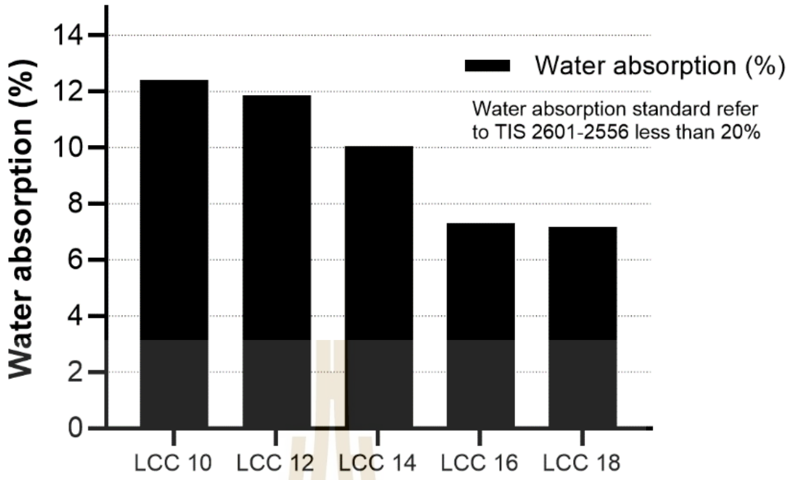

Figure 4.3 Water absorption results of LCC

Table 4.3 Water absorption results of LCC

Mix	Water absorption (%)
LCC 10	12.42
LCC 12	11.86
LCC 14	10.06
LCC 16	7.30
LCC 18	7.19

LCC 10 exhibits the highest water absorption at 12.42%, whereas LCC 18 shows the lowest at 7.19%. All tested samples meet the required minimum water absorption rates of less than 20% following the TIS 2601-2556 standard (Thai Industrial Standard, 2018).

The current study also aligns with other related studies where the water absorption of LCC was below 12% (Nurain Izzati et al., 2019). LCC samples with higher density show lower water absorption, while LCC 10 slightly exceeds 12%. LCCs with lower densities may need additional treatment or admixtures to reduce water absorption to optimal levels. Higher LCC demonstrates superior performance in reducing water absorption rates, lowering the risk of water leakage. Compared to normal concrete (NC), which has a water absorption rate of 7.93%, LCC exhibits higher water absorption, typically at or below 14%. However, the microstructure of NC reveals a total porosity of 25.42%, with an open porosity of 15.09% and a closed porosity of 10.62% (Cebeci, 1981). The interconnected nature of the open porosity suggests a higher potential for water leakage in NC. In this study, the microstructure of the LCC sample will be examined to obtain porosity data, which will be detailed in the results and discussion section.

LCC 12 and LCC 14 are potentially adopted due to their water absorption standard with the lower density. This enhances durability and minimizes the risk of water leakage, making them preferable for sustainable building practices.

4.1.4 Thermal conductivity

The thermal conductivity of LCC with varying densities was measured to assess its effectiveness in thermal performance for green roof applications. The results are summarised in Figure 4.4.

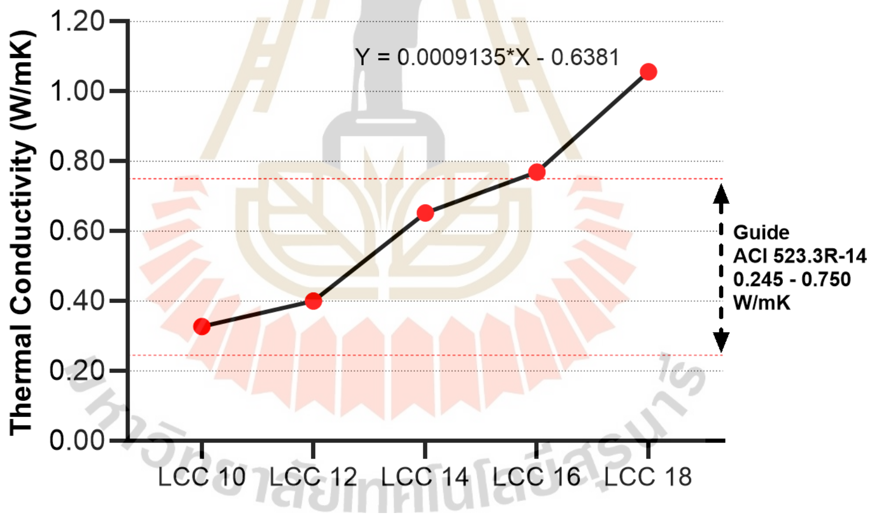

Figure 4.4 Thermal conductivity results of LCC

Table 4.4 Thermal conductivity results of LCC

Mix	Thermal Conductivity (W/mK)
LCC 10	0.32
LCC 12	0.40
LCC 14	0.65
LCC 16	0.77
LCC 18	1.05

As the density increases, its thermal conductivity also rises. LCC 10 exhibits the lowest thermal conductivity at 0.32 W/m·K, whereas LCC 18 demonstrates the highest conductivity at 1.05 W/m·K. According to the ACI 523.3R-14 standard, LCC 10 – LCC 18 thermal conductivity should ideally range between 0.245 to 0.750 W/m·K (American Concrete Institute, 1975). As shown in the result, LCC 10, LCC 12, and LCC 14 meet the requirement standard, while LCC 16 and LCC 18 exceed the standards.

Another related study revealed positive results, with the current study on thermal conductivity of 0.1 and 0.7 W/mK for LCC 6 to LCC 16. There are very high differences compared to normal concrete, which achieved 1.6 W/mK with 2200 kg/m^3 density (Zahari et al., 2009). As the cast density increases, there is a reduction in the median void diameter (D50). For a given density, thermal conductivity decreases as the median void diameter increases. Further investigation at the microstructural level is required to analyze the relationship between air voids in LCC and thermal conductivity (Batool & Bindiganavile, 2017).

Compared to normal concrete (NC) with a thermal conductivity around 2.25 W/mK, LCC can achieve 2 to 3 times lower thermal conductivity than NC, thereby enhancing its effectiveness in reducing heat transfer (Zahari et al., 2009). In conclusion, the study underscores that LCC materials, particularly those with lower densities, are highly suitable for green roof applications due to their superior thermal insulation properties. This characteristic enables these materials to contribute significantly to energy efficiency in buildings.

4.1.5 Flexural strength

The flexural strength of LCC with varying densities was evaluated to understand its performance under bending stress. The results are summarised in Figure 4.5. The accompanying line graph illustrates the flexural strength values for LCC 10 to LCC 18. LCC 10 exhibits the lowest flexural strength at 0.50 MPa, while LCC 18 shows the highest strength at 1.76 MPa.

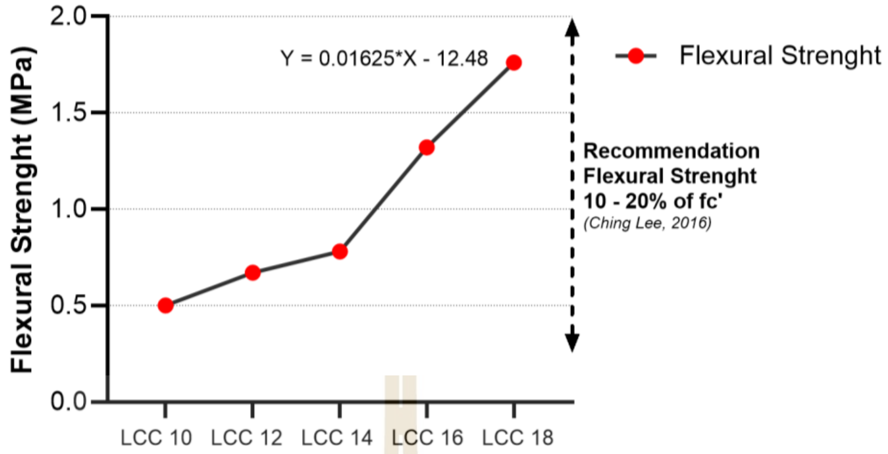

Figure 4.5 Flexural strength results of LCC

Table 4.5 Flexural strength results of LCC

Mix	Flexural Strength (MPa)
LCC 10	0.50
LCC 12	0.67
LCC 14	0.78
LCC 16	1.32
LCC 18	1.76

Higher-density LCC materials demonstrate superior flexural strength, rendering them more suitable for structural applications where resistance to bending stresses is critical. Theoretical guidelines suggest that flexural strength should ideally range between 10% and 20% of the compressive strength (Lee & Lee, 2016). The results align closely with these theoretical expectations, indicating the material's balanced mechanical properties. The flexural strength properties database can be used as data for structural design considerations in the future.

4.1.6 Tensile strength

The tensile strength of Lightweight Concrete (LCC) with varying densities was measured to evaluate its resistance to pulling forces. The results are summarised in Figure 4.6. The accompanying line graph illustrates the tensile strength values for LCC 10 – LCC 16. As the density of LCC increases, so does its tensile strength. LCC 10 exhibits the lowest tensile strength at 0.30 MPa, while LCC 18 shows the highest strength at 1.52 MPa.

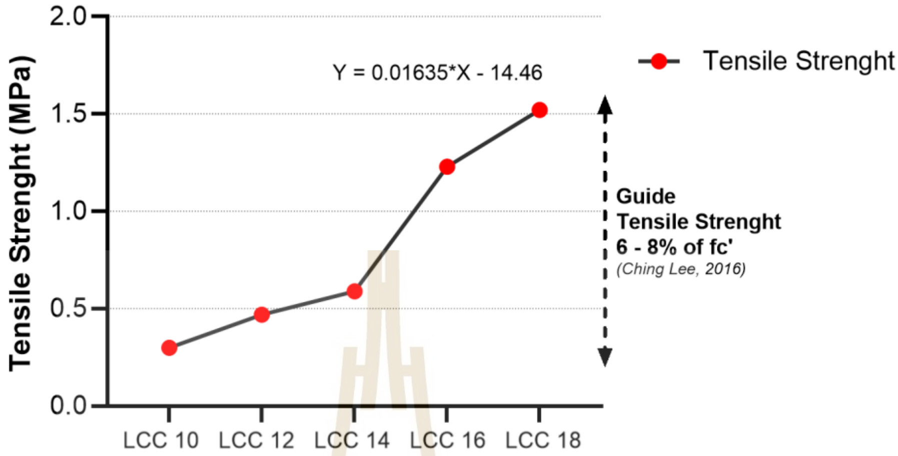

Figure 4.6 Tensile strength results of LCC

Table 4.6 Tensile strength results of LCC

Mix	Tensile Strength (MPa)
LCC 10	0.30
LCC 12	0.47
LCC 14	0.59
LCC 16	1.23
LCC 18	1.52

The study concludes that higher-density LCC materials demonstrate superior tensile strengths, making them highly suitable for structural applications requiring resistance to pulling forces. Theoretical guidelines suggest that flexural strength should ideally range between 6% to 8% of the compressive strength (Lee & Lee, 2016)

4.1.7 Modulus of elasticity

The elastic modulus of LCC with varying densities was assessed to determine its deformation characteristics under stress. The results are summarised in Figure 4.7.

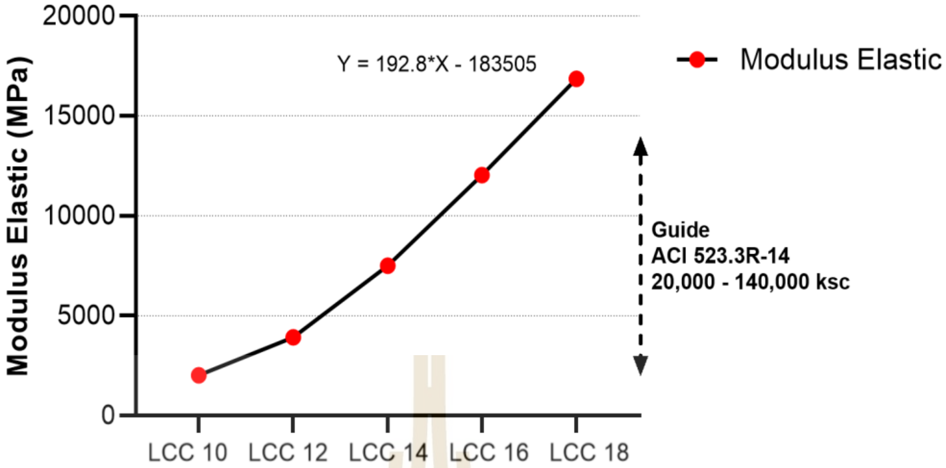

Figure 4.7 Modulus of elasticity results of LCC

Table 4.7 Modulus of elasticity results of LCC

Mix	Modulus elastic (MPa)
LCC 10	2023
LCC 12	3917
LCC 14	7512
LCC 16	12045
LCC 18	16865

As the density of LCC increases, so does its modulus of elasticity. LCC 10 exhibits the lowest modulus of elasticity at 2,023 MPa, while LCC 18 shows the highest modulus at 16,865 MPa. According to the ACI 523.3R-14 standard, the modulus of elasticity for LCC should ideally calculated between 2,000 and 14,000 MPa (American Concrete Institute, 2014). Higher-density LCC materials exhibit a higher modulus of elasticity, indicating enhanced stiffness and resistance to deformation under load. This characteristic is essential for structural applications where material rigidity is crucial. The studied LCC 10 to LCC 18 material properties align with the guideline range and can be applied to building construction. The results obtained in the database can be considered for any structural design calculation.

4.1.8 Conclusion: LCC mixed consideration for use on the green roof based on LCC properties test

The study aimed to obtain the physical properties of lightweight cellular concrete (LCC) materials as used to consider the employment of the LCC as a roof deck layer in green roof systems. Table 4.8 shows the overall result test on LCC properties.

Table 4.8 Physical properties of LCC in various density

Types	Compressive Strength (MPa)	Dry density (kg/m^3)	Water absorption (%)	Thermal conductivity (W/mK)	Flexural strength (MPa)	Tensile strength (MPa)	Modulus of elasticity (MPa)
NC*	31.2	2400	7.93	2.25	2.70	2.07	26300
LCC 10	2.47	980	12.42	0.32	0.50	0.30	2023
LCC 12	4.63	1274	11.86	0.40	0.67	0.47	3917
LCC 14	8.80	1436	10.06	0.65	0.78	0.59	7512
LCC 16	11.56	1619	7.30	0.77	1.32	1.23	12045
LCC 18	20.78	1894	7.19	1.05	1.76	1.52	16865
*) data of properties NC is secondary data from Ashraf et al. (2015)							

The results presented above demonstrate that density significantly influences the physical properties of both NC and LCC. The LCC maintained consistent stability at the target density, optimizing its properties. The properties tested, including compressive strength, water absorption, thermal conductivity, flexural strength, tensile strength, and modulus of elasticity, generally met the industrial standards set by the Thai Industrial Standard (2018) and the American Concrete Institute (2014). However, some samples in the LCC 16 and LCC 18 thermal conductivity tests exceeded the standard values. The high thermal conductivity could result from an inadequate mixing process, leading to an air-void structure that does not conform to the mix design. Further microstructural analysis is necessary to assess the volume and characteristics and establish the microstructural criteria of LCC.

Green roofs represent an advanced innovation that offers numerous benefits when integrated into buildings. The application of LCC on green roofs is intended to enhance their performance and address some of the limitations of conventional green roofs, particularly their excessive weight. Related studies have explored the potential use of LCC 14 in Indonesia, revealing positive outcomes, such as improved indoor temperatures compared to non-green roofs (Abdul Munir &

Afifuddin, 2020). However, further research is needed on LCC-based green roofs to understand the impact of using LCC as a green roof substrate better.

In the current study, the development of green roofs LCC focuses on investigating LCC 12 and LCC 14 at the microstructural level and testing them in open-air experiments. The literature review suggests that LCC 14 has the potential to replace conventional concrete as a roof deck, as it is classified as moderate-strength concrete (7–14 MPa). However, LCC 12 offers advantages in terms of lower thermal conductivity, which can enhance the thermal performance of green roofs. Additionally, LCC 12 exhibits higher water absorption, which could improve green roofs' water and drainage systems (Pratama et al., 2022).

In subsequent research, the microstructural characteristics of the air voids in LCC 12 and LCC 14 will be examined. The relationship between mix design, properties, and the quantity of air voids will be analyzed. Advanced technology will be employed to provide a comprehensive understanding of LCC.

4.2 Result and Discussion 2: LCC Microstructure Analysis

The Synchrotron Radiation X-ray Tomographic Microscopy (SRXTM) was conducted to investigate the selected samples, LCC 12 and LCC 14 in air-void volume, air-void distribution, and air-void stability structure. LCC 12 and LCC 14 were chosen to be investigated due to their potential to improve thermal performance when applied to green roofs. The following section presents a detailed discussion of the analysis results of the LCC microstructure.

4.2.1 Volume of air voids

The air-void volume in LCC 12 and LCC 14 was determined using Synchrotron Radiation X-ray Tomographic Microscopy (SRXTM). This technique enables precise measurement of the void water volume in LCC castings. Table 4.9 shows the variation of air voids' percentage volume with the foam added volume computed from mix design measurements and image analysis in LCC 12 and LCC 14.

Table 4.9 Variation of percentage volume of air voids with foam volume

Mix	Foam volume in the mix (%)	Percentage volume of air voids (%)		
		Total porosity	Closed porosity	Open porosity
LCC 12	45	39.23	38.74	0.49
LCC 14	38	29.82	29.47	0.35

The percentage of volume voids measured in cast LCC is marginally lower than the volume of voids calculated based on the mix design. The results showed the percentage of foam volume from mix design and the percentage of total porosity from SRXTM analysis. LCC 12 has 45% in a mix design and decreased by 5.77% in cast LCC, which is 39.23%, while LCC 14 has 38% in a mix design and decreased by 8.53%, 29.82%. Closed porosity represents the air voids wholly enclosed within the concrete matrix, contributing to thermal insulation and reduced permeability. The reduction in porosity at LCC 14 happened compared to LCC 12. This distinction is evident from the 2D and 3D visualizations generated by the SRXTM program. Figures 4.8 and 4.9 show the 2D section cut from three different area cuts of the sample.

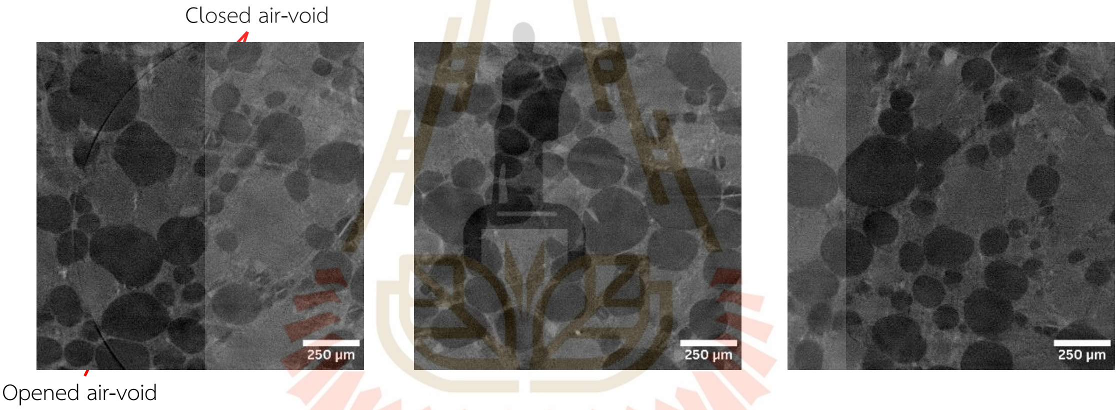

(UPPER SECTION) (MIDDLE SECTION) (BOTTOM SECTION)

Figure 4.8 2D section layer cut samples of LCC 12

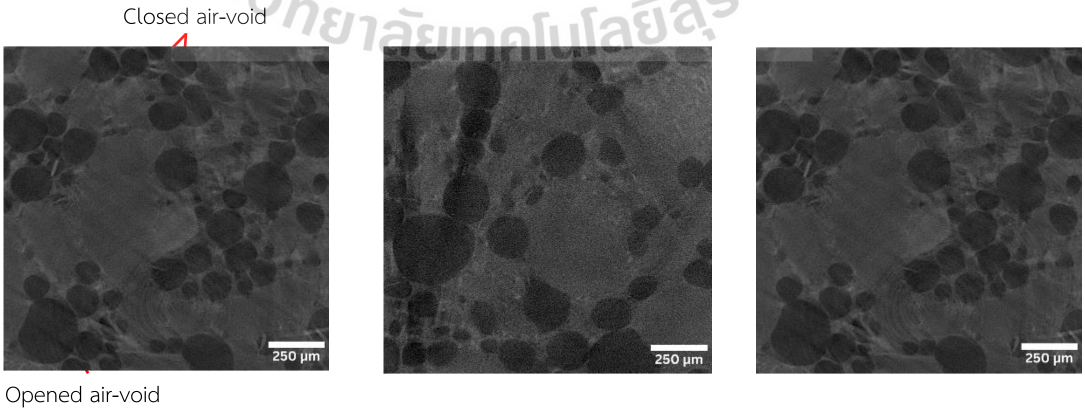

(UPPER SECTION) (MIDDLE SECTION) (BOTTOM SECTION)

Figure 4.9 2D section layer cut samples of LCC 14

The section cuts of LCC 12 and LCC 14 reveal distinct differences in the characteristics of air voids. LCC 12 exhibits a higher population of air voids compared to LCC 14. Although the diameters of air voids in both LCC 12 and LCC 14 appear similar, LCC 12 has a larger and more dominant diameter size. To understand the correlation between these characteristics and thermal conductivity, measuring the air void distribution in LCC 12 and LCC 14 is necessary. Analysis using the SRXTM technique has a high accuracy of up to 1 μm and has a 3D image output that can visualize the characteristics of the air void more clearly.

Figures 4.10 and 4.11 illustrate the separation of solid areas and air void areas in LCC 12 and LCC 14, respectively. 3D images reveal that the air void characteristics of LCC 12 are more uniform and predominant than LCC 14, consistent with the 2D image outputs from the section cuts.

(3D OVERALL IMAGE) (SOLID AREA) (AIR-VOID AREA)

Figure 4.10 3D output images SRXTM of LCC 12

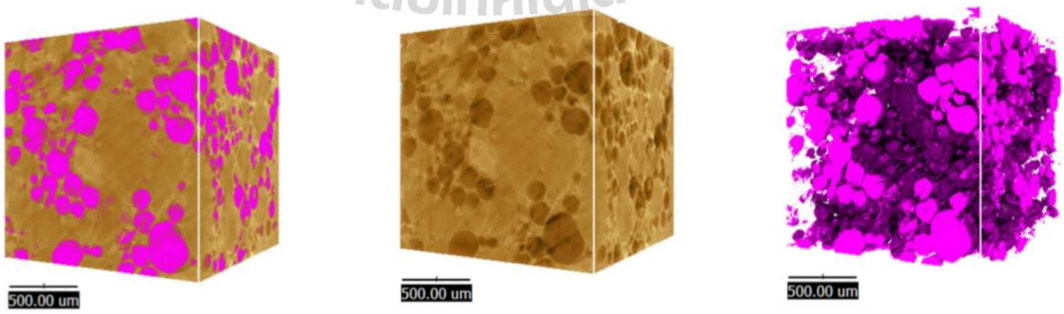

(3D OVERALL IMAGE) (SOLID AREA) (AIR-VOID AREA)

Figure 4.11 3D output images SRXTM of LCC 14

The observed decrease in porosity can be attributed to several factors, including variations in dry density of ±50 kg/m³, or approximately ±5%, which may influence the wet density. This aligns with related studies that report deviations in air voids in LCC research (Chung et al., 2020). A 5% variation in mix volume is acceptable, with a corresponding deviation in dry density, indicating the stability of air voids from mixing to LCC casting according to the mix design. However, the decrease in porosity for LCC 14 exceeding 5% could be due to heavier particles in the mix, potentially disrupting more air voids. Ensuring the stability of LCC air void volume is crucial for optimizing its properties.

The appropriate air void volume of LCC 12 indicates good insulation properties and resistance to water infiltration, enhancing the material's durability. The utilization of LCC 12 in green roofs holds significant potential for enhancing their thermal performance.

4.2.2 Air-void size distribution parameters

Section samples of LCC 12 and LCC 14 were analyzed in SRXTM to provide the data on air-void size distribution. The three cut sections were selected to analyze the air void size and distribution (upper, middle, and bottom sections). Typical binary images for the two mixes, LCC 12 and LCC 14 (cement–sand, and air-void), are shown in Table 4.10.

Table 4.10 2D output images SRXTM between LCC 12 and LCC 14

LCC 12	LCC 14
Upper section LCC 12 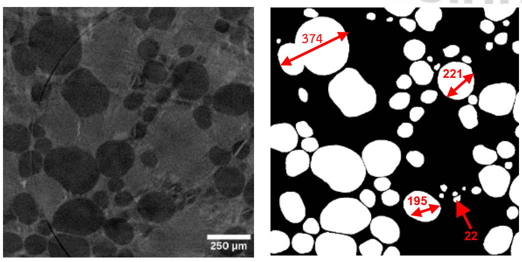 Biggest pores size: 374 µm Smalest pore size: 22 µm	Upper section LCC 14 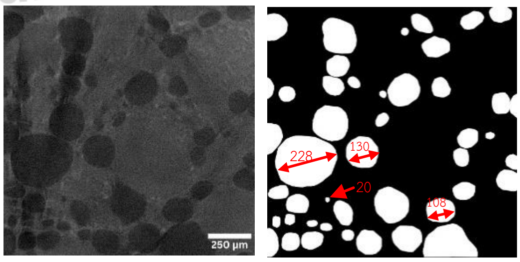 Biggest pores size: 228 µm Smalest pore size: 20 µm

Table 4.10 *2D* output images SRXTM between LCC 12 and LCC 14 (Cont.)

LCC 12	LCC 14
Middle section LCC 12 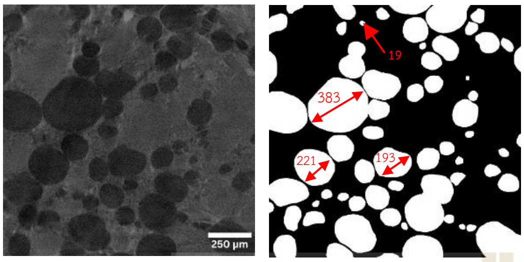 Biggest pores size: 383 µm Smalest pore size: 19 µm	Middle section LCC 14 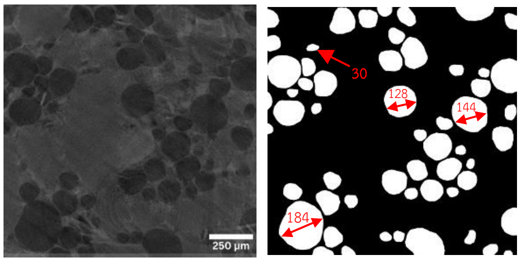 Biggest pores size: 184 µm Smalest pore size: 30 µm
Bottom section LCC 12 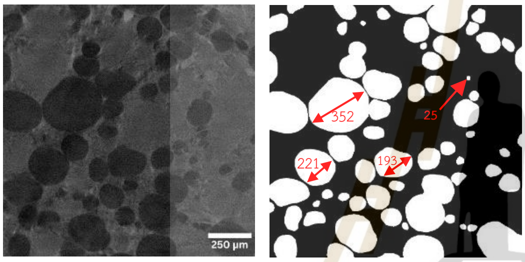 Biggest pores size: 352 µm Smalest pore size: 25 µm	Bottom section LCC 14 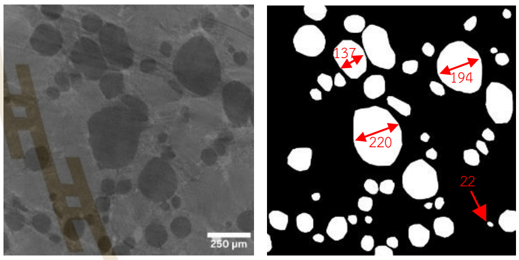 Biggest pores size: 220 µm Smalest pore size: 22 µm

Every image is digitized and converted into binary form, and a few morphological operations were done to refine the form of objects. Simple operations were only needed for this study as the air voids of white color contrast sharply with the surrounding matrix of black color, producing almost similar to a binary image before the microscopic examination. As observed from the binary images of LCC 12 and LCC 14, LCC 12 exhibits a denser form formation than LCC 14. Additionally, the diameter of LCC 12 is predominantly larger than that of LCC 14. One significant factor is that a greater number and size of air voids characterize the lower density of LCC. These numerous air voids result in lower thermal conductivity values, reduced compressive strength, and increased water absorption.

In addition, a few bigger air void diameter sizes ranging up to 383 µm are observed in LCC 12, while the maximum void diameter observed reaches 228 µm.

Figures 4.12 and 4.13 illustrate the air-void size distribution for LCC 12 and LCC 14, respectively, across three different cut sections: upper, middle, and bottom.

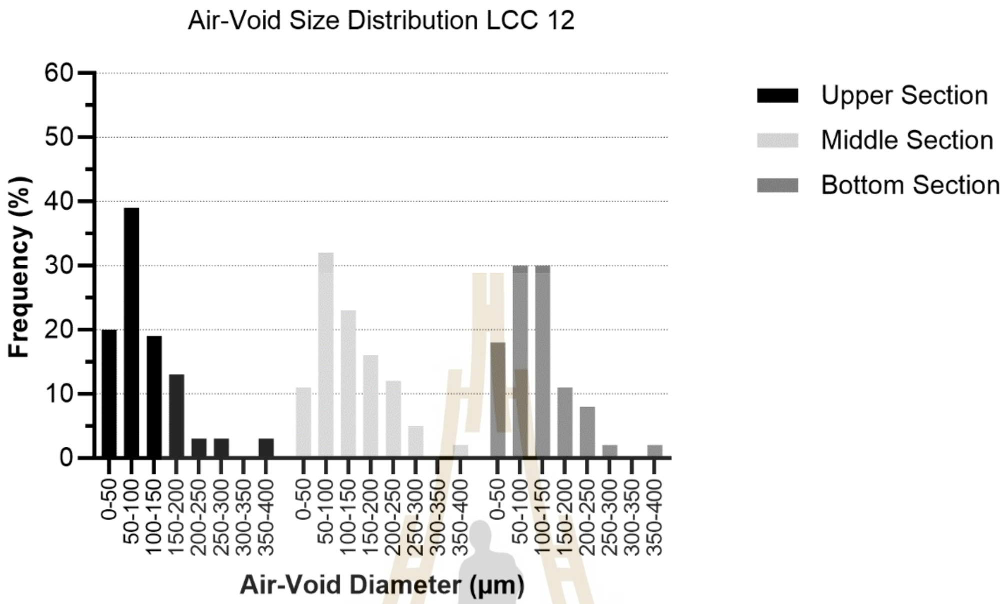

Figure 4.12 The frequency of air-void size distribution in LCC 12

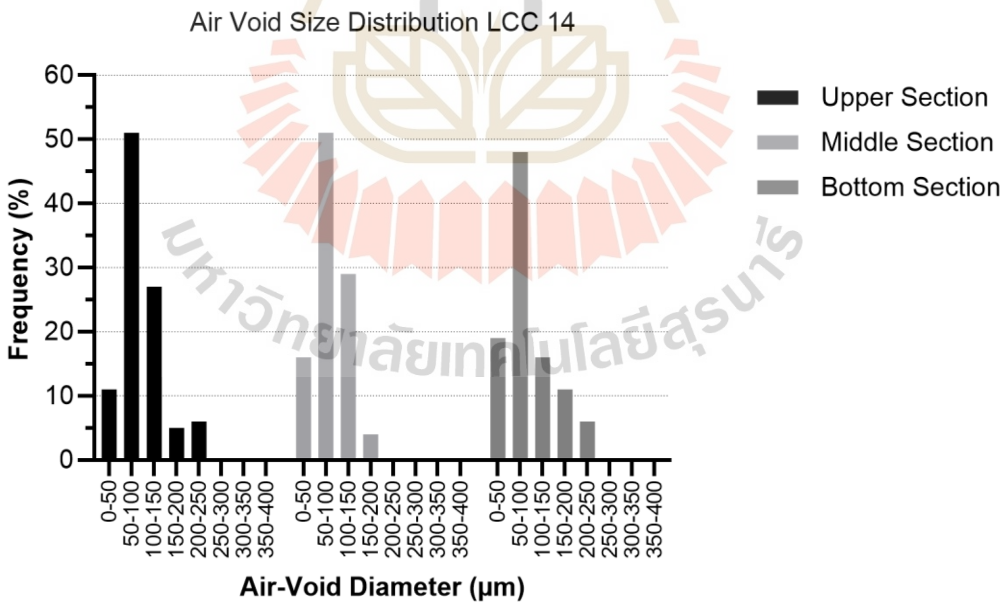

Figure 4.13 The frequency of air-void size distribution in LCC 14

The results indicated that the majority of voids in both LCC 12 and LCC 14 range between 50 and 150 µm. Specifically, air voids up to 150 µm constitute approximately 78% of the total in LCC 12, whereas in LCC 14, they account for about 95%. This demonstrates that LCC with lower density tends to have a higher proportion of larger air voids. Consequently, LCC 12, which contains larger air voids, exhibits lower compressive strength, reduced thermal conductivity, and increased water absorption.

Related research also investigates the frequency of air voids in LCC with a density of 1,300 kg/m³. The results indicate that air voids up to 150 μm comprise 60% of the total, slightly different from the current study's findings. Various factors can influence the size distribution of air voids, including the bubble size used and the stirring process. However, a uniform distribution of micro air voids can enhance compressive strength and reduce thermal conductivity. (Hilal et al., 2015). In more detail, Figures 4.14 and 4.15 quantify the air-void size distribution.

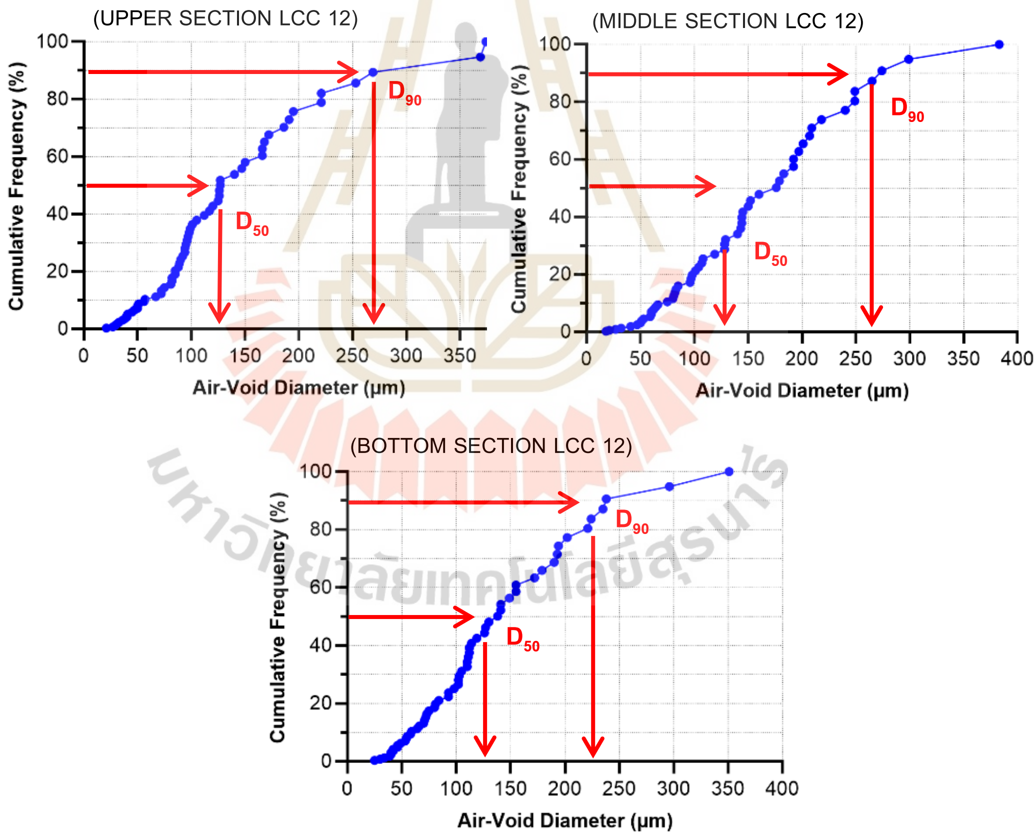

Figure 4.14 The cumulative frequency of air-void size in LCC 12

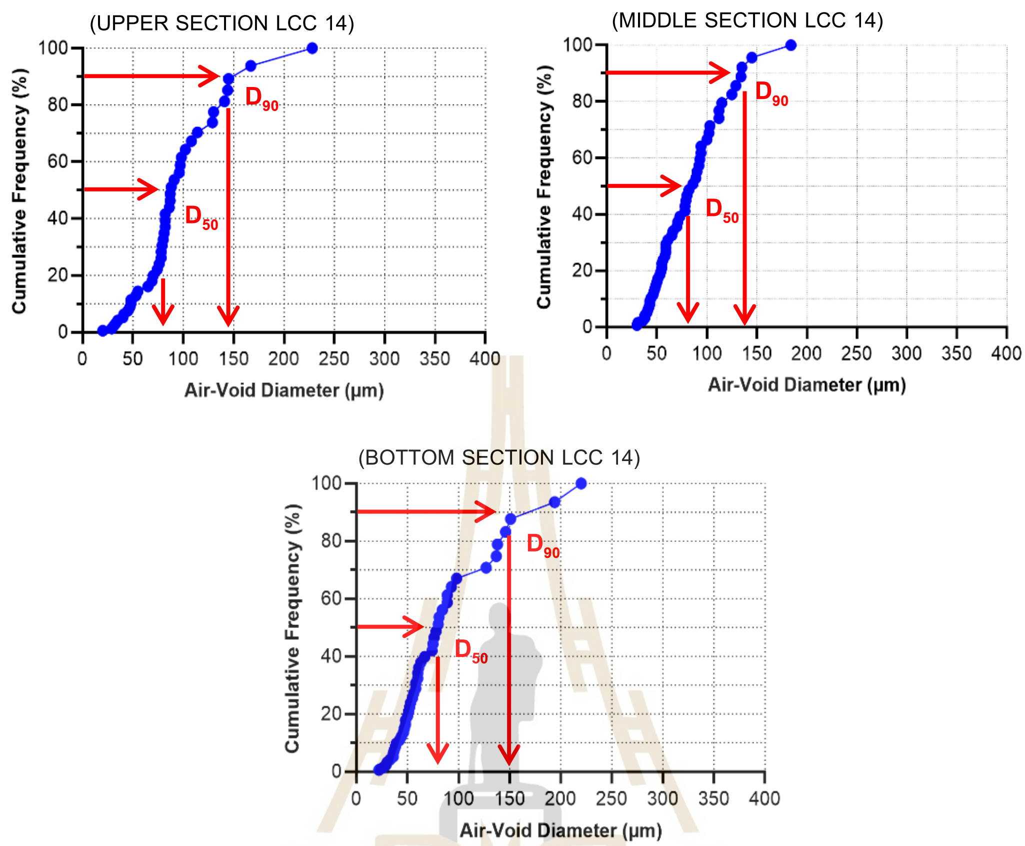

Figure 4.15 The cumulative frequency of air-void size in LCC 14

Table 4.11 Air-void size in D50 and D90 of LCC 12 and LCC 14

Mix Sample	LCC 12			LCC 14		
	Air-Void Size (D_{50}) (µm)	Air-Void Size (D_{90}) (µm)	Thermal Conductivity (W/mK)	Air-Void Size (D_{50}) (µm)	Air-Void Size (D_{90}) (µm)	Thermal Conductivity (W/mK)
Upper Sample	127	280		83	150	
Middle Sample	176	274	0.40	84	135	0.65
Bottom Sample	138	238		80	155	
Mean	**147**	**264**		**82**	**146**	

The cumulative distribution function is integral, which increases monotonically from 0 to 100, resulting in 50^{th} (D50) and 90th (D90) percentiles. The parameters used to quantify the air-void size distribution are D50 and D90 (Batool & Bindiganavile, 2017). The value of D50 for LCC 12 examined here was in the 127 – 176 μm range, and D50 for LCC 14 range of 80 – 84 μm. It shows that the increase in D50 leads to a reduction in thermal conductivity. Moreover, the value of D90 for LCC 12 ranges from 238 – 280 μm, and LCC 14 ranges from 135 – 155 μm. The mixes with a larger range of air-void size distribution showed higher conductivity, whereas, at higher density, smaller size of voids and narrower distribution of voids resulted in reduced thermal conductivity.

In conclusion, LCC 12 demonstrates favorable properties for reducing thermal conductivity due to its broader range of air-void size distribution. The D50 and D90 values for LCC 12 are between 147 and 264 μm. Previous research suggests that a higher D90 range in air-void distribution correlates with decreased thermal conductivity. In contrast, a lower D50 range indicates an increase in the compressive strength of LCC.

4.2.3 Stability of air-void

The stability of the air void is indicated by the form of the air void being intact, even, and closed. The stability of air voids within LCC 12 and LCC 14 is observed in Figures 4.16 and 4.17. The observation reveals a complex structure featuring intact bubble voids, solid phases, closed pores, opened pores, and micropores. Both opened, and closed pores indicate that while some air voids remain stable and intact pores. Only minor porosity is mergely observed. Other air voids are seemly separated by the solid phase, which gives LCC the advantages of low water absorption, high durability, and effective insulation.

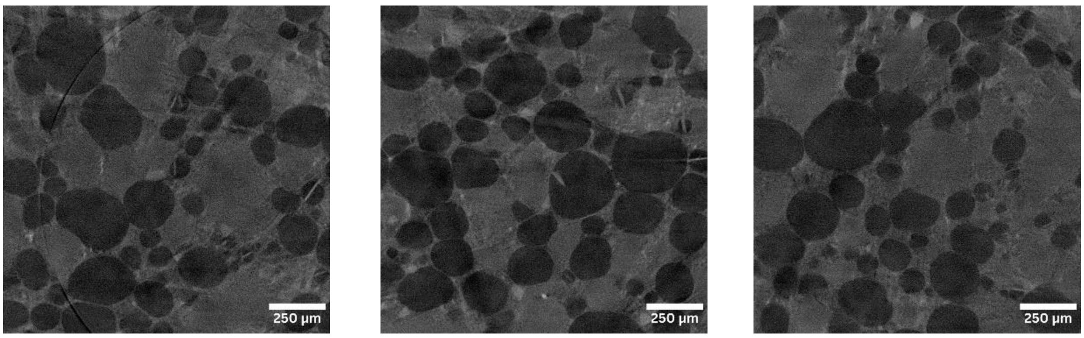

Figure 4.16 SRXTM projection images of LCC 12

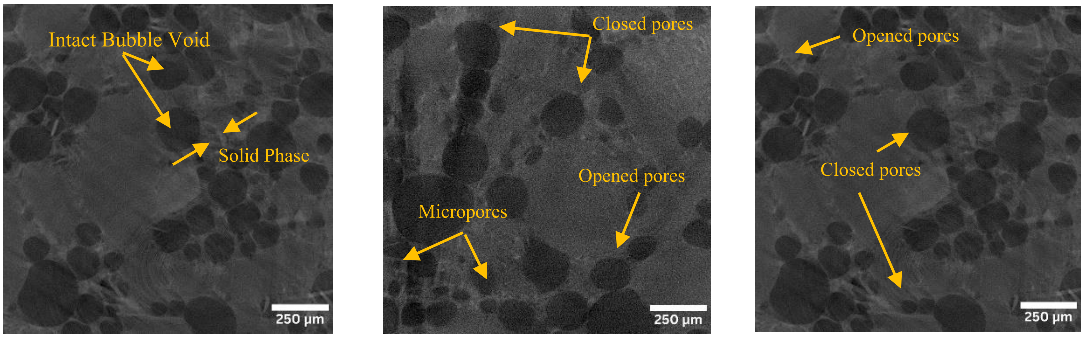

Figure 4.17 SRXTM projection images of LCC 14

The comparison between LCC 12 and LCC 14 reveals that the porosity stability is similar in both, with the primary difference being that LCC 14 has a smaller volume than LCC 12. Furthermore, SRXTM data indicate that LCC 14 has more open pores than LCC 12. This suggests that LCC 12 exhibits better thermal conductivity performance.

4.2.4 Conclusion: LCC microstructure analysis test to the thermal conductivity of physical properties LCC

The microstructure analysis test revealed that the SRXTM analysis provides accurate data about the volume, size, and structure of air voids in LCC samples. This study allows for a more in-depth examination of the microstructural characteristics and their relationship to the physical properties of LCC. Figure 4.18 illustrates the relationship between different types of porosity—total porosity, closed porosity, and opened porosity—and their corresponding thermal conductivity values across three roof types: NC, LCC 12, and LCC 14.

As observed, the increase in total porosity in LCC is associated with a reduction in thermal conductivity. The porosity not only influences the dry density, water absorption capacity, and compressive strength of LCC but also plays a critical role in determining its overall performance, including thermal conductivity (Nambiar & Ramamurthy, 2007). The LCC 12 and LCC 14 performed 0.40 and 0.65 W/mK of thermal conductivity in 39.23% and 29.82% of porosity, respectively. At the same time, it aligns with the observed report by Zhang et al. (2020) on the effects of increasing porosity to reduce the thermal conductivity value. NC also exhibits porosity but extremely high thermal conductivity. The key difference lies in the composition of closed porosity and open porosity.

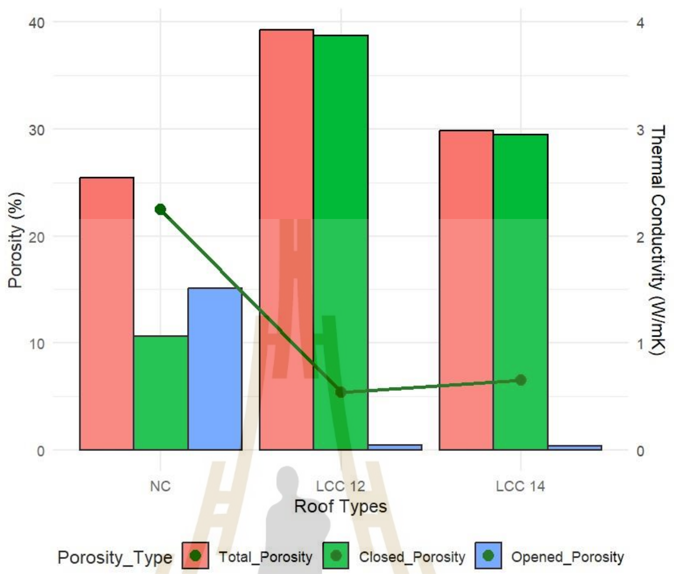

Figure 4.18 Relationship between the porosity and thermal conductivity for NC, LCC 12, and LCC 14

Relationship between the thermal conductivity and the air-void size parameters (D50 and D90) for NC, LCC 12, and LCC 14

Table 4.12 Data set of porosity and thermal conductivity

Type	Total Porosity (%)	Closed Porosity (%)	Opened Porosity (%)	Thermal Conductivity (W/mK)
NC*	25.42	10.62	15.09	2.25
LCC 12	39.23	38.74	0.49	0.40
LCC 14	29.82	29.47	0.35	0.65

*) data of porosity NC is secondary data from Kumar and Bhattacharjee (2003)

As the proportion of closed porosity increases, the thermal conductivity tends to decrease, particularly in the LCC 12 and LCC 14 roof types. This indicates a negative correlation between closed porosity and thermal conductivity, suggesting that closed pores effectively reduce heat transfer, thus lowering thermal conductivity. In contrast, the opened porosity, represented in blue, is relatively low across all roof types and appears to have a less significant impact on thermal conductivity. This may be because open pores are more likely to transfer heat through the material, increasing thermal conductivity if their proportions are higher. However, their levels are low in this dataset, so their influence is minimal.

The NC roof type shows a moderate level of total porosity with a balanced contribution from closed and opened pores, resulting in a thermal conductivity value lower than LCC 12 but higher than LCC 14. This suggests that while total porosity is a factor, the type of porosity—particularly the presence of closed pores—is more crucial in determining the material's thermal insulation properties.

Figure 4.19 shows the relationship between the Thermal Conductivity and the Air-Void Size Parameters (D50 and D90). The plot shows the thermal conductivity (W/mK) as a function of the air-void size parameters, D50 and D90 (in microns, µm), for three roof bases: NC, LCC 12, and LCC 14. D50 represents the median air-void size, while D90 represents the size below 90% of the air-voids are found.

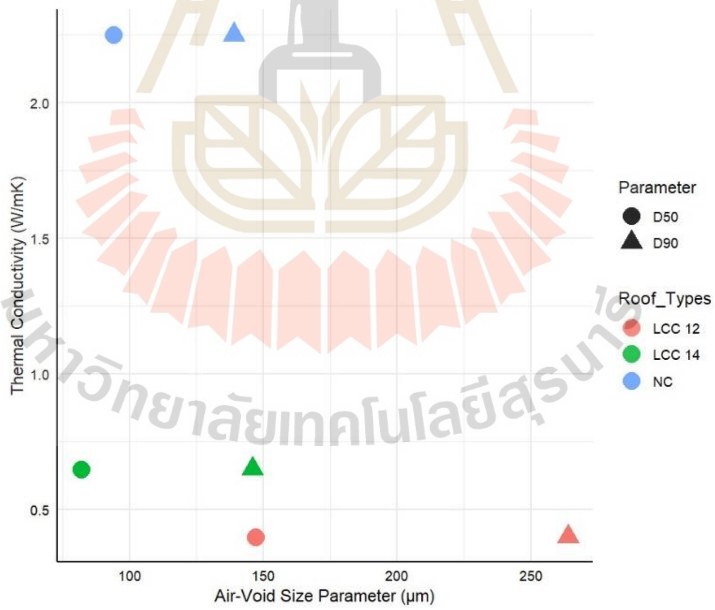

Figure 4.19 Relationship between the air-void size parameters (D50 and D90) and thermal conductivity for NC, LCC 12, and LCC 14

Table 4.13 Data set of air-void size on D50 and D90 for thermal conductivity

Type	D_{50}	D_{90}	Thermal Conductivity (W/mK)
NC*	94	139	2.25
LCC 12	147	264	0.54
LCC 14	82	146	0.65

*) data of porosity NC is secondary data from Kumar and Bhattacharjee (2003)

It is evident from the plot that an increase in D50 and D90 results in a decrease in thermal conductivity. Larger air-void sizes and a broader distribution of voids, particularly at lower densities, contribute to reduced thermal conductivity. This trend aligns with observations Coquard and Baillis (2006) reported for cellular polymeric solids and Nambiar and Ramamurthy (2007) for foam concrete, where larger void sizes correspond to lower thermal conductivity.

Overall, the data underscores the importance of closed porosity in reducing thermal conductivity, emphasizing its role in improving the insulating properties of materials used in roofing applications. By analyzing the microstructure in LCC, the quality of LCC 12, which has a high air void porosity, intact and closed pores, and lighter than LCC 14, is expected to improve the quality performance of green roofs. Section 4.3 reported the evaluation of the thermal transfer performance GR system using LCC 12 and LCC 14 on the open-air experimental.

4.3 Result and Discussion 3: Green Roof Experimental Test

The open-air experimental test of the green roof was conducted. The application of LCC 12 and LCC 14 on green roof samples will be conducted to assess the thermal performance of the green roof system when LCC serves as the roof deck base. Four samples will be utilized in this study: Normal concrete roof (Non GR), green roof conventional using normal concrete (GR-NC), Green roof LCC 12 (GR-LCC 12), and green roof LCC 14 (GR-LCC 14). The following section presents a detailed discussion of the various green roof types.

The open-air experimental study on green roof boxes was conducted at Suranaree University of Technology in February 2024 for 3 days respectively. Figure 4.8 shows Non GR, GR-NC, GR-LCC 12, and GR-LCC 14 roof experimental box. The sensors are installed on each material layer in 4 different types of green roofs, and one sensor outside to measure the outdoor temperature. As shown in Figure 4.20, the research observed gradient temperature across different types of roofs, specifically analyzing temperatures at various times throughout the day: 6:00 AM, 9:00 AM, 12:00 PM, 3:00 PM, and 6:00 PM.

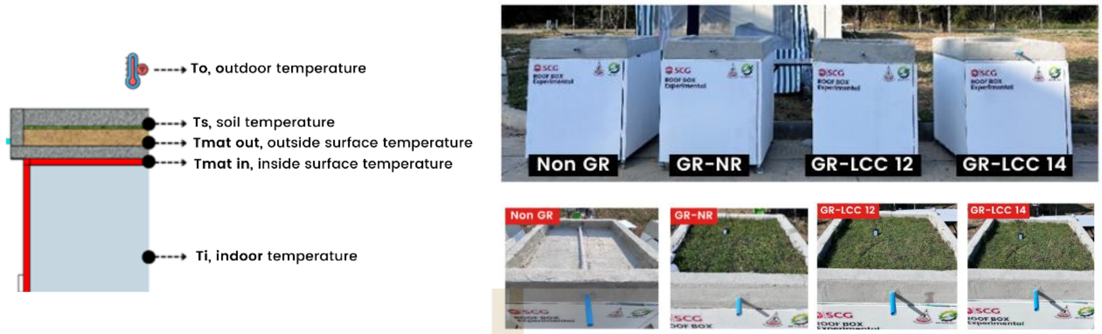

Figure 4.20 Open-air experimental green roofs

4.3.1 Gradient temperature

The results of the average gradient temperature of various roofs over three days are shown in Figure 4.21 and Table 4.14. The gradient temperature data indicates that GR-NC, GR-LCC 12, and GR-LCC 14 significantly reduce the external surface temperature compared to NC.

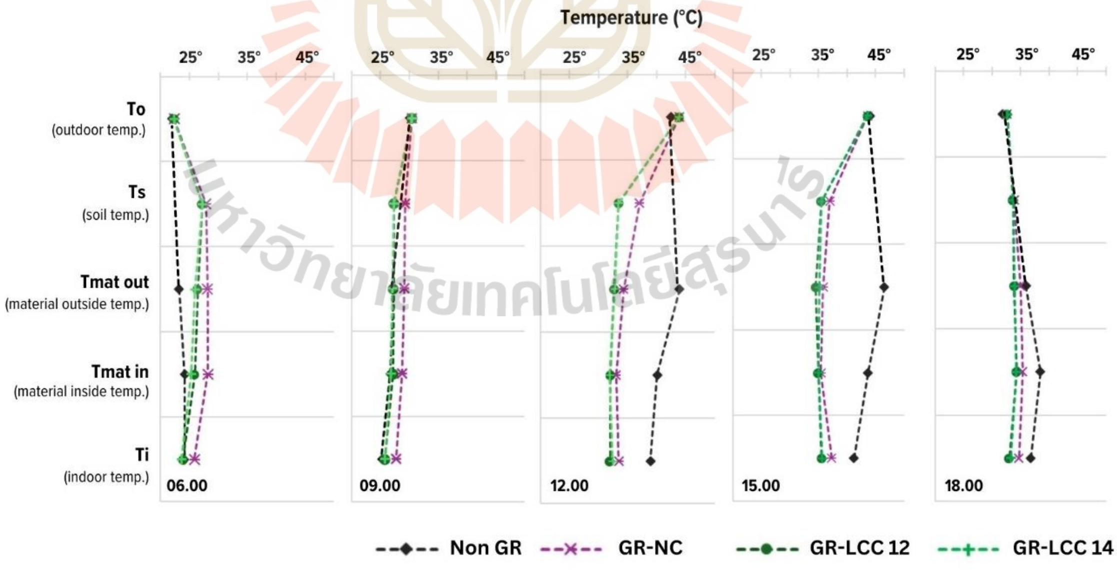

Figure 4.21 Result of gradient temperature on green roofs

Table 4.14 Data of gradient temperature on green roofs

Time	T_o	T_s	$T_{mat\ out}$	$T_{mat\ in}$	T_i	ΔT (T_o-T_i)
Non GR						
06:00	22.35	-	23.30	24.18	24.13	(-1.78)
09:00	30.45	-	27.34	26.66	25.17	5.28
12:00	43.85	-	43.91	40.09	38.91	4.94
15:00	43.63	-	46.56	43.70	41.23	2.40
18:00	32.69	-	36.00	38.52	36.80	(-4.11)
GR-NC						
06:00	22.35	27.87	28.11	28.21	25.90	(-3.55)
09:00	30.45	29.27	29.18	28.82	27.67	2.78
12:00	43.85	37.02	34.29	33.04	35.47	8.38
15:00	43.63	37.02	35.82	35.44	37.32	6.31
18:00	32.69	33.87	35.01	35.39	34.75	(-2.06)
GR-LCC 12						
06:00	22.35	27.22	26.48	25.92	23.90	(-1.55)
09:00	30.45	27.39	27.28	27.21	25.83	4.62
12:00	43.85	33.47	32.70	32.05	32.51	11.34
15:00	43.63	35.53	34.55	34.98	35.57	8.06
18:00	32.69	33.73	33.92	34.32	33.07	(-0.38)
GR-LCC 14						
06:00	22.35	27.23	26.02	25.34	23.60	(-1.25)
09:00	30.45	27.33	27.13	26.81	25.73	4.72
12:00	43.85	33.43	32.85	31.94	32.06	10.99
15:00	43.63	35.53	35.17	35.07	35.73	7.90
18:00	32.69	33.75	33.94	34.19	33.31	(-0.62)

As described in Figure 4.19, the green roof layers prevent heat from solar energy, so the indoor temperature does not accelerate sharply. The gradient temperature in the layers from the outdoors to the indoor temperature captured in the 3-hour interval to illustrate the different thermal behavior

In the morning, before being exposed to direct sunlight, the temperature of the green roof system is higher than that of the base model. As for the green roof model the surface temperature is still higher than the indoor air temperature, so heat is released from the roof into the room. After receiving direct solar heat until noon, the air temperature follows higher, which shows that the heat received indoors is more through the roof. As observed in Table 4.14, the room temperature for all green roof types (GR-NC, GR-LCC 12, and GR-LCC 14) is lower than that of the non-green roof. This reduction in room temperature is attributed to the green roof layer, which diminishes solar heat absorption and subsequently lowers the temperature on the material's outer surface ($T_{mat\ out}$). A reduced $T_{mat\ out}$ is correlated with a decrease in thermal distribution to the inner surface of the material ($T_{mat\ in}$), ultimately contributing to the reduction in indoor temperature (T_i).

The indoor temperature reduction is most notable at noon by 12:00 PM, where the GR-LCC 12 and GR-LCC 14 show a higher temperature difference (**Δ**T) at 11.34 °C and 10.99 °C respectively, compared to the **Δ**T GR-NC at 4.94 °C. During 15:00 PM, GR-LCC 12 and GR-LCC 14 maintained a significant temperature gap, and GR LCC 12 resulted in slightly better performance at 8.06 °C and 7.90 °C, respectively. Furthermore, when the temperature decreases in the evening, at 18:00 PM, the **Δ**T in GR-LCC 12 shows the closest temperature to the $T_{o,}$ which is only 0.38 °C different, indicating a relatively stable temperature condition. However, as the day progresses, the effectiveness of green roofs becomes more apparent. The GR-LCC 12, in particular, exhibits the smallest temperature gap, suggesting that it retains less heat and cools down faster than other roof types.

The gradient temperature comparison underscores the advantages of green roofs, especially those with LCC 12 and LCC 14, in mitigating heat transfer and improving energy efficiency in buildings. The application of GR-LCC 12 demonstrates positive outcomes compared to various studies on green roofs in tropical regions. GR-LCC 12 achieves an efficiency of up to 11.34 °C. Ahmed and Rumana (2009) conducted a study on GR-NC in Malaysia; the efficiency ranged at 3 °C. Abdul Munir and Afifuddin (2020) revealed that the GR-LCC 14 study in Indonesia reported an efficiency of approximately 10.2 °C. The present study's findings provide insights into the basic layers of the sub-base material, substrate, and vegetation. The performance of GR in this study could be further enhanced with the incorporation of additional supporting layers in future research.

4.3.2 Outdoor and Indoor Temperature

The temperature profiles of outdoor and indoor temperatures are shown in the detailed analysis of temperature fluctuations throughout three days, as shown in Figure 4.22.

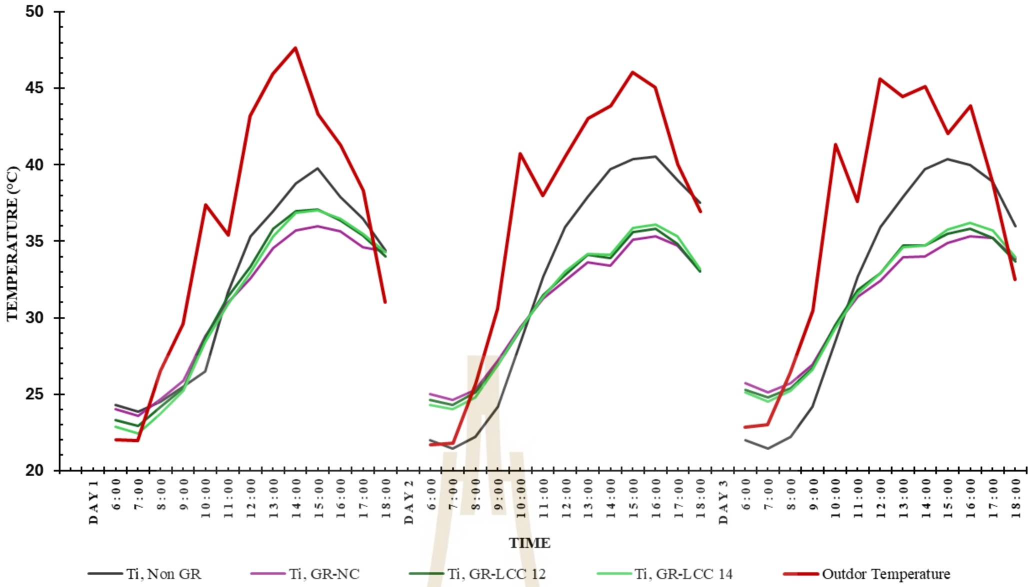

Figure 4.22 Result of outdoor and indoor temperature on green roof

Table 4.15 Data of outdoor and indoor temperature on green roofs

Data Temp.	To	Ti, Non GR	Ti, GR-NC	Ti, GR-LCC 12	Ti, GR-LCC 14
Day 1					
06:00	22.02	24.80	24.00	22.80	22.89
09:00	29.56	26.00	25.90	24.91	25.20
12:00	43.21	37.30	34.60	32.83	32.99
15:00	43.33	40.80	38.99	36.60	37.01
18.00	31.04	35.40	34.32	33.95	34.30
Day 2					
06:00	21.66	23.00	25.00	24.10	23.80
09:00	30.56	25.20	27.20	26.40	26.40
12:00	40.55	36.94	34.40	32.29	32.50
15:00	46.08	41.40	38.08	35.10	35.40
18.00	36.94	38.53	35.09	32.50	32.70
Day 3					
06:00	22.85	22.00	25.70	24.80	24.60
09:00	30.47	24.20	26.90	26.19	26.10
12:00	45.63	35.94	34.40	32.40	32.40
15:00	42.04	40.40	37.90	35.00	35.29
18.00	32.48	36.00	34.85	33.20	33.44

Table 4.15 revealed that outdoor temperatures fluctuate significantly, with daily minimum temperatures averaging around 22.16°C and maximum temperatures reaching up to 46.45°C. In contrast, the temperature profiles for different

roof types exhibit varying degrees of thermal insulation performance. Non GR showed the highest indoor temperature peaks, while the GR-LCC 12 had the lowest indoor temperature.

The highest recorded indoor temperatures for Non-GR, GR-NC, GR-LCC 12, and GR-LCC 14 were 41.40 °C, 38.99 °C, 36.60 °C, and 37.01 °C, respectively, while the lowest temperatures were 22.02 °C, 22.00 °C, 22.80 °C, and 22.89 °C. Green roofs (GR) offer significant insulation benefits, leading to a notable reduction in indoor temperatures. The application of LCC as a base material further higher the thermal resistance (R_t *value*) due to LCC's lower thermal conductivity (*k value*). The higher the R_t value, the lower the thermal transfer value (*Q-value*).

In green roof research conducted in tropical countries, the use of green roofs (GR) has been shown to effectively maintain indoor temperatures between 23°C and 38°C, a significant improvement compared to the higher indoor temperatures of 24°C to 51°C observed in buildings without green roofs (Pratama et al., 2023). The variation in temperature outcomes is influenced by multiple factors, including weather conditions, materials used, the composition of green roof layers, humidity, and more. This study demonstrates that GR-LCC 12 and GR-LCC 14 exhibit superior performance compared to conventional green roof systems. Notably, GR-LCC 12 performs slightly better than GR-LCC 14, and its lower density offers an additional advantage by reducing the structural load on the building.

The open-air experiment demonstrates that green roofs, especially those incorporating LCC, effectively lower indoor temperatures, highlighting their potential for energy savings in buildings. The implementation of such roofing systems is essential for sustainable building practices, as they not only promote energy efficiency but also help mitigate urban heat island effects. The recorded temperature data will be utilized to estimate the roof's thermal transfer, as detailed in the subsequent section.

4.3.3 Thermal transfer value of green roofs

The evaluation of the thermal transfer of green roofs by calculating the roof thermal transfer of four different roof types by using the real data of surface material. The calculation of thermal transfer divided to be two parts, 1) the thermal transfer of roof base concrete and LCC material and 2) the thermal transfer of green roof system.

These calculations are intended to assess the effectiveness of the roof base as thermal insulation, identifying areas that require enhancement. The calculations will be elaborated upon in the following section:

1) Thermal transfer of roof base concrete and LCC material

The single material thermal transfer calculate based on the conduction formula outlined in Section 2.4.2, utilizes the following formula:

$$Q = \frac{\mathrm{dT}}{R_t} = \frac{\mathrm{T_1} - \mathrm{T_2}}{(\mathrm{L}/k\mathrm{A})_1}$$

Figure 4.23 shows the different sections of roof samples and the point of the data temperature of surface material taken.

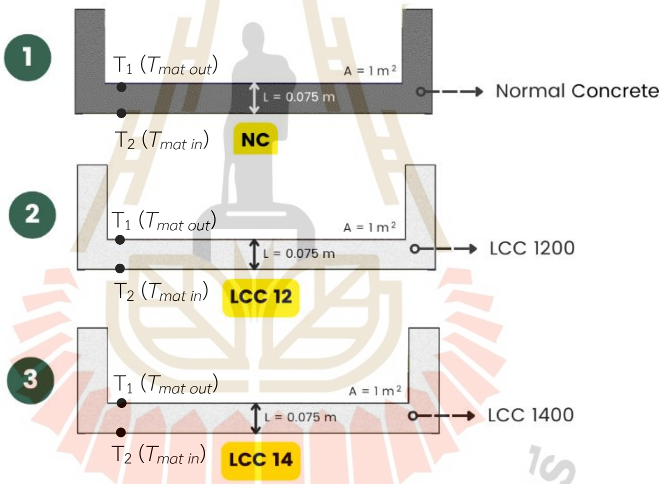

Figure 4.23 Roof base material sections

Additionally, Table 4.18 records the temperature outside surface material temperature (T_1), and inside surface material temperature (T_2) surface on three roof base material.

Table 4.16 Average temperature different (dT) of the three roof base material

Roof Types	Time	T_1 (°C)	T_2 (°C)	dT (°C)	Average dT (°C)
NC	06:00	23.20	24.18	-0.98	1.17
	09:00	27.34	26.66	0.69	
	12:00	43.91	38.09	5.83	
	15:00	46.56	43.70	2.86	
	18.00	36.00	38.52	-2.52	

Table 4.16 Average temperature different (dT) of the three roof base material (Continued)

Roof Types	Time	T_1 (°C)	T_2 (°C)	dT (°C)	Average dT (°C)
LCC 12	06:00	27.48	25.92	1.56	0.71
	09:00	28.28	27.21	1.07	
	12:00	34.00	33.05	0.95	
	15:00	36.05	35.48	0.57	
	18.00	33.73	34.32	-0.59	
LCC 14	06:00	26.52	25.34	1.18	0.75
	09:00	27.63	26.81	0.83	
	12:00	33.85	32.94	0.91	
	15:00	36.17	35.57	0.59	
	18.00	34.44	34.19	0.25	

The surface temperature comparison (dT) highlights that LCC 12 effectively creates a lower different temperature. This narrower temperature differential contributes to minimizing thermal transfer into buildings.

Once the value of dT is determined, the subsequent step involves calculating the thermal resistance (R-value). Table 4.17 provides the thermal conductivity (k-value) of the roof base material, which will be utilized in the R-value calculation.

Table 4.17 Thermal conductivity (k-value) of different roof base material

No	Material	Thermal Conductivity, k (W/mK)	Source
1	NC	2.25	Concrete Technology (Adam, Brooks)
2	LCC 12	0.40	Lab Test (Section 4.1.4)
3	LCC 14	0.65	Lab Test (Section 4.1.4)

The R-value in one unit area of single layer of roof base concrete, LCC 12., and LCC 14 should be determined. Table 4.18 shows the calculation of R-value of roof base material

Table 4.18 Thermal resistance (R-value) of different roof base material

No	Roof	Thickness	Thermal Conductivity	Thermal Resistance
		L, (m)	k, (W/mK)	R, (m^2K/W)
1	NC (Normal Concrete)	0.075	2.25	0.03
2	LCC 12 (LCC 1200 kg/m^3)	0.075	0.40	0.19
3	LCC 14 (LCC 1200 kg/m^3)	0.075	0.65	0.11

The R-value calculation represents the heat resistance of transfer rate through the roof material, shows significant differences between the NC, LC 12, and LCC 14. A higher R_t-value indicates better insulating properties. The NC has the lowest R-value of 0.03 m²K/W, reflecting its poor thermal insulation capability. In contrast, the LCC 12 and LCC 14, significantly improve insulation with higher R_t-value of 0.19 and 0.11 m²K/W, respectively.

With the values of d and R established, the thermal transfer (Q-value) can now be calculated. Table 4.19 presents the results of the Q-value calculations for various roof base materials.

Table 4.19 Q-value of different roof base material

Roof base material	Temperature different dT, (°C)	Total Thermal Resistance R_t, (m²K/W)	Thermal Transfer Value Q, (W/m²)
NC	1.17	0.03	39.00
LCC 12	0.71	0.19	3.74
LCC 14	0.75	0.11	6.82

The Q-value for LCC 12 is the lowest, demonstrating its high effectiveness in minimizing thermal transfer. Incorporating LCC 12 into the green roof system is anticipated to further enhance its thermal insulation properties. The following section presents calculations of the Q-value for the roof base material with the implementation of the green roof system.

2) Thermal transfer of green roof system

The application of multilayer techniques with green roofs can effectively reduce thermal transfer values. Consequently, the calculation of thermal transfer values for roof base materials incorporating a green roof system is taken into consideration. The multilayered material thermal transfer calculate based on the conduction formula outlined in Section 2.4.2, utilizes the following formula:

$$Q = \frac{\mathrm{dT}}{R_t} = \frac{\mathrm{T_1 - T_2}}{(\mathrm{L}/k\mathrm{A})_1 + (\mathrm{L}/k\mathrm{A})_2 + (\mathrm{L}/k\mathrm{A})_3}$$

Figure 4.24 shows the different sections of roof samples and the point of the data temperature of surface material taken.

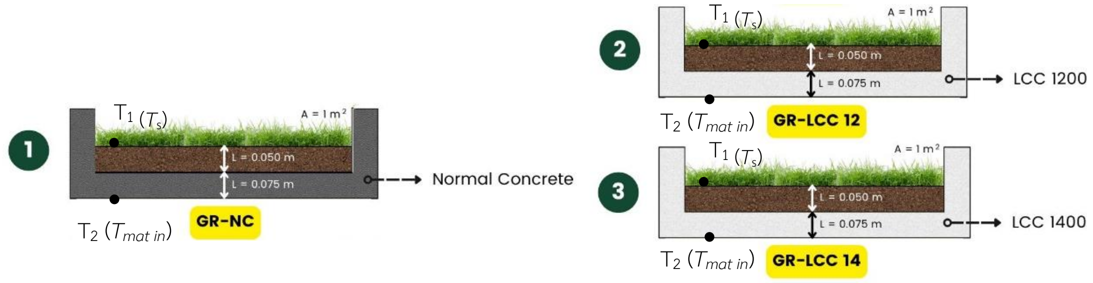

Figure 4.24 Green roof sections

Additionally, Table 4.20 records the temperature outside surface material temperature (T_1), and inside surface material temperature (T_2) surface on three various green roof with different roof base material.

Table 4.20 Average thermal different equivalent (TD_{eq}) of different roof material

Roof Types	Time	T_1 (°C)	T_2 (°C)	dT (°C)	Average dT (°C)
GR-NC	06:00	27.87	28.21	-0.35	0.63
	09:00	29.27	28.82	0.45	
	12:00	37.02	33.04	3.99	
	15:00	37.02	35.44	1.58	
	18.00	32.87	35.39	-2.52	
GR-LCC 12	06:00	27.22	25.92	1.30	0.27
	09:00	27.39	27.21	0.17	
	12:00	33.47	33.05	0.42	
	15:00	35.53	35.48	0.05	
	18.00	33.73	34.32	-0.59	
GR-LCC 14	06:00	27.23	25.34	1.89	0.49
	09:00	27.33	26.81	0.53	
	12:00	33.43	32.94	0.50	
	15:00	35.53	35.57	-0.04	
	18.00	33.75	34.19	-0.44	

The surface temperature comparison (dT) highlights that GR effectively creates a lower gap beetwen the surface. Furthermore, the GR-LCC 12 and GR-LCC 14 configurations exhibit consistently low and balanced dT values. This narrower temperature differential contributes to minimizing thermal transfer into buildings.

Based on the data presented, it is evident that different roof types exhibit varying degrees of thermal performance throughout the day, as measured by the difference in temperature dT between T_1 and T_2.

GR-NC shows the highest average dT of 0.63°C, indicating less effective thermal regulation compared to the other roof types. This suggests that the GR-NC roof allows more heat to pass through, making it less efficient in thermal insulation.

In contrast, GR-LCC 12 exhibits the lowest average dT of 0.27°C, signifying superior thermal insulation properties. The small temperature differential indicates that GR-LCC 12 is more effective at minimizing heat transfer, which is beneficial for maintaining stable indoor temperatures.

GR-LCC 14 has an intermediate performance with an average dT of 0.49°C, which is better than GR-NC but not as effective as GR-LCC 12. This indicates that while GR-LCC 14 provides some thermal insulation benefits, it does not perform as well as GR-LCC 12.

Once the value of dT is determined, the subsequent step involves calculating the total of thermal resistance value (R_t-value). Table 4.21 provides the thermal conductivity (k-value) of the roof base material, which will be utilized in the R-value calculation.

Table 4.21 Thermal conductivity of green roof material

No	Material	Thermal Conductivity	Source
1	NC	2.25	Concrete Technology (Adam, Brooks)
2	LCC 12	0.40	Lab Test (Section 4.1.4)
3	LCC 14	0.65	Lab Test (Section 4.1.4)
4	Substrate	0.44	Tetiana Nikiforova, et all (2013)
5	Vegetation	1.10	Jan Kleissl, et all (2010)

The R-value in one unit area of single layer of roof base concrete, LCC 12., and LCC 14 should be determined. Table 4.22 shows the calculation of R_t-value of roof base material.

Table 4.22 Thermal resistance (R_t-value) of green roof with different roof base

No	Roof	Material Configuration	Thickness	Thermal Conductivity	Thermal Resistance	Total Thermal Resistance
			L, (m)	k, (W/mK)	R, (m²K/W)	R_t, (m²K/W)
1	GR-NC	Normal Concrete	0.075	2.25	0.03	0.16
		Substrate	0.050	0.44	0.11	
		Vegetation	0.025	1.1	0.02	
2	GR-LCC 12	LCC 1200 kg/m^3	0.075	0.40	0.14	0.39
		Substrate	0.050	0.44	0.11	
		Vegetation	0.025	1.1	0.02	
3	GR-LCC 14	LCC 1400 kg/m^3	0.075	0.65	0.12	0.25
		Substrate	0.050	0.44	0.11	
		Vegetation	0.025	1.1	0.02	

The R_t-value calculation represents the heat resistance of transfer rate through the roof material, shows significant differences between the roof types, and a higher Rt-value indicates better insulating properties.

The NC without green roof which has R_t-value of 0.03 m²K/W, indicates receive an improvement when install the green roof system, the GR-NC, which incorporates a substrate and vegetation layer, significantly improves insulation with higher R_t-value of 0.16 m²K/W.

The GR-LCC roofs demonstrate better thermal performance. The GR-LCC 12 roof achieves the highest R_t-value of 0.39 m²K/W, the excellent insulating properties of the LCC 12 material combined with the substrate and vegetation layers. The GR-LCC 14 roof also performs well with a R_t-value of 0.25 m²K/W, slightly higher than GR-LCC 12 but still markedly better than GR-NC.

Overall, the data imply that using LCC materials, particularly GR-LCC 12, in green roof systems can significantly enhance thermal insulation, reducing the rate of heat transfer and contributing to energy efficiency. This analysis highlights the potential for optimizing building materials to improve thermal performance in green roof applications. The average calculation of dT from the open-air experimental data shows that the GR-LCC 12 provides the smallest dT. The calculation of thermal transfer from the roof will incorporate the data for thermal resistance (R_t) and the temperature difference (dT), as presented in Table 4.23

Table 4.23 Thermal transfer value of different green roof type material

Roof types	Temperature different dT, (°C)	Total Thermal Resistance R_t, (m²K/W)	Thermal Transfer Value Q, (W/m²)
GR-NC	0.63	0.16	3.94
GR-LCC 12	0.27	0.39	0.69
GR-LCC 14	0.49	0.25	1.96

The thermal transfer value (Q-value) were evaluated, the GR-NC roof demonstrates a lowest with an Q-value of 3.94 W/m². Moreover, GR-LCC 12 and GR-LCC 14 materials exhibit even better thermal performance at 0.69 W/m² and 1.96 W/m^2, respectively. GR-LCC 12, with a Q-value of 1.0 W/m², has the lowest value among the compared materials, underscoring its superior effectiveness in minimizing heat transfer.

4.3.4 Conclusion: Correlation of LCC in improving green roof performance

The open-air experiment on various roof types revealed that GR-LCC, both LCC 12 and LCC 14, have an excellent thermal transfer efficiency of green roof performance at 0.69 W/m^2 and 1.96 W/m^2, respectively. Thermal conductivity (k-value) is directly related to thermal resistance (R-value), as higher the k-value in a material results in greater the R-value, thereby decreasing thermal transfer (Q-value) (Humaish, 2020). Figure 4.25 shows the relation of k-value of NC, LCC 12, and LCC 14 with and without green roofs effects on the theirs R-value. Based on the data presented, it observe the impact of green roof systems on the thermal resistance of different roof types.

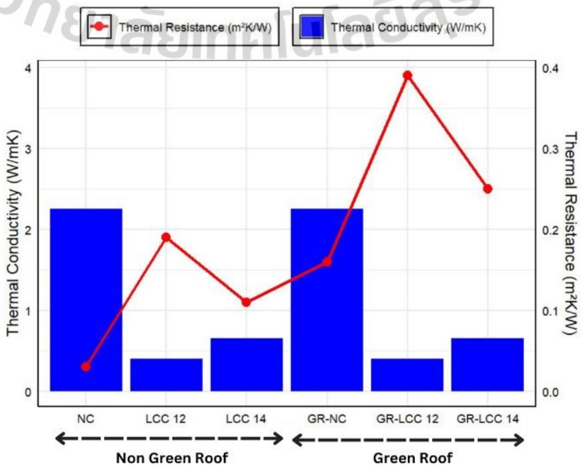

Figure 4.25 Relationship between the thermal conductivity and thermal resistance on single roof base material

Table 4.24 Data set of thermal resistance and thermal conductivity

Roof types	Thermal conductivity (k) (W/mK)	Thermal resistance (R_t) (m^2K/W)
Without green roof system		
NC	2.25	0.03
LCC 12	0.40	0.19
LCC 14	0.65	0.11
Installed green roof system		
GR-NC	2.25	0.16
GR-LCC 12	0.40	0.39
GR-LCC 14	0.65	0.25

The LCC 12 roof type demonstrates exceptional thermal performance, especially when combined with a green roof system. Without the green roof system, LCC 12 already shows a notable R-value of 0.19 m^2K/W, significantly higher than the NC roof type's 0.03 m^2K/W. This indicates that LCC 12 has better inherent insulation properties. When a green roof system is installed, the R-value of LCC 12 further increases to 0.39 m^2K/W, the highest among the studied configurations. This substantial enhancement suggests that the combination of LCC 12 material properties with a green roof system offers superior insulation capabilities, effectively minimizing heat thermal transfer. Figure 4.26 show the relation of thermal resistance (R_t-value) to the thermal transfer value (Q-value) of various roof-type parameters.

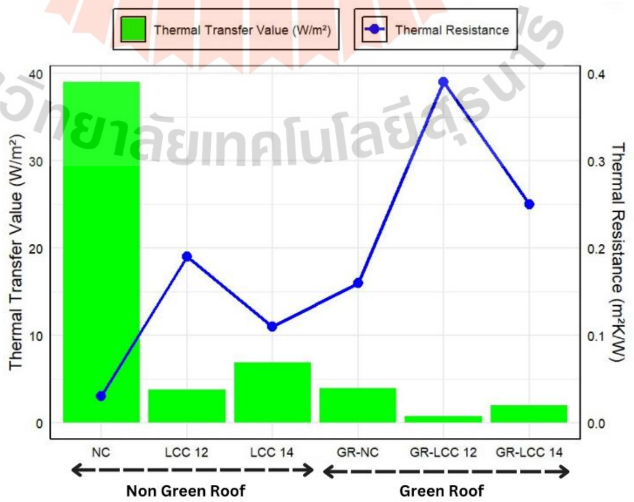

Figure 4.26 Relationship between the thermal resistance and thermal transfer value on single roof base material

Table 4.25 Data set of thermal transmittance and thermal transfer value

Roof types	Thermal resistance R_t, (m^2K/W)	Thermal transfer value Q, (W/m^2)
Without green roof system		
NC	0.03	39.00
LCC 12	0.19	3.74
LCC 14	0.11	6.82
Installed green roof system		
GR-NC	0.16	3.94
GR-LCC 12	0.39	0.69
GR-LCC 14	0.25	1.96

As observed, comparison of Q-value and R_t-value across different roof types. This figure was created using R programming language with the ggplot2 package. The data presented highlight the impact of different roof types on R-value and Q-value. The table compares various configurations both with and without green roof systems, showing a clear differentiation in thermal performance.

Without a green roof system, the roof type NC exhibits the lowest thermal resistance (0.03 m^2K/W) and the highest thermal transfer value (39.00 W/m^2), indicating poor insulation properties. In contrast, the LCC 12 roof type, even without the green roof system, demonstrates significantly better performance, with a thermal resistance of 0.19 m^2K/W and a much lower thermal transfer value of 3.74 W/m^2. This suggests that the LCC 12 material inherently possesses better insulating properties compared to the NC and LCC 14 types, which have thermal transfer values of 39.00 W/m^2 and 6.82 W/m^2, respectively.

The effectiveness of incorporating a green roof system is also evident from the table. For instance, the GR-LCC 12 configuration, which combines the LCC 12 roof base material with a green roof, exhibits an enhanced thermal resistance of 0.39 m^2K/W and an impressively low thermal transfer value of 0.69 W/m^2. This improvement indicates that the addition of a green roof not only enhances the inherent insulating properties of LCC 12 but also significantly minimizes the amount of thermal energy transferred through the roof. The GR-LCC 12 configuration, with the lowest Q-value among all the configurations, showcases the optimal balance between material properties and the additional thermal barrier provided by the green roof.

The data underscores the importance of material selection and the application of green roof systems in achieving energy-efficient building designs. The superior performance of the LCC 12 roof type, particularly when combined with a green roof system, highlights its potential as a preferred choice for minimizing heat transfer and enhancing overall thermal efficiency.

This reduction in heat transfer is reflected in the substantially lower Q-values for these roof types, highlighting the improved thermal performance of roofs that utilize LCC materials. The study of green roof calculation roof thermal transfer value by Y. He et al. (2021) in tropical countries shows a higher trend result ranges from 2.3 – 2.5 W/m^2. The current study demonstrates a lower trend of thermal transfer enhancement when green roofs are utilized in conjunction with LCC materials..

Thermal conductivity is a critical factor in minimizing thermal transfer within building materials. In comparison with findings from other studies, LCC 12 has demonstrated a lower thermal conductivity value of 0.48 W/mK, whereas LCC 14 exhibits a higher value of 0.74 W/mK. Higher thermal conductivity values correlate with increased Q-values when these materials are integrated into green roof systems. Table 4.22 provides a comparative analysis of the utilization of LCC 12 and LCC 14 materials between the current study and the reference study.

Table 4.26 Comparison of thermal transfer value on current study and reference study

Green roof types	Current study		Reference study*	
	Thermal Conductivity of LCC, W/mK	Thermal Transfer Value, W/m^2	Thermal Conductivity of LCC, W/mK	Thermal Transfer Value, W/m^2
GR-LCC 12	0.40	0.69	0.48	0.75
GR-LCC 14	0.65	1.96	0.74	2.04

Remark: the reference study gathered from Department of Alternative Energy Development and Efficiency (2009); Ganesan et al. (2015)

CHAPTER V
CASE PROJECT USING GREEN ROOF LCC

5.1 References Project 1: GR-LCC in Nakhon Ratchasima

The initial project for using Green Roof LCC was initiated in 2020 at the Nakhon Ratchasima commercial building project in Thailand. The idea of using LCC on a green roof is based on the reason that there is no green area in the building. However, the existing structure already exists and cannot accommodate the excessive weight if a conventional green roof is applied. Our research team initiated using LCC in green roofs because green roof properties are superior, have lighter weight than roof slabs, have good thermal performance, and have low water absorption.

Figure 5.1 GR-LCC Project in Nakhon Ratchasima

Figure 5.1 depicts the LCC green roof construction process. LCC roof deck casting is carried out before installing the green roof system. The application of LCC green roofs is more accessible because they do not use a supporting layer like conventional green roofs, and it is because LCC green roofs have good properties, indicating that green roofs can eliminate supporting layers on green roofs. That way, quality improvements and cost savings can be achieved.

This LCC green roof has been functioning well for approximately four years with minimal maintenance. Even though testing the thermal data collection process in the room under the LCC green roof, the temperature drop was 2 - 5 C cooler than the average room temperature. This proves that LCC green roofs can be used and applied to a broader market.

Figure 5.2 Layer system of GR-LCC 12

5.2 References Project 2: GR-LCC in Saraburi

Based on the research carried out in this thesis, it is concluded that GR-LCC 12 has the potential to be applied as a green roof. Research supported by SCG Roofing, Co. Ltd. is the forerunner of the development of GR-LCC, and it is hoped that it can be further developed and applied to many buildings in Thailand in the future.

Figure 5.3 GR-LCC 12 construction process

The GR-LCC pilot project was built as a real-time data collection center at the SCG Roofing Co. Ltd research site. The project also installed a conventional green roof, adopted from German technology. Figure 5.3 depicts the construction of a green roof pilot project in Saraburi.

Overall, GR-LCC has a more even and green vegetation growth rate. This is thought to be because GR-LCC stores sufficient soil moisture levels. Void water on the surface of the roof deck is indicated to help as a water storage reserve, which is used to maintain soil moisture.

Figure 5.4 Growth grass comparison between GR-NC and GR-LCC

Research in this thesis concludes that the thermal performance results show that GR-LCC performs better than conventional GR. Research on other aspects is recommended to be carried out to assess the performance of green roofs from different elements.

CHAPTER VI
CONCLUSIONS AND SUGGESTIONS

6.1 Summary and Conclusions

This study investigated the feasibility and performance of Lightweight Cellular Concrete (LCC) as a material for green roofs, focusing on its physical properties, microstructural stability, and thermal performance on green roofs. The findings from various experiments and analyses can be summarised as follows:

1) Physical properties: LCC exhibited superior thermal insulation properties. Considering these characteristics, LCC 12 and LCC 14 are anticipated for use in green roof construction due to their thermal conductivity values, which are three times lower than those of standard concrete, measuring 0.40 W/mK and 0.65 W/mK, respectively. The thermal conductivity values of LCC 12 and LCC 14 align with the thermal conductivity guideline specified in ACI 523.3R-93. These values also demonstrate a more favorable thermal conductivity trend compared to those reported in other studies and are significantly lower than those of conventional concrete.

2) Microstructural analysis: The superior thermal conductivity observed in LCC 12 compared to LCC 14 is influenced not only by its physical properties but also by its microstructural characteristics. Utilizing the SRXTM technique to analyze the porosity of air voids provides a detailed insight into the microstructure of these voids. Based on this study, the excellent thermal conductivity performance of LCC can be attributed to several factors:

    4) Adherence to the target dry density, ensuring it does not exceed ±50 kg/m³.
    5) The air void volume aligns with the mix design and is predominantly composed of closed pores.
    6) A lower thermal conductivity value is associated with larger air void sizes; LCC 12, which exhibits favorable thermal conductivity, features

air void sizes ranging from D50 to D90, approximately 147-264 μm in diameter.

7) The stability of the air void shape is crucial, requiring that the voids be completely round, closed, and uniformly distributed. An optimal arrangement of air voids is highly effective in enhancing the thermal conductivity value.

3) Thermal performance: LCC 12 is recommended for use in green roof construction due to its numerous advantages. In addition to its lightweight nature and low thermal conductivity compared to LCC 14, LCC 12 possesses adequate strength to function as a sub-base material on roof decks. Its minimal water absorption also suggests its potential for use in developing water storage systems within green roofs. When applied in green roof building applications, LCC 12 can cool indoor spaces by up to 11.34 °C below the outside air temperature at midday. This significant cooling effect is facilitated by its exceptionally low thermal transfer rate of 0.69 W/m², which is markedly lower than that of GR-LCC 14 and GR-NC.

Adopting LCC in green roof systems offers numerous environmental and economic advantages. Environmentally, LCC contributes to sustainability by reducing carbon emissions through improved energy efficiency and providing better insulation. Economically, the benefits include prolonged roof lifespan, reduced maintenance costs, and potential increases in property value due to the aesthetic and environmental advantages of green roofs. Additionally, using locally sourced materials for LCC production can further reduce the carbon footprint associated with transportation and manufacturing processes.

6.2 Recommendations for future work

Based on the findings, the following detailed suggestions are proposed for future research and practical applications:

1) Material Optimization: Future research should focus on optimizing the mix design of LCC to enhance its mechanical and thermal properties further. This includes experimenting with different foam agents, additives, and reinforcement materials to improve the overall performance of LCC in

green roof systems. Investigating using recycled materials in LCC production could also enhance its environmental benefits.

2) Long-term Performance Studies: Conducting long-term performance studies of LCC-based green roofs under various environmental conditions is essential to gather valuable data on their durability, maintenance requirements, and overall sustainability.
3) Integration with Renewable Energy: Exploring the integration of LCC-based green roofs with renewable energy systems, such as solar panels, could enhance buildings' energy efficiency and sustainability. Combining green roofs and solar energy can provide synergistic benefits, including improved thermal performance and increased energy production. Research into the optimal design and installation techniques for such integrated systems will be essential.
4) Cost-Benefit Analysis: Detailed cost-benefit analyses should quantify the economic advantages of using LCC in green roofs. These analyses should consider factors such as initial installation costs, long-term maintenance savings, energy efficiency improvements, and potential increases in property value. Clear economic justifications will help convince stakeholders and decision-makers of the benefits of adopting LCC-based green roofs.

Addressing these suggestions will fully realize LCC's potential as a key material in sustainable building practices, contributing to developing greener and more energy-efficient urban environments. The continued exploration and optimization of LCC will pave the way for its broader adoption, enhancing the sustainability and resilience of our built environment.

REFERENCES

Abass, F., Ismail, L. H., Wahab, I. A., & Elgadi, A. A. (2020). A Review of Green Roof: Definition, History, Evolution and Functions. *IOP Conference Series: Materials Science and Engineering*, *713*(1). https://doi.org/10.1088/1757-899X/713/1/012048

Ahmad, S., Umar, A., & Masood, A. (2017). Properties of Normal Concrete, Self-compacting Concrete and Glass Fibre-reinforced Self-compacting Concrete: An Experimental Study. *Procedia Engineering*, *173*, 807–813. https://doi.org/10.1016/j.proeng.2016.12.106

Ahmed, M. H. Bin, & Rumana, R. (2009). Thermal Performance of Rooftop Greenery system in Tropical Climate of Malaysia. *Journal of Architecture and Built Environmental*, *37*(1), 41–50.

American Concrete Institute. (1975). ACI 523.3R-14 : Guide for Cellular Concretes Above 50 Pcf, and for Aggregate Concretes Above 50 Pcf With Compressive Strengths Less Than 2500 Psi. *J Am Concr Inst*, *72*(2), 50–66. https://doi.org/10.14359/11115

American Concrete Institute. (2014). *ACI 523.3R-14: Guide for Cellular Concretes above 50 lb/ft3 (800 kg/m3).*

Ashraf, M. H., Fawkia, F. E.-H., & Hafez, R. D. A. (2015). Physical and Mechanical Properties of Concrete Incorporating Industrial and Agricultural Textile Wastes. *International Journal of Research in Engineering and Technology*, *04*(07), 166–176. https://doi.org/10.15623/ijret.2015.0407026

ASTM C869. (1999). *Standard Specification for Foaming Agents Used in Making Preformed Foam for*. *91*(Reapproved), 1–2.

Batool, F., & Bindiganavile, V. (2017). Air-void size distribution of cement based foam and its effect on thermal conductivity. *Construction and Building Materials*, *149*, 17–28. https://doi.org/10.1016/j.conbuildmat.2017.05.114

Beckstead, D., Wechsuwanarux, N., Chaianant, S., Limvichai, T., Saengpetch, D., PopunNgarm, S., Sombatsatapornkul, T., Onglaor, A., Phantophas, J., Pongthananikorn, S., & Soonyakanit, V. (2023). *Thailand's Energy transition*. https://www.chandlermhm.com/content/files/pdf/publications/Thailand Energy Transition Report - Outlook for 2024.pdf

Brunke, O. (2010). Comparison between X-ray-tube based and synchrotron based µCT. *10th European Conference on Non-Destructive Testing*.

Cascone, S. (2019). Green roof design: State of the art on technology and materials.

Sustainability (Switzerland), *11*(11). https://doi.org/10.3390/su11113020

Castleton, H. F., Stovin, V., Beck, S. B. M., & Davison, J. B. (2010). Green roofs; Building energy savings and the potential for retrofit. In *Energy and Buildings* (Vol. 42, Issue 10, pp. 1582–1591). Elsevier Ltd. https://doi.org/10.1016/j.enbuild.2010.05.004

Cebeci, Ö. Z. (1981). Pore structure of air-entrained hardened cement paste. *Cement and Concrete Research*, *11*(2), 257–265. https://doi.org/10.1016/0008-8846(81)90067-3

Chapirom, A., Sinsiri, T., Jaturapitakkul, C., & Chindaprasirt, P. (2019). Effect of speed rotation on the compressive strength of horizontal mixer for cellular lightweight concrete. *Suranaree Journal of Science and Technology*, *26*(2), 113–120. https://doi.org/10.13140/RG.2.2.25198.97609

Chica, L., & Alzate, A. (2019). Cellular concrete review: New trends for application in construction. *Construction and Building Materials*, *200*, 637–647. https://doi.org/10.1016/j.conbuildmat.2018.12.136

Chung, S. Y., Lehmann, C., Elrahman, M. A., & Stephan, D. (2017). Pore characteristics and their effects on the material properties of foamed concrete evaluated using micro-CT images and numerical approaches. *Applied Sciences (Switzerland)*, *7*(6). https://doi.org/10.3390/app7060550

Chung, S. Y., Sikora, P., Rucinska, T., Stephan, D., & Abd Elrahman, M. (2020). Comparison of the pore size distributions of concretes with different air-entraining admixture dosages using 2D and 3D imaging approaches. *Materials Characterization*, *162*(February), 110182. https://doi.org/10.1016/j.matchar.2020.110182

crisis24. (2024). Thailand: Heatwave forecast to persist across much of the country through at least April 30. *Https://Crisis24.Garda.Com/*, 1. https://crisis24.garda.com/alerts/2024/04/thailand-heatwave-forecast-to-persist-across-much-of-the-country-through-at-least-april-30

D'Orazio, M., DI PERNA, C., & DI GIUSEPPE, E. (2012). Green Roofs as passive cooling strategies under Temperate Climates. *Zemch 2012*, *January*, 561–570.

Department of Alternative Energy Development and Efficiency. (2009). *Ministry of Energy's notification on Criteria and Calculation Methods for Building Design of Various Systems, Overall Energy Consumption of Buildings and Use of Renewable Energy of Various Building Systems B.E. 2552*. http://www2.dede.go.th/%0Ahttp://www2.dede.go.th/km_berc/downloads/menu4/กฎหมายพลังงาน/english/08 ประกาศ ก พลังงาน เรื่อง หลักเกณฑ์และวิธีการคำนวณในการออกแ.pdf

Douglass, M., Kuhnel, D., Magnani, M., Hittner, L., Chodoronek, M., & Porter, S. (2017). Community outreach, digital heritage and private collections: a case study from the North American Great Plains. *World Archaeology*, *49*(5), 623–638. https://doi.org/10.1080/00438243.2017.1309299

Fernandez-Cañero, R., Emilsson, T., Fernandez-Barba, C., & Herrera Machuca, M. Á. (2013). Green roof systems: A study of public attitudes and preferences in southern Spain. *Journal of Environmental Management*, *128*, 106–115. https://doi.org/10.1016/j.jenvman.2013.04.052

Gallucci, E., Scrivener, K., Groso, A., Stampanoni, M., & Margaritondo, G. (2007). 3D experimental investigation of the microstructure of cement pastes using synchrotron X-ray microtomography (μCT). *Cement and Concrete Research*, *37*(3), 360–368. https://doi.org/10.1016/j.cemconres.2006.10.012

Ganesan, S., Othuman Mydin, M. A., Mohd Yunos, M. Y., & Mohd Nawi, M. N. (2015). Thermal Properties of Foamed Concrete with Various Densities and Additives at Ambient Temperature. *Applied Mechanics and Materials*, *747*(March), 230–233. https://doi.org/10.4028/www.scientific.net/amm.747.230

He, B. J. (2022). Green building: A comprehensive solution to urban heat. *Energy and Buildings*, *271*, 112306. https://doi.org/10.1016/j.enbuild.2022.112306

He, Y., Lin, E. S., Tan, C. L., Yu, Z., Tan, P. Y., & Wong, N. H. (2021). Model development of Roof Thermal Transfer Value (RTTV) for green roof in tropical area: A case study in Singapore. *Building and Environment*, *203*(February), 108101. https://doi.org/10.1016/j.buildenv.2021.108101

Hilal, A. A., Thom, N. H., & Dawson, A. R. (2015). On entrained pore size distribution of foamed concrete. *Construction and Building Materials*, *75*, 227–233. https://doi.org/10.1016/j.conbuildmat.2014.09.117

Humaish, H. H. (2020). Effect of porosity on thermal conductivity of porous materials. *IOP Conference Series: Materials Science and Engineering*, *737*(1). https://doi.org/10.1088/1757-899X/737/1/012185

IPCC. (2014). Part A: Global and Sectoral Aspects. (Contribution of Working Group II to the Fifth Assessment Report of the Intergovernmental Panel on Climate Change). In *Climate Change 2014: Impacts, Adaptation, and Vulnerability.* https://www.ipcc.ch/pdf/assessment-report/ar5/wg2/WGIIAR5-FrontMatterA_FINAL.pdf

Jones, M. R., & McCarthy, A. (2005). Preliminary views on the potential of foamed concrete as a structural material. *Magazine of Concrete Research*, *57*(1), 21–31. https://doi.org/10.1680/macr.2005.57.1.21

Jones, M. Roderick, Zheng, L., & Ozlutas, K. (2016). Stability and instability of foamed concrete. *Magazine of Concrete Research*, *68*(11), 542–549.

https://doi.org/10.1680/macr.15.00097

Kim, K. Y., Yun, T. S., Choo, J., Kang, D. H., & Shin, H. S. (2012). Determination of air-void parameters of hardened cement-based materials using X-ray computed tomography. *Construction and Building Materials*, *37*, 93–101. https://doi.org/10.1016/j.conbuildmat.2012.07.012

Kim, K. Y., Yun, T. S., & Park, K. P. (2013). Evaluation of pore structures and cracking in cement paste exposed to elevated temperatures by X-ray computed tomography. *Cement and Concrete Research*, *50*, 34–40. https://doi.org/10.1016/j.cemconres.2013.03.020

Koenders, S. J. M., Loonen, R. C. G. M., & Hensen, J. L. M. (2018). Investigating the potential of a closed-loop dynamic insulation system for opaque building elements. *Energy and Buildings*, *173*, 409–427. https://doi.org/10.1016/j.enbuild.2018.05.051

Kumar, R., & Bhattacharjee, B. (2003). Porosity, pore size distribution and in situ strength of concrete. *Cement and Concrete Research*, *33*(1), 155–164. https://doi.org/10.1016/S0008-8846(02)00942-0

Kurpinska, M., & Ferenc, T. (2017). Effect of porosity on physical properties of lightweight cement composite with foamed glass aggregate. *ITM Web of Conferences*, *15*, 06005. https://doi.org/10.1051/itmconf/20171506005

Landscape Development and Landscaping Research Society. (2018). *FFL: Guidelines for the Planning, Construction and Maintenance of Green Roofs*.

Lee, D. T. C., & Lee, T. S. (2016). The effect of aggregate condition during mixing on the mechanical properties of oil palm shell (OPS) concrete. *MATEC Web of Conferences*, *87*, 0–4. https://doi.org/10.1051/matecconf/20178701019

Lei, Y., Duan, Y., He, D., Zhang, X., Chen, L., Li, Y., Gao, Y. G., Tian, G., & Zheng, J. (2018). Effects of urban greenspace patterns on particulate matter pollution in metropolitan Zhengzhou in Henan, China. *Atmosphere*, *9*(5), 1–15. https://doi.org/10.3390/ATMOS9050199

Leo A, L. (1960). Cellular Concrete. *Industrial and Engineering Chemistry*, *52*(11), 28A-32A. https://doi.org/10.1021/i650611a718

Lu, H., Alymov, E., Shah, S., & Peterson, K. (2017). Measurement of air void system in lightweight concrete by X-ray computed tomography. *Construction and Building Materials*, *152*, 467–483. https://doi.org/10.1016/j.conbuildmat.2017.06.180

Ma, H. (2014). Mercury intrusion porosimetry in concrete technology: Tips in measurement, pore structure parameter acquisition and application. *Journal of Porous Materials*, *21*(2), 207–215. https://doi.org/10.1007/s10934-013-9765-4

Mohd Sari, K. A., & Mohammed Sani, A. R. (2017). Applications of Foamed Lightweight Concrete. *MATEC Web of Conferences*, *97*, 1–5. https://doi.org/10.1051/matecconf/20179701097

Munir, A., Muslimsyah, Afifuddin, M., & Mahlil. (2020a). Application of precast foamed concrete panels for the structural deck of green roof system. *IOP Conference Series: Materials Science and Engineering*, *796*(1). https://doi.org/10.1088/1757-899X/796/1/012039

Munir, A., Muslimsyah, Afifuddin, M., & Mahlil. (2020b). Application of precast foamed concrete panels for the structural deck of green roof system. *IOP Conference Series: Materials Science and Engineering*, *796*(1). https://doi.org/10.1088/1757-899X/796/1/012039

Munir, Abdul, Abdullah, Afifuddin, M., & Muslimsyah. (2020). Thermal Performance of Precast Foam Concrete Integrated with Green Roofs System. *Advances in Engineering Research*, *192*(November).

Munir, Abdul, & Afifuddin, M. (2020). *Thermal Performance of Precast Foam Concrete Integrated with Green Roofs System*.

Nambiar, E. K. K., & Ramamurthy, K. (2007). Air-void characterisation of foam concrete. *Cement and Concrete Research*, *37*(2), 221–230. https://doi.org/10.1016/j.cemconres.2006.10.009

Narayanan, N., & Ramamurthy, K. (2000). Structure and properties of aerated concrete: A review. *Cement and Concrete Composites*, *22*(5), 321–329. https://doi.org/10.1016/S0958-9465(00)00016-0

Niachou, A., Papakonstantinou, K., Santamouris, M., Tsangrassoulis, A., & Mihalakakou, G. (2001). Analysis of the green roof thermal properties and investigation of its energy performance. *Energy and Buildings*, *33*(7), 719–729. https://doi.org/10.1016/S0378-7788(01)00062-7

Niu, H., Clark, C., Zhou, J., & Adriaens, P. (2010). Scaling of economic benefits from green roof implementation in Washington, DC. *Environmental Science and Technology*, *44*(11), 4302–4308. https://doi.org/10.1021/es902456x

Nurain Izzati, M. Y., Suraya Hani, A., Shahiron, S., Sallehuddin Shah, A., Mohamad Hairi, O., Zalipah, J., Noor Azlina, A. H., Mohamad Nor Akasyah, W. A., & Nurul Amirah, K. (2019). Strength and water absorption properties of lightweight concrete brick. *IOP Conference Series: Materials Science and Engineering*, *513*(1). https://doi.org/10.1088/1757-899X/513/1/012005

Othman, R., Jaya, R. P., Muthusamy, K., Sulaiman, M., Duraisamy, Y., Abdullah, M. M. A. B., Przybył, A., Sochacki, W., Skrzypczak, T., Vizureanu, P., & Sandu, A. V. (2021).

Relation between density and compressive strength of foamed concrete. *Materials*, *14*(11). https://doi.org/10.3390/ma14112967

Othman, R., Muthusamy, K., Sulaiman, M. A., Duraisamy, Y., Jaya, R. P., Wei, C. B., Al Bakri Abdullah, M. M., Mangi, S. A., Nabiałek, M., & Sliwa, A. (2022). Compressive strength and durability of foamed concrete incorporating Processed Spent Bleaching Earth. *Archives of Civil Engineering*, *68*(2), 627–643. https://doi.org/10.24425/ace.2022.140663

Pan, Y. H., Wong, K. W., & Hui, C. M. (2007). Cost Comparison between the Construction of Lightweight and Conventional Partitions in Chongqing, China. *International Journal of Construction Management*, *7*(1), 57–70. https://doi.org/10.1080/15623599.2007.10773095

Pianella, A., Aye, L., Chen, Z., & Williams, N. S. G. (2017). Substrate depth, vegetation and irrigation affect green roof thermal performance in a mediterranean type climate. *Sustainability (Switzerland)*, *9*(8). https://doi.org/10.3390/su9081451

Pratama, H. C., Sinsiri, T., & Chapirom, A. (2022). *Development of a Mixture of Lightweight Cell Crete for Green Roof Construction in Thailand*. 1–5.

Pratama, H. C., Sinsiri, T., & Chapirom, A. (2023). Green Roof Development in ASEAN Countries: The Challenges and Perspectives. *Sustainability (Switzerland)*, *15*(9). https://doi.org/10.3390/su15097714

Raj, A., Sathyan, D., & Mini, K. M. (2019). Physical and functional characteristics of foam concrete: A review. *Construction and Building Materials*, *221*, 787–799. https://doi.org/10.1016/j.conbuildmat.2019.06.052

Ramamurthy, K., Kunhanandan Nambiar, E. K., & Indu Siva Ranjani, G. (2009). A classification of studies on properties of foam concrete. *Cement and Concrete Composites*, *31*(6), 388–396. https://doi.org/10.1016/j.cemconcomp.2009.04.006

Santamouris, M. (2014). Cooling the cities - A review of reflective and green roof mitigation technologies to fight heat island and improve comfort in urban environments. *Solar Energy*, *103*, 682–703. https://doi.org/10.1016/j.solener.2012.07.003

Shandilya, A., Hauer, M., & Streicher, W. (2020). Optimization of thermal behavior and energy efficiency of a residential house using energy retrofitting in different climates. *Civil Engineering and Architecture*, *8*(3), 335–349. https://doi.org/10.13189/cea.2020.080318

Sudprasert, S., & Klinsmith, S. (2014). Assessment of Overall Thermal Transfer Value (OTTV) in Buildings with Inclined Glass Wall. *Journal of Architectural/Planning Research and Studies (JARS)*, *11*(1), 109–118.

https://doi.org/10.56261/jars.v11i1.23882

Talebi, A., Bagg, S., Sleep, B. E., & O'Carroll, D. M. (2019). Water retention performance of green roof technology: A comparison of canadian climates. *Ecological Engineering*, *126*(May 2018), 1–15. https://doi.org/10.1016/j.ecoleng.2018.10.006

Thai Industrial Standard. (2018). TIS 2601-2556: Industrial Product Standards of Lightweight Cellular Concrete Blocks. In *Announcement of the Ministry of Industry* (Vol. 1, Issue 1). http://dx.doi.org/10.1016/j.cirp.2016.06.001%0Ahttp://dx.doi.org/10.1016/j.powtec.2016.12.055%0Ahttps://doi.org/10.1016/j.ijfatigue.2019.02.006%0Ahttps://doi.org/10.1016/j.matlet.2019.04.024%0Ahttps://doi.org/10.1016/j.matlet.2019.127252%0Ahttp://dx.doi.o

Vijayaraghavan, K. (2016). Green roofs: A critical review on the role of components, benefits, limitations and trends. In *Renewable and Sustainable Energy Reviews* (Vol. 57, pp. 740–752). Elsevier Ltd. https://doi.org/10.1016/j.rser.2015.12.119

Wan Ibrahim, M. H., Jamaludin, N., Irwan, J. M., Ramadhansyah, P. J., & Suraya Hani, A. (2014). Compressive and flexural strength of foamed concrete containing polyolefin fibers. *Advanced Materials Research*, *911*(March), 489–493. https://doi.org/10.4028/www.scientific.net/AMR.911.489

Wen, B., Musa, S. N., Onn, C. C., Ramesh, S., Liang, L., Wang, W., & Ma, K. (2020). The role and contribution of green buildings on sustainable development goals. *Building and Environment*, *185*(August). https://doi.org/10.1016/j.buildenv.2020.107091

Wildenschild, D., Rivers, M. L., Porter, M. L., Iltis, G. C., Armstrong, R. T., & Davit, Y. (2015). Using synchrotron-based X-ray microtomography and functional contrast agents in environmental applications. *Soil- Water- Root Processes: Advances in Tomography and Imaging*, 1–22. https://doi.org/10.2136/sssaspecpub61.c1

Yang, W., Pang, M., Xie, H., Xiao, M., Pei, J., & Zhuo, L. (2023). Investigation and Analysis of the Influence of Environmental Factors on the Temperature Distribution of Thin-Walled Concrete. *Applied Sciences (Switzerland)*, *13*(22). https://doi.org/10.3390/app132212157

Yu, W., Liang, X., Ni, F. M. W., Oyeyi, A. G., & Tighe, S. (2020). Characteristics of lightweight cellular concrete and effects on mechanical properties. *Materials*, *13*(12), 1–17. https://doi.org/10.3390/ma13122678

Zahari, N. M., Rahman, I. A., Mujahid, A., Zaidi, A., Ismail, H., & Rahman, A. (2009). Foamed Concrete: Potential Application in Thermal Insulation. *Malaysian Technical Universities on Engineering and Techonology*, 47–52.

Zhang, X., Yang, Q., Shi, Y., Zheng, G., Li, Q., Chen, H., & Cheng, X. (2020). Effects of different control methods on the mechanical and thermal properties of ultra-light foamed concrete. *Construction and Building Materials*, *262*, 120082. https://doi.org/10.1016/j.conbuildmat.2020.120082

APPENDIX A

PROPERTIES LCC TEST RESULT

อว 7432(5)/Rep.0958

17 ตุลาคม 2566

ห้องปฏิบัติการทดสอบวัสดุก่อสร้าง
ศูนย์เครื่องมือวิทยาศาสตร์และเทคโนโลยี
มหาวิทยาลัยเทคโนโลยีสุรนารี

รายงานผลทดสอบกำลังต้านแรงอัดของแท่ง คอนกรีตมวลเบาทรงลูกบาศก์

เรียน: มหาวิทยาลัยเทคโนโลยีสุรนารี ที่อยู่: 111 ถนนมหาวิทยาลัย ตำบลสุรนารี อำเภอเมือง จังหวัดนครราชสีมา 30000	คำขอรับบริการเลขที่ : CMT 0556/66 รายงานผลทดสอบเลขที่: RepCMT660556(6)
เจ้าของตัวอย่าง: นาย ลิขิต ชีวาสวัสดิ์ โครงการ: คอนกรีตมวลเบา ชื่อตัวอย่าง: แท่งคอนกรีตมวลเบารูปทรงลูกบาศก์ ขนาด 150 x 150 x 150 มม. วิธีการทดสอบ: มอก.2601-2556	หมายเลขตัวอย่าง : CMT S0556/66-6 ชั้นคุณภาพ : - วันรับตัวอย่าง : 6 กันยายน 2566 วันทดสอบ : 6 กันยายน 2566

No.	Mix/ Product Code	Casting Date	Age (days)	Density (kg/m^3)	Cure Type	Condition Before Test	Condition Fracture Type	Compressive Strength Load (kN)	Compressive Strength Stress (MPa)	Compressive Strength Uncert. (MPa)	Remark
1	-	03/09/66	3	1,010.7	F	1,8	S	39.8	1.74	-	(1000)
2	-	03/09/66	3	998.5	F	1,8	S	38.3	1.63	-	
3	-	03/09/66	3	978.5	F	1,8	S	34.5	1.48	-	

Cure Type : L = Laboratory ; F = Field

Condition of Specimens

Before Test : 1= สภาพปรกติ ,2 =แตกบิ่น ,3 =มีวัสดุแปลกปลอม ,4 =มีรูพรุน
5=ผิวหน้าเอียงไม่ได้ฉาก ,6=ผิวข้างไม่เรียบ ,7=ผิวชื้น ,8=ผิวแห้ง

Fracture Type : according to BS EN 12390-3-2002

Satisfy : S

Unsatisfy : 1 , 2 , 3 , 4 , 5 , 6 , 7 , 8 , 9

The reported expanded uncertainty measurement calculation procedure providing a level of approximately 95 %

ลงชื่อ .... ผู้รับรอง
(ผู้ช่วยศาสตราจารย์ ดร.ทิพย์วรรณ ฟังสุวรรณรักษ์)
รองผู้อำนวยการศูนย์เครื่องมือวิทยาศาสตร์และเทคโนโลยี
ปฏิบัติการแทนผู้อำนวยการศูนย์เครื่องมือวิทยาศาสตร์และเทคโนโลยี
17 ตุลาคม 2566

- รายงานนี้รับรองเฉพาะตัวอย่างที่ทำการทดสอบตามที่ระบุไว้ข้างต้นเท่านั้น
- ห้ามตัด ห้ามถ่ายสำเนาใบรายงานผลการทดสอบแต่เพียงบางส่วนยกเว้นทำทั้งฉบับ โดยไม่ได้รับความยินยอมเป็นลายลักษณ์อักษรจากห้องปฏิบัติการ

End of Report

อว 7432(5)/Rep.0953

17 ตุลาคม 2566

ห้องปฏิบัติการทดสอบวัสดุก่อสร้าง
ศูนย์เครื่องมือวิทยาศาสตร์และเทคโนโลยี
มหาวิทยาลัยเทคโนโลยีสุรนารี

รายงานผลทดสอบกำลังต้านแรงอัดของแท่งคอนกรีตมวลเบาทรงลูกบาศก์

เรียน: มหาวิทยาลัยเทคโนโลยีสุรนารี ที่อยู่: 111 ถนนมหาวิทยาลัย ตำบลสุรนารี อำเภอเมือง จังหวัดนครราชสีมา 30000	คำขอรับบริการเลขที่ : CMT 0556/66 รายงานผลทดสอบเลขที่: RepCMT660556(1)
เจ้าของตัวอย่าง: นาย ลิขิต ชีวาสวัสดิ์ โครงการ: คอนกรีตมวลเบา ชื่อตัวอย่าง: แท่งคอนกรีตมวลเบารูปทรงลูกบาศก์ ขนาด 150 x 150 x 150 มม. วิธีการทดสอบ: มอก.2601-2556	หมายเลขตัวอย่าง : CMT S0556/66-1 ชั้นคุณภาพ : - วันรับตัวอย่าง : 1 กันยายน 2566 วันทดสอบ : 1 กันยายน 2566

No.	Mix/ Product Code	Casting Date	Age (days)	Density (kg/m^3)	Cure Type	Condition		Compressive Strength			Remark
						Before Test	Fracture Type	Load (kN)	Stress (MPa)	Uncert. (MPa)	
1	-	29/08/66	3	1,221.9	F	1,8	S	67.9	2.87	-	(1200)
2	-	29/08/66	3	1,235.7	F	1,8	S	58.1	2.54	-	
3	-	29/08/66	3	1,239.6	F	1,8	S	59.6	2.51	-	

Cure Type : L = Laboratory ; F = Field
Condition of Specimens
Before Test : 1= สภาพปรกติ ,2 =แตกบิ่น ,3 =มีวัสดุแปลกปลอม ,4 =มีรูพรุน
5=ผิวหน้าเอียงไม่ได้ฉาก ,6=ผิวข้างไม่เรียบ ,7=ผิวชื้น ,8=ผิวแห้ง
Fracture Type : according to BS EN 12390-3-2002
Satisfy : S
Unsatisfy : 1 , 2 , 3 , 4 , 5 , 6 , 7 , 8 , 9

The reported expanded uncertainty measurement calculation procedure providing a level of approximately 95 %

ลงชื่อ .... ผู้รับรอง
(ผู้ช่วยศาสตราจารย์ ดร.ทิพย์วรรณ ฟังสุวรรณรักษ์)
รองผู้อำนวยการศูนย์เครื่องมือวิทยาศาสตร์และเทคโนโลยี
ปฏิบัติการแทนผู้อำนวยการศูนย์เครื่องมือวิทยาศาสตร์และเทคโนโลยี
17 ตุลาคม 2566

- รายงานนี้รับรองเฉพาะตัวอย่างที่ทำการทดสอบตามที่ระบุไว้ข้างต้นเท่านั้น
- ห้ามตัด ห้ามถ่ายสำเนาใบรายงานผลการทดสอบแต่เพียงบางส่วนยกเว้นทำทั้งฉบับ โดยไม่ได้รับความยินยอมเป็นลายลักษณ์อักษรจากห้องปฏิบัติการ

End of Report

อว 7432(5)/Rep.0954

17 ตุลาคม 2566

ห้องปฏิบัติการทดสอบวัสดุก่อสร้าง
ศูนย์เครื่องมือวิทยาศาสตร์และเทคโนโลยี
มหาวิทยาลัยเทคโนโลยีสุรนารี

รายงานผลทดสอบกำลังต้านแรงอัดของแท่ง คอนกรีตมวลเบาทรงลูกบาศก์

เรียน: มหาวิทยาลัยเทคโนโลยีสุรนารี ที่อยู่: 111 ถนนมหาวิทยาลัย ตำบลสุรนารี อำเภอเมือง จังหวัดนครราชสีมา 30000	คำขอรับบริการเลขที่ : CMT 0556/66 รายงานผลทดสอบเลขที่: RepCMT660556(2)
เจ้าของตัวอย่าง: นาย ลิขิต ชีวาสวัสดิ์ โครงการ: คอนกรีตมวลเบา ชื่อตัวอย่าง: แท่งคอนกรีตมวลเบารูปทรงลูกบาศก์ ขนาด 150 x 150 x 150 มม. วิธีการทดสอบ: มอก.2601-2556	หมายเลขตัวอย่าง : CMT S0556/66-2 ชั้นคุณภาพ : - วันรับตัวอย่าง : 1 กันยายน 2566 วันทดสอบ : 1 กันยายน 2566

No.	Mix/ Product Code	Casting Date	Age (days)	Density (kg/m^3)	Cure Type	Condition Before Test	Condition Fracture Type	Compressive Strength Load (kN)	Compressive Strength Stress (MPa)	Compressive Strength Uncert. (MPa)	Remark
1	-	30/08/66	2	1,403.2	F	1,8	S	80.6	3.48	-	(1400)
2	-	30/08/66	2	1,452.6	F	1,8	S	107.3	4.67	-	
3	-	30/08/66	2	1,426.0	F	1,8	S	91.4	3.92	-	

Cure Type : L = Laboratory ; F = Field

Condition of Specimens

Before Test : 1= สภาพปรกติ ,2 =แตกบิ่น ,3 =มีวัสดุแปลกปลอม ,4 =มีรูพรุน
5=ผิวหน้าเอียงไม่ได้ฉาก ,6=ผิวข้างไม่เรียบ ,7=ผิวชื้น ,8=ผิวแห้ง

Fracture Type : according to BS EN 12390-3-2002

Satisfy : S

Unsatisfy : 1 , 2 , 3 , 4 , 5 , 6 , 7 , 8 , 9

The reported expanded uncertainty measurement calculation procedure providing a level of approximately 95 %

ลงชื่อ .... ผู้รับรอง
(ผู้ช่วยศาสตราจารย์ ดร.ทิพย์วรรณ ฟังสุวรรณรักษ์)
รองผู้อำนวยการศูนย์เครื่องมือวิทยาศาสตร์และเทคโนโลยี
ปฏิบัติการแทนผู้อำนวยการศูนย์เครื่องมือวิทยาศาสตร์และเทคโนโลยี
17 ตุลาคม 2566

- รายงานนี้รับรองเฉพาะตัวอย่างที่ทำการทดสอบตามที่ระบุไว้ข้างต้นเท่านั้น
- ห้ามตัด ห้ามถ่ายสำเนาใบรายงานผลการทดสอบแต่เพียงบางส่วนยกเว้นทำทั้งฉบับ โดยไม่ได้รับความยินยอมเป็นลายลักษณ์อักษรจากห้องปฏิบัติการ

End of Report

อว 7432(5)/Rep.0955

17 ตุลาคม 2566

ห้องปฏิบัติการทดสอบวัสดุก่อสร้าง
ศูนย์เครื่องมือวิทยาศาสตร์และเทคโนโลยี
มหาวิทยาลัยเทคโนโลยีสุรนารี

รายงานผลทดสอบกำลังต้านแรงอัดของแท่ง คอนกรีตมวลเบาทรงลูกบาศก์

เรียน: มหาวิทยาลัยเทคโนโลยีสุรนารี ที่อยู่: 111 ถนนมหาวิทยาลัย ตำบลสุรนารี อำเภอเมือง จังหวัดนครราชสีมา 30000	คำขอรับบริการเลขที่ : CMT 0556/66 รายงานผลทดสอบเลขที่: RepCMT660556(3)
เจ้าของตัวอย่าง: นาย ลิขิต ชีวาสวัสดิ์ โครงการ: คอนกรีตมวลเบา ชื่อตัวอย่าง: แท่งคอนกรีตมวลเบารูปทรงลูกบาศก์ ขนาด 150 x 150 x 150 มม. วิธีการทดสอบ: มอก.2601-2556	หมายเลขตัวอย่าง : CMT S0556/66-3 ชั้นคุณภาพ : - วันรับตัวอย่าง : 4 กันยายน 2566 วันทดสอบ : 4 กันยายน 2566

No.	Mix/ Product Code	Casting Date	Age (days)	Density (kg/m^3)	Cure Type	Condition		Compressive Strength			Remark
						Before Test	Fracture Type	Load (kN)	Stress (MPa)	Uncert. (MPa)	
1	-	01/09/66	3	1,596.9	F	1,8	S	189.8	8.22	-	(1600)
2	-	01/09/66	3	1,587.4	F	1,8	S	183.9	7.89	-	
3	-	01/09/66	3	1,602.4	F	1,8	S	188.0	8.07	-	

Cure Type : L = Laboratory ; F = Field

Condition of Specimens

Before Test : 1= สภาพปรกติ ,2 =แตกบิ่น ,3 =มีวัสดุแปลกปลอม ,4 =มีรูพรุน
5=ผิวหน้าเอียงไม่ได้ฉาก ,6=ผิวข้างไม่เรียบ ,7=ผิวชื้น ,8=ผิวแห้ง

Fracture Type : according to BS EN 12390-3-2002

Satisfy : S

Unsatisfy : 1 , 2 , 3 , 4 , 5 , 6 , 7 , 8 , 9

The reported expanded uncertainty measurement calculation procedure providing a level of approximately 95 %

ลงชื่อ .... ผู้รับรอง
(ผู้ช่วยศาสตราจารย์ ดร.ทิพย์วรรณ ฟังสุวรรณรักษ์)
รองผู้อำนวยการศูนย์เครื่องมือวิทยาศาสตร์และเทคโนโลยี
ปฏิบัติการแทนผู้อำนวยการศูนย์เครื่องมือวิทยาศาสตร์และเทคโนโลยี
17 ตุลาคม 2566

- รายงานนี้รับรองเฉพาะตัวอย่างที่ทำการทดสอบตามที่ระบุไว้ข้างต้นเท่านั้น
- ห้ามตัด ห้ามถ่ายสำเนาใบรายงานผลการทดสอบแต่เพียงบางส่วนยกเว้นทำทั้งฉบับ โดยไม่ได้รับความยินยอมเป็นลายลักษณ์อักษรจากห้องปฏิบัติการ

End of Report

อว 7432(5)/Rep.0957

17 ตุลาคม 2566

ห้องปฏิบัติการทดสอบวัสดุก่อสร้าง
ศูนย์เครื่องมือวิทยาศาสตร์และเทคโนโลยี
มหาวิทยาลัยเทคโนโลยีสุรนารี

รายงานผลทดสอบกำลังต้านแรงอัดของแท่ง คอนกรีตมวลเบาทรงลูกบาศก์

เรียน: มหาวิทยาลัยเทคโนโลยีสุรนารี ที่อยู่: 111 ถนนมหาวิทยาลัย ตำบลสุรนารี อำเภอเมือง จังหวัดนครราชสีมา 30000	คำขอรับบริการเลขที่ : CMT 0556/66 รายงานผลทดสอบเลขที่: RepCMT660556(5)
เจ้าของตัวอย่าง: นาย ลิขิต ชีวาสวัสดิ์ โครงการ: คอนกรีตมวลเบา ชื่อตัวอย่าง: แท่งคอนกรีตมวลเบารูปทรงลูกบาศก์ ขนาด 150 x 150 x 150 มม. วิธีการทดสอบ: มอก.2601-2556	หมายเลขตัวอย่าง : CMT S0556/66-5 ชั้นคุณภาพ : - วันรับตัวอย่าง : 5 กันยายน 2566 วันทดสอบ : 5 กันยายน 2566

No.	Mix/ Product Code	Casting Date	Age (days)	Density (kg/m^3)	Cure Type	Condition: Before Test	Condition: Fracture Type	Compressive Strength: Load (kN)	Compressive Strength: Stress (MPa)	Compressive Strength: Uncert. (MPa)	Remark
1	-	02/09/66	3	1,886.8	F	1,8	S	312.6	13.73	-	(1800)
2	-	02/09/66	3	1,897.3	F	1,8	S	342.3	14.49	-	
3	-	02/09/66	3	1,862.6	F	1,8	S	312.2	13.51	-	

Cure Type : L = Laboratory ; F = Field

Condition of Specimens

Before Test : 1= สภาพปรกติ ,2 =แตกบิ่น ,3 =มีวัสดุแปลกปลอม ,4 =มีรูพรุน
5=ผิวหน้าเอียงไม่ได้ฉาก ,6=ผิวข้างไม่เรียบ ,7=ผิวชื้น ,8=ผิวแห้ง

Fracture Type : according to BS EN 12390-3-2002

Satisfy : S

Unsatisfy : 1 , 2 , 3 , 4 , 5 , 6 , 7 , 8 , 9

The reported expanded uncertainty measurement calculation procedure providing a level of approximately 95 %

ลงชื่อ .... ผู้รับรอง
(ผู้ช่วยศาสตราจารย์ ดร.ทิพย์วรรณ ฟังสุวรรณรักษ์)
รองผู้อำนวยการศูนย์เครื่องมือวิทยาศาสตร์และเทคโนโลยี
ปฏิบัติการแทนผู้อำนวยการศูนย์เครื่องมือวิทยาศาสตร์และเทคโนโลยี
17 ตุลาคม 2566

- รายงานนี้รับรองเฉพาะตัวอย่างที่ทำการทดสอบตามที่ระบุไว้ข้างต้นเท่านั้น
- ห้ามตัด ห้ามถ่ายสำเนาใบรายงานผลการทดสอบแต่เพียงบางส่วนยกเว้นทำทั้งฉบับ โดยไม่ได้รับความยินยอมเป็นลายลักษณ์อักษรจากห้องปฏิบัติการ

End of Report

อว 7432(5)/Rep.0961

17 ตุลาคม 2566

ห้องปฏิบัติการทดสอบวัสดุก่อสร้าง
ศูนย์เครื่องมือวิทยาศาสตร์และเทคโนโลยี
มหาวิทยาลัยเทคโนโลยีสุรนารี

รายงานผลทดสอบกำลังต้านแรงอัดของแท่ง คอนกรีตมวลเบาทรงลูกบาศก์

เรียน: มหาวิทยาลัยเทคโนโลยีสุรนารี ที่อยู่: 111 ถนนมหาวิทยาลัย ตำบลสุรนารี อำเภอเมือง จังหวัดนครราชสีมา 30000	คำขอรับบริการเลขที่ : CMT 0556/66 รายงานผลทดสอบเลขที่: RepCMT660556(9)
เจ้าของตัวอย่าง: นาย ลิขิต ชีวาสวัสดิ์ โครงการ: คอนกรีตมวลเบา ชื่อตัวอย่าง: แท่งคอนกรีตมวลเบารูปทรงลูกบาศก์ ขนาด 150 x 150 x 150 มม. วิธีการทดสอบ: มอก.2601-2556	หมายเลขตัวอย่าง : CMT S0556/66-9 ชั้นคุณภาพ : - วันรับตัวอย่าง : 11 กันยายน 2566 วันทดสอบ : 11 กันยายน 2566

No.	Mix/ Product Code	Casting Date	Age (days)	Density (kg/m^3)	Cure Type	Condition Before Test	Condition Fracture Type	Compressive Strength Load (kN)	Compressive Strength Stress (MPa)	Compressive Strength Uncert. (MPa)	Remark
1	-	03/09/66	8	1,006.2	F	1,8	S	40.4	1.74	-	(1000)
2	-	03/09/66	8	925.8	F	1,8	S	26.3	1.13	-	
3	-	03/09/66	8	958.9	F	1,8	S	35.5	1.51	-	

Cure Type : L = Laboratory ; F = Field

Condition of Specimens

Before Test : 1= สภาพปรกติ ,2 =แตกบิ่น ,3 =มีวัสดุแปลกปลอม ,4 =มีรูพรุน
5=ผิวหน้าเอียงไม่ได้ฉาก ,6=ผิวข้างไม่เรียบ ,7=ผิวชื้น ,8=ผิวแห้ง

Fracture Type : according to BS EN 12390-3-2002

Satisfy : S

Unsatisfy : 1 , 2 , 3 , 4 , 5 , 6 , 7 , 8 , 9

The reported expanded uncertainty measurement calculation procedure providing a level of approximately 95 %

ลงชื่อ .... ผู้รับรอง
(ผู้ช่วยศาสตราจารย์ ดร.ทิพย์วรรณ ฟังสุวรรณรักษ์)
รองผู้อำนวยการศูนย์เครื่องมือวิทยาศาสตร์และเทคโนโลยี
ปฏิบัติการแทนผู้อำนวยการศูนย์เครื่องมือวิทยาศาสตร์และเทคโนโลยี
17 ตุลาคม 2566

- รายงานนี้รับรองเฉพาะตัวอย่างที่ทำการทดสอบตามที่ระบุไว้ข้างต้นเท่านั้น
- ห้ามตัด ห้ามถ่ายสำเนาใบรายงานผลการทดสอบแต่เพียงบางส่วนยกเว้นทำทั้งฉบับ โดยไม่ได้รับความยินยอมเป็นลายลักษณ์อักษรจากห้องปฏิบัติการ

End of Report

อว 7432(5)/Rep.0956

17 ตุลาคม 2566

ห้องปฏิบัติการทดสอบวัสดุก่อสร้าง
ศูนย์เครื่องมือวิทยาศาสตร์และเทคโนโลยี
มหาวิทยาลัยเทคโนโลยีสุรนารี

รายงานผลทดสอบกำลังต้านแรงอัดของแท่ง คอนกรีตมวลเบาทรงลูกบาศก์

เรียน: มหาวิทยาลัยเทคโนโลยีสุรนารี
ที่อยู่: 111 ถนนมหาวิทยาลัย ตำบลสุรนารี อำเภอเมือง จังหวัดนครราชสีมา 30000
เจ้าของตัวอย่าง: นาย ลิขิต ชีวาสวัสดิ์
โครงการ: คอนกรีตมวลเบา
ชื่อตัวอย่าง: แท่งคอนกรีตมวลเบารูปทรงลูกบาศก์ ขนาด 150 x 150 x 150 มม.
วิธีการทดสอบ: มอก.2601-2556

คำขอรับบริการเลขที่ : CMT 0556/66
รายงานผลทดสอบเลขที่: RepCMT660556(4)
หมายเลขตัวอย่าง : CMT S0556/66-4
ชั้นคุณภาพ : -
วันรับตัวอย่าง : 5 กันยายน 2566
วันทดสอบ : 5 กันยายน 2566

No.	Mix/ Product Code	Casting Date	Age (days)	Density (kg/m^3)	Cure Type	Condition		Compressive Strength			Remark
						Before Test	Fracture Type	Load (kN)	Stress (MPa)	Uncert. (MPa)	
1	-	29/08/66	7	1,249.5	F	1,8	S	89.9	3.89	-	(1200)
2	-	29/08/66	7	1,206.1	F	1,8	S	76.3	3.25	-	
3	-	29/08/66	7	1,240.3	F	1,8	S	90.4	3.93	-	

Cure Type : L = Laboratory ; F = Field
Condition of Specimens
Before Test : 1= สภาพปรกติ ,2 =แตกบิ่น ,3 =มีวัสดุแปลกปลอม ,4 =มีรูพรุน
5=ผิวหน้าเอียงไม่ได้ฉาก ,6=ผิวข้างไม่เรียบ ,7=ผิวชื้น ,8=ผิวแห้ง
Fracture Type : according to BS EN 12390-3-2002
Satisfy : S
Unsatisfy : 1 , 2 , 3 , 4 , 5 , 6 , 7 , 8 , 9

The reported expanded uncertainty measurement calculation procedure providing a level of approximately 95 %

ลงชื่อ .... ผู้รับรอง
(ผู้ช่วยศาสตราจารย์ ดร.ทิพย์วรรณ ฟังสุวรรณรักษ์)
รองผู้อำนวยการศูนย์เครื่องมือวิทยาศาสตร์และเทคโนโลยี
ปฏิบัติการแทนผู้อำนวยการศูนย์เครื่องมือวิทยาศาสตร์และเทคโนโลยี
17 ตุลาคม 2566

- รายงานนี้รับรองเฉพาะตัวอย่างที่ทำการทดสอบตามที่ระบุไว้ข้างต้นเท่านั้น
- ห้ามตัด ห้ามถ่ายสำเนาใบรายงานผลการทดสอบแต่เพียงบางส่วนยกเว้นทำทั้งฉบับ โดยไม่ได้รับความยินยอมเป็นลายลักษณ์อักษรจากห้องปฏิบัติการ

End of Report

อว 7432(5)/Rep.0959

17 ตุลาคม 2566

ห้องปฏิบัติการทดสอบวัสดุก่อสร้าง
ศูนย์เครื่องมือวิทยาศาสตร์และเทคโนโลยี
มหาวิทยาลัยเทคโนโลยีสุรนารี

รายงานผลทดสอบกำลังต้านแรงอัดของแท่ง คอนกรีตมวลเบาทรงลูกบาศก์

เรียน: มหาวิทยาลัยเทคโนโลยีสุรนารี ที่อยู่: 111 ถนนมหาวิทยาลัย ตำบลสุรนารี อำเภอเมือง จังหวัดนครราชสีมา 30000	คำขอรับบริการเลขที่ : CMT 0556/66 รายงานผลทดสอบเลขที่:
เจ้าของตัวอย่าง: นาย ลิขิต ชีวาสวัสดิ์ โครงการ: คอนกรีตมวลเบา ชื่อตัวอย่าง: แท่งคอนกรีตมวลเบารูปทรงลูกบาศก์ ขนาด 150 x 150 x 150 มม. วิธีการทดสอบ: มอก.2601-2556	RepCMT660556(7) หมายเลขตัวอย่าง : CMT S0556/66-7 ชั้นคุณภาพ : - วันรับตัวอย่าง : 6 กันยายน 2566 วันทดสอบ : 6 กันยายน 2566

No.	Mix/ Product Code	Casting Date	Age (days)	Density (kg/m^3)	Cure Type	Condition Before Test	Condition Fracture Type	Compressive Strength Load (kN)	Compressive Strength Stress (MPa)	Compressive Strength Uncert. (MPa)	Remark
1	-	30/08/66	7	1,399.4	F	1,8	S	103.0	4.42	-	(1400)
2	-	30/08/66	7	1,420.4	F	1,8	S	133.5	5.76	-	
3	-	30/08/66	7	1,394.0	F	1,8	S	116.1	5.02	-	

Cure Type : L = Laboratory ; F = Field

Condition of Specimens

Before Test : 1= สภาพปรกติ ,2 =แตกบิ่น ,3 =มีวัสดุแปลกปลอม ,4 =มีรูพรุน
5=ผิวหน้าเอียงไม่ได้ฉาก ,6=ผิวข้างไม่เรียบ ,7=ผิวชื้น ,8=ผิวแห้ง

Fracture Type : according to BS EN 12390-3-2002

Satisfy : S

Unsatisfy : 1 , 2 , 3 , 4 , 5 , 6 , 7 , 8 , 9

The reported expanded uncertainty measurement calculation procedure providing a level of approximately 95 %

ลงชื่อ .... ผู้รับรอง

(ผู้ช่วยศาสตราจารย์ ดร.ทิพย์วรรณ ฟังสุวรรณรักษ์)

รองผู้อำนวยการศูนย์เครื่องมือวิทยาศาสตร์และเทคโนโลยี

ปฏิบัติการแทนผู้อำนวยการศูนย์เครื่องมือวิทยาศาสตร์และเทคโนโลยี

17 ตุลาคม 2566

- รายงานนี้รับรองเฉพาะตัวอย่างที่ทำการทดสอบตามที่ระบุไว้ข้างต้นเท่านั้น
- ห้ามตัด ห้ามถ่ายสำเนาใบรายงานผลการทดสอบแต่เพียงบางส่วนยกเว้นทำทั้งฉบับ โดยไม่ได้รับความยินยอมเป็นลายลักษณ์อักษรจากห้องปฏิบัติการ

End of Report

อว 7432(5)/Rep.0960

17 ตุลาคม 2566

ห้องปฏิบัติการทดสอบวัสดุก่อสร้าง
ศูนย์เครื่องมือวิทยาศาสตร์และเทคโนโลยี
มหาวิทยาลัยเทคโนโลยีสุรนารี

รายงานผลทดสอบกำลังต้านแรงอัดของแท่ง คอนกรีตมวลเบาทรงลูกบาศก์

เรียน: มหาวิทยาลัยเทคโนโลยีสุรนารี ที่อยู่: 111 ถนนมหาวิทยาลัย ตำบลสุรนารี อำเภอเมือง จังหวัดนครราชสีมา 30000	คำขอรับบริการเลขที่ : CMT 0556/66 รายงานผลทดสอบเลขที่:
เจ้าของตัวอย่าง: นาย ลิขิต ชีวาสวัสดิ์ โครงการ: คอนกรีตมวลเบา ชื่อตัวอย่าง: แท่งคอนกรีตมวลเบารูปทรงลูกบาศก์ ขนาด 150 x 150 x 150 มม. วิธีการทดสอบ: มอก.2601-2556	RepCMT660556(8) หมายเลขตัวอย่าง : CMT S0556/66-8 ชั้นคุณภาพ : - วันรับตัวอย่าง : 8 กันยายน 2566 วันทดสอบ : 8 กันยายน 2566

No.	Mix/ Product Code	Casting Date	Age (days)	Density (kg/m^3)	Cure Type	Condition Before Test	Fracture Type	Compressive Strength Load (kN)	Stress (MPa)	Uncert. (MPa)	Remark
1	-	01/09/66	7	1,587.2	F	1,8	S	214.1	9.08	-	(1600)
2	-	01/09/66	7	1,739.6	F	1,8	S	289.7	12.34	-	
3	-	01/09/66	7	1,583.0	F	1,8	S	198.0	8.50	-	

Cure Type : L = Laboratory ; F = Field
Condition of Specimens
Before Test : 1= สภาพปรกติ ,2 =แตกบิ่น ,3 =มีวัสดุแปลกปลอม ,4 =มีรูพรุน
5=ผิวหน้าเอียงไม่ได้ฉาก ,6=ผิวข้างไม่เรียบ ,7=ผิวขึ้น ,8=ผิวแห้ง
Fracture Type : according to BS EN 12390-3-2002
Satisfy : S
Unsatisfy : 1 , 2 , 3 , 4 , 5 , 6 , 7 , 8 , 9

The reported expanded uncertainty measurement calculation procedure providing a level of approximately 95 %

ลงชื่อ .... ผู้รับรอง
(ผู้ช่วยศาสตราจารย์ ดร.ทิพย์วรรณ ฟังสุวรรณรักษ์)
รองผู้อำนวยการศูนย์เครื่องมือวิทยาศาสตร์และเทคโนโลยี
ปฏิบัติการแทนผู้อำนวยการศูนย์เครื่องมือวิทยาศาสตร์และเทคโนโลยี
17 ตุลาคม 2566

- รายงานนี้รับรองเฉพาะตัวอย่างที่ทำการทดสอบตามที่ระบุไว้ข้างต้นเท่านั้น
- ห้ามตัด ห้ามถ่ายสำเนาใบรายงานผลการทดสอบแต่เพียงบางส่วนยกเว้นทำทั้งฉบับ โดยไม่ได้รับความยินยอมเป็นลายลักษณ์อักษรจากห้องปฏิบัติการ

End of Report

อว 7432(5)/Rep.0962

17 ตุลาคม 2566

ห้องปฏิบัติการทดสอบวัสดุก่อสร้าง
ศูนย์เครื่องมือวิทยาศาสตร์และเทคโนโลยี
มหาวิทยาลัยเทคโนโลยีสุรนารี

รายงานผลทดสอบกำลังต้านแรงอัดของแท่ง คอนกรีตมวลเบาทรงลูกบาศก์

เรียน: มหาวิทยาลัยเทคโนโลยีสุรนารี ที่อยู่: 111 ถนนมหาวิทยาลัย ตำบลสุรนารี อำเภอเมือง จังหวัดนครราชสีมา 30000	คำขอรับบริการเลขที่ : CMT 0556/66 รายงานผลทดสอบเลขที่:
เจ้าของตัวอย่าง: นาย ลิขิต ชีวาสวัสดิ์ โครงการ: คอนกรีตมวลเบา ชื่อตัวอย่าง: แท่งคอนกรีตมวลเบารูปทรงลูกบาศก์ ขนาด 150 x 150 x 150 มม. วิธีการทดสอบ: มอก.2601-2556	RepCMT660556(10) หมายเลขตัวอย่าง : CMT S0556/66-10 ชั้นคุณภาพ : - วันรับตัวอย่าง : 11 กันยายน 2566 วันทดสอบ : 11 กันยายน 2566

No.	Mix/ Product Code	Casting Date	Age (days)	Density (kg/m^3)	Cure Type	Condition Before Test	Condition Fracture Type	Compressive Strength Load (kN)	Compressive Strength Stress (MPa)	Compressive Strength Uncert. (MPa)	Remark
1	-	02/09/66	9	1,828.9	F	1,8	S	375.8	15.82	-	(1800)
2	-	02/09/66	9	1,880.0	F	1,8	S	354.3	15.11	-	
3	-	02/09/66	9	1,822.9	F	1,8	S	393.2	16.40	-	

Cure Type : L = Laboratory ; F = Field
Condition of Specimens
Before Test : 1= สภาพปรกติ ,2 =แตกบิ่น ,3 =มีวัสดุแปลกปลอม ,4 =มีรูพรุน
5=ผิวหน้าเอียงไม่ได้ฉาก ,6=ผิวข้างไม่เรียบ ,7=ผิวชื้น ,8=ผิวแห้ง
Fracture Type : according to BS EN 12390-3-2002
Satisfy : S
Unsatisfy : 1 , 2 , 3 , 4 , 5 , 6 , 7 , 8 , 9

The reported expanded uncertainty measurement calculation procedure providing a level of approximately 95 %

ลงชื่อ .... ผู้รับรอง
(ผู้ช่วยศาสตราจารย์ ดร.ทิพย์วรรณ ฟังสุวรรณรักษ์)
รองผู้อำนวยการศูนย์เครื่องมือวิทยาศาสตร์และเทคโนโลยี
ปฏิบัติการแทนผู้อำนวยการศูนย์เครื่องมือวิทยาศาสตร์และเทคโนโลยี
17 ตุลาคม 2566

- รายงานนี้รับรองเฉพาะตัวอย่างที่ทำการทดสอบตามที่ระบุไว้ข้างต้นเท่านั้น
- ห้ามตัด ห้ามถ่ายสำเนาใบรายงานผลการทดสอบแต่เพียงบางส่วนยกเว้นทำทั้งฉบับ โดยไม่ได้รับความยินยอมเป็นลายลักษณ์อักษรจากห้องปฏิบัติการ

End of Report

อว 7432(5)/Rep.0966

17 ตุลาคม 2566

ห้องปฏิบัติการทดสอบวัสดุก่อสร้าง
ศูนย์เครื่องมือวิทยาศาสตร์และเทคโนโลยี
มหาวิทยาลัยเทคโนโลยีสุรนารี

รายงานผลทดสอบกำลังต้านแรงอัดของแท่ง คอนกรีตมวลเบาทรงลูกบาศก์

เรียน: มหาวิทยาลัยเทคโนโลยีสุรนารี ที่อยู่: 111 ถนนมหาวิทยาลัย ตำบลสุรนารี อำเภอเมือง จังหวัดนครราชสีมา 30000	คำขอรับบริการเลขที่ : CMT 0556/66 รายงานผลทดสอบเลขที่: RepCMT660556(14)
เจ้าของตัวอย่าง: นาย ลิขิต ชีวาสวัสดิ์ โครงการ: คอนกรีตมวลเบา ชื่อตัวอย่าง: แท่งคอนกรีตมวลเบารูปทรงลูกบาศก์ ขนาด 150 x 150 x 150 มม. วิธีการทดสอบ: มอก.2601-2556	หมายเลขตัวอย่าง : CMT S0556/66-14 ชั้นคุณภาพ : - วันรับตัวอย่าง : 18 กันยายน 2566 วันทดสอบ : 19 กันยายน 2566

No.	Mix/ Product Code	Casting Date	Age (days)	Density (kg/m^3)	Cure Type	Condition Before Test	Fracture Type	Compressive Strength Load (kN)	Stress (MPa)	Uncert. (MPa)	Remark
1	-	03/09/66	16	922.4	F	1,8	S	36.5	1.56	-	(1000)
2	-	03/09/66	16	944.8	F	1,8	S	49.8	2.12	-	
3	-	03/09/66	16	1,008.8	F	1,8	S	49.7	2.11	-	

Cure Type : L = Laboratory ; F = Field

Condition of Specimens

Before Test : 1= สภาพปรกติ ,2 =แตกบิ่น ,3 =มีวัสดุแปลกปลอม ,4 =มีรูพรุน
5=ผิวหน้าเอียงไม่ได้ฉาก ,6=ผิวข้างไม่เรียบ ,7=ผิวชื้น ,8=ผิวแห้ง

Fracture Type : according to BS EN 12390-3-2002

Satisfy : S

Unsatisfy : 1 , 2 , 3 , 4 , 5 , 6 , 7 , 8 , 9

The reported expanded uncertainty measurement calculation procedure providing a level of approximately 95 %

ลงชื่อ .... ผู้รับรอง

(ผู้ช่วยศาสตราจารย์ ดร.ทิพย์วรรณ ฟังสุวรรณรักษ์)
รองผู้อำนวยการศูนย์เครื่องมือวิทยาศาสตร์และเทคโนโลยี
ปฏิบัติการแทนผู้อำนวยการศูนย์เครื่องมือวิทยาศาสตร์และเทคโนโลยี
17 ตุลาคม 2566

- รายงานนี้รับรองเฉพาะตัวอย่างที่ทำการทดสอบตามที่ระบุไว้ข้างต้นเท่านั้น
- ห้ามตัด ห้ามถ่ายสำเนาใบรายงานผลการทดสอบแต่เพียงบางส่วนยกเว้นทำทั้งฉบับ โดยไม่ได้รับความยินยอมเป็นลายลักษณ์อักษรจากห้องปฏิบัติการ

End of Report

อว 7432(5)/Rep.0963

17 ตุลาคม 2566

ห้องปฏิบัติการทดสอบวัสดุก่อสร้าง
ศูนย์เครื่องมือวิทยาศาสตร์และเทคโนโลยี
มหาวิทยาลัยเทคโนโลยีสุรนารี

รายงานผลทดสอบกำลังต้านแรงอัดของแท่ง คอนกรีตมวลเบาทรงลูกบาศก์

เรียน: มหาวิทยาลัยเทคโนโลยีสุรนารี ที่อยู่: 111 ถนนมหาวิทยาลัย ตำบลสุรนารี อำเภอเมือง จังหวัดนครราชสีมา 30000	คำขอรับบริการเลขที่ : CMT 0556/66 รายงานผลทดสอบเลขที่: RepCMT660556(11)
เจ้าของตัวอย่าง: นาย ลิขิต ชีวาสวัสดิ์ โครงการ: คอนกรีตมวลเบา ชื่อตัวอย่าง: แท่งคอนกรีตมวลเบารูปทรงลูกบาศก์ ขนาด 150 x 150 x 150 มม. วิธีการทดสอบ: มอก.2601-2556	หมายเลขตัวอย่าง : CMT S0556/66-11 ชั้นคุณภาพ : - วันรับตัวอย่าง : 12 กันยายน 2566 วันทดสอบ : 12 กันยายน 2566

No.	Mix/ Product Code	Casting Date	Age (days)	Density (kg/m^3)	Cure Type	Condition Before Test	Condition Fracture Type	Compressive Strength Load (kN)	Compressive Strength Stress (MPa)	Compressive Strength Uncert. (MPa)	Remark
1	-	29/08/66	14	1,246.2	F	1,8	S	101.0	4.37	-	(1200)
2	-	29/08/66	14	1,249.3	F	1,8	S	98.7	4.27	-	
3	-	29/08/66	14	1,253.3	F	1,8	S	88.7	3.93	-	

Cure Type : L = Laboratory ; F = Field

Condition of Specimens

Before Test : 1= สภาพปรกติ ,2 =แตกบิ่น ,3 =มีวัสดุแปลกปลอม ,4 =มีรูพรุน
5=ผิวหน้าเอียงไม่ได้ฉาก ,6=ผิวข้างไม่เรียบ ,7=ผิวชื้น ,8=ผิวแห้ง

Fracture Type : according to BS EN 12390-3-2002

Satisfy : S

Unsatisfy : 1 , 2 , 3 , 4 , 5 , 6 , 7 , 8 , 9

The reported expanded uncertainty measurement calculation procedure providing a level of approximately 95 %

ลงชื่อ .... ผู้รับรอง
(ผู้ช่วยศาสตราจารย์ ดร.ทิพย์วรรณ ฟังสุวรรณรักษ์)
รองผู้อำนวยการศูนย์เครื่องมือวิทยาศาสตร์และเทคโนโลยี
ปฏิบัติการแทนผู้อำนวยการศูนย์เครื่องมือวิทยาศาสตร์และเทคโนโลยี
17 ตุลาคม 2566

- รายงานนี้รับรองเฉพาะตัวอย่างที่ทำการทดสอบตามที่ระบุไว้ข้างต้นเท่านั้น
- ห้ามตัด ห้ามถ่ายสำเนาใบรายงานผลการทดสอบแต่เพียงบางส่วนยกเว้นทำทั้งฉบับ โดยไม่ได้รับความยินยอมเป็นลายลักษณ์อักษรจากห้องปฏิบัติการ

End of Report

อว 7432(5)/Rep.0964

17 ตุลาคม 2566

ห้องปฏิบัติการทดสอบวัสดุก่อสร้าง
ศูนย์เครื่องมือวิทยาศาสตร์และเทคโนโลยี
มหาวิทยาลัยเทคโนโลยีสุรนารี

รายงานผลทดสอบกำลังต้านแรงอัดของแท่ง คอนกรีตมวลเบาทรงลูกบาศก์

เรียน: มหาวิทยาลัยเทคโนโลยีสุรนารี ที่อยู่: 111 ถนนมหาวิทยาลัย ตำบลสุรนารี อำเภอเมือง จังหวัดนครราชสีมา 30000	คำขอรับบริการเลขที่ : CMT 0556/66 รายงานผลทดสอบเลขที่: RepCMT660556(12)
เจ้าของตัวอย่าง: นาย ลิขิต ชีวาสวัสดิ์ โครงการ: คอนกรีตมวลเบา ชื่อตัวอย่าง: แท่งคอนกรีตมวลเบารูปทรงลูกบาศก์ ขนาด 150 x 150 x 150 มม. วิธีการทดสอบ: มอก.2601-2556	หมายเลขตัวอย่าง : CMT S0556/66-12 ชั้นคุณภาพ : - วันรับตัวอย่าง : 13 กันยายน 2566 วันทดสอบ : 13 กันยายน 2566

No.	Mix/ Product Code	Casting Date	Age (days)	Density (kg/m^3)	Cure Type	Condition Before Test	Condition Fracture Type	Compressive Strength Load (kN)	Compressive Strength Stress (MPa)	Compressive Strength Uncert. (MPa)	Remark
1	-	30/08/66	14	1,457.5	F	1,8	S	151.1	6.62	-	(1400)
2	-	30/08/66	14	1,453.4	F	1,8	S	140.5	6.03	-	
3	-	30/08/66	14	1,421.2	F	1,8	S	106.1	4.59	-	

Cure Type : L = Laboratory ; F = Field

Condition of Specimens

Before Test : 1= สภาพปรกติ ,2 =แตกบิ่น ,3 =มีวัสดุแปลกปลอม ,4 =มีรูพรุน
5=ผิวหน้าเอียงไม่ได้ฉาก ,6=ผิวข้างไม่เรียบ ,7=ผิวชื้น ,8=ผิวแห้ง

Fracture Type : according to BS EN 12390-3-2002

Satisfy : S

Unsatisfy : 1 , 2 , 3 , 4 , 5 , 6 , 7 , 8 , 9

The reported expanded uncertainty measurement calculation procedure providing a level of approximately 95 %

ลงชื่อ .... ผู้รับรอง

(ผู้ช่วยศาสตราจารย์ ดร.ทิพย์วรรณ ฟังสุวรรณรักษ์)
รองผู้อำนวยการศูนย์เครื่องมือวิทยาศาสตร์และเทคโนโลยี
ปฏิบัติการแทนผู้อำนวยการศูนย์เครื่องมือวิทยาศาสตร์และเทคโนโลยี
17 ตุลาคม 2566

- รายงานนี้รับรองเฉพาะตัวอย่างที่ทำการทดสอบตามที่ระบุไว้ข้างต้นเท่านั้น
- ห้ามตัด ห้ามถ่ายสำเนาใบรายงานผลการทดสอบแต่เพียงบางส่วนยกเว้นทำทั้งฉบับ โดยไม่ได้รับความยินยอมเป็นลายลักษณ์อักษรจากห้องปฏิบัติการ

End of Report

อว 7432(5)/Rep.0965

17 ตุลาคม 2566

ห้องปฏิบัติการทดสอบวัสดุก่อสร้าง
ศูนย์เครื่องมือวิทยาศาสตร์และเทคโนโลยี
มหาวิทยาลัยเทคโนโลยีสุรนารี

รายงานผลทดสอบกำลังต้านแรงอัดของแท่ง คอนกรีตมวลเบาทรงลูกบาศก์

เรียน: มหาวิทยาลัยเทคโนโลยีสุรนารี ที่อยู่: 111 ถนนมหาวิทยาลัย ตำบลสุรนารี อำเภอเมือง จังหวัดนครราชสีมา 30000	คำขอรับบริการเลขที่ : CMT 0556/66 รายงานผลทดสอบเลขที่: RepCMT660556(13)
เจ้าของตัวอย่าง: นาย ลิขิต ชีวาสวัสดิ์ โครงการ: คอนกรีตมวลเบา ชื่อตัวอย่าง: แท่งคอนกรีตมวลเบารูปทรงลูกบาศก์ ขนาด 150 x 150 x 150 มม. วิธีการทดสอบ: มอก.2601-2556	หมายเลขตัวอย่าง : CMT S0556/66-13 ชั้นคุณภาพ : - วันรับตัวอย่าง : 15 กันยายน 2566 วันทดสอบ : 15 กันยายน 2566

No.	Mix/ Product Code	Casting Date	Age (days)	Density (kg/m^3)	Cure Type	Condition Before Test	Fracture Type	Compressive Strength Load (kN)	Stress (MPa)	Uncert. (MPa)	Remark
1	-	01/09/66	14	1,638.2	F	1,8	S	250.3	10.99	-	(1600)
2	-	01/09/66	14	1,578.6	F	1,8	S	242.9	10.58	-	
3	-	01/09/66	14	1,600.1	F	1,8	S	250.2	10.77	-	

Cure Type : L = Laboratory ; F = Field

Condition of Specimens

Before Test : 1= สภาพปรกติ ,2 =แตกบิ่น ,3 =มีวัสดุแปลกปลอม ,4 =มีรูพรุน
5=ผิวหน้าเอียงไม่ได้ฉาก ,6=ผิวข้างไม่เรียบ ,7=ผิวชื้น ,8=ผิวแห้ง

Fracture Type : according to BS EN 12390-3-2002
Satisfy : S
Unsatisfy : 1 , 2 , 3 , 4 , 5 , 6 , 7 , 8 , 9

The reported expanded uncertainty measurement calculation procedure providing a level of approximately 95 %

ลงชื่อ .... ผู้รับรอง
(ผู้ช่วยศาสตราจารย์ ดร.ทิพย์วรรณ ฟังสุวรรณรักษ์)
รองผู้อำนวยการศูนย์เครื่องมือวิทยาศาสตร์และเทคโนโลยี
ปฏิบัติการแทนผู้อำนวยการศูนย์เครื่องมือวิทยาศาสตร์และเทคโนโลยี
17 ตุลาคม 2566

- รายงานนี้รับรองเฉพาะตัวอย่างที่ทำการทดสอบตามที่ระบุไว้ข้างต้นเท่านั้น
- ห้ามตัด ห้ามถ่ายสำเนาใบรายงานผลการทดสอบแต่เพียงบางส่วนยกเว้นทำทั้งฉบับ โดยไม่ได้รับความยินยอมเป็นลายลักษณ์อักษรจากห้องปฏิบัติการ

End of Report

อว 7432(5)/Rep.0967

17 ตุลาคม 2566

ห้องปฏิบัติการทดสอบวัสดุก่อสร้าง
ศูนย์เครื่องมือวิทยาศาสตร์และเทคโนโลยี
มหาวิทยาลัยเทคโนโลยีสุรนารี

รายงานผลทดสอบกำลังต้านแรงอัดของแท่ง คอนกรีตมวลเบาทรงลูกบาศก์

เรียน: มหาวิทยาลัยเทคโนโลยีสุรนารี ที่อยู่: 111 ถนนมหาวิทยาลัย ตำบลสุรนารี อำเภอเมือง จังหวัดนครราชสีมา 30000	คำขอรับบริการเลขที่ : CMT 0556/66 รายงานผลทดสอบเลขที่: RepCMT660556(15)
เจ้าของตัวอย่าง: นาย ลิขิต ชีวาสวัสดิ์ โครงการ: คอนกรีตมวลเบา ชื่อตัวอย่าง: แท่งคอนกรีตมวลเบารูปทรงลูกบาศก์ ขนาด 150 x 150 x 150 มม. วิธีการทดสอบ: มอก.2601-2556	หมายเลขตัวอย่าง : CMT S0556/66-15 ชั้นคุณภาพ : - วันรับตัวอย่าง : 18 กันยายน 2566 วันทดสอบ : 19 กันยายน 2566

No.	Mix/ Product Code	Casting Date	Age (days)	Density (kg/m^3)	Cure Type	Condition Before Test	Condition Fracture Type	Compressive Strength Load (kN)	Compressive Strength Stress (MPa)	Compressive Strength Uncert. (MPa)	Remark
1	-	02/09/66	17	1,797.0	F	1,8	S	375.3	16.11	-	(1800)
2	-	02/09/66	17	1,853.3	F	1,8	S	393.2	17.30	-	
3	-	02/09/66	17	1,804.6	F	1,8	S	423.9	18.51	-	

Cure Type : L = Laboratory ; F = Field

Condition of Specimens

Before Test : 1= สภาพปรกติ ,2 =แตกบิ่น ,3 =มีวัสดุแปลกปลอม ,4 =มีรูพรุน 5=ผิวหน้าเอียงไม่ได้ฉาก ,6=ผิวข้างไม่เรียบ ,7=ผิวชื้น ,8=ผิวแห้ง

Fracture Type : according to BS EN 12390-3-2002

Satisfy : S

Unsatisfy : 1 , 2 , 3 , 4 , 5 , 6 , 7 , 8 , 9

The reported expanded uncertainty measurement calculation procedure providing a level of approximately 95 %

ลงชื่อ .... ผู้รับรอง

(ผู้ช่วยศาสตราจารย์ ดร.ทิพย์วรรณ ฟังสุวรรณรักษ์)
รองผู้อำนวยการศูนย์เครื่องมือวิทยาศาสตร์และเทคโนโลยี
ปฏิบัติการแทนผู้อำนวยการศูนย์เครื่องมือวิทยาศาสตร์และเทคโนโลยี
17 ตุลาคม 2566

- รายงานนี้รับรองเฉพาะตัวอย่างที่ทำการทดสอบตามที่ระบุไว้ข้างต้นเท่านั้น
- ห้ามตัด ห้ามถ่ายสำเนาใบรายงานผลการทดสอบแต่เพียงบางส่วนยกเว้นทั้งฉบับ โดยไม่ได้รับความยินยอมเป็นลายลักษณ์อักษรจากห้องปฏิบัติการ

End of Report

อว 7432(5)/Rep.0970

17 ตุลาคม 2566

ห้องปฏิบัติการทดสอบวัสดุก่อสร้าง
ศูนย์เครื่องมือวิทยาศาสตร์และเทคโนโลยี
มหาวิทยาลัยเทคโนโลยีสุรนารี

รายงานผลทดสอบกำลังต้านแรงอัดของแท่ง คอนกรีตมวลเบาทรงลูกบาศก์

เรียน: มหาวิทยาลัยเทคโนโลยีสุรนารี ที่อยู่: 111 ถนนมหาวิทยาลัย ตำบลสุรนารี อำเภอเมือง จังหวัดนครราชสีมา 30000	คำขอรับบริการเลขที่ : CMT 0556/66 รายงานผลทดสอบเลขที่: RepCMT660556(18)
เจ้าของตัวอย่าง: นาย ลิขิต ชีวาสวัสดิ์ โครงการ: คอนกรีตมวลเบา ชื่อตัวอย่าง: แท่งคอนกรีตมวลเบารูปทรงลูกบาศก์ ขนาด 150 x 150 x 150 มม. วิธีการทดสอบ: มอก.2601-2556	หมายเลขตัวอย่าง : CMT S0556/66-18 ชั้นคุณภาพ : - วันรับตัวอย่าง : 2 ตุลาคม 2566 วันทดสอบ : 3 ตุลาคม 2566

No.	Mix/ Product Code	Casting Date	Age (days)	Density (kg/m³)	Cure Type	Condition Before Test	Fracture Type	Compressive Strength Load (kN)	Stress (MPa)	Uncert. (MPa)	Remark
1	-	03/09/66	30	980.8	F	1,8	S	40.4	1.75	-	(1000)
2	-	03/09/66	30	940.1	F	1,8	S	44.4	1.91	-	
3	-	03/09/66	30	1,019.8	F	1,8	S	56.8	2.47	-	

Cure Type : L = Laboratory ; F = Field

Condition of Specimens

Before Test : 1= สภาพปรกติ ,2 =แตกบิ่น ,3 =มีวัสดุแปลกปลอม ,4 =มีรูพรุน 5=ผิวหน้าเอียงไม่ได้ฉาก ,6=ผิวข้างไม่เรียบ ,7=ผิวชื้น ,8=ผิวแห้ง

Fracture Type : according to BS EN 12390-3-2002

Satisfy : S

Unsatisfy : 1 , 2 , 3 , 4 , 5 , 6 , 7 , 8 , 9

The reported expanded uncertainty measurement calculation procedure providing a level of approximately 95 %

ลงชื่อ .... ผู้รับรอง

(ผู้ช่วยศาสตราจารย์ ดร.ทิพย์วรรณ ฟังสุวรรณรักษ์)

รองผู้อำนวยการศูนย์เครื่องมือวิทยาศาสตร์และเทคโนโลยี

ปฏิบัติการแทนผู้อำนวยการศูนย์เครื่องมือวิทยาศาสตร์และเทคโนโลยี

17 ตุลาคม 2566

- รายงานนี้รับรองเฉพาะตัวอย่างที่ทำการทดสอบตามที่ระบุไว้ข้างต้นเท่านั้น
- ห้ามตัด ห้ามถ่ายสำเนาใบรายงานผลการทดสอบแต่เพียงบางส่วนยกเว้นทำทั้งฉบับ โดยไม่ได้รับความยินยอมเป็นลายลักษณ์อักษรจากห้องปฏิบัติการ

End of Report

อว 7432(5)/Rep.0968

17 ตุลาคม 2566

ห้องปฏิบัติการทดสอบวัสดุก่อสร้าง
ศูนย์เครื่องมือวิทยาศาสตร์และเทคโนโลยี
มหาวิทยาลัยเทคโนโลยีสุรนารี

รายงานผลทดสอบกำลังต้านแรงอัดของแท่ง คอนกรีตมวลเบาทรงลูกบาศก์

เรียน: มหาวิทยาลัยเทคโนโลยีสุรนารี ที่อยู่: 111 ถนนมหาวิทยาลัย ตำบลสุรนารี อำเภอเมือง จังหวัดนครราชสีมา 30000	คำขอรับบริการเลขที่ : CMT 0556/66 รายงานผลทดสอบเลขที่: RepCMT660556(16)
เจ้าของตัวอย่าง: นาย ลิขิต ชีวาสวัสดิ์ โครงการ: คอนกรีตมวลเบา ชื่อตัวอย่าง: แท่งคอนกรีตมวลเบารูปทรงลูกบาศก์ ขนาด 150 x 150 x 150 มม. วิธีการทดสอบ: มอก.2601-2556	หมายเลขตัวอย่าง : CMT S0556/66-16 ชั้นคุณภาพ : - วันรับตัวอย่าง : 26 กันยายน 2566 วันทดสอบ : 26 กันยายน 2566

No.	Mix/ Product Code	Casting Date	Age (days)	Density (kg/m^3)	Cure Type	Condition Before Test	Condition Fracture Type	Compressive Strength Load (kN)	Compressive Strength Stress (MPa)	Compressive Strength Uncert. (MPa)	Remark
1	-	29/08/66	28	1,263.9	F	1,8	S	93.8	4.06	-	(1200)
2	-	29/08/66	28	1,263.6	F	1,8	S	114.1	4.90	-	
3	-	29/08/66	28	1,293.2	F	1,8	S	112.9	4.94	-	

Cure Type : L = Laboratory ; F = Field

Condition of Specimens

Before Test : 1= สภาพปรกติ ,2 =แตกบิ่น ,3 =มีวัสดุแปลกปลอม ,4 =มีรูพรุน
5=ผิวหน้าเอียงไม่ได้ฉาก ,6=ผิวข้างไม่เรียบ ,7=ผิวชื้น ,8=ผิวแห้ง

Fracture Type : according to BS EN 12390-3-2002

Satisfy : S

Unsatisfy : 1 , 2 , 3 , 4 , 5 , 6 , 7 , 8 , 9

The reported expanded uncertainty measurement calculation procedure providing a level of approximately 95 %

ลงชื่อ .... ผู้รับรอง

(ผู้ช่วยศาสตราจารย์ ดร.ทิพย์วรรณ ฟังสุวรรณรักษ์)
รองผู้อำนวยการศูนย์เครื่องมือวิทยาศาสตร์และเทคโนโลยี
ปฏิบัติการแทนผู้อำนวยการศูนย์เครื่องมือวิทยาศาสตร์และเทคโนโลยี
17 ตุลาคม 2566

- รายงานนี้รับรองเฉพาะตัวอย่างที่ทำการทดสอบตามที่ระบุไว้ข้างต้นเท่านั้น
- ห้ามตัด ห้ามถ่ายสำเนาใบรายงานผลการทดสอบแต่เพียงบางส่วนยกเว้นทำทั้งฉบับ โดยไม่ได้รับความยินยอมเป็นลายลักษณ์อักษรจากห้องปฏิบัติการ

End of Report

อว 7432(5)/Rep.0972

17 ตุลาคม 2566

ห้องปฏิบัติการทดสอบวัสดุก่อสร้าง
ศูนย์เครื่องมือวิทยาศาสตร์และเทคโนโลยี
มหาวิทยาลัยเทคโนโลยีสุรนารี

รายงานผลทดสอบกำลังต้านแรงอัดของแท่ง คอนกรีตมวลเบาทรงลูกบาศก์

เรียน: มหาวิทยาลัยเทคโนโลยีสุรนารี ที่อยู่: 111 ถนนมหาวิทยาลัย ตำบลสุรนารี อำเภอเมือง จังหวัดนครราชสีมา 30000	คำขอรับบริการเลขที่ : CMT 0556/66 รายงานผลทดสอบเลขที่: RepCMT660556(20)
เจ้าของตัวอย่าง: นาย ลิขิต ชีวาสวัสดิ์ โครงการ: คอนกรีตมวลเบา ชื่อตัวอย่าง: แท่งคอนกรีตมวลเบารูปทรงลูกบาศก์ ขนาด 150 x 150 x 150 มม. วิธีการทดสอบ: มอก.2601-2556	หมายเลขตัวอย่าง : CMT S0556/66-20 ชั้นคุณภาพ : - วันรับตัวอย่าง : 27 กันยายน 2566 วันทดสอบ : 27 กันยายน 2566

No.	Mix/ Product Code	Casting Date	Age (days)	Density (kg/m^3)	Cure Type	Condition		Compressive Strength			Remark
						Before Test	Fracture Type	Load (kN)	Stress (MPa)	Uncert. (MPa)	
1	-	30/08/66	28	1,434.5	F	1,8	S	155.8	6.83	-	(1400)
2	-	30/08/66	28	1,410.1	F	1,8	S	154.4	6.63	-	
3	-	30/08/66	28	1,463.5	F	1,8	S	131.7	5.76	-	

Cure Type : L = Laboratory ; F = Field

Condition of Specimens

Before Test : 1= สภาพปรกติ ,2 =แตกบิ่น ,3 =มีวัสดุแปลกปลอม ,4 =มีรูพรุน
5=ผิวหน้าเอียงไม่ได้ฉาก ,6=ผิวข้างไม่เรียบ ,7=ผิวชื้น ,8=ผิวแห้ง

Fracture Type : according to BS EN 12390-3-2002

Satisfy : S

Unsatisfy : 1 , 2 , 3 , 4 , 5 , 6 , 7 , 8 , 9

The reported expanded uncertainty measurement calculation procedure providing a level of approximately 95 %

ลงชื่อ .... ผู้รับรอง
(ผู้ช่วยศาสตราจารย์ ดร.ทิพย์วรรณ ฟังสุวรรณรักษ์)
รองผู้อำนวยการศูนย์เครื่องมือวิทยาศาสตร์และเทคโนโลยี
ปฏิบัติการแทนผู้อำนวยการศูนย์เครื่องมือวิทยาศาสตร์และเทคโนโลยี
17 ตุลาคม 2566

- รายงานนี้รับรองเฉพาะตัวอย่างที่ทำการทดสอบตามที่ระบุไว้ข้างต้นเท่านั้น
- ห้ามตัด ห้ามถ่ายสำเนาใบรายงานผลการทดสอบแต่เพียงบางส่วนยกเว้นทำทั้งฉบับ โดยไม่ได้รับความยินยอมเป็นลายลักษณ์อักษรจากห้องปฏิบัติการ

End of Report

อว 7432(5)/Rep.0969

17 ตุลาคม 2566

ห้องปฏิบัติการทดสอบวัสดุก่อสร้าง
ศูนย์เครื่องมือวิทยาศาสตร์และเทคโนโลยี
มหาวิทยาลัยเทคโนโลยีสุรนารี

รายงานผลทดสอบกำลังต้านแรงอัดของแท่ง คอนกรีตมวลเบาทรงลูกบาศก์

เรียน: มหาวิทยาลัยเทคโนโลยีสุรนารี ที่อยู่: 111 ถนนมหาวิทยาลัย ตำบลสุรนารี อำเภอเมือง จังหวัดนครราชสีมา 30000	คำขอรับบริการเลขที่ : CMT 0556/66 รายงานผลทดสอบเลขที่:
เจ้าของตัวอย่าง: นาย ลิขิต ชีวาสวัสดิ์ โครงการ: คอนกรีตมวลเบา ชื่อตัวอย่าง: แท่งคอนกรีตมวลเบารูปทรงลูกบาศก์ ขนาด 150 x 150 x 150 มม. วิธีการทดสอบ: มอก.2601-2556	RepCMT660556(17) หมายเลขตัวอย่าง : CMT S0556/66-17 ชั้นคุณภาพ : - วันรับตัวอย่าง : 29 กันยายน 2566 วันทดสอบ : 2 ตุลาคม 2566

No.	Mix/ Product Code	Casting Date	Age (days)	Density (kg/m^3)	Cure Type	Condition Before Test	Condition Fracture Type	Compressive Strength Load (kN)	Compressive Strength Stress (MPa)	Compressive Strength Uncert. (MPa)	Remark
1	-	01/09/66	31	1,561.3	F	1,8	S	229.9	9.82	-	(1600)
2	-	01/09/66	31	1,661.1	F	1,8	S	214.5	9.33	-	
3	-	01/09/66	31	1,635.8	F	1,8	S	353.4	15.53	-	

Cure Type : L = Laboratory ; F = Field

Condition of Specimens

Before Test : 1= สภาพปรกติ ,2 =แตกบิ่น ,3 =มีวัสดุแปลกปลอม ,4 =มีรูพรุน
5=ผิวหน้าเอียงไม่ได้ฉาก ,6=ผิวข้างไม่เรียบ ,7=ผิวชื้น ,8=ผิวแห้ง

Fracture Type : according to BS EN 12390-3-2002

Satisfy : S

Unsatisfy : 1 , 2 , 3 , 4 , 5 , 6 , 7 , 8 , 9

The reported expanded uncertainty measurement calculation procedure providing a level of approximately 95 %

ลงชื่อ .... ผู้รับรอง

(ผู้ช่วยศาสตราจารย์ ดร.ทิพย์วรรณ ฟังสุวรรณรักษ์)
รองผู้อำนวยการศูนย์เครื่องมือวิทยาศาสตร์และเทคโนโลยี
ปฏิบัติการแทนผู้อำนวยการศูนย์เครื่องมือวิทยาศาสตร์และเทคโนโลยี
17 ตุลาคม 2566

- รายงานนี้รับรองเฉพาะตัวอย่างที่ทำการทดสอบตามที่ระบุไว้ข้างต้นเท่านั้น
- ห้ามตัด ห้ามถ่ายสำเนาใบรายงานผลการทดสอบแต่เพียงบางส่วนยกเว้นทำทั้งฉบับ โดยไม่ได้รับความยินยอมเป็นลายลักษณ์อักษรจากห้องปฏิบัติการ

End of Report

อว 7432(5)/Rep.0971

17 ตุลาคม 2566

ห้องปฏิบัติการทดสอบวัสดุก่อสร้าง
ศูนย์เครื่องมือวิทยาศาสตร์และเทคโนโลยี
มหาวิทยาลัยเทคโนโลยีสุรนารี

รายงานผลทดสอบกำลังต้านแรงอัดของแท่ง คอนกรีตมวลเบาทรงลูกบาศก์

เรียน: มหาวิทยาลัยเทคโนโลยีสุรนารี ที่อยู่: 111 ถนนมหาวิทยาลัย ตำบลสุรนารี อำเภอเมือง จังหวัดนครราชสีมา 30000	คำขอรับบริการเลขที่ : CMT 0556/66 รายงานผลทดสอบเลขที่: RepCMT660556(19)
เจ้าของตัวอย่าง: นาย ลิขิต ชีวาสวัสดิ์ โครงการ: คอนกรีตมวลเบา ชื่อตัวอย่าง: แท่งคอนกรีตมวลเบารูปทรงลูกบาศก์ ขนาด 150 x 150 x 150 มม. วิธีการทดสอบ: มอก.2601-2556	หมายเลขตัวอย่าง : CMT S0556/66-19 ชั้นคุณภาพ : - วันรับตัวอย่าง : 2 ตุลาคม 2566 วันทดสอบ : 3 ตุลาคม 2566

No.	Mix/ Product Code	Casting Date	Age (days)	Density (kg/m^3)	Cure Type	Condition		Compressive Strength			Remark
						Before Test	Fracture Type	Load (kN)	Stress (MPa)	Uncert. (MPa)	
1	-	02/09/66	31	1,859.6	F	1,8	S	423.2	18.69	-	(1800)
2	-	02/09/66	31	1,921.6	F	1,8	S	529.1	22.99	-	
3	-	02/09/66	31	1,899.5	F	1,8	S	475.5	20.65	-	

Cure Type : L = Laboratory ; F = Field

Condition of Specimens

Before Test : 1= สภาพปรกติ ,2 =แตกบิ่น ,3 =มีวัสดุแปลกปลอม ,4 =มีรูพรุน
5=ผิวหน้าเอียงไม่ได้ฉาก ,6=ผิวข้างไม่เรียบ ,7=ผิวขึ้น ,8=ผิวแห้ง

Fracture Type : according to BS EN 12390-3-2002

Satisfy : S

Unsatisfy : 1 , 2 , 3 , 4 , 5 , 6 , 7 , 8 , 9

The reported expanded uncertainty measurement calculation procedure providing a level of approximately 95 %

ลงชื่อ .... ผู้รับรอง
(ผู้ช่วยศาสตราจารย์ ดร.ทิพย์วรรณ ฟังสุวรรณรักษ์)
รองผู้อำนวยการศูนย์เครื่องมือวิทยาศาสตร์และเทคโนโลยี
ปฏิบัติการแทนผู้อำนวยการศูนย์เครื่องมือวิทยาศาสตร์และเทคโนโลยี
17 ตุลาคม 2566

- รายงานนี้รับรองเฉพาะตัวอย่างที่ทำการทดสอบตามที่ระบุไว้ข้างต้นเท่านั้น
- ห้ามตัด ห้ามถ่ายสำเนาใบรายงานผลการทดสอบแต่เพียงบางส่วนยกเว้นทำทั้งฉบับ โดยไม่ได้รับความยินยอมเป็นลายลักษณ์อักษรจากห้องปฏิบัติการ

End of Report

อว 7432(5)/Rep. 0973

17 ตุลาคม 2566
แผ่นที่ 1/1

ห้องปฏิบัติการทดสอบวัสดุก่อสร้าง

ศูนย์เครื่องมือวิทยาศาสตร์และเทคโนโลยี มหาวิทยาลัยเทคโนโลยีสุรนารี

ผลทดสอบแรงดึงแยกของแท่งคอนกรีต (Tensile Splitting Test)

เรียน : มหาวิทยาลัยเทคโนโลยีสุรนารี
ที่อยู่ : 111 ถนนมหาวิทยาลัย ตำบลสุรนารี อำเภอเมือง จังหวัดนครราชสีมา 30000

โครงการ	: คอนกรีตมวลเบา	หมายเลขรับงาน :	CMT0556/66
สถานที่	: -	หมายเลขตัวอย่าง :	CMT0556/66-21
เจ้าของตัวอย่าง	: นาย ลิขิต ชีวาสวัสดิ์	วันรับตัวอย่าง :	30-09-2566
วัสดุตัวอย่าง	: แท่งตัวอย่างคอนกรีตมวลเบารูปทรงกระบอก ขนาด 150 x 300 มม. Density 1000 kg/cu.m	วันทดสอบ :	03-10-2566
		ผู้ทดสอบ :	นายจักรฤษณ์ ธนะมณีวุฒิ

Specimen No.	Size		Casting Date	Age	Cure Type	Max Load	Splitting Tensile Strength
	Diameter (mm)	Length (mm)		(days)		(kN)	(ksc)
1	152.22	302.17	3/9/2566	30	F	21.1	2.98
2	151.96	303.38	3/9/2566	30	F	23.2	3.27
3	152.32	302.55	3/9/2566	30	F	21.5	3.03

Cure Type : L = Laboratory ; F = Field

ลงชื่อ ผู้รับรอง

(ผู้ช่วยศาสตราจารย์ ดร.ทิพย์วรรณ ฟังสุวรรณรักษ์)

รองผู้อำนวยการศูนย์เครื่องมือวิทยาศาสตร์และเทคโนโลยี

ปฏิบัติการแทนผู้อำนวยการศูนย์เครื่องมือวิทยาศาสตร์และเทคโนโลยี

17 ตุลาคม 2566

- รายงานนี้รับรองเฉพาะตัวอย่างที่ทำการทดสอบตามที่ระบุไว้ข้างต้นเท่านั้น
- ห้ามตัด ห้ามถ่ายสำเนาใบรายงานผลการทดสอบแต่เพียงบางส่วน ยกเว้นทำทั้งฉบับ โดยไม่ได้รับความยินยอมเป็นลายลักษณ์อักษรจากห้องปฏิบัติการ

End of Report

อว 7432(5)/Rep. 0974

17 ตุลาคม 2566

แผ่นที่ 1/1

ห้องปฏิบัติการทดสอบวัสดุก่อสร้าง

ศูนย์เครื่องมือวิทยาศาสตร์และเทคโนโลยี มหาวิทยาลัยเทคโนโลยีสุรนารี

ผลทดสอบแรงดึงแยกของแท่งคอนกรีต (Tensile Splitting Test)

เรียน	: มหาวิทยาลัยเทคโนโลยีสุรนารี
ที่อยู่	: 111 ถนนมหาวิทยาลัย ตำบลสุรนารี อำเภอเมือง จังหวัดนครราชสีมา 30000

โครงการ	: คอนกรีตมวลเบา	หมายเลขรับงาน :	CMT0556/66
สถานที่	: -	หมายเลขตัวอย่าง :	CMTNS0556/66-22
เจ้าของตัวอย่าง	: นาย ลิขิต ชีวาสวัสดิ์	วันรับตัวอย่าง :	27-09-2566
วัสดุตัวอย่าง	: แท่งตัวอย่างคอนกรีตมวลเบารูปทรงกระบอก ขนาด 150 x 300 มม. Density 1200 kg/cu.m	วันทดสอบ :	28-09-2566
		ผู้ทดสอบ :	นายจักรกฤษณ์ ธนะมณีวุฒิ

Specimen No.	Size		Casting Date	Age (days)	Cure Type	Max Load (kN)	Splitting Tensile Strength (ksc)
	Diameter (mm)	Length (mm)					
1	150.54	307.25	29/8/2566	30	F	34.6	4.86

Cure Type : L = Laboratory ; F = Field

ลงชื่อ ทิพ ฟัง ผู้รับรอง

(ผู้ช่วยศาสตราจารย์ ดร.ทิพย์วรรณ ฟังสุวรรณรักษ์)

รองผู้อำนวยการศูนย์เครื่องมือวิทยาศาสตร์และเทคโนโลยี

ปฏิบัติการแทนผู้อำนวยการศูนย์เครื่องมือวิทยาศาสตร์และเทคโนโลยี

17 ตุลาคม 2566

- รายงานนี้รับรองเฉพาะตัวอย่างที่ทำการทดสอบตามที่ระบุไว้ข้างต้นเท่านั้น
- ห้ามตัด ห้ามถ่ายสำเนาใบรายงานผลการทดสอบแต่เพียงบางส่วน ยกเว้นทำทั้งฉบับ โดยไม่ได้รับความยินยอมเป็นลายลักษณ์อักษรจากห้องปฏิบัติการ

End of Report

อว 7432(5)/Rep. 0975

17 ตุลาคม 2566

แผ่นที่ 1/1

ห้องปฏิบัติการทดสอบวัสดุก่อสร้าง

ศูนย์เครื่องมือวิทยาศาสตร์และเทคโนโลยี มหาวิทยาลัยเทคโนโลยีสุรนารี

ผลทดสอบแรงดึงแยกของแท่งคอนกรีต (Tensile Splitting Test)

เรียน	: มหาวิทยาลัยเทคโนโลยีสุรนารี		
ที่อยู่	: 111 ถนนมหาวิทยาลัย ตำบลสุรนารี อำเภอเมือง จังหวัดนครราชสีมา 30000		
โครงการ	: คอนกรีตมวลเบา	หมายเลขรับงาน :	CMT0556/66
สถานที่	: -	หมายเลขตัวอย่าง :	CMT0556/66-23
เจ้าของตัวอย่าง	: นาย ลิขิต ชีวาสวัสดิ์	วันรับตัวอย่าง :	27-09-2566
วัสดุตัวอย่าง	: แท่งตัวอย่างคอนกรีตมวลเบารูปทรงกระบอก ขนาด 150 x 300 มม.	วันทดสอบ :	28-09-2566
	Density 1400 kg/cu.m	ผู้ทดสอบ :	นายจักรกฤษณ์ ธนะมณีวุฒิ

Specimen No.	Size Diameter (mm)	Size Length (mm)	Casting Date	Age (days)	Cure Type	Max Load (kN)	Splitting Tensile Strength (ksc)
1	152.40	303.79	30/8/2566	29	F	40.8	5.72
2	152.75	307.45	30/8/2566	29	F	46.3	6.40
3	153.25	303.92	30/8/2566	29	F	43.2	6.02

Cure Type : L = Laboratory ; F = Field

ลงชื่อ ทิพ ฟัง ผู้รับรอง

(ผู้ช่วยศาสตราจารย์ ดร.ทิพย์วรรณ ฟังสุวรรณรักษ์)

รองผู้อำนวยการศูนย์เครื่องมือวิทยาศาสตร์และเทคโนโลยี

ปฏิบัติการแทนผู้อำนวยการศูนย์เครื่องมือวิทยาศาสตร์และเทคโนโลยี

17 ตุลาคม 2566

- รายงานนี้รับรองเฉพาะตัวอย่างที่ทำการทดสอบตามที่ระบุไว้ข้างต้นเท่านั้น
- ห้ามตัด ห้ามถ่ายสำเนาใบรายงานผลการทดสอบแต่เพียงบางส่วน ยกเว้นทำทั้งฉบับ โดยไม่ได้รับความยินยอมเป็นลายลักษณ์อักษรจากห้องปฏิบัติการ

End of Report

อว 7432(5)/Rep. 0976

17 ตุลาคม 2566

แผ่นที่ 1/1

ห้องปฏิบัติการทดสอบวัสดุก่อสร้าง

ศูนย์เครื่องมือวิทยาศาสตร์และเทคโนโลยี มหาวิทยาลัยเทคโนโลยีสุรนารี

ผลทดสอบแรงดึงแยกของแท่งคอนกรีต (Tensile Splitting Test)

เรียน	: มหาวิทยาลัยเทคโนโลยีสุรนารี		
ที่อยู่	: 111 ถนนมหาวิทยาลัย ตำบลสุรนารี อำเภอเมือง จังหวัดนครราชสีมา 30000		
โครงการ	: คอนกรีตมวลเบา	หมายเลขรับงาน :	CMT0556/66
สถานที่	: -	หมายเลขตัวอย่าง :	CMT0556/66-24
เจ้าของตัวอย่าง	: นาย ลิขิต ชีวาสวัสดิ์	วันรับตัวอย่าง :	02-10-2566
วัสดุตัวอย่าง	: แท่งตัวอย่างคอนกรีตมวลเบารูปทรงกระบอก ขนาด 150 x 300 มม. Density 1600 kg/cu.m	วันทดสอบ :	02-10-2566
		ผู้ทดสอบ :	นายจักรกฤษณ์ ธนะมณีวุฒิ

Specimen No.	Size		Casting Date	Age	Cure Type	Max Load	Splitting Tensile Strength
	Diameter (mm)	Length (mm)		(days)		(kN)	(ksc)
1	150.67	302.15	1/9/2566	31	F	86.8	12.38
2	150.58	301.32	1/9/2566	31	F	85.4	12.22
3	151.26	301.73	1/9/2566	31	F	91.8	13.06

Cure Type : L = Laboratory ; F = Field

ลงชื่อ ผู้รับรอง

(ผู้ช่วยศาสตราจารย์ ดร.ทิพย์วรรณ ฟังสุวรรณรักษ์)

รองผู้อำนวยการศูนย์เครื่องมือวิทยาศาสตร์และเทคโนโลยี

ปฏิบัติการแทนผู้อำนวยการศูนย์เครื่องมือวิทยาศาสตร์และเทคโนโลยี

17 ตุลาคม 2566

- รายงานนี้รับรองเฉพาะตัวอย่างที่ทำการทดสอบตามที่ระบุไว้ข้างต้นเท่านั้น
- ห้ามตัด ห้ามถ่ายสำเนาใบรายงานผลการทดสอบแต่เพียงบางส่วน ยกเว้นทำทั้งฉบับ โดยไม่ได้รับความยินยอมเป็นลายลักษณ์อักษรจากห้องปฏิบัติการ

End of Report

อว 7432(5)/Rep. 0977

17 ตุลาคม 2566

แผ่นที่ 1/1

ห้องปฏิบัติการทดสอบวัสดุก่อสร้าง

ศูนย์เครื่องมือวิทยาศาสตร์และเทคโนโลยี มหาวิทยาลัยเทคโนโลยีสุรนารี

ผลทดสอบแรงดึงแยกของแท่งคอนกรีต (Tensile Splitting Test)

เรียน	: มหาวิทยาลัยเทคโนโลยีสุรนารี		
ที่อยู่	: 111 ถนนมหาวิทยาลัย ตำบลสุรนารี อำเภอเมือง จังหวัดนครราชสีมา 30000		
โครงการ	: คอนกรีตมวลเบา	หมายเลขรับงาน :	CMT0556/66
สถานที่	: -	หมายเลขตัวอย่าง :	CMT0556/66-25
เจ้าของตัวอย่าง	: นาย ลิขิต ชีวาสวัสดิ์	วันรับตัวอย่าง :	30-09-2566
วัสดุตัวอย่าง	: แท่งตัวอย่างคอนกรีตมวลเบารูปทรงกระบอก ขนาด 150 x 300 มม. Density 1800 kg/cu.m	วันทดสอบ :	03-10-2566
		ผู้ทดสอบ :	นายจักรกฤษณ์ ธนะมณีวุฒิ

Specimen No.	Size		Casting Date	Age	Cure Type	Max Load	Splitting Tensile Strength
	Diameter (mm)	Length (mm)		(days)		(kN)	(ksc)
1	152.58	303.84	2/9/2566	31	F	114.1	15.98
2	152.29	303.10	2/9/2566	31	F	111.1	15.63
3	152.01	304.24	2/9/2566	31	F	108.1	15.17

Cure Type : L = Laboratory ; F = Field

ลงชื่อ ผู้รับรอง

(ผู้ช่วยศาสตราจารย์ ดร.ทิพย์วรรณ ฟังสุวรรณรักษ์)

รองผู้อำนวยการศูนย์เครื่องมือวิทยาศาสตร์และเทคโนโลยี

ปฏิบัติการแทนผู้อำนวยการศูนย์เครื่องมือวิทยาศาสตร์และเทคโนโลยี

17 ตุลาคม 2566

- รายงานนี้รับรองเฉพาะตัวอย่างที่ทำการทดสอบตามที่ระบุไว้ข้างต้นเท่านั้น
- ห้ามตัด ห้ามถ่ายสำเนาใบรายงานผลการทดสอบแต่เพียงบางส่วน ยกเว้นทำทั้งฉบับ โดยไม่ได้รับความยินยอมเป็นลายลักษณ์อักษรจากห้องปฏิบัติการ

End of Report

อว 7432(5)/Rep. 0978

17 ตุลาคม 2566

แผ่นที่ 1/1

ห้องปฏิบัติการทดสอบวัสดุก่อสร้าง

ศูนย์เครื่องมือวิทยาศาสตร์และเทคโนโลยี มหาวิทยาลัยเทคโนโลยีสุรนารี

Flexural Strength of Concrete (Third Point Loading)

โครงการ : คอนกรีตมวลเบา

เจ้าของตัวอย่าง : นายลิขิต ชีวาสวัสดิ์

หมายเลขรับงาน : CMT0556/66

วัสดุตัวอย่าง : Concrete Beam 150 x 150 x 500 mm.

หมายเลขตัวอย่าง : CMTNS0556/66-26

มาตรฐานทดสอบ : ASMT C78

วันรับตัวอย่าง : 02-10-2566

ระยะจุดรองรับ : 450 มิลลิเมตร

วันทดสอบ : 09-10-2566

ผู้ทดสอบ : นายอาทิ นครเรียบ

Sample No.	Dimension (mm) Wd.(b) - Tk.(d)	Age (day)	Maximum Load (N)	Flexural Strength (MPa)	Flexural Strength (kgf/cm^2)	Ave. Flexural Strength (kgf/cm^2)	Remark
1	150 x 150	36	4,216	0.56	5.73	5.18	(1000 kg/cu.m)
2	150 x 150	36	4,226	0.56	5.75		(1000 kg/cu.m)
3	150 x 150	36	3,888	0.40	4.05		(1000 kg/cu.m)

- รายงานนี้รับรองเฉพาะตัวอย่างที่ทำการทดสอบตามที่ระบุไว้ข้างต้นเท่านั้น
- ห้ามตัด ห้ามถ่ายสำเนาใบรายงานผลการทดสอบแต่เพียงบางส่วน ยกเว้นทำทั้งฉบับ โดยไม่ได้รับความยินยอมเป็นลายลักษณ์อักษรจากห้องปฏิบัติการ

ลงชื่อ .... ผู้รับรอง

(ผู้ช่วยศาสตราจารย์ ดร.ทิพย์วรรณ ฟังสุวรรณรักษ์)

รองผู้อำนวยการศูนย์เครื่องมือวิทยาศาสตร์และเทคโนโลยี

ปฏิบัติการแทนผู้อำนวยการศูนย์เครื่องมือวิทยาศาสตร์และเทคโนโลยี

17 ตุลาคม 2566

End of Report

อว 7432(5)/Rep. 0979

17 ตุลาคม 2566

แผ่นที่ 1/1

ห้องปฏิบัติการทดสอบวัสดุก่อสร้าง

ศูนย์เครื่องมือวิทยาศาสตร์และเทคโนโลยี มหาวิทยาลัยเทคโนโลยีสุรนารี

Flexural Strength of Concrete (Third Point Loading)

โครงการ : คอนกรีตมวลเบา

เจ้าของตัวอย่าง : นายลิขิต ชีวาสวัสดิ์

หมายเลขรับงาน : CMT0556/66

วัสดุตัวอย่าง : Concrete Beam 150 x 150 x 500 mm.

หมายเลขตัวอย่าง : CMTNS0556/66-27

มาตรฐานทดสอบ : ASMT C78

วันรับตัวอย่าง : 02-10-2566

ระยะจุดรองรับ : 450 มิลลิเมตร

วันทดสอบ : 09-10-2566

ผู้ทดสอบ : นายอาทิ นครเรียบ

Sample No.	Dimension (mm) Wd.(b) - Tk.(d)	Age (day)	Maximum Load (N)	Flexural Strength (MPa)	Flexural Strength (kgf/cm^2)	Ave. Flexural Strength (kgf/cm^2)	Remark
1	150 x 150	41	4,778	0.64	6.50	6.70	(1200 kg/cu.m)
2	150 x 150	41	4,863	0.65	6.61		(1200 kg/cu.m)
3	150 x 150	41	5,145	0.69	6.99		(1200 kg/cu.m)

- รายงานนี้รับรองเฉพาะตัวอย่างที่ทำการทดสอบตามที่ระบุไว้ข้างต้นเท่านั้น
- ห้ามตัด ห้ามถ่ายสำเนาใบรายงานผลการทดสอบแต่เพียงบางส่วน ยกเว้นทำทั้งฉบับ โดยไม่ได้รับความยินยอมเป็นลายลักษณ์อักษรจากห้องปฏิบัติการ

ลงชื่อ .... ผู้รับรอง

(ผู้ช่วยศาสตราจารย์ ดร.ทิพย์วรรณ ฟังสุวรรณรักษ์)

รองผู้อำนวยการศูนย์เครื่องมือวิทยาศาสตร์และเทคโนโลยี

ปฏิบัติการแทนผู้อำนวยการศูนย์เครื่องมือวิทยาศาสตร์และเทคโนโลยี

17 ตุลาคม 2566

End of Report

อว 7432(5)/Rep. 0980

17 ตุลาคม 2566

แผ่นที่ 1/1

ห้องปฏิบัติการทดสอบวัสดุก่อสร้าง

ศูนย์เครื่องมือวิทยาศาสตร์และเทคโนโลยี มหาวิทยาลัยเทคโนโลยีสุรนารี

Flexural Strength of Concrete (Third Point Loading)

โครงการ : คอนกรีตมวลเบา

เจ้าของตัวอย่าง : นายลิขิต ชีวาสวัสดิ์

วัสดุตัวอย่าง : Concrete Beam 150 x 150 x 500 mm.

มาตรฐานทดสอบ : ASMT C78

ระยะจุดรองรับ : 450 มิลลิเมตร

หมายเลขรับงาน : CMT0556/66

หมายเลขตัวอย่าง : CMTNS0556/66-28

วันรับตัวอย่าง : 02-10-2566

วันทดสอบ : 09-10-2566

ผู้ทดสอบ : นายอาทิ นครเรียบ

Sample No.	Dimension (mm) Wd.(b) - Tk.(d)	Age (day)	Maximum Load (N)	Flexural Strength (MPa)	Flexural Strength (kgf/cm^2)	Ave. Flexural Strength (kgf/cm^2)	Remark
1	150 x 150	40	4,818	0.64	6.55	7.88	(1400 kg/cu.m)
2	150 x 150	40	6,938	0.93	9.43		(1400 kg/cu.m)
3	150 x 150	40	5,622	0.75	7.64		(1400 kg/cu.m)

- รายงานนี้รับรองเฉพาะตัวอย่างที่ทำการทดสอบตามที่ระบุไว้ข้างต้นเท่านั้น
- ห้ามตัด ห้ามถ่ายสำเนาใบรายงานผลการทดสอบแต่เพียงบางส่วน ยกเว้นทำทั้งฉบับ โดยไม่ได้รับความยินยอมเป็นลายลักษณ์อักษรจากห้องปฏิบัติการ

ลงชื่อ .... ผู้รับรอง

(ผู้ช่วยศาสตราจารย์ ดร.ทิพย์วรรณ ฟังสุวรรณรักษ์)

รองผู้อำนวยการศูนย์เครื่องมือวิทยาศาสตร์และเทคโนโลยี

ปฏิบัติการแทนผู้อำนวยการศูนย์เครื่องมือวิทยาศาสตร์และเทคโนโลยี

17 ตุลาคม 2566

End of Report

อว 7432(5)/Rep. 0981

17 ตุลาคม 2566

แผ่นที่ 1/1

ห้องปฏิบัติการทดสอบวัสดุก่อสร้าง

ศูนย์เครื่องมือวิทยาศาสตร์และเทคโนโลยี มหาวิทยาลัยเทคโนโลยีสุรนารี

Flexural Strength of Concrete (Third Point Loading)

โครงการ : คอนกรีตมวลเบา

เจ้าของตัวอย่าง : นายลิขิต ชีวาสวัสดิ์

วัสดุตัวอย่าง : Concrete Beam 150 x 150 x 500 mm.

มาตรฐานทดสอบ : ASMT C78

ระยะจุดรองรับ : 450 มิลลิเมตร

หมายเลขรับงาน : CMT0556/66

หมายเลขตัวอย่าง : CMTNS0556/66-29

วันรับตัวอย่าง : 02-10-2566

วันทดสอบ : 09-10-2566

ผู้ทดสอบ : นายอาทิ นครเรียบ

Sample No.	Dimension (mm) Wd.(b) - Tk.(d)	Age (day)	Maximum Load (N)	Flexural Strength (MPa)	Flexural Strength (kgf/cm^2)	Ave. Flexural Strength (kgf/cm^2)	Remark
1	150 x 150	38	11,021	1.47	14.98	13.55	(1600 kg/cu.m)
2	150 x 150	38	9,148	1.22	12.44		(1600 kg/cu.m)
3	150 x 150	38	9,724	1.30	13.22		(1600 kg/cu.m)

- รายงานนี้รับรองเฉพาะตัวอย่างที่ทำการทดสอบตามที่ระบุไว้ข้างต้นเท่านั้น
- ห้ามตัด ห้ามถ่ายสำเนาใบรายงานผลการทดสอบแต่เพียงบางส่วน ยกเว้นทำทั้งฉบับ โดยไม่ได้รับความยินยอมเป็นลายลักษณ์อักษรจากห้องปฏิบัติการ

ลงชื่อ .... ผู้รับรอง

(ผู้ช่วยศาสตราจารย์ ดร.ทิพย์วรรณ ฟังสุวรรณรักษ์)

รองผู้อำนวยการศูนย์เครื่องมือวิทยาศาสตร์และเทคโนโลยี

ปฏิบัติการแทนผู้อำนวยการศูนย์เครื่องมือวิทยาศาสตร์และเทคโนโลยี

17 ตุลาคม 2566

End of Report

อว 7432(5)/Rep. 0982

17 ตุลาคม 2566

แผ่นที่ 1/1

มหาวิทยาลัยเทคโนโลยีสุรนารี

ห้องปฏิบัติการทดสอบวัสดุก่อสร้าง

ศูนย์เครื่องมือวิทยาศาสตร์และเทคโนโลยี มหาวิทยาลัยเทคโนโลยีสุรนารี

Flexural Strength of Concrete (Third Point Loading)

โครงการ : คอนกรีตมวลเบา

เจ้าของตัวอย่าง : นายลิขิต ชีวาสวัสดิ์

วัสดุตัวอย่าง : Concrete Beam 150 x 150 x 500 mm.

มาตรฐานทดสอบ : ASMT C78

ระยะจุดรองรับ : 450 มิลลิเมตร

หมายเลขรับงาน : CMT0556/66

หมายเลขตัวอย่าง : CMTNS0556/66-30

วันรับตัวอย่าง : 02-10-2566

วันทดสอบ : 09-10-2566

ผู้ทดสอบ : นายอาทิ นครเรียบ

Sample No.	Dimension (mm) Wd.(b) - Tk.(d)	Age (day)	Maximum Load (N)	Flexural Strength (MPa)	Flexural Strength (kgf/cm^2)	Ave. Flexural Strength (kgf/cm^2)	Remark
1	150 x 150	37	16,876	2.25	22.95	18.00	(1800 kg/cu.m)
2	150 x 150	37	12,593	1.68	17.12		(1800 kg/cu.m)
3	150 x 150	37	10,252	1.37	13.94		(1800 kg/cu.m)

- รายงานนี้รับรองเฉพาะตัวอย่างที่ทำการทดสอบตามที่ระบุไว้ข้างต้นเท่านั้น
- ห้ามตัด ห้ามถ่ายสำเนาใบรายงานผลการทดสอบแต่เพียงบางส่วน ยกเว้นทำทั้งฉบับ โดยไม่ได้รับความยินยอมเป็นลายลักษณ์อักษรจากห้องปฏิบัติการ

ลงชื่อ .... ผู้รับรอง

UNOFFICIAL

รองผู้อำนวยการศูนย์เครื่องมือวิทยาศาสตร์และเทคโนโลยี

ปฏิบัติการแทนผู้อำนวยการศูนย์เครื่องมือวิทยาศาสตร์และเทคโนโลยี

17 ตุลาคม 2566

End of Report

อว 7432(5)/Rep. 0983

17 ตุลาคม 2566

แผ่นที่ 1/1

มหาวิทยาลัยเทคโนโลยีสุรนารี

ห้องปฏิบัติการทดสอบวัสดุก่อสร้าง

ศูนย์เครื่องมือวิทยาศาสตร์และเทคโนโลยี มหาวิทยาลัยเทคโนโลยีสุรนารี

ผลทดสอบการดูดซึมน้ำของคอนกรีตบล็อกมวลเบา มอก. 2601-2556

เจ้าของตัวอย่าง : นาย ลิขิต ชีวาสวัสดิ์	หมายเลขคำขอ : CMT 0556/66
โครงการ : คอนกรีตมวลเบา	หมายเลขตัวอย่าง : CMT NS0556/66-31
	วันที่รับตัวอย่าง : 02-10-2566
ประเภท : คอนกรีตบล็อกมวลเบา แบบเติมฟองอากาศ	วันที่ทดสอบ : 09-10-2566
ความหนาระบุ : - มม.	ผู้ทดสอบ : จักรกฤษณ์
ความสูงระบุ : - มม.	
ความยาวระบุ : - มม.	

Specimen No.	Dimension (mm) w x l x t	Weight Dry (g)	Weight Saturate (g)	Absoption (%)	Average Absoption (%)	Remark
1	150.3 x 151.6 x 152.9	3,138.5	3,674.5	17.08	17.32	(Density 1000 kg/cu.m)
2	151.8 x 150.5 x 151.5	2,932.4	3,453.3	17.76		
3	150.3 x 150.3 x 152.4	2,939.4	3,442.5	17.12		

- รายงานนี้รับรองเฉพาะตัวอย่างที่ทำการทดสอบตามที่ระบุไว้ข้างต้นเท่านั้น
- ห้ามตัด ห้ามถ่ายสำเนาใบรายงานผลการทดสอบแต่เพียงบางส่วน ยกเว้นทำทั้งฉบับ โดยไม่ได้รับความยินยอมเป็นลายลักษณ์อักษรจากห้องปฏิบัติการ

ลงชื่อ ทิพย์ ฟัง ผู้รับรอง

(ผู้ช่วยศาสตราจารย์ ดร.ทิพย์วรรณ ฟังสุวรรณรักษ์)

รองผู้อำนวยการศูนย์เครื่องมือวิทยาศาสตร์และเทคโนโลยี

ปฏิบัติการแทนผู้อำนวยการศูนย์เครื่องมือวิทยาศาสตร์และเทคโนโลยี

17 ตุลาคม 2566

End of Report

อว 7432(5)/Rep. 0984

17 ตุลาคม 2566
แผ่นที่ 1/1

ห้องปฏิบัติการทดสอบวัสดุก่อสร้าง

ศูนย์เครื่องมือวิทยาศาสตร์และเทคโนโลยี มหาวิทยาลัยเทคโนโลยีสุรนารี

ผลทดสอบการดูดซึมน้ำของคอนกรีตบล็อกมวลเบา มอก. 2601-2556

เจ้าของตัวอย่าง : นาย ลิขิต ชีวาสวัสดิ์	หมายเลขคำขอ : CMT 0556/66
โครงการ : คอนกรีตมวลเบา	หมายเลขตัวอย่าง : CMT NS0556/66-32
	วันที่รับตัวอย่าง : 26-09-2566
ประเภท : คอนกรีตบล็อกมวลเบา แบบเติมฟองอากาศ	วันที่ทดสอบ : 27-09-2566
ความหนาระบุ : - มม.	ผู้ทดสอบ : จักรกฤษณ์
ความสูงระบุ : - มม.	
ความยาวระบุ : - มม.	

Specimen No.	Dimension (mm) w x l x t	Weight Dry (g)	Weight Saturate (g)	Absoption (%)	Average Absoption (%)	Remark
1	151.2 x 152.5 x 152.2	3,935.8	4,491.2	14.11	14.00	(Density 1200 kg/cu.m)
2	151.0 x 151.4 x 152.8	3,812.8	4,353.2	14.17		
3	151.2 x 150.8 x 152.4	3,887.3	4,421.0	13.73		

- รายงานนี้รับรองเฉพาะตัวอย่างที่ทำการทดสอบตามที่ระบุไว้ข้างต้นเท่านั้น
- ห้ามตัด ห้ามถ่ายสำเนาใบรายงานผลการทดสอบแต่เพียงบางส่วน ยกเว้นทำทั้งฉบับ โดยไม่ได้รับความยินยอมเป็นลายลักษณ์อักษรจากห้องปฏิบัติการ

ลงชื่อ ผู้รับรอง

(ผู้ช่วยศาสตราจารย์ ดร.ทิพย์วรรณ ฟังสุวรรณรักษ์)

รองผู้อำนวยการศูนย์เครื่องมือวิทยาศาสตร์และเทคโนโลยี

ปฏิบัติการแทนผู้อำนวยการศูนย์เครื่องมือวิทยาศาสตร์และเทคโนโลยี

17 ตุลาคม 2566

End of Report

อว 7432(5)/Rep. 0985

17 ตุลาคม 2566
แผ่นที่ 1/1

ห้องปฏิบัติการทดสอบวัสดุก่อสร้าง
ศูนย์เครื่องมือวิทยาศาสตร์และเทคโนโลยี มหาวิทยาลัยเทคโนโลยีสุรนารี
ผลทดสอบการดูดซึมน้ำของคอนกรีตบล็อกมวลเบา มอก. 2601-2556

เจ้าของตัวอย่าง : นาย ลิขิต ชีวาสวัสดิ์	หมายเลขคำขอ : CMT 0556/66
โครงการ : คอนกรีตมวลเบา	หมายเลขตัวอย่าง : CMT NS0556/66-33
	วันที่รับตัวอย่าง : 26-09-2566
ประเภท : คอนกรีตบล็อกมวลเบา แบบเติมฟองอากาศ	วันที่ทดสอบ : 28-09-2566
ความหนาระบุ : - มม.	ผู้ทดสอบ : จักรกฤษณ์
ความสูงระบุ : - มม.	
ความยาวระบุ : - มม.	

Specimen No.	Dimension (mm) w x l x t	Weight Dry (g)	Weight Saturate (g)	Absoption (%)	Average Absoption (%)	Remark
1	152.4 x 152.7 x 151.5	4,478.6	5,008.8	11.84	10.42	(Density 1400 kg/cu.m)
2	153.4 x 151.5 x 152.7	4,527.4	4,952.6	9.39		
3	150.7 x 152.1 x 150.4	4,575.7	5,034.4	10.02		

- รายงานนี้รับรองเฉพาะตัวอย่างที่ทำการทดสอบตามที่ระบุไว้ข้างต้นเท่านั้น
- ห้ามตัด ห้ามถ่ายสำเนาใบรายงานผลการทดสอบแต่เพียงบางส่วน ยกเว้นทำทั้งฉบับ โดยไม่ได้รับความยินยอมเป็นลายลักษณ์อักษรจากห้องปฏิบัติการ

ลงชื่อ ทิพย์ ผู้รับรอง
(ผู้ช่วยศาสตราจารย์ ดร.ทิพย์วรรณ ฟังสุวรรณรักษ์)
รองผู้อำนวยการศูนย์เครื่องมือวิทยาศาสตร์และเทคโนโลยี
ปฏิบัติการแทนผู้อำนวยการศูนย์เครื่องมือวิทยาศาสตร์และเทคโนโลยี
17 ตุลาคม 2566

End of Report

อว 7432(5)/Rep. 0986

17 ตุลาคม 2566
แผ่นที่ 1/1

มหาวิทยาลัยเทคโนโลยีสุรนารี

ห้องปฏิบัติการทดสอบวัสดุก่อสร้าง
ศูนย์เครื่องมือวิทยาศาสตร์และเทคโนโลยี มหาวิทยาลัยเทคโนโลยีสุรนารี
ผลทดสอบการดูดซึมน้ำของคอนกรีตบล็อกมวลเบา มอก. 2601-2556

เจ้าของตัวอย่าง	: นาย ลิขิต ชีวาสวัสดิ์	หมายเลขคำขอ	: CMT 0556/66
โครงการ	: คอนกรีตมวลเบา	หมายเลขตัวอย่าง	: CMT NS0556/66-34
		วันที่รับตัวอย่าง	: 02-10-2566
ประเภท	: คอนกรีตบล็อกมวลเบา แบบเติมฟองอากาศ	วันที่ทดสอบ	: 05-10-2566
ความหนาระบุ	: - มม.	ผู้ทดสอบ	: จักรกฤษณ์
ความสูงระบุ	: - มม.		
ความยาวระบุ	: - มม.		

Specimen No.	Dimension (mm) w x l x t	Weight Dry (g)	Weight Saturate (g)	Absoption (%)	Average Absoption (%)	Remark
1	151.6 x 150.3 x 152.5	5,196.5	5,744.8	10.55	9.29	(Density 1600 kg/cu.m)
2	150.5 x 151.9 x 152.1	5,102.5	5,537.8	8.53		
3	151.4 x 152.7 x 152.4	5,128.8	5,579.6	8.79		

- รายงานนี้รับรองเฉพาะตัวอย่างที่ทำการทดสอบตามที่ระบุไว้ข้างต้นเท่านั้น
- ห้ามตัด ห้ามถ่ายสำเนาใบรายงานผลการทดสอบแต่เพียงบางส่วน ยกเว้นทำทั้งฉบับ โดยไม่ได้รับความยินยอมเป็นลายลักษณ์อักษรจากห้องปฏิบัติการ

ลงชื่อ ทิพย์ ฟัง ผู้รับรอง

(ผู้ช่วยศาสตราจารย์ ดร.ทิพย์วรรณ ฟังสุวรรณรักษ์)
รองผู้อำนวยการศูนย์เครื่องมือวิทยาศาสตร์และเทคโนโลยี
ปฏิบัติการแทนผู้อำนวยการศูนย์เครื่องมือวิทยาศาสตร์และเทคโนโลยี
17 ตุลาคม 2566

End of Report

อว 7432(5)/Rep. 0987

17 ตุลาคม 2566

แผ่นที่ 1/1

มหาวิทยาลัยเทคโนโลยีสุรนารี

ห้องปฏิบัติการทดสอบวัสดุก่อสร้าง

ศูนย์เครื่องมือวิทยาศาสตร์และเทคโนโลยี มหาวิทยาลัยเทคโนโลยีสุรนารี

ผลทดสอบการดูดซึมน้ำของคอนกรีตบล็อกมวลเบา มอก. 2601-2556

เจ้าของตัวอย่าง : นาย ลิขิต ชีวาสวัสดิ์	หมายเลขคำขอ : CMT 0556/66
โครงการ : คอนกรีตมวลเบา	หมายเลขตัวอย่าง : CMT NS0556/66-35
	วันที่รับตัวอย่าง : 02-10-2566
ประเภท : คอนกรีตบล็อกมวลเบา แบบเติมฟองอากาศ	วันที่ทดสอบ : 09-10-2566
ความหนาระบุ : - มม.	ผู้ทดสอบ : จักรกฤษณ์
ความสูงระบุ : - มม.	
ความยาวระบุ : - มม.	

Specimen No.	Dimension (mm) w x l x t	Weight Dry (g)	Weight Saturate (g)	Absoption (%)	Average Absoption (%)	Remark
1	151.7 x 152.2 x 152.7	6,022.3	6,402.0	6.30		
2	150.7 x 151.7 x 153.6	6,354.1	6,744.4	6.14	6.13	(Density 1800 kg/cu.m)
3	151.3 x 151.7 x 152.9	6,250.5	6,622.2	5.95		

- รายงานนี้รับรองเฉพาะตัวอย่างที่ทำการทดสอบตามที่ระบุไว้ข้างต้นเท่านั้น
- ห้ามตัด ห้ามถ่ายสำเนาใบรายงานผลการทดสอบแต่เพียงบางส่วน ยกเว้นทำทั้งฉบับ โดยไม่ได้รับความยินยอมเป็นลายลักษณ์อักษรจากห้องปฏิบัติการ

ลงชื่อ ผู้รับรอง

(ผู้ช่วยศาสตราจารย์ ดร.ทิพย์วรรณ ฟังสุวรรณรักษ์)

รองผู้อำนวยการศูนย์เครื่องมือวิทยาศาสตร์และเทคโนโลยี

ปฏิบัติการแทนผู้อำนวยการศูนย์เครื่องมือวิทยาศาสตร์และเทคโนโลยี

17 ตุลาคม 2566

End of Report

อว 7432(5)/Rep. 0988

17 ตุลาคม 2566

แผ่นที่ 1/1

ห้องปฏิบัติการทดสอบวัสดุก่อสร้าง

ศูนย์เครื่องมือวิทยาศาสตร์และเทคโนโลยี มหาวิทยาลัยเทคโนโลยีสุรนารี

ผลทดสอบมอดูลัสยืดหยุ่นของแท่งคอนกรีต (Elastic Modulus of Concrete Test)

เรียน	: มหาวิทยาลัยเทคโนโลยีสุรนารี		
ที่อยู่	: 111 ถนนมหาวิทยาลัย ตำบลสุรนารี อำเภอเมือง จังหวัดนครราชสีมา 30000		
โครงการ	: คอนกรีตมวลเบา	หมายเลขรับงาน	: CMT 0556/66
สถานที่	: -	หมายเลขตัวอย่าง	: CMTNS 0556/66-36
เจ้าของตัวอย่าง	: นายลิขิต ชีวาสวัสดิ์	วันรับตัวอย่าง	: 02-10-2566
วัสดุตัวอย่าง	: แท่งคอนกรีตมวลเบารูปทรงกระบอก ขนาด 150 x 300 มม.	วันทดสอบ	: 09-10-2566
		ผู้ทดสอบ	: นายจักรกฤษณ์ ธนะมณีวุฒิ

Specimen No.	Casting Date	Age (days)	Cure Type	Gauge Reading		Force Reading		Modulus of Elasticity (ksc)	Remark
				initial (mm)	at 0.4fc' (mm)	initial (kN)	at 0.4fc' (kN)		
1	3/9/2566	36	F	0.052	0.216	10	28	19,000	(Density 1000 kg/cu.m)
2	3/9/2566	36	F	0.056	0.196	10	28	22,257	(Density 1000 kg/cu.m)
3	29/8/2566	41	F	0.024	0.154	10	40	39,949	(Density 1200 kg/cu.m)
4	30/8/2566	40	F	0.014	0.128	10	60	75,926	(Density 1400 kg/cu.m)
5	30/8/2566	40	F	0.016	0.128	10	60	77,282	(Density 1400 kg/cu.m)

Cure Type : L = Laboratory ; F = Field

ลงชื่อ ผู้รับรอง

(ผู้ช่วยศาสตราจารย์ ดร.ทิพย์วรรณ ฟังสุวรรณรักษ์)

รองผู้อำนวยการศูนย์เครื่องมือวิทยาศาสตร์และเทคโนโลยี

ปฏิบัติการแทนผู้อำนวยการศูนย์เครื่องมือวิทยาศาสตร์และเทคโนโลยี

17 ตุลาคม 2566

- รายงานนี้รับรองเฉพาะตัวอย่างที่ทำการทดสอบตามที่ระบุไว้ข้างต้นเท่านั้น
- ห้ามตัด ห้ามถ่ายสำเนาใบรายงานผลการทดสอบแต่เพียงบางส่วน ยกเว้นทำทั้งฉบับ โดยไม่ได้รับความยินยอมเป็นลายลักษณ์อักษรจากห้องปฏิบัติการ

End of Report

อว 7432(5)/Rep. 0989

17 ตุลาคม 2566

แผ่นที่ 1/1

ห้องปฏิบัติการทดสอบวัสดุก่อสร้าง

ศูนย์เครื่องมือวิทยาศาสตร์และเทคโนโลยี มหาวิทยาลัยเทคโนโลยีสุรนารี

ผลทดสอบมอดูลัสยืดหยุ่นของแท่งคอนกรีต (Elastic Modulus of Concrete Test)

เรียน	: มหาวิทยาลัยเทคโนโลยีสุรนารี
ที่อยู่	: 111 ถนนมหาวิทยาลัย ตำบลสุรนารี อำเภอเมือง จังหวัดนครราชสีมา 30000
โครงการ	: คอนกรีตมวลเบา
สถานที่	: -
เจ้าของตัวอย่าง	: นายลิขิต ชีวาสวัสดิ์
วัสดุตัวอย่าง	: แท่งคอนกรีตมวลเบารูปทรงกระบอก ขนาด 150 x 300 มม.
หมายเลขรับงาน	: CMT 0556/66
หมายเลขตัวอย่าง	: CMTNS 0556/66-37
วันรับตัวอย่าง	: 02-10-2566
วันทดสอบ	: 09-10-2566
ผู้ทดสอบ	: นายจักรกฤษณ์ ธนะมณีวุฒิ

Specimen No.	Casting Date	Age (days)	Cure Type	Gauge Reading initial (mm)	Gauge Reading at 0.4fc' (mm)	Force Reading initial (kN)	Force Reading at 0.4fc' (kN)	Modulus of Elasticity (ksc)	Remark
1	1/9/2566	38	F	0.006	0.150	10	110	120,217	(Density 1600 kg/cu.m)
2	1/9/2566	38	F	0.006	0.144	10	110	125,444	(Density 1600 kg/cu.m)
3	2/9/2566	37	F	0.006	0.122	10	130	179,082	(Density 1800 kg/cu.m)
4	2/9/2566	37	F	0.006	0.132	10	130	164,869	(Density 1800 kg/cu.m)

Cure Type : L = Laboratory ; F = Field

ลงชื่อ ผู้รับรอง

(ผู้ช่วยศาสตราจารย์ ดร.ทิพย์วรรณ ฟังสุวรรณรักษ์)

รองผู้อำนวยการศูนย์เครื่องมือวิทยาศาสตร์และเทคโนโลยี

ปฏิบัติการแทนผู้อำนวยการศูนย์เครื่องมือวิทยาศาสตร์และเทคโนโลยี

17 ตุลาคม 2566

- รายงานนี้รับรองเฉพาะตัวอย่างที่ทำการทดสอบตามที่ระบุไว้ข้างต้นเท่านั้น
- ห้ามตัด ห้ามถ่ายสำเนาใบรายงานผลการทดสอบแต่เพียงบางส่วน ยกเว้นทำทั้งฉบับ โดยไม่ได้รับความยินยอมเป็นลายลักษณ์อักษรจากห้องปฏิบัติการ

End of Report

APPENDIX B

PUBLICATIONS

List of Publications

Pratama, H.C., Sinsiri, T., Chapirom, A., 2022. **Development of a Mixture of Lightweight Cell Crete for Green Roof Construction in Thailand**. The 27th National Convention on Civil Engineering. August, 2022, Chiang Rai, Thailand. 5

Pratama, H.C., Sinsiri, T., Chapirom, A., 2023. **Green Roof Development in ASEAN Countries: The Challenges and Perspectives**. Sustainability. 15.

Pratama, H.C., Sinsiri, T., Chapirom, A., 2024. **A Study of Roof Thermal Transfer Value (RTTV) Efficiency on Green Roofs**. Annual Concrete Conference 18. January, 2024, Nakhon Ratchasima, Thailand. 5

In Process

Pratama, H.C., Sinsiri, T., Chapirom, A., 2024. **The Role of Energy Efficiency for the New Green Roofs Construction Techniques by Using Lightweight Cellular Concrete.** The 18th East Asia-Pacific Conference on Structural Engineering & Construction (EASEC-18). November, 2024, Chiang Mai, Thailand

Development of a Mixture of Lightweight Cell Crete for Green Roof Construction in Thailand

Hanny Chandra Pratama[1] Theerawat Sinsiri [1,2*] and Aphai Chapirom[2]

[1] *Civil Engineering Program, School of Engineering, Suranaree University of Technology, Nakhon Ratchasima, THAILAND*
[2] *Sustainable Innovative and Energy – Efficient Construction Materials (SIE-CON) School of Engineering, Suranaree University of Technology, Nakhon Ratchasima, THAILAND*
**Corresponding author; E-mail address: sinsiri@g.sut.ac.th*

Abstract

Green roofs are still not widely known in Thailand. It is caused by the complicated construction process, the need of imported materials, and the higher cost compared to conventional roofs. Green roofs are considered a new alternative due to their ability to reduce power usage, noise, air pollution. develop an urban ecosystem, and so on. Thus, the researcher is interested in using lightweight cell crete (LCC) as a load structural material to support the weight of the soil used to grow plants, since the lightweight cell crete has the following properties: strength, resistance to heat, waterproofness, soundproofness, and light weight. Moreover, the construction cost will be more affordable. The purpose of this study is to determine lightweight cell crete for applying on green roof. The density of lightweight cell crete is set range 600 – 1,800 kg/m^3. The result found that the properties of lightweight cell crete 1,200 and 1,400 kg/m^3 meets the standard to substitute the normal concrete. In addition, the researcher put the green roof with lightweight cell crete structure to the test in actual site and found that it can contribute to the increase of green space in urban life. The cost of construction was reduced, as was the temperature inside the building. It is advantageous for Thailand's green roof industry.

Keywords: green roof, energy-saving roof, lightweight cell crete, green roof lightweight cell crete

1. Introduction

Temperatures in cities continue to rise as a result of urban heat islands (UHI) and the consequences of climate change. As a result, energy consumption has increased over past four decades [1]. The Electricity Generating Authority of Thailand (EGAT) has collected electricity-related data and report in its Annual Report. In the past 13 years (2000 – 2012), Thailand's overall electricity usage has risen to 75.01 percent and is continuing to rise [2]. The air conditioning system consumes the majority of energy in order to cool the indoor air due to the high rate of thermal heat transfer into the room. Researchers are interested in resolving the UHI issue through the use of green roofs [3].

Reduction of surface temperature and thermal comfort are the two important functions of the green roof in urban areas. Green roofs offer a natural and sustainable way to cover building envelopes with vegetation to bring multiple benefit in urban life. Moreover, Green roofs limit heat transfer through building roofs by around 80% in the summer [4]. In tropical countries, green roof has an important performance of rainwater detention and retention. Because of the significant water content storage on humid-tropical green roofs, thermal performance is twice as effective as in temperate zones [5]. However, green roofs on buildings are not widely used in Thailand. Some of the reasons for not implementing green roofs are the high cost of heavy structure and layer installation, as well as the maintenance costs.

Lightweight Cell Crete (LCC) can be presented as a solution for load-supporting construction, taking into consideration building weight and cost. LCC is created by injecting air from a foam agent into a slurry concrete mixture. The essential benefit of LCC as a roof material is its low density and low thermal conductivity. LCC has a density range of 600 to 1800 kg/m3, which is significantly lower than normal concrete, and a thermal conductivity range of 0.1–0.7 W/m.K, which decreases with density [6].

This study is an experimental study of the properties of LCC to identify the feasibility standard for using LCC as load structural supports for green roofs. By analyzing the data on LCC properties and the green roof standard, it will be feasible to develop a potential guideline for integrating LCC in green roofs in order to enhance the efficiency of green roofs and minimize the cost problems.

2. Materials and Methods

2.1 Lightweight Cell Crete Materials

This study is a development mixture from the previous study, where the result obtains a recommended method to provide a proper LCC properties by horizontal mixer with 45 rpm [7]. The consistency of 45 rpm speed used to improve the quality of LCC properties better than those on general used in 60-70 rpm. Excessive rotation over 45 rpm can damage the mortar's foam bubbles. Fig 1 shows the horizontal mixer developed by Suranaree University of Technology.

Fig 1. Horizontal Concrete Machine

The LCC composition consists of Portland Cement Type-I, fine sand, foam agent, and water follows the requirements of ASTM C150 with the water to cement ratio (w/c = 0.5).

This current study, we used the SUT V2.1 foam agent (Suranaree University of Technology foam agent version 2.1) since it is made by natural protein to relate with green issues with a pH of 8.55, SG of 1-1.05, and foam density of 40-50 kg/m^3. Therefore, all of appliance material in LCC is found and made by local materials. Table 1 shows the composition of LCC mixed design.

Table 1 Composition of LCC density range 600 – 1800 kg/m^3

Density (kg/m^3)	Cement (kg)	Fine Sand (kg)	Water (kg)	Foam (kg)
600	460	0	205	30
800	429	160	184	27
900	417	280	177	25
1,000	408	395	172	24
1,200	396	617	165	20
1,400	388	834	160	17
1,600	382	1,047	157	14
1,800	377	1,258	154	10

The process of mix-design is described in Fig.2. Firstly, pour the cement, fine sand, and water into the horizontal mixer follows the composition of specified LCC density. After the mortar mixed well, in Fig. 3, the specified amount of foam agent is injected and mixed until the mortar has bubble textures following the guideline of ACI 523.3R-14. Last step before molding process, the mortar will be weighed to check the wet density according to the target density we want by a tolerance range ± 50 kg/m^3.

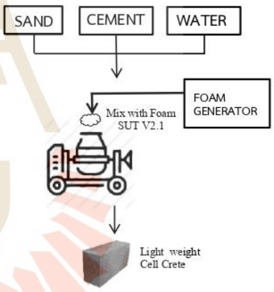

Fig 2. Method of LCC mix design

Fig 3. Adding foam agent into mortar

The following step is poured into the prepared molds. The mortar was poured into the mold immediately after preparation to get a target density range of 600 - 1,800 kg/m^3 of fresh concrete. The molds are the cubic shape at 150 x 150 x 150 mm and the rectangular shape at 300 x 300 x 75 mm., as shown in Fig. 4

Fig 4. LCC molding process

The curing treatment of the samples was by wet covering method (moist curing) for 28 days before the test.

2.2 Test Method

2.2.1 Thermal conductivity test

In determining the thermal conductivity of the LCC samples, the test was conducted accordance to ASTM C 177 – 97 [8]. The three samples of 300 x 300 x 75 mm. were examined using two isothermal cold surface assemblies and a guarded hot plate.

2.2.2. Compressive strength test

Compressive strength test for this study was conducted according to the BS EN 12390-3 [9]. For this test, three samples 150 x 150 x 150 mm. have been prepared for laboratories test. The testing machine will apply the selected load to the specimen and increase continuously until no greater load can be sustained. The maximum load will be recorded.

2.2.3. Water absorption test

Water absorption test was conducted in order to determine the percentage of the water absorption by the LCC. The test was accordance to the TIS 2601-2556 [10]. Initially, the LCC samples were dried in the oven at 100°C for 24 hours. The samples were then cooled down before immerse in the water tank for another 24 hours. In order to assess the percentage of water absorption, the weight of samples was measured before and after immersion in the tank

3. Results and Discussions

3.1. Thermal Conductivity

The thermal conductivity results of LCC range 600 – 1,800 kg/m^3 illustates in Fig. 5. The results shows that the number of thermal conductivity will increase follow the density.

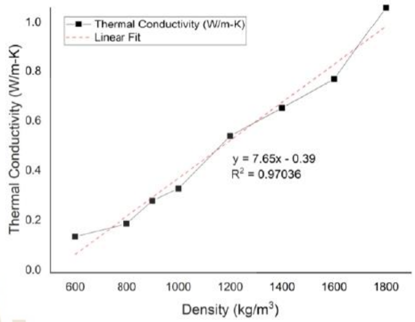

Fig 5. Thermal conductivity result

The LCC density (600, 800, 900, and 1,000 kg/m^3) reach the thermal conductivity at 0.134, 0.186, 0.276, and 0.327 W/m.K. The thermal conductivity is starting to significantly increase on LCC density 1,200, 1,400, and 1,600 kg/m^3 at 0.540, 0.652, and 0.769 W/m.K respectively. The highest density samples in this study, 1,800 kg/m^3 density reach at 1.059 W/m.K.

Based on general result in some previous studies, LCC has a lower thermal conductivity than conventional concrete [11-12]. It indicates that the prospective combination of a green roof and LCC as the roof deck will enhance the heat transfer resistance and result in a room with a cooler temperature than conventional concrete.

3.2. Compressive Strength

Compressive strength testing shows in Table 2. From the data, we can categorize the types of LCC based on the strength.

There are three different lightweight concrete type divisions in terms of strength range, which are low-density concretes (0.7-7.0 MPa), moderate-strength concretes (7-14 MPa) and structural concretes (17-63 MPa) [13]. The moderate-strength concretes are recommended to apply as a load bearing for supporting the roof deck of green roof.

Table 2 LCC categorizes based on the strength

Density (kg/m^3)	Compressive Strength (MPa)	Lightweight Concrete Category
600	1.2	low-density concretes
800	2.0	low-density concretes
900	2.8	low-density concretes
1,000	3.5	low-density concretes
1,200	4.8	low-density concretes
1,400	8.8	Moderate-strength concretes
1,600	16.4	Structural concretes
1,800	18.3	Structural concretes

3.3. Water Absorption

The percentage of water absorption for each density type illustrates in Fig 6. As can be seen, low-density concretes (600 and 800 kg/m^3) with high porosity exhibit substantial water absorption (42.94 and 28.54 percent, respectively). LCC with density 900 and 1,000 kg/m^3 decrease significantly to 16.92% and 12.42% respectively. The percentage of water absorption continuous to decrease where water absorption of LCC (1,200 and 1,400 kg/m^2) are 11.86% and 10.06%. The water absorption of LCC 1,600 and 1,800 kg/m^3 reach the slightly result at 7.30% and 7.19%. The result meets the recommendation since the percentage of water absorption of LCC 1,200 – 1,800 kg/m^3 less than 12% [14].

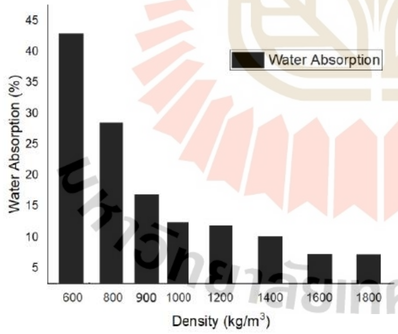

Fig 6. Water absorption result

4. Conclusions

1. LCC has a lower thermal conductivity more than normal concrete. Due to its low thermal conductivity, it indicates that green roof heat transmission will be enhanced when LCC is used as the roof deck material.
2. The outcome indicates that LCC with density 1,400 kg/m^3 has the potential to replace normal concrete as a roof deck since it categorized as moderate-strength concrete. Therefore, the roof deck will be more efficient in structure load, cost, and strength.
3. The aims of a green roof are to retain moisture content and nourish plant life. In other hand, the roof deck is also holding the important role to prevent the water leakage. Therefore, water absorption is an important factor to consider while utilizing a green roof's quality. The LCC range of 1,200 to 1,400 kg/m^3 is a suitable option for retaining water absorption since the value is less than 12%.

6. Recommendation and Future Works

Green roofs offer a natural and sustainable way to bring multiple environmental benefits, including improving building energy efficiency. Passive design with a green roof system offers a solution to reduce heat gain from solar radiation through the roof.

(a)

(b)

(c)

Fig 7. (a) Roof deck from LCC, (b) Planting the vegetation on green roof, and (c) Green roof integrated LCC

In addition, as shown in Fig. 7, the researcher put the green roof with LCC 1,200 kg/m^3 with extra adding structure support to test in actual site and found that it can contribute to the increase of green space in urban life.

This research studied the development of a mixture of lightweight cell crete for green roof construction in Thailand. According to the results, an LCC range of 1,200 to 1,400 kg/m^3 is recommended for use in green roof systems. By using LCC, the structure load and the cost of construction was reduced. It is advantageous for Thailand's green roof industry.

The application of LCC on green roof still requires additional research into the broader green roof system. The water leakage might be a main problem of the LCC green roof system in a long-term application. Therefore, the future research suggested the additional research concern on the drainage system model in LCC green roof system to prevent the water leakage and may reduce the installation cost and maintenance cost more than normal green roof.

Acknowledgement

This study is supported by research funds to extend knowledge from Thailand Science Research and Innovation (TSRI) on Precast Cellular Concrete. The authors are grateful to the Suranaree University of Technology, Sustainable Innovative and Energy Efficient Construction Material (SIE-CON), and Infinity Concrete Technology, Co. Ltd for providing support both financially and using its facilities.

References

[1] Santamouris, M. (2014). Cooling the cities - A review of reflective and green roof mitigation technologies to fight heat island and improve comfort in urban environments, *Sol. Energy*, vol. 103, pp. 682–703..

[2] Suwapaet, N. (2016). Thailand electricity consumption during 2000 – 2012 ; facts and trends. no. September 2013.

[3] Munir, A. and Afifuddin, M. (2020). Thermal Performance of Precast Foam Concrete Integrated with Green Roofs System.

[4] Besir, A. B. and Cuce, e. (2018). Green roofs and facades: A comprehensive review, *Renew. Sustain. Energy Rev.*, vol. 82, no. July 2017, pp. 915–939.

[5] Hashemi, S. S. G., Bin Mahmud, H. and Ashraf, M. A. (2015). Performance of green roofs with respect to water quality and reduction of energy consumption in tropics: A review. *Renew. Sustain. Energy Rev.*, vol. 52, pp. 669–679.

[6] Chica, L. and Alzate, A. (2019). Cellular concrete review: New trends for application in construction. *Constr. Build. Mater.*, vol. 200, pp. 637–647.

[7] Chapirom, A., Sinsiri, T., Jaturapitakkul, C., and Chindaprasirt, P. (2019). Effect of speed rotation on the compressive strength of horizontal mixer for cellular lightweight concrete, *Suranaree J. Sci. Technol.*, vol. 26, no. 2, pp. 113–120.

[8] ASTM C177. (1997). Standard Test Method for Steady-State Heat Flux Measurements and Thermal Transmission Properties by Means of the Guarded-Hot-Plate," p. 22.

[9] British Standard Institute. (2001). BS EN 12390-3:2001 Testing hardened concrete - Part 3: Compressive strength of test specimens," *BSI Standards Publication.* pp. 4–10.

[10] TIS 2601-2556. (2018). Lightweight Foamed Concrete, *Announc. Minist. Ind.*, vol. 1, no. 1, pp. 1–10.

[11] Ganesan, S., Othuman Mydin, M. A., Mohd Yunos, M. Y., and Mohd Nawi, M. N. (2015). Thermal Properties of Foamed Concrete with Various Densities and Additives at Ambient Temperature. *Appl. Mech. Mater.*, vol. 747, no. March, pp. 230–233.

[12] Tasdemir, C., Sengul, O., and Tasdemir, M. A. (2017). A comparative study on the thermal conductivities and mechanical properties of lightweight concretes. *Energy Build.*, vol. 151, pp. 469–475.

[13] Chaipanich, A. and Chindaprasirt, P. (2015). *The properties and durability of autoclaved aerated concrete masonry blocks*. Elsevier Ltd.

[14] Nurain Izzati, M. Y. *et al.*, (2019). Strength and water absorption properties of lightweight concrete brick. *IOP Conf. Ser. Mater. Sci. Eng.*, vol. 513, no. 1.

sustainability

MDPI

Review

Green Roof Development in ASEAN Countries: The Challenges and Perspectives

Hanny Chandra Pratama [1], Theerawat Sinsiri [1,2,*] and Aphai Chapirom [2]

[1] School of Civil Engineering, Suranaree University of Technology, Nakhon Ratchasima 30000, Thailand; hannychandra.arch@gmail.com

[2] Sustainable Innovation and Energy-Efficient Construction Materials (SIE-CON), Suranaree University of Technology, Nakhon Ratchasima 30000, Thailand; aphai_ch@g.sut.ac.th

* Correspondence: sinsiri@sut.ac.th; Tel.: +66-803347718

Abstract: Green roofs (GRs) have emerged as an essential component for the sustainability of buildings, as they reduce the need for cooling energy by limiting heat transmission into building space. The benefits of implementing GRs are appropriate in tropical regions with hot temperatures. The entire Association of Southeast Asian Nations (ASEAN) is located in a tropical climate and receives about 12 h of sunlight every day throughout the year, which offers excellent opportunities to install GRs. This research reviews the literature on GR knowledge in ASEAN countries over the past decade (2012–2022) and discusses two main points including (i) GR development level status and (ii) GR performance regarding drivers, motivations, and barriers. The review reveals that Singapore and Malaysia are two among ten countries with significant developments in GRs. Barriers to expertise, government regulations, and public awareness of green roofs represent the most challenging aspects of GR implementation in ASEAN countries. Although research regarding the use of green roofs has been conducted widely, ASEAN countries still need to investigate regulatory breakthroughs, incentives, and technology applications to encourage the use of GRs. The review recommends promoting the use of GRs, which have the potential to reduce energy consumption by up to fifty percent, outdoor surface temperature up to 23.8 °C, and room temperature to 14 °C. The use of GRs can also mitigate runoff issues by up to 98.8% to avoid the risk of flooding in ASEAN countries, which have high rainfall. In addition, this review sheds new insights on providing future potential research to improve GR development in the ASEAN region.

Keywords: green roofs; tropical green roofs; cities; sustainable development

check for updates

Citation: Pratama, H.C.; Sinsiri, T.; Chapirom, A. Green Roof Development in ASEAN Countries: The Challenges and Perspectives. *Sustainability* **2023**, *15*, 7714. https://doi.org/10.3390/su15097714

Academic Editors: Pingping Luo, Guangwei Huang, Binaya Kumar Mishra and Mohd Remy Rozainy Bin Mohd Arif Zainol

Received: 4 March 2023
Revised: 18 April 2023
Accepted: 25 April 2023
Published: 8 May 2023

1. Introduction

Changes in a city's appearance caused by population density have a substantial effect on land-use change, replacing green spaces and vacant land with urban infrastructure [1]. Among all the continents in the world, Asia has the biggest population, which accounts for around 61% of the global population (4.7 billion). The world's most populated country is China (1438 million), followed by India (1380 million), the United States (331 million), Indonesia (273 million), and Pakistan (220 million), and four of the top five most populous countries are located in mainland Asia [2]. Population density can lead to numerous issues, such as: greenhouse gas emissions, climate change, the urban heat island (UHI) effect, air and water pollution, and frequent flooding, owing to the lack of green spaces, which have necessitated the development of innovative responses to the issues of urban living [3–5].

Green (vegetated, eco, or living) roofs are basically roofs planted with vegetation on top of a growth medium (substrate). The concept was designed and developed to be incorporated into urban infrastructure to offset the effects of climate change, urban expansion issues, and other potential difficulties related to human intervention in ecosystems. GRs generally comprise several components, including vegetation, substrate, filter fabric, drainage material, root barrier, and insulation. Each component plays a mutually beneficial role in the system that forms the benefits of GRs [6,7].

GRs can enhance the energy efficiency of buildings and help mitigate the UHI effect by lowering the ambient temperature and improving thermal comfort for humans [8,9]. Additionally, GRs help to store rainwater and delay peak flow, reducing the risk of floods. Some of the rainwater will be absorbed by the substrate or trapped in the pore spaces. It can also be absorbed by plants and retained in plant tissues or transpired back into the atmosphere [10]. GRs buffer acidic rain and theoretically retain pollutants, thereby producing good quality stormwater runoff [10,11]. Sound absorption is another feature of GRs; sound can be minimized by absorbing sound waves diffracting over roofs [12]. The GR system is a popular approach that could help to mitigate air pollution in urban environments. More precisely, on a sunny day, GRs may lower the CO_2 concentration in the nearby region [13,14]. GRs also aid in restoring biodiversity that has been lost due to urban development and offer a safe place for birds, insects, and different plants to grow [15].

GRs can be classified by their purposes and characteristics into two major types: intensive roofs and extensive roofs. Intensive green roofs (IGRs) need a deep substrate and require skilled labor, irrigation, and constant maintenance. IGRs are usually associated with roof gardens and need additional structural support due to the heavy weight of the substrate [16,17], while extensive green roofs (EGRs) have a relatively thin layer of soil and grow sedums or moss. EGRs require lower maintenance and cost less, resulting in more widespread application compared to IGRs [18–20].

As GRs have become more popular in the recent decades and their implementation has expanded beyond Europe, the urge to understand how this novel ecosystem functions has arisen in many areas. Various studies have been conducted to assess the novelty and suitability of green roofs in non-tropical areas, but only few have been conducted in tropical areas [21]. The tropical region contains a greater amount of daylight than does the temperate zone. For this reason, an evaluation is needed to measure how to adapt the design to the climatic features of tropical green roofs.

In recent years, there have been many publications on GRs. According to Web of Science, more than 2400 articles, reviews, book chapters, and proceedings papers on green roofs have been published in the last 30 years (1989–2018). Individual continents show that most publications were issued in Europe (37.84%), followed by Asia (29.11%), North America (24.93%), Australia (4.72%), and South America (2.49%), with the lowest number of publications in Africa (0.91%) [22]. In Asia, a closer examination shows that research has come from only several countries, including China, Japan, South Korea, India, Taiwan, and Iran. Even though ASEAN countries dominate the tropical region in Asia, relatively little green roof literature has been published. Out of approximately 10 ASEAN member states, including Brunei, Cambodia, Indonesia, Laos, Malaysia, Myanmar, the Philippines, Singapore, Thailand, and Vietnam, only Singapore has made significant green roof research contributions [23].

Therefore, this paper aims to identify the current conditions and perspectives related to GRs in ASEAN countries by reviewing the research articles based on ASEAN cases. The paper then addresses the GR development level in ASEAN countries as well as discusses the key findings observed in the drivers, motivations, and barriers of GRs. We anticipate the study will provide qualified support to urban planners and policymakers for urgent future research to advance the development of GRs in ASEAN countries.

2. Materials and Methods

This study uses a systematic literature review (SLR) to eliminate bias and increase scientific value. According to Uman [24], systematic literature review examines the findings of previous studies in order to recognize recurring and consistent patterns. The three pillars of rigor, transparency, and replicability form the basis of a systematic literature review (SLR), which allows deeper understanding of a subject and identification of knowledge gaps [25]. The SLR adopted in this article follows the PRISMA protocol according to Moher et al. [26], and the number of stages of the PRISMA protocol varies according to the authors.

For this study, a comprehensive literature search was undertaken to identify papers specifically published between 2012 and 2023. To search for the articles, we utilized Scopus, MDPI, Science Direct, and industry reports. There were ten search country terms within the title, abstract, and keywords of the articles on the significance of green roofs in ASEAN countries, including ("green roofs") AND ("Brunei" OR "Cambodia" OR "Indonesia" OR "Laos" OR "Malaysia" OR "Myanmar" OR "Philippines" OR "Singapore" OR "Thailand" OR "Vietnam"). Inclusion and exclusion criteria include language, timeline, and literature type.

For data analysis, the title, abstract, keywords, journal name, authors' names, and year of publication of the searched records were exported to an MS Excel spreadsheet. Two independent authors screened the paper titles and abstracts independently. Then, two independent reviewers performed an eligible assessment by carefully screening the full text of papers that were screened in the first screening process to assess their fit with the inclusion criteria. During this stage, disagreements between reviewers were resolved through arbitration by the other two reviewers.

Data that were exported to an MS Excel spreadsheet were modified by adding items for which data were sought for data management. As shown in Figure 1, the PRISMA approach includes two rounds of elimination. The first round of screening classifies the articles into conceptual, theoretical, and empirical studies. The second screening is an evaluation that involves reading the full texts and classifying them into one of six GR development level categories according to Zhang's methods [27]. From the review of 99 total full-text articles, we selected 70 articles, which were included for qualitative synthesis review. Out of these 70 full-text articles, with publication dates ranging between 2012 and 2022, 47 articles (67%) were qualitative, and 23 articles (33%) were quantitative.

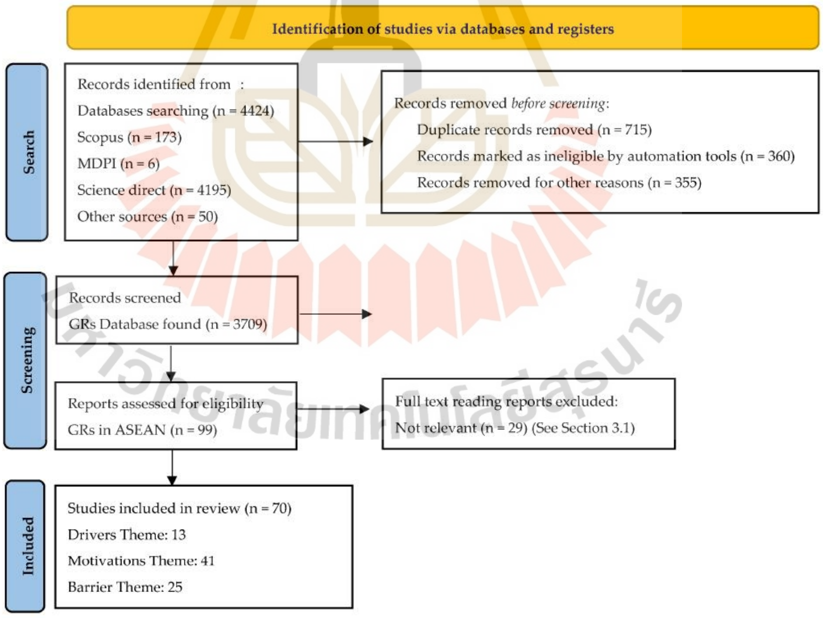

Figure 1. PRISMA flow diagram for green roof database in ASEAN countries.

Selected literature refers to the number of studies providing evidence, despite the fact that clearly, not all studies provide evidence of equal quality. We extrude all the result data in selected literature by systematically presenting the group theme of research (drivers, motivations, and barriers) to determine the scope and gaps in the ASEAN countries' study of GRs. We anticipate the study will provide qualified support and can help researchers design urgent GR future research in ASEAN countries.

3. Results

3.1. Mapping of Selected Literatures

The academic journals gathered using searching strategies resulted in a total of 99 papers.

The filtering process outlined in the previous section selected the 70 most relevant studies for a full-text review. Studies that did not meet the eligibility criteria comprised reviews, studies comparing green roofs with other technologies but not nongreen roofs, and studies presenting no comparisons. Such studies were not included in the selected literature.

Figure 2 provides the details of the papers obtained initially, regarding the number of papers selected for the review based on the ASEAN country cases. It is shown that Malaysia has a significant amount of literature available on the contribution of GRs as compared to other countries for the GR drivers; this includes studies reporting policy pressure from government as encouragement to use GRs (e.g., Ismail et al. [28], Fauzi et al. [29,30]) and advance technology of GRs (e.g., Munir et al. [31], Mahdiyar et al. [32]). When it comes to the motivations behind using GRs, several studies have provided examples, including those related to the energy efficiency of GRs (e.g., Sittipong and Pichai [33]); the urban heat island (UHI) effect, such as studies that report the benefits of GRs to outdoor surfaces (e.g., Munir et al. [34]); and indoor room temperature (e.g., Irsyad et al. [35]) as compared to conventional roofs. Moreover, motivation to use GRs is also derived from their capacity to control runoff, including storm water retention (e.g., Orozco et al. [36]) and runoff water quality (e.g., Romali et al. [37]). There are also data regarding the motivation for using GRs to increase biodiversity (e.g., Sananunsakul [38]). Lastly, in investigating barriers of GRs in ASEAN countries, a large number of studies addressed the problem. These could be grouped into three categories: government policy and technological barriers, which were only found in Singapore and Malaysia; economic barriers, as when installation costs are highly volatile (e.g., high price GRs in Brunei [39] and low price GRs in Vietnam [40]); social acceptability and feasibility barriers, which are discussed in numerous studies.

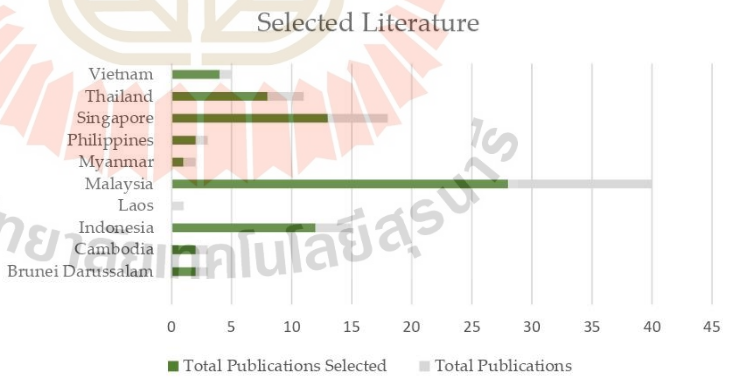

Figure 2. Schematic representing total search findings and the number of studies sorted for full-text review.

Figure 3 shows that the majority of studies conducted in ASEAN countries focused on the motivations for implementing GRs, totaling 52%. The motivations are still the focus since ASEAN societies are still attempting to validate the advantages of using GRs and overcome the main barriers. On the other hand, driver research is still insufficient. Drivers are urgently needed to help ASEAN countries accelerate the development of GRs. The findings of each selection criteria will be described in the stages of green roofs in ASEAN countries (Section 3.2). In addition, the reviews of green roofs' potential in ASEAN countries as well as the social acceptability and feasibility issues will be provided (Section 3.3).

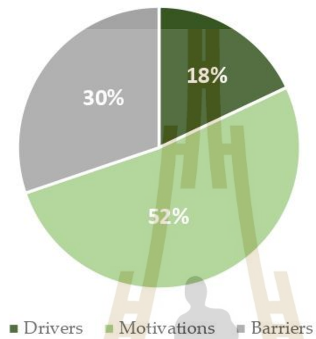

Figure 3. Schematic representing total type of selected literature, including drivers, motivations, and barriers.

3.2. Stages of Green Roofs in ASEAN Countries

The existence of green buildings as approaches to environmental restoration has increased in urban green spaces during the past decade to reduce climate change. Figure 4 illustrates the number of urban green spaces in various major Asian cities.

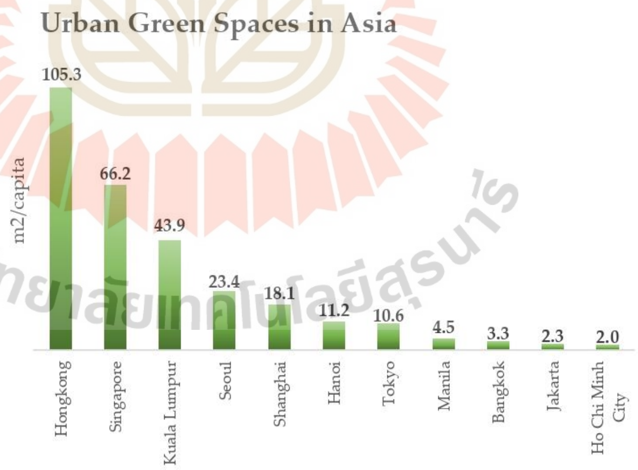

Figure 4. Number of urban green spaces in several countries in Asia. (This figure is illustrated using the data from Hasnan, available online in theaseanpost.com [41]).

In the data, there are several metropolises that are included in ASEAN countries, Singapore (66.2 m^2/capita); Kuala Lumpur, Malaysia (43.9 m^2/capita); Hanoi, Vietnam (11.2 m^2/capita); Manila, Phillipines (4.5 m^2/capita); Bangkok, Thailand (3.3 m^2/capita); Jakarta, Indonesia (2.3 m^2/capita); and Ho Chi Minh City, Vietnam (2.0 m^2/capita) [41]. However, WHO suggested a standard of 9 square meters per capita. Moreover, a previous study mentioned the ideal urban green space value of a modern city is 50 m^2 per capita. [34,42]. Singapore, Malaysia, and Vietnam are the three leading ASEAN nations that have met the minimum standards for green space. In addition, Singapore has exceeded the ideal indicator of urban green space, making Singapore a modern ASEAN city. As observed, Singapore's approach is similar to Hong Kong's, which includes the implementation of a three-dimensional green space system. This is demonstrated by the existence of numerous green projects, including Gardens by the Bay, Singapore Botanic Garden, and NUT Green Roof. Malaysia, on the other hand, has to add approximately 7 m^2/capita to resemble Singapore as a modern city. The implementation of an ideal green area could increase the city's wealth and property values. This is also related to the fact that GRs can boost people's happiness and lower the risk of depression [43,44]. In addition, according to UNICEF, the creation of urban green areas can considerably enhance the physical, mental, and social development of children [45].

GR technology has developed as a solution for combating the lack of urban green space. However, GR growth in developing countries is slower than in developed nations. This is also influenced by the number of GR research publications in developed countries, with USA, China, and Italy dominating the contributions with total percentages of around 22%, 13%, and 9% while developing countries (India and Iran) are below 2%. Interestingly, Singapore, a developed country in the ASEAN region, cannot contribute much to green roof research, as it only contributes under 2% [22]. Lack of interest, applicable policies, and standards, as well as incompetence, are the most frequently cited obstacles to knowledge and awareness in developing countries [46].

GR implementation is a complicated issue concerning many aspects. According to Zhang [27], GR implementations are started from "Environmental and Social Problems" that plague cities in Stage 1 (e.g., heatwaves, urban warming, and urban flooding). The problems resulting from "Diverse Pressure", such as in environmental pressure (e.g., energy, water, and air), social pressure (e.g., health, safety, mortality, and morbidity), economic pressure (e.g., expenditure, productivity, and market) and policy pressure (e.g., urban sustainability, energy saving, and water saving) are included in Stage 2. The pressure from various aspects drives a response for tackling the problem through "GR Research and Development" in Stage 3, where some studies have been conducted to monitor, model, and assess GR performance.

After the preliminary approach from Stages 1 to 3, GRs have actually been implemented in the "Promotion" Stage 4, where regulation and stimulation have been started to support further steps in GR development. In "GR Implementation" Stage 5, a systematic process is relevant to practical GR application in cities, including design, construction, contract and supply, operation, and maintenance. "Performance Evaluation" Stage 6 is evaluation in terms of GRs' function in addressing environmental and social issues in cities. Figure 5 shows the framework of green roof development. Furthermore, several studies or actual projects in ASEAN countries will be briefly evaluated and classified according to their stages of development below.

Figure 5. The framework for green roof development, promotion, and application. (This figure is adapted from the previous study by Zhang [27]).

Brunei is also known as Brunei Darussalam. The country, which is one of the relatively small countries in the ASEAN region, is still considered to be in "Diverse Pressure" (Stage 2) as a result of several challenges in developing GRs. GR development in Brunei started from Stage 1, where increasing temperature increases electrical consumption. The government is interested in implementing GRs in an effort to reduce energy consumption by an estimated 30 percent [47]. This energy issue necessitates Stage 2 to evaluate public interest in GRs. According to results of an actual survey in Bandar Sri Bengawan, the capital city of Brunei, only 7% of the 414 buildings constructed using flat-roof reinforced concrete have the potential for GR installation. People prefer pitched roofs because of their strength and prevention of leaks. Moreover, GRs' appeal to society is as of yet minimal. A survey of building owners' interest in the usage of GRs revealed that only 24% of respondents supported the implementation of GRs [48] The level of public awareness of GRs could be increased by educating buildings' owners and increasing the involvement of professional knowledge and government sectors.

For the past decade, Cambodia has experienced flood problems in the capital city of Phnom Penh. This is due to limited capacity of the city's drainage system. Lyna mentioned that several areas in Phnom Penh were affected by flooding with a height of more than one meter [48]. The current issue in Cambodia is classified as Stage 1, which motivates researchers to solve the flood problem by improving green infrastructure. Tree canopies, bioswales, permeable pavements, and green roofs are some of the green infrastructure options proposed by Nou in his study [49]. In the development of green infrastructure, the use of GRs can be suggested according to previous research by Sarkar indicating that GRs can reduce runoff control by 18 to 29% [50].

Indonesia is located in the equatorial zone with high average temperatures during daytime and relative exposure time. The high temperatures in Indonesia appear to be a major issue in Stage 1 for Indonesia. Jakarta, as the metropolitan city in Indonesia, has average daytime temperatures that could reach up to 35 °C. The surface of a roof exposed to the sun during the day can be affected by temperatures as high as 50 °C [51]. In order to limit the heat absorption into buildings, the development of GRs in Indonesia is important. An evaluation study in Bandung has undertaken Stage 2 to analyze the deployment of GRs in the targeted area. GRs can be applied on the slab concrete roofs of 53 out of 222 dwellings. Sloped roofs that may not be suitable for GRs installation are still prevalent in Indonesia [52]. Several GR research studies and developments, which are categorized as Stage 3, are also being conducted. A study by Munir found that the use of lightweight foamed concrete and a green roof reduces construction loads and cooling loads for air conditioning systems [51]. Moreover, as an alternative to concrete, corrugated zinc roofing could be used as the base of a building's green roof. Yuliani mentioned that corrugated zinc roofs have the fastest response to cold down to 2 °C compared to concrete-based GRs [53]. Unfortunately, there is no research for GR-supporting regulations in Indonesia.

Malaysia is one of the ASEAN member countries with positive GR development. It accounted for 28 papers in the research database on GRs, the highest of all ASEAN countries. Based on a survey by Rahman, the 30 cases where projects integrated GRs categorized it as Stage 5. Interestingly, GRs are popularly implemented in condominiums and offices with 11 projects and 5 projects, respectively [53]. However, mostly, GR projects in Malaysia are privately accessed only for those who own condominiums or work at offices. It may be an obstacle to promote GRs on small scales such as with residential housing, schools, or low-rise buildings. However, some research projects in Malaysia have reached Stage 6, and performance evaluations of the implementation of GRs on public buildings have been reviewed by Rahmat [54]. He mentioned that GRs might reduce the average surface temperature by between 3.6 °C and 11.1 °C compared to conventional roofs. Evaluations of the performance of actual buildings are expected to present to the market the fact that GRs increase building performance.

Myanmar's government initiated implementation of smart city projects in Yangon and Mandalay. However, references and standards for green buildings in Myanmar remain inadequate. Lwin mentioned that "energy efficiency" and "water efficiency" are the most crucial problems, categorized as Stage 1 [55]. Lwin also mentioned the necessity of further development of a green building rating system for Myanmar, which should be considered along with the domestic conditions of the country and categorized as Stage 2 [55]. In addition, there is still no specific information on GR development in Myanmar. GRs can reduce building electricity consumption and improve water quality through absorption, making them a viable option for future research in Myanmar to increase energy efficiency and water efficiency.

Urbanization from rural to urban areas in the Philippines has resulted in 51.2% of the population moving and residing in cities, categorized as Stage 1 [56]. The development of Stage 3 GRs has also been carried out through research to increase water retention. The results show that adding 0.6% hydrogel to the soil can increase water retention to 45.46%, which is higher than the 30.07% achieved by GRs without hydrogel [57]. GRs have been implemented in the Philippines, and it is evident that there are several GR suppliers in the Philippine construction market, which is classified as Stage 5. Orozco surveyed a number of local GR suppliers in the Philippines. The results revealed that green roofs generally met minimum standards [36]. By adjusting GR products based on environmental and climatic conditions of the Philippines, providing local materials, and developing GR experts, it is possible to overcome the aforementioned problems. However, a study about "Promotion" Stage 4 from the government has not been found.

Currently, Singapore is a thriving, world-class urban center with limited land and resources. However, Singapore's high level of greenery is largely the result of decades of careful planning. The Singapore Sustainable Development Blueprint maximizes land use while maintaining 8 m^2 of green space per person and increasing the amount of greenery in high-rise buildings to 50 ha by 2030 [23]. Another government institution, Singapore National Parks (NParks), has introduced a GR incentive to encourage owners of existing buildings to have GRs, which is categorized as Stage 4. The program supported approximately 50% of GR installation costs in order to promote GR application and create a green urban environment [58]. Referring to the installation of GRs as categorized as Stage 5, Singapore has remarkable GR projects that have attracted many building owners in Singapore. Projects such as Nanyang Technological University (NTU) have been known all around the world as stunning works of architecture (See Figure 6). NTU received the Green Mark Platinum Award from the Singapore Building and Construction Authority (BCA) for adopting best practices in environmental sustainability. The GR performance evaluation, which is categorized as Stage 6, showed that the GRs in NTU help with energy savings of nearly 120,000 kWh per year and water savings of over 1170 m^3 per year, resulting in lower operation and maintenance costs. The green roof, high-performance glass, and carbon dioxide sensors in its air-handling units also contribute to the building's energy efficiency and healthy indoor air quality [59]. From the references above, it shows that government and architects have played a significant role in promoting GRs, particularly from a design perspective. The integrated development of GRs, from Stage 1 of "Environmental and Social Problems" with land availability to Stage 6 of "Performance Evaluation" with the large green roof project at NTU, demonstrates Singapore's position as the ASEAN leader in the development of green roofs.

Moving to Thailand, one of the big countries in the ASEAN region, the major obstacles to adoption are the absence of adequate subsidy programs and deficient knowledge and skilled labor force; these typical ASEAN pressures are categorized as Stage 2. The interview study of Sangkakol [60] mentioned that the roof is the last part of a building to be completed—typically after the majority of available funds have been allocated. Therefore, the absence of GR subsidies make GRs unlikely to be installed, and GRs might be skipped even if planned initially. Interestingly, in Thailand, as shown in Figure 6, Thammasat University (TU) built a magnificent structure known as the largest urban rooftop farm in Asia, which we categorized as Stage 5. The 22,000-square-meter TU GR combats climate change by combining modern landscape architecture with traditional agricultural ingenuity, urban farming, a solar roof, and green public space [61]. However, research articles on GRs in Thailand are still limited. The expansion of research and promotion in Thailand has the potential to increase development of GRs for all segments of society.

(**a**) (**b**)

Figure 6. The magnificent green roof projects in ASEAN countries: (**a**) Nanyang Technological University (NTU), Singapore and (**b**) urban rooftop farm, Thammasat University (TU), Thailand.

Several major Vietnamese cities, including Hanoi and Ho Chi Minh City, have minimal green space areas. Hanoi has only 11.2 m^2/capita of urban green space, while Ho Chi Minh City has only 2.0 m^2/capita [41]. Pam's responder poll, which is an evaluation of "Diverse Pressure" (Stage 2), received a positive response, with 64 percent of building users and 62 percent of specialists agreeing to promote green space [62]. This response is far better than the poll in Brunei, where just 24% of building users participated. A study that can be classified as Stage 3 showed that the price of green roof construction in Vietnam is approximately 15 to 45 USD/m^2, which is fairly inexpensive compared to other green roof pioneering nations such as Hong Kong at around 400 to 1000 USD/m^2 [63] or Singapore at approximately 89 to 197 USD/m^2 [63]. It is well demonstrated that Vietnam's potential for green roofs is highly promising [40]. As a recommendation, it is necessary to conduct additional studies on Stages 4 to 6 in light of Vietnam's vast potential for GR development.

Identifying research on GRs conducted in ASEAN countries, shown in Figure 7, allowed us to pinpoint the critical stages of GR development level. In general, 6 of 10 ASEAN countries are still restricted under Stage 3 "GR Research and Development". However, only Singapore is stable in all aspects of highest stage development. Malaysia, who is on an equal level of development as Singapore, is still attempting to tackle deficiencies, such as the "Promotion" aspect of Stage 4, where government regulations are still limited (shown in Table 1). Subsidies for constructing GRs as a development strategy in Singapore are an effective strategy. However, GR subsidy programs are not implemented in Malaysia. Moving on to the Philippines and Thailand, these two nations have adopted GRs up to Stage 5, but they face the same issues: a lack of regulatory support from the government, subsidies, end-user desire, and green roof expertise. Indonesia and Vietnam are still in Stage 3 of green roof development and research. Implementation remains low in Indonesia and Vietnam. Even though Indonesia's green roof research database is ranked third, research on green roof technological improvements remains limited. This results in stagnation of GR development at Stage 3. Therefore, research on the promotion, implementation, and performance evaluation of GRs is urgently required in order to expand the use of GRs. Brunei, Cambodia, Laos, and Myanmar are lagging behind the other ASEAN nations in the development of GRs. Particularly, in Laos it is still quite difficult to find previously published studies on GRs. It is recommended that those four countries conduct more research on GR benefits to obtain potential data on GR efficiency in specified locations in the countries.

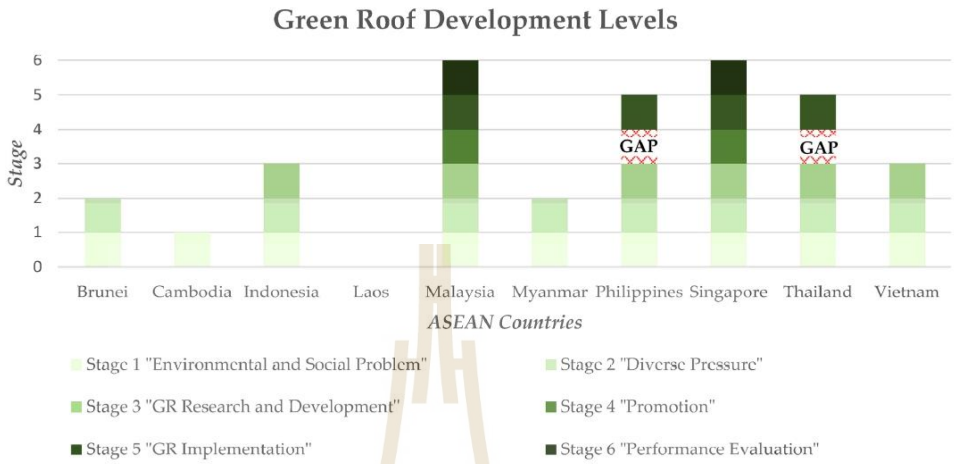

Figure 7. The green roof development levels in ASEAN Countries.

3.3. Green Roof Performance in ASEAN Countries

In this study, green roof performance is categorized into three review groups: drivers, motivations, and barriers research. In total, 70 research studies are included in this section.

3.3.1. Drivers of Green Roofs in ASEAN Countries

In this section, we report the results of "5 articles on Policy Pressure" and "7 articles on Advance Innovation Technology", which discuss drivers of GRs in ASEAN countries. The factors below are crucial and can accelerate the development of green roofs in the ASEAN region:

- Policy Pressure.

To fully implement GRs, mandatory or voluntary policies, regulations, guidance, standards, or initiatives are necessarily established. Some examples of developed cities and countries that encourage the development of GRs are Toronto and Canada, who implement policy pressures that aim to legislate sustainable construction [64].

Regulations and standards have a significant role in the development of GRs in Singapore and Malaysia because of the existence of a handbook in Singapore and maintenance guidelines in Malaysia, as shown in Table 1.

Table 1. Policy pressure to drive GR implementation, as reported in the literature.

Authors	Key Findings		Country
	Subsidy Scheme	Regulations and Standards	
Ismail et al. [28]	The scheme supported 50% of green roof installation costs by Singapore National Parks (NParks) to encourage owners to have green roofs	Standards for Singapore GRs, • Introduction to Vertical Greenery • Handbook of Skyrise Greening in Singapore • Vertical Greenery for the Tropics	Singapore

Table 1. *Cont.*

Authors	Key Findings		Country
	Subsidy Scheme	Regulations and Standards	
Fauzi et al. [29,30], Siew et al. [65], Zaid et al. [66]	None	• Applying GR will improve the green building assessment standards up to 7–10% • BREEM code is suitably used for assessment. • Evaluation of roof penetration barrier, drainage, filter, substrate, vegetation, green building credit, and thermal performance guides. 9 guidelines for GR maintenance	Malaysia

However, this appears to be inextricable from the subsidy scheme. In Singapore, the subsidy scheme has been implemented for quite some time, making building owners more interested in installing GRs. However, there is no report found that Malaysia implemented this subsidy scheme. Abdul Rahim [67] also reports that the lack of subsidies in Malaysia is one of the obstacles to enormous propagation of GRs in society. The study concludes that government has a significant impact on the development of green roofs. Government action in the form of subsidies is a highly successful way of encouraging building proprietors to install green roofs.

- Advance Innovation Technology.

GR technology's first appearance was in Ziggurat of Ancient Mesopotamia, from the fourth millennium until 600 BC. The GRs were located in the courtyard temples, and shrubs and trees were planted on terraces formed by a gran-stepped pyramid [64]. GRs have become more successful over time as a result of technical developments. Environmental considerations influence the development of GR technology in every country; thus, there are always variations in the application of technology between nations. Therefore, technological innovation is one of the drivers encouraging the advancement of GR development.

Table 2 shows the advanced innovation technology literature that has been researched in ASEAN countries. There are notable differences in the technological development of GRs. The countries in Stage 6 development focus on developing smart and efficient green roof construction technology. Mahdiyar's research on prototypes established which style of GR was most suitable for a building [32]. In addition, Singapore also has artificial technology as one of its advanced technologies [68]. Meanwhile, in other countries, green roof research is still concentrated on adapting GR implementation to the country's culture. In Indonesia and Thailand, for instance, alternative materials are developed for GR optimization in cost and performance [31,69]. However, the development of advanced technology for GRs in ASEAN countries is still limited compared to the total GR articles in the ASEAN region.

Table 2. Advanced innovation technology to drive GR implementation, as reported in the literature.

Authors	Findings	Details
Mahdiyar et al. [32]	Development of a decision support system (DSS) for selecting the optimum type of GR for residential buildings in Kuala Lumpur	Malaysia, All types GR, System to selection GRs
He et al. [68]	Artificial neural network (ANN) models had a better average prediction for accurate modelling of thermal and hydrological performance	Singapore, EGR, Evaluate plant evapotranspiration
He et al. [70]	A methodology for a quick evaluation of thermal performance of a green roof during the early stages of design	Singapore, EGR, Model development of RTTV

Table 2. *Cont.*

Authors	Findings	Details
Phoomirat et al. [33]	Develop a rapid assessment checklist (RAC) to assess GR services	Thailand, All GRs, Assessment tools
Munir et al. [31]	The panel 400 mm width is an optimal form for the structural roof deck of the green roof system	Indonesia, EGR, Structural deck precast foamed concrete for GRs
Shahid et al. [71]	Palm oil clinker has good ability to drain excess water, and there is no side effect in terms of plant development	Malaysia, EGR, Palm oil clinker as drainage layer
Chandra et al. [69]	Lightweight cellular concrete 1200 and 1400 kg/m^3 meets the standard to substitute normal concrete	Thailand, EGR, Structural deck alternative for GRs

3.3.2. Motivations for Green Roofs in ASEAN Countries

In this section, we report the results of total 41 research articles including eight studies in "Energy Efficiency", 15 articles in "Urban Heat Island Mitigation", 16 articles in "Runoff Control", and two articles in "Biodiversity Increase". The factors below are important and can validate the benefits of applying GRs in ASEAN countries:

- Energy Efficiency.

In the five studies reporting on annual energy consumption, the effect of green roofs ranged from savings of 1–57% (Table 3). Installing GRs in tropical countries effects a in reduction heat gain and leads to decrease in cooling loads. Energy savings is affected by a number of factors, including layer thickness, moisture content, and vegetation selection [72]. Sittipong [73] reported that an increase in the thickness of the soil layer reduces the building energy consumption. As shown in Figure 8, two different thickness layers were compared by installing multiple sensors within a GR's layers. Wong [74] discovered that shrubs are recommended because they effectively reduce the energy consumption of buildings. The findings also agreed that an increase in soil thickness would further lower the building's energy consumption. In addition, the moisture content of the soil, which is influenced by vegetation, can have a significant impact on the outcome. Apart from this, in the case of multi-story structures, green roofs reduce energy consumption significantly on the floors directly below the green roof. Azis [75] collected data of electrical usage on the top floor and lower floor. The results show that the top floor was directly impacted by the green roof and consumed 40% less electricity.

Figure 8. Experimental set of GR model in Thailand [73]. "Reproduced with permission from Sittipong Permpituck, Pichai Namprakai, The energy consumption performance of roof lawn gardens in Thailand; published by Elsevier, 2012".

Table 3. Energy savings due to GR implementation, as per the selected literature.

Authors	Energy Savings	Details
Wong et al. [74]	1–15% reduction in energy consumption	Singapore, EGR, Comparison rooftop garden with turfing, shrubs, and tree
Dewi et al. [76]	11.24–21% reduction in cooling load	Indonesia, EGR, GR simulations by planting *Tradescantia Spathacea* and Sedum acre
Sittipong and Pichai [73]	GR thickness 0.10 m–31.07% GR thickness 0.20 m–37.11%	Thailand, EGR, Increasing soil depth improves energy savings by around 6%
Azis et al. [75]	37–40% reduction in energy consumption	Johor Bahru, Malaysia, EGR and IGR GR integration with 17-floor apartment
Yuliani et al. [77]	Concrete GRs, 57.1% reduction in heat flow Corrugated Zinc GRs, 50.8% reduction in heat flow	Surakarta, Indonesia, EGR, A corrugated zinc roof with plants could improve thermal conditions in a building

- Urban Heat Island Mitigation.

Green roofs are regarded as one of the most practical tools in mitigating the UHI effect because they reduce air and surface temperatures in cities through the provision of shading, removal of heat from the air, and reduction of temperatures of the roof surface. In this section, we report the results of 15 studies and discuss the impact of GRs on the UHI effect. Outdoor surface and indoor room temperature in green roof studies will be discussed:

1. Outside Surface Temperature.

The maximum reduction ranges for outside surface temperature fell between 10.4 and 23.8 °C compared to conventional roofs (Table 4) according to the 11 studies including actual survey, experimental, and simulation studies. The results of an actual survey on constructed GRs are lower than those of an experimental study that was merely a trial model. However, the reduction performance of GRs in ASEAN countries is highly effective. Green roofs are more effective in reducing temperature during warm temperatures. ASEAN countries, located in tropical climate areas, have consistent temperature radiation throughout the year. Moreover, six out of ten ASEAN countries have reached a maximum temperature above 40 °C [78]. Therefore, the application of green roofs in the ASEAN region is highly recommended.

Aside from climate, material selection has an influence on decreasing performance due to temperature. In Indonesia, Munir [51] revealed that lightweight foamed concrete in combination with roof slabs for green roofs has positive results on cooling as well as on construction loads, which will also impact cost effectiveness. Based on a simulation study, another alternative from Yuliana [53] claimed that corrugated zinc with plants can be used instead of green roof concrete.

Table 4. Reduction of outdoor surface temperature after implementing GRs, as reported in the selected studies.

Authors	Max. Outdoor Surface Temperature Reduction	Ambient Temperature	Remarks
Sunakorn [79]	10.4 °C	30 °C	Thailand, Actual Survey Study, EGR, Local material Thailand (Green Mat) can be applied on GRs

Table 4. *Cont.*

Authors	Max. Outdoor Surface Temperature Reduction	Ambient Temperature	Remarks
Qin [80], Yang et al. [81]	19 °C	24–32 °C	Singapore, Simulation study, Cool roofs, Insulation layer on cool roofs plays a negligible role in heat flux values
Munir et al. [51]	19.1 °C	28–57 °C	Aceh, Indonesia, Experimental study, EGR, Precast foamed concrete, Combination of lightweight foamed concrete and GR
Ahmed and Rumana [82], Ismail et al. [83]	19.8 °C	30.2 °C	Malaysia, Actual survey study, Roof garden, GRs performed better than white concrete roof and gardening roof
Yuliani et al. [53,77]	20 °C	24–35 °C	Surakarta, Indonesia, Experimental study, EGR, Concrete and corrugated zinc, A corrugated zinc roof with plants could improve thermal conditions in a building
Azis et al. [75], Rahmat et al. [54], Rahman et al. [84]	23.8 °C	30–36 °C	Kuala Lumpur and Putrajaya, Malaysia, Experimental study, EGR, Green roof improving public environment
Yuliani et al. [53,77]	20 °C	24–35 °C	Surakarta, Indonesia, Experimental study, EGR, Concrete and corrugated zinc, A corrugated zinc roof with plants could improve thermal conditions in a building
Azis et al. [75], Rahmat et al. [54], Rahman et al. [84]	23.8 °C	30–36 °C	Kuala Lumpur and Putrajaya, Malaysia, Experimental study, EGR, Green roof improving public environment

2. Indoor Room Temperature.

Indoor room temperature has an effect on human thermal comfort. According to Ahmed [82], the temperature comfort zone for humans is between 23.5 °C and 28.5 °C; thus, if the room temperature is within this range, humans can be present without the need for heating or cooling. Implementing GRs reduces the thermal transfer in building, which will also impact indoor room temperature reductions.

The maximum reduction ranges for indoor temperature are from 3 to 14 °C (Table 5) according to nine studies, including actual survey, experimental, and simulation studies. According to several studies [35,82,85], the application of a roof garden has the same favorable effects as the usage of GRs. Combining the use of GRs and a roof garden will improve GR heat resistance.

The materials used also affect the performance of GRs at inside room temperatures. Munir [51] used lightweight foamed concrete for GRs with an effective outdoor decrease up to 10.2 °C. The use of GRs can result in significant energy savings since the temperature of a room that applies GRs deviates less from the comfort zone than the temperature of a room that does not apply GRs. This allows cooling to operate more efficiently in spaces with GRs.

Table 5. Reduction of indoor temperature after implementing GRs, as reported in the selected studies.

Authors	Max. Indoor Temperature Reduction	Temperature Comparison	Remarks
Yuliani et al. [77]	3 °C	GR 23–28 °C NON-GR 27–31 °C	Surakarta, Indonesia, Experimental study, EGR, Concrete and corrugated zinc, A corrugated zinc roof with plants could improve thermal conditions in a building
Pahm et al. [62]	3 °C	GR 31 °C NON-GR 34 °C	Ho Chi Minh City, Vietnam, Actual survey study, roof garden In cooler area, GR still resulted lower than non-GR temperature
Ahmed and Rumana [82], Ismail et al. [83], Rahman et al. [84]	3 °C	GR 24.5–31.5 °C NON-GR 25.5–33 °C	Malaysia, Actual survey study, roof garden, GRs performed better than white concrete roof and gardening roof
Irsyad et al. [35]	6.8 °C	GR 23–26 °C NON-GR 24–32 °C	Bandung, Indonesia, Experimental study, EGR, The use of Amaranta and Bromelia plants can inhibit heat transfer into the room
Sunakorn [79]	7 °C	GR 24.6–27.9 °C NON-GR 29.6–39.9 °C	Thailand, Actual survey study, EGR, Local material Thailand (Green Mat) can be applied on GRs
Munir et al. [51]	10.2 °C	GR 35–38 °C NON-GR 42–51 °C	Aceh, Indonesia, Experimental study, EGR, Precast foamed concrete Combination of lightweight foamed concrete and green roof
Yang et al. [81]	14 °C	GR 26–27 °C NON-GR 28–41 °C	Singapore, Simulation study, EGR, Insulation layer on cool roofs plays a negligible role in heat flux values

- Runoff Control.

1. Storm Water Retention.

Retention is the process of holding water on the green roof and preventing water from draining off the green roof [86]. Table 6 presents the water retention capacities given in the selected literature in several ASEAN countries. The overview of studies reported that GRs in ASEAN countries can have a maximum water retention capacity up to 98.8%. The main parameters affecting the retention values are rainfall intensity and duration. Comparatively, subtropical regions in China receive approximately 1058 mm of precipitation annually, allowing them to retain up to 100 percent of precipitation [86]. In contrast, the Philippines' tropical rainfall of 2348 mm per year can retain up to 75 percent. In addition to rainfall, the ability of GRs to retain water is affected by factors such as sunshine intensity, temperature, soil media depth, and plant selection.

2. Runoff Water Quality.

Stormwater runoff carries non-point source pollution from cities, impacting water quality. GRs have the potential to reduce runoff quantity, while their impact on runoff quality is also considered. GRs are a source of pollutant reduction if the pollutants are fewer in the runoff than in the rainwater or in the runoff from bare roofs [11]. Figure 9 shows the example of runoff model based experiment in Singapore.

Table 6. Water retention capacity on GRs, as reported in the selected studies.

Authors	Water Retention Capacity	Remarks and Influence Factors
Chanrachna et al. [49]	37.90%	Phnom Penh, Cambodia, Comparison study, GI (Green Infrastructure) scenario by installation tree, bioswales, permeable pavements, and green roofs
Cuong et al. [85]	42%	Hanoi, Vietnam, Experimental study, EGR, Four models with different irrigation systems
Asinas et al. [57]	46%	Philippines, Experimental study, EGR, Waterproof substrate improving water retention by adding hydrogel to substrate media
Chai et al. [87]	72.5%	Kuching, Malaysia, Simulation study, EGR, Green roof water balance by virtual modelling approach
Orozco et al. [36]	75%	Metro Manila, Philippines, Comparison study, EGR, Suppliers company, Comparison of suppliers with six different GR technologies
Ayub et al. [88], Fai et al. [89], Chow et al. [90], Romali et al. [37], Kok et al. [91], Chai et al. [87], Musa et al. [92]	86%	Malaysia, Simulation study, EGR, GRs decrease of stormwater runoff, Types of substrates resulting in different runoff, Mixture of plant species was the most effective vegetation at reducing runoff water
Vergroesen and Joshi [93]	98.8%	Singapore, Experimental study, EGR, 3-day experiment, Different sedum comparison

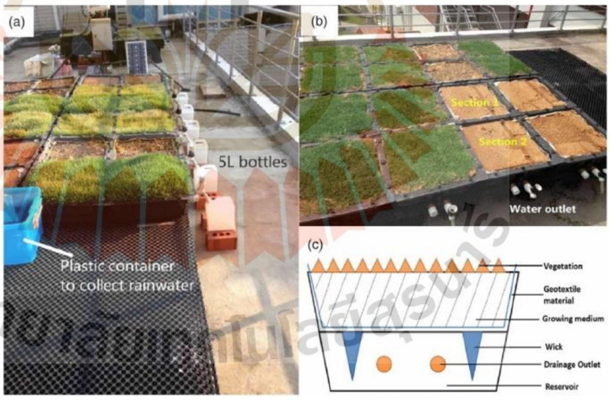

Figure 9. (**a**–**c**) Experimental set of runoff-model-based experiment in Singapore by Lim et al. [94].

In several studies in developed countries, GR runoff released higher concentrations of total phosphorus, total nitrogen, nitrates, and phosphates, meaning GRs are a source of these nutrients [95,96].

Studies on runoff quality are currently limited; Malaysia and Singapore have a few studies on this matter from GRs. Table 7 shows the runoff quality studies in Malaysia and Singapore. However, study of runoff quality in other ASEAN countries needs to be carried out to develop and validate the benefits of green roofs to improve water quality.

Table 7. Runoff quality on GRs, as reported in the selected studies.

Authors	Findings	Remarks and Influence Factors
Romali et al. [37]	GRs with beach morning glory improve the COD up to 99% GRs with creeping oxeye reduce the BOD up to 17%	Malaysia, Experimental study, EGR, Green roof with beach morning glory and creeping oxeye
Lim et al. [94]	Mixture substrate clay (5–30%), silt (5–60%), and sand (20–75%) can decline in chemical concentration level	Singapore, Experimental study, EGR, Substrate comparison
Vijayaraghavan et al. [97]	The concentrations of most of the chemical components in runoff were highest during the beginning of rain events and subsided in the subsequent rain events	Singapore, Experimental study, EGR, Real rain events and ten different simulated rain events

- Biodiversity Increase.

Green roofs can promote urban biodiversity through the provision of complex vegetation structures, greater foraging and roosting options for animals, and enhanced habitat connectivity [94].

An observation study of biodiversity of GRs in Singapore revealed that spontaneous species had approximately 28.9% site cover in a year apart from planting seeds at the beginning. In addition, after installing the GRs, the fauna increased up to 69 fauna species, including species of birds, bees, hornets, wasps, butterflies, moths, etc. [98]. Sananunsakul stated a similar perspective that green roof characteristics may influence bird communities utilizing these urban ecosystems [38].

3.3.3. Barriers to Green Roofs in ASEAN Countries

GR implementation is also constrained by barriers of government policy, technology barriers, economic issues, social acceptability, and feasibility issues. A search with the green roof database in ASEAN countries found that the study of barriers is dominant compared to other green roof topics. We report the results total 25 articles including five studies in "Economics" and 20 articles in "Social Acceptability and Feasibility Issues":

- Government Policy and Technology Barriers.

As described above, regarding ASEAN drivers with green roofs, green roofs can be developed with governmental support and technological advancements. Singapore and Malaysia are the only two ASEAN countries supported by government regulations and rigorous programs. On the other hand, eight other ASEAN countries did not have any research or archives pertaining to government sponsorship and technology. This is the biggest barrier in ASEAN countries that must be addressed for the green roofs of ASEAN countries to advance.

- Economy.

In this section, we discuss the findings from our review in terms of economic barriers. We shortlisted five studies that discussed the economic feasibility of GRs with the inclusion of several costs and benefits. Figure 10 presents the types of GRs and their costs in each of the studies. A study in developed countries showed that the installation cost for extensive green roofs can range between 55 and 220 USD/m^2 [99]. The high cost of installation is a major barrier to the development of GRs in ASEAN countries. This is demonstrated by

Rahman in Brunei Darussalam with typical green roof installations ranging from 208 to 318 USD/m^2. The roof slab's design for excessive strength has a significant impact on the high-cost green roof. As a recommendation, the structural load design that meets the load requirements of the green roof will be extremely cost-effective [39].

Figure 10. The green roof development level in ASEAN countries. (Source: Brunei Darussalam [39], Indonesia [100], Philippines [36], Singapore [101], and Vietnam [40].

More importantly, Vietnam's pricing range is significantly lower than the average price in industrialized markets. This may be because conventional green roofs are still manufactured in Vietnam [40]. The advancement of the application of green roof technology is urgently required to enhance the performance of green roofs while maintaining market-competitive pricing.

Research on the cost of green roofs in Singapore reveals that prices are comparable to the global average for green roofs. In addition, a complete green roof system and excellent performance back this claim [101]. The rise of green roof construction in ASEAN countries will be stimulated by the creation of high-quality green roofs at prices that are far lower than the world average.

- Social Acceptability and Feasibility Issues in ASEAN Countries.

We discovered around 12 studies examining the perspectives of possible GR implementers and users, such as architects, engineers, property developers, and building owners. Social acceptability from numerous studies shown in Table 8 can represent the major obstacle points. According to most studies, initial building expenses, maintenance costs, and lack of knowledge are the primary obstacles to the broad use of GRs. Moreover, the lack of implementation knowledge and qualified labor, as well as the absence of government incentives, are additional causes for concern.

According to the findings of Shams, survey research on user perception in Brunei resulted less interest in GRs [48]. Several studies in Malaysia indicated that the lack of GR expertise in the country remained a significant issue [67,102]. Arif [103] described that a method for enhancing public interest in green roofs can be initiated by introducing GRs to the community in public places. This will enhance the user's ability to experience the advantages of a green roof.

Table 8. Social acceptability according to GR implementers and users.

Challenge	Brunei	Malaysia	Indonesia	Thailand	Vietnam	Myanmar	References
Lack of Interest using GRs	✓	✓	✓		✓		[48,52,104–107]
Lack of Guidelines		✓				✓	[67,102,108]
Less Government Intensive		✓		✓		✓	[60,103,109]
High Installation Cost		✓					[110]
Lack of Expertise			✓				[105,106]

Observing the absence of social acceptability in ASEAN countries also has an effect on building aspects. Table 9 describes research studies discussing the current building feasibility for applying GRs. Briefly, most limitations have been found in studies. Shams [48] mentioned that the application of GRs on structures in Brunei is quite limited. Luthfiyyah conveyed a similar result [52], in which the city demonstrates the absence of potential buildings for applying GRs. Additionally, Chow mentioned the warnings and concerns regarding use of GRs in industrial buildings.

Table 9. Current building feasibility for applying GRs.

Authors	Findings	Remarks
Suparwoko and Taufani [111]	The potential to use GRs as an urban farming space	Sleman, Indonesia, Survey study, Feasibility of buildings
Chow and Abu Bakar [102]	Industries were very cautious about having rooftop gardens due to the unknown risk on maintenance aspects	Malaysia, Survey study, Feasibility of buildings
Rahman et al. [112]	GRs help to regenerate and revitalize the commercial setting in urbanized areas	Malaysia, Survey study, Feasibility of buildings
Hwang and Roscoe [113]	Green roofs as a platform for the interaction between humans and nature is a possibility that is yet to be fully explored, especially in a tropical context	Singapore, Actual study, Feasibility of buildings
Naing et al. [114]	47% of selected buildings in sampling area were possible to retrofit for a green roof	Thailand, Survey study, Feasibility of buildings
Jalanugroh and Tikul [115]	Of twenty-six education buildings, three can be built with an intensive green roof, seven can be built but gardeners are needed, and sixteen can be built with extensive green roofs	Thailand, Survey study, Feasibility of buildings
Lwin and Panuwatwanich [108]	Energy efficiency, water efficiency, and waste and pollution, are the most crucial categories that should be concerned	Myanmar, Survey study, Feasibility of buildings

According to our findings, ASEAN society is still unaware of GRs. However, if GRs have an affordable and visually acceptable design, they have the potential for social acceptability. Furthermore, user-specific experiences and expectations are essential to consider. To expand their awareness, there is a need to directly introduce the benefits of GRs to society.

4. Discussion

4.1. Challenges of GR Development in ASEAN Countries

The study presented here stems from the phenomena of uneven development of GRs in the ASEAN countries, even though the ASEAN region has potential topographical characteristics for maximizing the benefits of green roofs. This is evident from the skewed distribution of the 70 GR research articles in ASEAN, Malaysia, and Singapore, which accounted for more than half of the distribution with a total of 41 articles. (There were 28 articles for Malaysia and 13 articles for Singapore). This results Malaysia and Singapore's acceleration toward an advanced level of GRs.

Based on the inclusion criteria for a paper in the review, the evidence for the drivers in ASEAN countries was limited to thirteen articles, which were dominated by Malaysia and Singapore. To increase the level of development in each ASEAN country, it is suggested that the other countries in ASEAN develop a proper technology regarding GR development. As for studies in GR motivations, the 38 studies are significantly higher than for the other two criteria, making the level of evidence pertaining to this service strong. To validate the benefits of using GRs in ASEAN countries, research focusing on motivation appears to remain popular. The research on barriers is also quite dominant, with 25 articles demonstrating that the development of GRs in ASEAN countries still faces numerous obstacles.

The grouping of GR development levels is determined by a sequence of development scenarios from Stage 1 to Stage 6 based on the 70 research papers gathered. An extensive variety of papers, from analyzing urban issues to evaluating GRs, have been compiled. In terms of Singapore and Malaysia, the GR performance evaluation articles reveal that GR implementation has been accomplished and examined for quality (e.g., Azis et al. [72], Hwang [98]). However, Malaysia also reported numerous barriers (Table 9). The community's reluctance to implement GRs is a result of the government's lack of emphasis on their widespread installation.

Thailand and the Philippines occupied Stage 5 despite having few research articles on the development of GRs because the GR system has been implemented on the largest green roof farm building in Thailand. In the Philippines, a comparative analysis of the quality and prices of GR suppliers reveals that the market for GR suppliers in the Philippines is competitive. However, the disparity in the government's "Promotion" stage is still relatively small. To accelerate development in Thailand and the Philippines, government assistance such as guidebooks and regulations is necessary.

Indonesia and Vietnam are in Stage 3 of "GR Research and Development," despite the fact that Indonesia has quite a few articles containing sixteen study GRs. Indonesia continues to struggle with benefit validation despite conducting a great deal of research on the topic of motivation with nine studies, the majority of whose results were model-based. This imbalance between model and actual survey results is shown in several parameters of UHI effects (Section 3.2). In the meantime, the number of GR study articles in Vietnam remains very low. In addition to a dearth of interest in using GRs and a lack of expertise, the development of GRs in these two nations has stalled at Stage 3.

Brunei, Myanmar, Cambodia, and Laos have conducted limited research on GRs, resulting in a low level of development in these four nations. In Brunei and Myanmar, evaluation is still limited to barriers to the implementation of GRs. Laos has not conducted any research on GRs, whereas Cambodia is still evaluating their ability to combat flooding.

Compared to all challenges, the challenge in ASEAN countries is clearly reported to increase the interest of using GRs. This must also be supported by government regulations that are still minimally implemented in ASEAN nations. In some instances, there is no definitive standard for the development of GRs, so price fluctuations remain highly variable. Several GR development alternatives are explained in Section 4.2.

4.2. Perspective and Future Needs of GR Development in ASEAN Countries

The literature review highlights some important findings of drivers where policy pressure can increase green roof development level (this is the case reported, e.g., by Ismail [28] and Fauzi [29]). Moreover, differences in Singapore's and Malaysia's rules indicate that each nation's regulations are created according to its own needs. It is important to point out, ASEAN countries without the support of government regulations have difficulty developing green roofs. The advancement of technology is an additional factor that contributes to the development of GRs. However, through examining the reviews, just a limited source pertaining to advanced technology was discovered. This is also a significant gap that makes it difficult for other countries outside of Singapore and Malaysia to grow in GR development.

The present investigation on factors that motivate GR implementation in ASEAN countries has been found up to ten in all ASEAN countries. Some of the aspects that can be highlighted are:

- GRs can reduce energy consumption in buildings by up to 57%, reduce roof surface temperatures when compared to bare roofs up to 23.8 °C, and reduce the room temperature to 14 °C. It should be noted that heating load reductions can be influenced by substrate [73], vegetation [76], and insulating material [81]. Some researchers describe alternative material such as lightweight concrete deck that can improve GR properties [40,51].
- GRs aid in water management, owing to their high water retention potential and increased runoff quality. The application of GRs in ASEAN countries is highly appropriate due to the region's abundant precipitation. GRs can control up to 98.8% of flood water retention. However, the retention is high only for low- to moderate-intensity rainfall. Countries with significant precipitation, such as the Philippines, are highly interested in GR water management research (e.g., as described in the case reported by Orozco [36]). The use of hydrogel to increase water retention on the substrate is an interesting innovation to be developed (from research by Asinas [57]). Other countries with heavy precipitation, such as Indonesia, are encouraged to conduct studies on the water management of GRs.
- The present review study also signals biodiversity, which is the fact that GRs can promote urban biodiversity and enhanced habitat connectivity between flora and fauna as was shown in research in Singapore [113]. A habitat is created from many environmental factors. We found no literature on biodiversity in other ASEAN nations during our search. We need further research on the effect of environment and topography on the biodiversity of the GR.

However, the study of GR barriers in ASEAN countries is particularly prominent. Of the 70 studies in the literature, 25 studies on the barriers of GRs in ASEAN countries were majorly discussed in Section 4.2. All barriers can be overcome by conducting and developing more research on the drivers. Several prospective research recommendations on the topic of drivers are as follows:

1. Investigating alternative materials that can enhance the efficacy of GRs and reduce installation costs.
2. Developing intelligent technology that can expedite the retrieval of GR data in order to accelerate the pre-development, construction, and maintenance processes.
3. Planning guidelines and economic schemes that can be referred to in the future when creating government regulations.
4. Conducting research on the benefits of GRs at each city scale (e.g., residential buildings, commercial buildings, and high-rise buildings) to educate users on the advantages of GR use.
5. At this time, numerous diverse data can be suggested for calculating the mean and median value for each parameter. Due to the heterogeneity of the parameters in the calculated studies, it was deemed statistically invalid to compute such values. Evaluation of performance can serve as an indicator for evaluating the performance of green roofs in ASEAN countries.

5. Conclusions

This study systematically reviewed the recent literature to identify the current development of green roofs in ASEAN countries.

According to our findings, GRs give multiple benefits to both users and the ecosystem. GRs effectiveness is influenced by many factors such as the weather and the location of ASEAN nations that is ideal for optimizing the properties of GRs.

However, a review of the literature on GR research in ASEAN countries revealed that the level of development of GRs in ASEAN countries is not evenly distributed. Most notably, the key challenges are similar, because of a lack of supporting regulations, lack of expertise in green roofs, and expensive installation prices. Regulatory concerns, in the opinion of the present authors, must be issued through the governments' technical authority so that they have the capacity and legal basis. While the regulations are being finalized, the development of green roof technology in accordance with the climate features of ASEAN countries must be prioritized by implementing the appropriate green roof technology, so the installation costs for building GRs can be decreased.

The scientific potential of the present work is that it allows us to understand the specific beneficial performance of green roofs in ASEAN countries and propose a future strategy to overcome the barriers. Increased public awareness is expected to increase the ASEAN region's GR level in the long term.

Author Contributions: Conceptualization, H.C.P., T.S. and A.C.; methodology, H.C.P., T.S. and A.C.; formal analysis, H.C.P.; writing—original draft preparation, H.C.P.; writing—review and editing, H.C.P., T.S. and A.C.; revisions, H.C.P., T.S. and A.C.; supervision, T.S. and A.C.; project administration, T.S. and A.C.; funding acquisition, T.S. and A.C. All authors have read and agreed to the published version of the manuscript.

Funding: This study is supported by research funds to extend knowledge from OROG Thailand Scholarship, Sustainable Innovative and Energy Efficient Construction Material (SIE-CON); and Infinity Concrete Technology, Co., Ltd.

Institutional Review Board Statement: Not applicable.

Informed Consent Statement: Not applicable.

Data Availability Statement: Not applicable.

Acknowledgments: The authors are grateful to the Suranaree University of Technology; Sustainable Innovative and Energy Efficient Construction Material (SIE-CON); and Infinity Concrete Technology, Co., Ltd. for providing support financially and for allowing us to use its facilities.

Conflicts of Interest: The authors declare no conflict of interest.

References

1. Shao, H.; Kim, G. A Comprehensive Review of Different Types of Green Infrastructure to Mitigate Urban Heat Islands: Progress, Functions, and Benefits. *Land* **2022**, *11*, 1792. [CrossRef]
2. Gaigbe-Togbe, V.; Bassarsky, L.; Gu, D.; Spoorenberg, T.; Zeifman, L. *World Population Prospects 2022*; United Nations: New York, NY, USA, 2022; ISBN 978-92-1-148373-4.
3. Grullón-Penkova, I.F.; Zimmerman, J.K.; González, G. Green Roofs in the Tropics: Design Considerations and Vegetation Dynamics. *Heliyon* **2020**, *6*, e04712. [CrossRef] [PubMed]
4. Mondal, M.S.H. The Implications of Population Growth and Climate Change on Sustainable Development in Bangladesh. *Jamba J. Disaster Risk Stud.* **2019**, *11*, 535. [CrossRef] [PubMed]
5. Stone, B. Urban Sprawl and Air Quality in Large US Cities. *J. Environ. Manag.* **2008**, *86*, 688–698. [CrossRef] [PubMed]
6. Vijayaraghavan, K. Green Roofs: A Critical Review on the Role of Components, Benefits, Limitations and Trends. Renew. *Sustain. Energy Rev.* **2016**, *57*, 740–752. [CrossRef]
7. Auer, T.; Radi, M.; Brkovi, M. Green Facades and Living Walls—A Review Establishing the Classification of Construction Types and Mapping the Benefits. *Sustainability* **2019**, *11*, 4579. [CrossRef]
8. Schade, J.; Lidelöw, S.; Lönnqvist, J. The Thermal Performance of a Green Roof on a Highly Insulated Building in a Sub-Arctic Climate. *Energy Build.* **2021**, *241*, 110961. [CrossRef]
9. Samuel, K.A.; Bamfo-Agyei, E. Minimization of Heat Gains in Buildings: The Case of Domestic Buildings in Cape Coast Metropolis–Ghana. *Int. J. Dev. Sustain.* **2012**, *1*, 315–326. [CrossRef]
10. Oberndorfer, E.; Lundholm, J.; Bass, B.; Coffman, R.R.; Doshi, H.; Dunnett, N.; Gaffin, S.; Köhler, M.; Liu, K.K.Y.; Rowe, B. Green Roofs as Urban Ecosystems: Ecological Structures, Functions, and Services. *Bioscience* **2007**, *57*, 823–833. [CrossRef]
11. Berndtsson, J.C. Green Roof Performance towards Management of Runoff Water Quantity and Quality: A Review. *Ecol. Eng.* **2010**, *36*, 351–360. [CrossRef]
12. Van Renterghem, T.; Botteldooren, D. In-Situ Measurements of Sound Propagating over Extensive Green Roofs. *Build. Environ.* **2011**, *46*, 729–738. [CrossRef]

13. Pandit, R.; Laband, D.N. Energy Savings from Tree Shade. *Ecol. Econ.* **2010**, *69*, 1324–1329. [CrossRef]
14. Akbari, H.; Pomerantz, M.; Taha, H. Cool Surfaces and Shade Trees to Reduce Energy Use and Improve Air Quality in Urban Areas. *Sol. Energy* **2001**, *70*, 295–310. [CrossRef]
15. Liu, K.; Baskaran, B. Thermal Performance of Green Roofs through Field Evaluation. In Proceedings of the First North American Green Roof Infrastructure Conference, Awards and Trade Show, Chicago, IL, USA, 29–30 May 2003; pp. 1–10.
16. Mohammed Ahmed, R.; Halil Alibaba, A.Z. An Evaluation of Green Roofing in Buildings. *Int. J. Sci. Res. Publ.* **2016**, *6*, 366–2250.
17. Kosareo, L.; Ries, R. Comparative Environmental Life Cycle Assessment of Green Roofs. *Build. Environ.* **2007**, *42*, 2606–2613. [CrossRef]
18. Li, H.; Ye, J. The Comparison of the Forms of Ecological Green Roof Based on the Full Life Cycle Theory. *ICEOE 2011—2011 Int. Conf. Electron. Optoelectron. Proc.* **2011**, *1*, V1-294–V1-296. [CrossRef]
19. Grant, G.; Lane, C. Extensive Green Roofs in London. *Urban Habitats* **2006**, *4*, 51–65.
20. Blackhurst, M.; Hendrickson, C.; Matthews, H.S. Cost-Effectiveness of Green Roofs. *J. Archit. Eng.* **2010**, *16*, 136–143. [CrossRef]
21. Lugo, A.E.; Rullán, J. *The Conservation Message of the Rehabilitated Facilities of the International Institute of Tropical Forestry*; Res. Note IITF-RN-2; U.S. Department of Agriculture: Washington, DC, USA, 2015; p. 49.
22. Suszanowicz, D.; Kolasa-Więcek, A. The Impact of Green Roofs on the Parameters of the Environment in Urban Areas-Review. *Atmosphere* **2019**, *10*, 792. [CrossRef]
23. Mithraratne, N. Green Roofs in Singapore: How Green Are They? In Proceedings of the SB 13 Singapore—Realising Sustainability in the Tropics, Singapore, 9–10 September 2013; Volume 5, pp. 978–981.
24. Uman, L. Systematic Reviews and Meta-Analyses. *J. Can. Acad. Child Adolesc. Psychiatry* **2011**, *20*, 57–59. [CrossRef] [PubMed]
25. Wilt, T.J.; Fink, H.A. Systematic Reviews and Meta-Analyses. *Clin. Res. Methods Surg.* **2007**, 311–325. [CrossRef]
26. Moher, D.; Liberati, A.; Tetzlaff, J.; Altman, D.G. Preferred Reporting Items for Systematic Reviews and Meta-Analyses: The PRISMA Statement. *BMJ* **2009**, *339*, 332–336. [CrossRef]
27. Zhang, G.; He, B.J. Towards Green Roof Implementation: Drivers, Motivations, Barriers and Recommendations. *Urban For. Urban Green.* **2021**, *58*, 126992. [CrossRef]
28. Ismail, Z.; Aziz, H.A.; Nasir, N.M.; Taib, M.Z.M. Comparative Study on Green Roof Mechanism in Developed Countries. In Proceedings of the 2012 IEEE Symposium on Business, Engineering and Industrial Applications, Bandung, Indonesia, 23–26 September 2012; pp. 678–683. [CrossRef]
29. Fauzi, M.A.; Malek, N.A.; Othman, J. Evaluation of Green Roof System for Green Building Projects in Malaysia. *Int. J. Environ. Ecol. Eng.* **2013**, *7*, 75–81.
30. Fauzi, M.A.; Malek, N.A. Green Building Assessment Tools: Evaluating Different Tools for Green Roof System. *Int. J. Educ. Res.* **2013**, *1*, 1–14.
31. Munir, A.; Afifuddin, M. Application of Precast Foamed Concrete Panels for the Structural Deck of Green Roof System. *IOP Conf. Ser. Mater. Sci. Eng.* **2020**, *796*, 012039. [CrossRef]
32. Mahdiyar, A.; Tabatabaee, S.; Durdyev, S.; Ismail, S.; Abdullah, A.; Wan Mohd Rani, W.N.M. A Prototype Decision Support System for Green Roof Type Selection: A Cybernetic Fuzzy ANP Method. Sustain. *Cities Soc.* **2019**, *48*, 101532. [CrossRef]
33. Phoomirat, R.; Disyatat, N.R.; Park, T.Y.; Lee, D.K.; Dumrongrojwatthana, P. Rapid Assessment Checklist for Green Roof Ecosystem Services in Bangkok, Thailand. *Ecol. Process.* **2020**, *9*, 1–17. [CrossRef]
34. WHO Regional Office for Europe. *Urban Green Spaces: A Brief for Action*; WHO: Geneva, Switzerland, 2017.
35. Irsyad, M.; Pasek, A.D.; Indartono, Y.S. An Investigation of Green Roof Deployment in Bandung City, Indonesia. *J. Eng. Appl. Sci.* **2016**, *11*, 2528–2534. [CrossRef]
36. Orozco, C.R.; Madriaga, D.A.D. Assessment of Green Roofs in the Philippines Using Sustainability Indicators and Cost-Benefit Analysis. *Int. J. Environ. Stud.* **2021**, *79*, 810–821. [CrossRef]
37. Romali, N.S.; Othman, N.S.; Mhd Ramli, N.N. The Application of Green Roof for Stormwater Quantity and Quality Improvement. *IOP Conf. Ser. Earth Environ. Sci.* **2021**, *682*, 012029. [CrossRef]
38. Sananunsakul, P.; Dumrongrojwatthana, P.; Disyatat, N.R. Species Diversity of Birds Utilizing Green Roofs in Bangkok. In Proceedings of the Burapha University International Conference, Chonburi, Thailand, 3–4 August 2017; pp. 426–434.
39. Rahman, M.M.; Shams, S.; Ismail, P.H.R.I.P. Green Roof Retrofit: A Case Study. *Int. J. Integr. Eng.* **2021**, *13*, 81–88. [CrossRef]
40. Dang, H.; Nguyen, V.; Cuong, D.V. Cost Assessment of Green Roofs—Case Study in Hanoi. In *International Workshop on Environmental & Architectural Design for Sustainable Development*; Construction Publishing House: Ha Noi, Vietnam, 2016; pp. 83–93.
41. Hasnan, L. ASEAN's Green Spaces Disappearing Fast. Available online: https://theaseanpost.com/article/aseans-green-spaces-disappearing-fast (accessed on 23 June 2019).
42. Russo, A.; Cirella, G.T. Modern Compact Cities: How Much Greenery Do We Need? *Int. J. Environ. Res. Public Health* **2018**, *15*, 2180. [CrossRef] [PubMed]
43. Kwon, O.H.; Hong, I.; Yang, J.; Wohn, D.Y.; Jung, W.S.; Cha, M. Urban Green Space and Happiness in Developed Countries. *EPJ Data Sci.* **2021**, *10*, 28. [CrossRef] [PubMed]
44. Kusumaning Asri, A.; Lee, H.Y.; Pan, W.C.; Tsai, H.J.; Chang, H.T.; Candice Lung, S.C.; Su, H.J.; Yu, C.P.; Ji, J.S.; Wu, C.; et al. Is Green Space Exposure Beneficial in a Developing Country? *Landsc. Urban Plan.* **2021**, *215*, 104226. [CrossRef]
45. UNICEF. *The Necessity of Urban Green Space for Children's Optimal Development*; United Nations Children's Fund: New York, NY, USA, 2021; pp. 1–37.

46. Durdyev, S.; Koc, K.; Karaca, F.; Gurgun, A.P. Strategies for Implementation of Green Roofs in Developing Countries. *Eng. Constr. Archit. Manag.* **2022**, *29*. [CrossRef]
47. Razzaghmanesh, M.; Beecham, S.; Salemi, T. The Role of Green Roofs in Mitigating Urban Heat Island Effects in the Metropolitan Area of Adelaide, South Australia. *Urban For. Urban Green.* **2016**, *15*, 89–102. [CrossRef]
48. Shams, S.; Ismail, P.H.R.I.B.P.; Zania, A.B.H.; Mohamad, A.B.H. Challenges and Opportunities of Green Roof in Building Design: A Case Study in Bandar Seri Begawan. *Malays. Constr. Res. J.* **2018**, *5*, 113–123.
49. Chanrachna, N.; Sasima, C. The Potential of Green Infrastructure (GI) for Reducing Stormwater Runoff in a Phnom Penh Neighborhood. *Geogr. Tech.* **2016**, *11*, 39–50. [CrossRef]
50. Sarkara, S.; Butcher, J.B.; Johnson, T.E.; Clark, C.M. Simulated Sensitivity of Urban Green Infrastructure Practices to Climate Change. *Earth Interact.* **2018**, *22*, 1–37. [CrossRef]
51. Munir, A.; Afifuddin, M. Thermal Performance of Precast Foam Concrete Integrated with Green Roofs System. *Adv. Eng. Res.* **2020**, *192*, 202–206.
52. Luthfiyyah, D.N.; Widjajanti, R. Green Roof to Overcome Urban Heat Island Effects in the Center of Semarang. *E3S Web Conf.* **2019**, *125*, 7–11. [CrossRef]
53. Yuliani, S.; Hardiman, G.; Setyowati, E. A Comparison of Heat Performance Between Green Roofs on Concrete and Green Roofs on Corrugated Zinc. *DIMENSI J. Archit. Built Environ.* **2021**, *47*, 55–64. [CrossRef]
54. Rahmat, M.H.; Mohkatar, M.H.; Abd Wahab, I.; Abd Salam, N.N.; Abdul Aziz, H.; Abas, N.H. Assessing the Efficiency of Green Roof Technology: A Case Study of Masjid Kota Iskandar, Nusajaya, Johor. *MATEC Web Conf.* **2018**, *250*, 06011. [CrossRef]
55. Lwin, M.; Panuwatwanich, K. Identification and Evaluation of Green Building Assessment Indicators for Myanmar. *J. Green Build.* **2021**, *16*, 143–172. [CrossRef]
56. Republic of the Philippines Highlights of the Philippine Population 2015 Census of Population. Available online: https://psa.gov.ph/content/highlights-philippine-population-2015-census-population (accessed on 7 February 2023).
57. Asinas, J.A.T.; Iii, J.V.B.; Cabanes, J.R.; Domino, R.J.; Abestilla, G.A.D.; Lictaoa, C.S. Utilization of Super Absorbent Polymers (SAP) in Extensive Green Roof as Water Retention in Urban Area. *BIMP-EAGA Reg. Dev.* **2019**, *5*, 93–107. [CrossRef]
58. National Parks Board New Incentives to Promote Skyrise Greenery in Singapore. Available online: https://www.nparks.gov.sg/news/2011/3/new-incentives-to-promote-skyrise-greenery-in-singapore (accessed on 8 February 2023).
59. Nanyang Technology University Nanyang Technological University (NTU) School of Art, Design and Media (ADM). Available online: https://www.greenroofs.com/projects/nanyang-technological-university-ntu-school-of-art-design-and-media-adm/ (accessed on 8 February 2023).
60. Sangkakool, T.; Techato, K.; Zaman, R.; Brudermann, T. Prospects of Green Roofs in Urban Thailand—A Multi-Criteria Decision Analysis. *J. Clean. Prod.* **2018**, *196*, 400–410. [CrossRef]
61. Holmes, D. Thammasat University—The Largest Urban Rooftop Farm in Asia. Available online: https://worldlandscapearchitect.com/thammasat-university-the-largest-urban-rooftop-farm-in-asia/?v=5b79c40fa7c2#.Y-MGfHYzaUk (accessed on 8 February 2023).
62. Pham, L.H.; Vo, T.P.N.; Tran, T.T.; Tran, T.M.H. Optimizing the Benefits of Housing Roofers in Ho Chi Minh City to Adapt to the Current Climate Change Context. *AIP Conf. Proc.* **2021**, *2406*, 060024. [CrossRef]
63. Townshend, D. *Study on Green Roof Application in Hong Kong*; Architectural Services Department: Hong Kong, China, 2007; pp. 1–157.
64. Banting, D.; Hitesh, D.; Li, J.; Missios, P. Report on the Environmental Benefits and Costs of Green Roof Technology for the City of Toronto. In *City of Toronto and Ontario Centres for Excellence—Earth and Environmental Technologies*; Ryerson University: Toronto, ON, Canada, 2005; pp. 1–88.
65. Siew, Z.B.; Chin, C.M.M.; Sakundarini, N. Designing a Guideline for Green Roof System in Malaysia. *J. Clean WAS* **2019**, *3*, 5–10. [CrossRef]
66. Zaid, S.; Zaid, L.M.; Esfandiari, M.; Abu Hasan, Z.F. Green Roof Maintenance for Non-Residential Buildings in Tropical Climate: Case Study of Kuala Lumpur. *Environ. Dev. Sustain.* **2022**, *24*, 2471–2496. [CrossRef]
67. Abdul Rahim, N.N.; Mohamad Bohari, A.A.; Adnan, A.S.; Khalil, N.; Olanipekun, A.O. Challenges and Way Forward for Implementing Green Roof in Construction Industry in Sarawak, Malaysia. *J. Smart Sci. Technol.* **2021**, *1*, 40–47. [CrossRef]
68. He, Y.; Lin, E.S.; Tan, C.L.; Tan, P.Y.; Wong, N.H. Quantitative Evaluation of Plant Evapotranspiration Effect for Green Roof in Tropical Area: A Case Study in Singapore. *Energy Build.* **2021**, *241*, 110973. [CrossRef]
69. Pratama, H.C.; Sinsiri, T.; Chapirom, A. Development of a Mixture of Lightweight Cell Crete for Green Roof Construction in Thailand. In Proceedings of the the 27th National Convention on Civil Engineering, Chiang Rai, Thailand, 24–26 August 2022; pp. 1–5.
70. He, Y.; Lin, E.S.; Tan, C.L.; Yu, Z.; Tan, P.Y.; Wong, N.H. Model Development of Roof Thermal Transfer Value (RTTV) for Green Roof in Tropical Area: A Case Study in Singapore. *Build. Environ.* **2021**, *203*, 108101. [CrossRef]
71. Shahid, K.A.; Sulaiman, M.A.; Ghazali, N.; Rahman, W.A.; Zukri, A. Palm Oil Clinker as Drainage Layer in Green Roof System under Malaysia Climatic Conditions. *Malays. Tech. Univ. Conf. Eng. Technol.* **2013**, *5*, 2013–2014.
72. Peng, L.L.H.; Yang, X.; He, Y.; Hu, Z.; Xu, T.; Jiang, Z.; Yao, L. Thermal and Energy Performance of Two Distinct Green Roofs: Temporal Pattern and Underlying Factors in a Subtropical Climate. *Energy Build.* **2019**, *185*, 247–258. [CrossRef]
73. Permpituck, S.; Namprakai, P. The Energy Consumption Performance of Roof Lawn Gardens in Thailand. *Renew. Energy* **2012**, *40*, 98–103. [CrossRef]

74. Wong, N.H.; Cheong, D.K.W.; Yan, H.; Soh, J.; Ong, C.L.; Sia, A. The Effects of Rooftop Garden on Energy Consumption of a Commercial Building in Singapore. *Energy Build.* **2003**, *35*, 353–364. [CrossRef]
75. Shareena, S.; Azis, A.B.; Ismail, I.Z.; Sipan, I.; Mohd, H.; Nur, A.L.I.; Aina, A.; Najib, M. Energy Saving and Maintenance Expediture of Green Roof: An Empirical Study in Johor Bahru. In Proceedings of the 26th Annual Pacific Rim Real Estate Society Conference, Canberra, Australia, 19–22 January 2020.
76. Dewi, C.P.; Paramitha, P.A. An Analysis of the Efficiency of Green Roofs on Cooling Energy Demand in Residential Building. *AIP Conf. Proc.* **2021**, *2447*, 030027. [CrossRef]
77. Yuliani, S.; Hardiman, G.; Setyowati, E.; Setyaningsih, W.; Winarto, Y. Thermal Behaviour of Concrete and Corrugated Zinc Green Roofs on Low-Rise Housing in the Humid Tropics. *Archit. Sci. Rev.* **2021**, *64*, 247–261. [CrossRef]
78. Living Asean The Highest Recorded Temperatures in the Asean. Available online: https://livingasean.com/special-scoop/highest-recorded-temperatures-asean/ (accessed on 8 February 2023).
79. Sunakorn, P. Thermal Performance of Green Roof Mat. In Proceedings of the Annual International Conference on Architecture and Civil Engineering, Singapore, 18–19 March 2013; pp. 1–6. [CrossRef]
80. Qin, X. A Green Roof Test Bed for Stormwater Management and Reduction of Urban Heat Island Effect in Singapore. *Br. J. Environ. Clim. Chang.* **2013**, *2*, 410–420. [CrossRef]
81. Yang, J.; Kumar, D.L.M.; Pyrgou, A.; Chong, A.; Santamouris, M.; Kolokotsa, D.; Lee, S.E. Green and Cool Roofs' Urban Heat Island Mitigation Potential in Tropical Climate. *Sol. Energy* **2018**, *173*, 597–609. [CrossRef]
82. Ahmed, M.H.B.; Rashid, R. Thermal Performance of Rooftop Greenery System in Tropical Climate of Malaysia. *J. Archit. Built Environ.* **2009**, *37*, 41–50.
83. Ismail, A.; Samad, M.H.A.; Rahman, A.M.A. The Investigation of Green Roof and White Roof Cooling Potential on Single Storey Residential Building in the Malaysian Climate. *World Acad. Sci. Eng. Technol.* **2011**, *76*, 129–137.
84. Rahman, A.A.; Zaid, S.M.; Mohammad Shuhaimi, N.D.A. Effects of Green Roof in Reducing Surface Temperature and Addressing Urban Heat Island in Tropical Climate of Malaysia. *J. Des. Built Environ.* **2022**, *22*, 1–20. [CrossRef]
85. Cuong, D.V.; Nguyen, V.; Dang, H. Evaluation of Storm-Water Runoff Control by Green Roofs: A Case Study in Hanoi, Vietnam. In Proceedings of the Water and Environment Technology Conference, Sapporo, Japan, 22–23 July 2017.
86. VanWoert, N.D.; Rowe, D.B.; Andresen, J.A.; Rugh, C.L.; Fernandez, R.T.; Xiao, L. Green Roof Stormwater Retention. *J. Environ. Qual.* **2005**, *34*, 1036–1044. [CrossRef]
87. Chai, C.T.; Putuhena, F.J.; Selaman, O.S. A Modelling Study of the Event-Based Retention Performance of Green Roof under the Hot-Humid Tropical Climate in Kuching. *Water Sci. Technol.* **2017**, *76*, 2988–2999. [CrossRef]
88. Ayub, K.R.; Ghani, A.A.; Zakaria, N.A. Green Roof: Vegetation Response towards Lead and Potassium. In Proceedings of the 1st Young Scientist International Conference of Water Resources Development and Environmental Protection, Malang, Indonesia, 5–7 June 2015; pp. 5–7.
89. Fai, C.M.; Bakar, M.F.; Roslan, M.A.; Fadzailah, F.A.; Idrus, M.F.; Ismail, N.F.; Sidek, L.M.; Basri, H. Hydrological Performance of Native Plant Species within Extensive Green Roof System in Malaysia. *ARPN J. Eng. Appl. Sci.* **2015**, *10*, 6419–6423.
90. Chow, M.F.; Bakar, M.F.A.; Arenanda, V. Influence of Native Plant Species on Substrate Moisture Content Behaviour within Extensive Green Roof System. *AIP Conf. Proc.* **2019**, *2129*, 020020. [CrossRef]
91. Kok, K.H.; Mohd Sidek, L.; Chow, M.F.; Zainal Abidin, M.R.; Basri, H.; Hayder, G. Evaluation of Green Roof Performances for Urban Stormwater Quantity and Quality Controls. *Int. J. River Basin Manag.* **2016**, *14*, 1–7. [CrossRef]
92. Musa, S.; Arish, M.; Arshad, N.; Jalil, M.; Kasmin, H. Potential of Storm Water Capacity Using Vegetated Roofs in Malaysia. In Proceedings of the International Conference on Civil Engineering Practice (ICCE08), Kuantan, Malaysia, 12–14 May 2011.
93. Vergroesen, T.; Joshi, U.M. Green Roof Runoff Experiments in Singapore. In Proceedings of the NOVATECH 2010, Lyon, France, 27 June–1 July 2010; pp. 1–11.
94. Lim, H.S.; Segovia, E.; Ziegler, A.D. Water Quality Impacts of Young Green Roofs in a Tropical City: A Case Study from Singapore. *Blue-Green Syst.* **2021**, *3*, 145–163. [CrossRef]
95. Kuoppamäki, K.; Hagner, M.; Lehvävirta, S.; Setälä, H. Biochar Amendment in the Green Roof Substrate Affects Runoff Quality and Quantity. *Ecol. Eng.* **2016**, *88*, 1–9. [CrossRef]
96. Chai, H.; Tang, Y.; Su, X.; Wang, W.; Lu, H.; Shao, Z.; He, Q. Annual Variation Patterns of the Effluent Water Quality from a Green Roof and the Overall Impacts of Its Structure. *Environ. Sci. Pollut. Res.* **2018**, *25*, 30170–30179. [CrossRef] [PubMed]
97. Vijayaraghavan, K.; Joshi, U.M.; Balasubramanian, R. A Field Study to Evaluate Runoff Quality from Green Roofs. *Water Res.* **2012**, *46*, 1337–1345. [CrossRef]
98. Hwang, Y.H.; Yue, Z.E.J. Observation of Biodiversity on Minimally Managed Green Roofs in a Tropical City. *J. Living Archit.* **2015**, *2*, 9–26. [CrossRef]
99. Liberalesso, T.; Oliveira Cruz, C.; Matos Silva, C.; Manso, M. Green Infrastructure and Public Policies: An International Review of Green Roofs and Green Walls Incentives. *Land Use Policy* **2020**, *96*, 104693. [CrossRef]
100. Utomo, C.; Astarini, S.D.; Rahmawati, F.; Setijanti, P.; Nurcahyo, C.B. The Influence of Green Building Application on High-Rise Building Life Cycle Cost and Valuation in Indonesia. *Buildings* **2022**, *12*, 2180. [CrossRef]
101. Wong, N.H.; Tay, S.F.; Wong, R.; Ong, C.L.; Sia, A. Life Cycle Cost Analysis of Rooftop Gardens in Singapore. *Build. Environ.* **2003**, *38*, 499–509. [CrossRef]

102. Chow, M.F.; Abu Bakar, M.F. A Review on the Development and Challenges of Green Roof Systems in Malaysia. *Int. J. Civil Environ. Struct. Constr. Archit. Eng.* **2016**, *10*, 16–20.
103. Ali Ariff, A.A.; Ahmad Zawawi, E.M.; Yunus, J.; Kwong, Q.J. A Systematic Review for a Highly Accessible Green Roof for Malaysian Public Institution Buildings. *J. Facil. Manag.* **2022**, *3*, 17. [CrossRef]
104. Rahman, S.R.A.; Ahmad, H.; Rosley, M.S.F. Green Roof: Its Awareness Among Professionals and Potential in Malaysian Market. *Procedia Soc. Behav. Sci.* **2013**, *85*, 443–453. [CrossRef]
105. Yuliani, S.; Hardiman, G.; Setyowati, E. Green-Roof: The Role of Community in the Substitution of Green-Space toward Sustainable Development. *Sustainability* **2020**, *12*, 1429. [CrossRef]
106. Yuliani, S.; Hardiana, A.; Sumadyo, A.; Iswati, T.Y. Green Roof on Tropical House as Architectural Innovation Responding COVID-19 Pandemic. *ARTEKS J. Tek. Arsit.* **2022**, *7*, 347–356. [CrossRef]
107. Le, V.T.; Tran, T.; Truong, T.; Chi, H.; City, M.; Minh, H.C. Towards Eco-Social Housing Challenges and Opportunities in Vietnam: Montly Income Quintile of Urban Households. *MATEC Web Conf.* **2018**, *193*, 01001. [CrossRef]
108. Lwin, M.; Panuwatwanich, K. Current Situation and Development of Green Building Rating System in Myanmar. *MATEC Web Conf.* **2020**, *312*, 01003. [CrossRef]
109. Sanmargaraja, S.; Nair, J.S.; Wee, S.T.; Zhi, T.Z. Constraints of Green Roof System Implementation in Malaysia. *AIP Conf. Proc.* **2019**, *2157*, 020037. [CrossRef]
110. Ismail, Z.; Aziz, H.A.; Nasir, N.M.; Taib, M.Z.M. Obstacles to Adopt Green Roof in Malaysia. In Proceedings of the 2012 IEEE Colloquium on Humanities, Science And Engineering, Kota Kinabalu, Malaysia, 3–4 December 2012; pp. 357–361. [CrossRef]
111. Suparwoko; Taufani, B. Urban Farming Construction Model on the Vertical Building Envelope to Support the Green Buildings Development in Sleman, Indonesia. *Procedia Eng.* **2017**, *171*, 258–264. [CrossRef]
112. Rahman, S.R.A.; Ahmad, H.; Mohammad, S.; Rosley, M.S.F. Perception of Green Roof as a Tool for Urban Regeneration in a Commercial Environment: The Secret Garden, Malaysia. *Procedia Soc. Behav. Sci.* **2015**, *170*, 128–136. [CrossRef]
113. Hwang, Y.H.; Roscoe, C. Perceptions of a Wild Green Roof in Singapore. In Proceedings of the Cities Alive 13th Annual Green Rood Wall Conference, New York, NY, USA, 5–8 October 2015; pp. 1–12.
114. Naing, Y.M.; Nitivattananon, V.; Shipin, O.V. Green Roof Retrofitting: Assessment of the Potential for Academic Campus. *Eng. J.* **2017**, *21*, 57–74. [CrossRef]
115. Jalanugroh, C.; Tikul, N. Evaluation of Education Buildings for Green Roof Construction in Maejo University, Chiang Mai, Thailand. *J. Clean Energy Technol.* **2017**, *5*, 433–437. [CrossRef]

การประชุมวิชาการคอนกรีตประจำปี ครั้งที่ 18

Annual Concrete Conference 18

A STUDY OF ROOF THERMAL TRANSFER VALUE (RTTV) EFFICIENCY ON GREEN ROOFS

Hanny Chandra Pratama[1]
ธีรวัฒน์ สินศิริ (Theerawat Sinsiri)[2]
อภัย ชาภิรมย์ (Aphai Chapirom)[3]

[1]นักศึกษาปริญญาเอก สาขาวิชาวิศวกรรมโยธา สำนักวิชาวิศวกรรมศาสตร์ มหาวิทยาลัยเทคโนโลยีสุรนารี จังหวัดนครราชสีมา 30000 Email: hannychandra.arch@gmail.com

[2]ผู้ช่วยศาสตราจารย์ สาขาวิชาวิศวกรรมโยธา สำนักวิชาวิศวกรรมศาสตร์ มหาวิทยาลัยเทคโนโลยีสุรนารี จังหวัดนครราชสีมา Email: sinsiri@g.sut.ac.th

[3]เลขานุการกลุ่มวิจัยนวัตกรรมวัสดุก่อสร้างอนุรักษ์พลังงานและสิ่งแวดล้อมอย่างยั่งยืน มหาวิทยาลัยเทคโนโลยีสุรนารี จังหวัดนครราชสีมา Email: aphai_ch@g.sut.ac.th

ABSTRACT: In the pursuit of energy-efficient building designs, understanding the Roof Thermal Transfer Value (RTTV) is pivotal, especially in the context of green roof systems. This research conducts a comprehensive comparative analysis of RTTV across various roof types, emphasizing the significance of green roofs in mitigating thermal transfer. The study systematically investigates clay roofs, galvanized iron roof, concrete roof, lightweight cellular concrete roof, and green roof system by exploring their respective RTTV performances under virtual calculation model.

Furthermore, the green roofs to be used in this study will be integrated with lightweight cellular concrete. This combination of systems is expected to enhance the performance of the green roof following the recommendations outlined in the FLL guidelines 2018.

Through rigorous experimentation and calculation modelling, this research quantifies the impact of roof material, insulation, and vegetative cover on RTTV. The results provide a nuanced understanding of how different roofing systems influence the thermal properties of buildings. Specifically, the study highlights the substantial reduction in thermal transfer offered by green roofs, emphasizing their role as superior insulators compared to conventional and green roofs.

KEYWORDS: lightweight cellular concrete, green roofs, energy efficiency, sustainability

1. Introduction

In the relentless pursuit of sustainable urban development, the integration of environmentally conscious technologies into a building has become pivotal. It is observed that 20% - 40% of energy consumption is based on buildings, especially on the cooling load [1]. Thailand, located in a tropical region characterized by consistently high temperatures, is very considered about energy regulation. It is shown that Thailand's government has issued Ministerial regulations on building envelopes by selecting a method to reduce the Overall Thermal Transfer Value (OTTV) and Roof Thermal Transfer Value (RTTV) as an important strategy [2].

The major reason for the cooling load is heat transfer through the building envelope, in particular the roof by approximately 60% of heat gain transfer [3]. However, the fact in urban buildings relies on that many buildings still do not consider this issue, such as using non-thermal resistance roof materials such as metal sheet roofing due to their affordable price. the heat conduction implications of these materials are resulting in elevated indoor temperatures that necessitate increased reliance on cooling systems.

Among these solutions, green roofs have emerged as a promising strategy to mitigate the adverse effects of urban development on the environment. Green roofs offer a natural and sustainable way to cover building envelopes with vegetation to bring multiple benefits to urban life. Moreover, Green roofs limit heat transfer through building roofs by around 80% in the summer [4]. It is observed that green roofs on buildings are not widely used in Thailand due to the high cost of heavy structure and layer installation, as well as the maintenance costs [5]. In this study, the author refers to a green roof that was integrated with lightweight cellular concrete (GR-LCC). The use of lightweight cellular concrete innovation on green roofs can overcome factors inhibiting the application of green roofs in Thailand.

Therefore, this study is proposed to assess the suitability of several roofing materials commonly used in buildings in Thailand and their effectiveness in reducing energy in buildings in Thailand by calculating the RTTV value. By calculating the RTTV value in the building design process, we can predict the suitability of the building to create a sustainable green environment.

2. Material and Methods

This study uses a virtual roof model with dimensions of 100 x 100 cm. Fig. 1 shows the variable of roof type studied, or in detail as follows:

- Clay roof (CR)
- Galvanized iron (GI)
- Concrete slab (CON)
- Lightweight cellular concrete slab (LCC)
- Green roof + lightweight cellular concrete (GR-LCC)

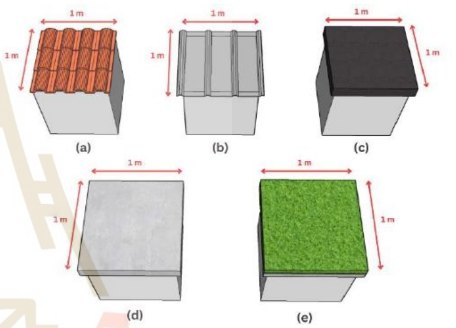

Fig.1. Virtual roof model, a) clay roof, b) galvanized iron, c) concrete slab, d) lightweight cellular concrete slab, and e) green roof lightweight cellular concrete.

Various RTTV values from virtual roof models will be calculated by the formula as shown in Eq. (1).

$$RTTV = \frac{(Ar \,.\, Ur \,.\, TDeq) + (As \,.\, Us \,.\, \Delta T) + (As \,.\, SC \,.\, SF)}{Ao} \quad (1)$$

RTTV	= Roof Thermal Transfer Value (W/m^2)
Ar	= Opaque roof area (m^2)
Ur	= Thermal transmittance of *Ar* (W/m^{2}K)
TDeq	= Equivalent temperature difference (K), Ex. (10 K)
As	= Skylight area (m^2)
Us	= Thermal transmittance of skylight area (W/m^2)
ΔT	= the temperature difference between exterior and interior design conditions (5 K)
SC	= Shading coefficient of skylight
SF	= Solar factor (W/m^2)
Ao	= Gross roof area (m^2), where Ao = Ar + As

The RTTV value is influenced by the properties of the material, especially the thermal conductivity (*K*) and the thickness of the material (*t*). Table 1 describes the properties of data and the calculation of the thermal transmittance (*Ur*).

Table 1 Roof material properties

Material	Thick-ness (m)	Thermal Conductivity (W/mK)	Thermal Resistance (m2k/W)	U Value (W/m2K)
CR	0.100	0.85	0.118	8.5
GI	0.015	5.60	0.003	373.3
CON	0.150	1.30	0.115	8.7
LCC	0.150	0.54	0.278	3.6
GR-LCC	0.075	0.10	0.750	1.1
	0.075	0.54	0.139	
	0.015	5.60	0.003	

*GR-LCC layers consist of GI, LCC and GR
Source : [1], [6], [7]

The relation of thermal transmittance (*R*) is described in Eq. 2.

$$Roof\ U\ Value = \frac{1}{R} \tag{2}$$

After obtaining the relative RTTV values for each model, the study continued with simulation calculations and onsite measurements in a room with GR-LCC roof types of 4 x 2.5 meters in Nakhon Ratchasima, Thailand as shown in Fig 2.

Fig.2. Actual temperature measurement of GR-LCC in Nakhon Ratchasima, Thailand

Measurements use a thermal type (T) sensor from the National Instrument as shown in Fig. 3. Measurements were carried out for 3 days to determine the estimated variations in outdoor and indoor temperature differences at 06.00, 09.00, 12.00, 15.00, and 18.00.

Fig.3. Instrument of temperature measurement

Lastly, after getting the RTTV value from a room with a GR-LCC roof, a calculation simulation is carried out by substituting the calculation with another roof type. The RTTV value from the simulation calculations for various types of roofs will be calculated entirely using OTTV on 4 sides of the building envelope. Therefore, the efficiency value of RTTV is more visible, the OTTV value will be defaulted to 30 W/m2 according to the maximum limit for environmentally friendly OTTV set by the Thai government [2].

3. Results and Discussions

3.1. RTTV calculation on various roof materials

Table 2 shows the RTTV calculation of various roof types on virtual model 1.00 x 1.00 m. The RTTV calculation will uncount the skylight value because the roof study currently selected is a fully solid roof.

Table 2 RTTV of selected roof materials

Material	Solid Roof			Total RTTV (W/m^2)
	Ar	*Ur*	*TDeq*	
CR	1	8.5	10	85
GI	1	373.3	10	3733
CON	1	8.7	10	87
LCC	1	3.6	10	36
GR-LCC	1	1.1	10	11

Based on the RTTV standard recommended by the government of 25 W/m^2, only GR-LCC material has a high effectiveness value and passed the standard. Apart from that, the use of GI in buildings has a very high RTTV value. High RTTV will burden the cooling load and impact the building's energy consumption, especially during the daytime. The use of additional heat-resistant layers can be an alternative to reduce the RTTV value.

3.2. Actual Temperature Measurement

Fig. 4 describes the result of actual temperature measurement for 3 days testing on the room areas 10 m^2 (4 x 2.5 m). The use of GR-LCC in buildings can maintain indoor temperatures cooler than outside temperatures. However, at nighttime, the absorbed thermal energy remains stored in the material where the room will be warmer than the outside temperatures.

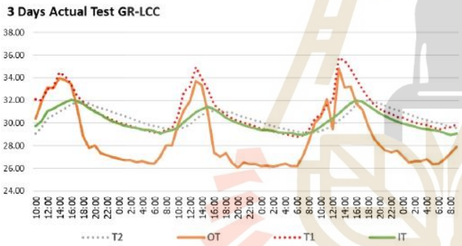

Fig.4. Actual Temperature Test of GR-LCC

The performance of GR-LCC in maintaining room temperature is fabulous. In 3 days of sampling, the highest room temperature point was 32°C. When compared with a similar study [1], rooms with CR, GI, and CON roofs have higher room temperatures, which on 35°C, 42°C, and 38°C, respectively.

Table 3 explains the ability of GR-LCC to withstand thermal transfer into the building. The effectiveness of GR-LCC works optimally during daytime. It is shown based on the times of 9.00, 12.00, and 15.00, the average temperature difference between the outside and inside temperature is on positive value. By using the GR-LCC roofing, energy use for the cooling load becomes more efficient.

Table 3 Effectiveness of GR-LCC on Daytime

Day	Outdoor Temp.	Indoor Temp.	ΔT	Average Temp.
Time 06.00				
Day 1	26.39	29.29	-2.89	-2.85°C
Day 2	26.22	29.01	-2.79	
Day 3	26.41	29.28	-2.87	
Time 09.00				
Day 1	30.40	29.74	0.66	0.91°C
Day 2	28.05	29.38	-1.34	
Day 3	30.06	29.34	0.71	
Time 12.00				
Day 1	33.14	31.07	2.07	0.82°C
Day 2	31.90	30.52	1.38	
Day 3	29.46	30.43	-0.97	
Time 15.00				
Day 1	33.78	31.84	1.94	1°C
Day 2	31.02	31.46	-0.44	
Day 3	33.25	31.75	1.50	
Time 18.00				
Day 1	28.86	31.68	-2.82	-2.59°C
Day 2	27.31	30.47	-3.16	
Day 3	29.71	31.52	-1.81	

* Average + , Indoor temperature is cooler
* Average - , Indoor temperature is warmer

3.3. Efficiency RTTV of various roof materials on buildings

The assessment of the effectiveness of RTTV cannot simply be done by comparing the value of one roof with another. RTTV calculations must be combined with OTTV calculations on all four sides of the building envelopes.

The authors use RTTV effectiveness calculations with the same room area in the actual GR-LCC temperature test and simulate the room area using other roof types.

GR-LCC has an effectiveness of 19%, the highest in reducing energy use in buildings as shown in Table 4. Meanwhile, the use of GI causes energy waste that is 10x that of general clay roofs.

Table 4 Efficiency of Roof Materials on the Building Energy Calculation

Material	Area (m^2)	OTTV	RTTV	Total Overall	Efficiency (%)
CR	10	30	85	39	0 %
GI			3733	403	-948 %
CON			87	39	0 %
LCC			36	34	13 %
GR-LCC			11	31	19 %

*CR is referred to be a control material

4. Conclusions

The proposed research approach can help us in quantifying the efficiency of RTTV, especially the green roof system. As it is known, even though green roofs have the best effectiveness in reducing energy in buildings. Green roofs are still not widely known in Thailand. Through this research, the author encourages to promotion of a green roof system combined with lightweight cellular concrete as a solution to building energy problems in Thailand.

Apart from that, several important conclusions that can be obtained from this study include:

• The RTTV value is influenced by the thermal resistance value and the thickness of the material used. A combination of heat-retaining materials can be an option to increase thermal resistance performance.

• GR-LCC is very effective in preventing thermal transfer during the daytime approximately reducing the room temperature by 2°C cooler than room temperature.

• The effectiveness of GR-LCC in reducing energy consumption in buildings is very efficient with an efficiency value of 19%.

• Although the use of GI roofs is very common because of their affordable price and easy installation, it has an energy load impact that is 10 times greater than clay roofs or concrete roofs.

Acknowledgements

This study is supported by research funds to extend knowledge from OROG Thailand Scholarship and SCG Roofing, CO. Ltd. The authors are grateful to Sustainable Innovative and Energy Efficient Construction Material (SIE-CON); and Infinity Concrete Technology, Co., Ltd. for leading this research.

References

[1] V. V. Joshi, "Heat transfer characterization of test rooms with six different roofs," *Int. J. Heat Technol.*, vol. 38, no. 1, pp. 131–136, 2020.

[2] C. Singhpoo, N. Punnucharoenwong, and C. Benjapiyaporn, *Study of the Effect of Temperature Differences on the Overall Thermal Transfer Value of buildings*, vol. 79. Elsevier B.V., 2015.

[3] S. Sudprasert and S. Klinsmith, "Assessment of Overall Thermal Transfer Value (OTTV) in Buildings with Inclined Glass Wall," *J. Archit. Res. Stud.*, vol. 11, no. 1, pp. 109–118, 2014.

[4] M. D'Orazio, C. DI PERNA, and E. DI GIUSEPPE, "Green Roofs as passive cooling strategies under Temperate Climates," *Zemch 2012*, no. January, pp. 561–570, 2012.

[5] H. C. Pratama, T. Sinsiri, and A. Chapirom, "Green Roof Development in ASEAN Countries: The Challenges and Perspectives," *Sustain.*, vol. 15, no. 9, 2023.

[6] H. C. Pratama, T. Sinsiri, and A. Chapirom, "Development of a Mixture of Lightweight Cell Crete for Green Roof Construction in Thailand," pp. 1–5, 2022.

[7] N. Somboonwit and N. Sahachaisaeree, "Healthcare Building: Modelling the Impacts of Local Factors for Building Energy Performance Improvement in Thailand," *Procedia - Soc. Behav. Sci.*, vol. 50, no. May, pp. 549–562, 2012.

The 18th East Asia-Pacific Conference on Structural Engineering & Construction (EASEC-18)
"Construction Engineering for a Responsible Growth and Sustainable Future"
November 13–15, 2024, Chiang Mai, Thailand

The Role of Energy Efficiency for the New Green Roofs Construction Techniques by Using Lightweight Cellular Concrete

Hanny Chandra Pratama[1], Theerawat Sinsiri[2*], and Aphai Chapirom[3]

[1] Ph.D. Student in Civil Engineering, Suranaree University of Technology, Nakhon Ratchasima, Thailand
Email: hannychandra.arch@gmail.com
[2] Assistant Proffesor in Civil Engineering, Suranaree University of Technology, Nakhon Ratchasima, Thailand
Email: sinsiri@g.sut.ac.th
[3] Researcher in Sustainable Innovative and Energy – Efficient Construction Materials (SIE-CON), Civil Engineering, Suranaree University of Technology, Nakhon Ratchasima, Thailand
Email: aphai_ch@g.sut.ac.th
*Corresponding Author

Abstract. As the world seeks innovative solutions to address the urgent challenges of climate change and resource depletion, the integration of sustainable practices in the construction industry is of paramount importance. This manuscript explores the role of energy efficiency in the utilization of ightweight cellular concrete (LCC) in green roofs. Green roofs have emerged as a promising strategy for mitigating the heat transfer impacts in buildings. However, conventional green roofs face limitations in Thailand. The introduction of LCC in green roofs offers a new solution. This study investigates the energy performance assessment by calculating the thermal transfer of material by using Roof Thermal Transfer Value (RTTV), obtaining temperature data from open-air experiments, and comparing the cooling load estimation. The study shows that LCC material contributes to energy savings in buildings up to 58.35 % compared with concrete roofs. When LCC is integrated with a green roof system, its efficiency is further enhanced up to 86.26 %. While the efficiency level of LCC green roofs is marginally behind that of conventional green roofs, the utilization of LCC in green roof installations yields notable advantages. These include cost savings attributed to its lightweight materials, reduced installation expenses, and simplified maintenance requirements. The incorporation of LCC in green roof constructions not only fosters energy conservation but also offers practical benefits that make it a cost-effective and sustainable option for urban development initiatives, especially in Thailand.

Keywords: lightweight cellular concrete, green roofs, energy efficiency, sustainability

1. Introduction

The government continues to strive for the development of energy-efficient buildings to achieve the global goals of SDG on year of 2030, particularly in addressing the issue of sustainable cities and communities (Kufeoglu, 2022). The rising temperature of the earth has led to an increased demand for cooling loads in buildings. It is observed that between 20% to 40% of energy consumption in buildings is used for cooling loads (Joshi, 2020). Thailand, located in a tropical region characterized by persistently high temperatures, prioritizes energy regulation by establishing benchmarks on building energy values, as an assessment using the Roof Thermal Transfer Value (RTTV) standards for assesing roof performance (Singhpoo et al., 2015). The utilization of energy-efficient roof is strongly recommended as a means to mitigate cooling loads.

Among these green innovations, green roofs stand out as multifaceted solutions, offering benefits ranging from energy conservation, stormwater management, and to biodiversity conservation (D'Orazio et al., 2012). Parizotto, et al. studied the green roof thermal performance of an experimental single-family residence in Florianopolis, SC, Brazil. In his studies during the warm period, the green roof reduced heat gain by 92% and 97% in comparison to ceramic and metallic roofs, respectively (Parizotto and Lamberts, 2011). In a study in Malaysia, the results showed that internal surface temperature of the green roof model is considerably smaller at peak with 10.2 ºC of temperature differences on average compared to the non-green roof model (Munir and Afifuddin, 2020). Several studies above show that green roofs have an important role in building efficiency. However, the adoption of green roofs on buildings in Thailand remains relatively uncommon, primarily due to the high costs associated with heavy structure and layer installation, as well as maintenance costs (Pratama et al., 2023). In this study, the author refers to a green roof that was integrated with lightweight cellular concrete (GR-LCC). The main advantages of LCC compared to conventional concrete are weight reduction up to 80%; excellent acoustic and thermal isolation; high resistance to fire; lower costs in raw materials, easier pumping and application (Chica and Alzate, 2019). The use of LCC innovation on green roofs can overcome factors inhibiting the application of green roofs in Thailand.

Therefore, this study is proposed to observe the performance of four roof types, concrete roof, LCC roof, GR-Concrete, and GR-LCC. Comparisons through RTTV calculations, data collection through open air experiments, and cooling load estimation calculations will provide an overview of the relationship between the efficiency levels of the various types of roofs studied.

2. Material and Methods

2.1. Lightweight Cellular Concrete for Green Roof

The lightweight cellular concrete material that will be used to develop on green roofs is LCC 1,200 kg/m^3 in accordance with recommendations in previous studies. LCC density 1,200 kg/m^3 has water absorption performance at 11.86%, thermal conductivity at 0.54 W/mK, and compressive strength at 4.8 MPa (Pratama et al., 2022).

The LCC composition consists of Portland cement type-I, fine sand, water, and foam agent following the requirements of ASTM C150 with the water-to-cement ratio (w/c= 0.5). The SUT V2.1 foam agent (Suranaree University of Technology foam agent version 2.1) will be used for this GR-LCC development since the foam agent is made by natural protein and related to green environmental issues with a pH of 8.55, SG of 1-1.05, and foam density of 40-60 kg/m^3 (Chapirom et al., 2019). The LCC mortar was molded in a square 1.00 x 1.00 x 0.075 m as a base deck for growing a green roof. In addition, the normal concrete roof will also be molded as a control sample.

(a) (b) (c)

Figure 1. (a) LCC Mixing Process; (b) LCC base for green roof; and (c) Concrete base for geen roof

2.2. Characteristics of the Experimental Box

Models of the experimental boxes were made in four stands, with one prepared as a Concrete roof (as a control sample), LCC roof, GR-Concrete, and GR-LCC (Figure 2). The dimensions of all stands were 1.00 x 1.00 m x 1.00 m.

Figure 2. Roof experimental boxes for oncrete roof, LCC roof, GR-Concrete, and GR-LCC

The construction of each box is made from a reinforcing iron structure covered by a wooden base and styrofoam board insulation on every side except the top side. The top side can be installed with roof materials that will be researched and can be replaced. The styrofoam board provides thermal insulation for the wall and the floor so that the heat flows to/from the room mainly through the top side. Based on this assumption, the heat flow rate value through the roof into the room and the temperature changes will express the thermal performance of each building model. The single layer green roof is constructed above the roof deck in accordance with FLL guidelines as shown in Table 1 (Losken et al., 2018).

Table 1. Characteristics of the roof experimental box

Abbreviated Name	Concrete Roof	LCC Roof	GR-Concrete	GR-LCC
Extensive Vegetation, 2.5 cm thick	None	None	Zoysia grass mat	Zoysia grass mat
Extensive Substrate, 7.5 cm thick	None	None	Mixture of fine sand and compost	Mixture of fine sand and compost
Drainage Layer	None	None	Drainage geotextile mat, 2 cm thick	A pipe-wrapped geotextile mat
Base	Concrete, Density of 2,400 kg/m^3	LCC,Density of 1,200 kg/m^3	Concrete, Density of 2,400 kg/m^3	LCC, Density of 1,200 kg/m^3
Room Test	Wooden base and styrofoam board insulation, 100 x 100 x 100 cm			

2.3. Parameters Analysis of Conventional Roofs and Green Roofs

The objective of this study is to evaluate the energy efficiency of four types of roofs. The comparison started by calculating RTTV calculation of experimental roof boxes. Various RTTV values from experimental roof boxes will be calculated by the formula as shown in Eq. 1

$$RTTV = \frac{(Ar\,.\,Ur\,.\,TDeq) + (Ag\,.\,Ug\,.\,\Delta T) + (Ag\,.\,SC\,.\,SF)}{At} \qquad (1)$$

$RTTV$ = Overall/Roof Thermal Transfer Value (W/m^2)
$A_{(roof)}$ = Opaque wall/roof area (m^2)
$U_{(roof)}$ = Thermal transmittance of Ar (W/m^{2}K)
$TDeq$ = Equivalent temperature difference (K), Ex. (10 K)
$A_{(glass)}$ = Glassing area (m^2)
$U_{(glass)}$ = Thermal transmittance of glassing area (W/m^2)
ΔT = The temperature difference between exterior and interior design conditions (5 K)
SC = Shading coefficient of glassing
SF = Solar factor (W/m^2)
$A_{(total)}$ = Gross wall/roof area (m^2), where $At = Ao + Ag$

The RTTV calculations in this study will be calculated excluding the glassing calculation due to all surface is an opaque surfaces. The thermal transfer value in buildings is influenced by the use of the type of material which is described as the thermal transmittance value (Uo), described in Eq. 2

$$U\ Value = \frac{1}{R}, \text{where R} = \frac{t}{K} \tag{2}$$

R = Thermal resistance (m^{2}k/W)
K = Thermal conductivity of material (W/m.K)
t = Thickness of material (m)

Table 2 describes the properties of data and the calculation of the thermal transmittance (Uo) on roof as a factor to calculate the RTTV.

Table 2. U-value calculation of material surfaces

Surfaces	Material Configuration	Thickness (m)	Thermal Conductivity (W/m.K)	Thermal Resistance (m^{2}k/W)	U Value (W/m^{2}K)
Concrete Roof	Normal Concrete	0.075	1.40	0.05	18.67
GR-Concrete	Normal Concrete	0.075	1.40	0.05	1.35
	Drainage Layer	0.020	0.04	0.50	
	Substrate	0.050	0.30	0.17	
	Vegetation	0.025	1.10	0.02	
LCC Roof	LCC 1200 kg/m^3	0.075	0.54	0.14	7.20
GR-LCC	LCC 1200 kg/m^3	0.075	0.54	0.14	3.05
	Substrate	0.050	0.30	0.17	
	Vegetation	0.025	1.10	0.02	

*GR-LCC will not calculate the drainage pipe due to uncovered a whole surface
Source : (Asadi et al., 2018), (Yaghoobian et al., 2010), and (Scape, 2019)

The calculation of RTTV value from the experimental test boxes will be calculated to obtain the data of thermal transfer of the test boxes influenced by various of roof types. The study will continue to compare the temperature profiles between the four various roof types which were performed during the period of February 2024 for 3 days along. The test boxes located at Suranaree University of Technology, Thailand (33° 55' 56.028" S 18° 38' 23.46" E). The change in the temperature of every layer on each roof types was carried out. The enviromental factors (i.e. air temperature, air humidity) were measured using outdoor temperature and humidity sensor Modela AM2306 (RH accuracy ± 2%, Temperature accuracy ± 0.3 °C). The soil temperature and humidity were measured using a needle probe sensor Modela SFP001 (RH accuracy ± 2%, Temperature accuracy ± 0.5 °C) . The probes were placed horizontally at each of the depths. The outdoor and indoor roof deck surfaces were measured using thermal type (T) sensor from the National Instruments. Indoor temperatures and its humidity were measured using hanging temperature and humidity sensor Modela AM2305 (RH accuracy ± 2%, Temperature accuracy ± 0.3 °C). Fig 3 summarize the details of measurement items and measurement points.

(a) (b) (c)

Figure 3. (a) Croos section of sensor instalation; (b) concrete roof & LCC roof experimental; and (c) GR-Concrete and GR-LCC experimental

The test box will be exposed to an open ambient environment with direct sunlight, the data logger recorded the data in 10 minutes intervals for 3 day's experiment to observe thermal responses of the models continually. The experiment took place in the inner court of a building where direct sunlight was available during the days. Only the direct sunlight of early morning at 6.00 am until late afternoon at 6.00 pm. The temperature gradient analysis will be available through this data collection. The difference in indoor temperature obtained from research data will be used to calculate the cooling load.

Cooling load is the rate at which a cooling system or process must remove heat from a conditioned zone to maintain it at a constant dry bulb temperature and humidity. The calculation methods using the cooling load temperature difference effects from the heat loads of surface materials following the reccomendation method of ASHRAE (Hashim et al., 2018). The calculation cooling load will be calculated by the formula as shown in Eq. 3.

$$Q = \mathrm{U}\,.\,\mathrm{A}\,.\,(\mathrm{To} - \mathrm{Ti})\,.\;24 \tag{3}$$

Q	= Watt hours / per day heat load (Wh)
U	= U insulation value of sandwich panel (W / m^2.K)
A	= Surface area of ceiling, wall, and floor(m^3)
Ti	= Air temperature inside the room (°C)
To	= Ambient temperature (°C)
24	= Hours in a day

This load calculation will bring to an understanding of the cooling load energy efficiency in every 3 hours interval in daytime started from 6.00 am to 18.00 pm.

3. Results and Discussion

3.1 RTTV calculation on various roof types

Table 3 shows the RTTV calculation of various roof types on experimental roof box 1.00 x 1.00 x 1.00 m. The calculation will uncount the glassing value because the roof of selected study are fully opaque.

Table 3. OTTV and RTTV calculation

Material	Solid Roof			Total RTTV (W/m^2)	Standard RTTV ($10 - 15\ W/m^2$)
	Ar	*Ur*	*TDeq*		
Concrete Roof	1	18.67	10	187	✗
LCC Roof	1	7.20	10	72	✗
GR-Concrete	1	1.35	10	14	✓
GR-LCC	1	3.05	10	31	✗

According to the RTTV standard recommended by the government of 10 - 15 W/m^2 (Chirarattananon et al., 2007). It is observed that only GR-Concrete comply the prescribed standard. Concrete roofs, LCC roofs fail to meet the standards due to their propensity for rapid heat conduction. GR-LCC does not yet meet RTTV standards, but it can be seen that there is significant potential for reducing the thermal transfer value of GR-LCC. Next step, various roofs will be placed in an open air for temperature measurements.

3.2 Open-air temperature test

Figure 4 shows the indoor temperature on 4 different types of roof compared to the outside room temperature.

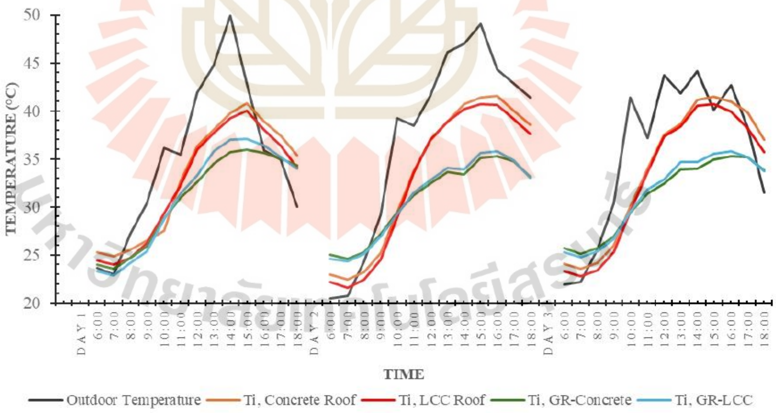

Figure 4. Indoor temperature in 3 days measurement compared to outdoor temperature.

The graph above illustrates that rooms without green roofs reveal higher temperatures compared to those with green roofs, with a temperature variance ranging from 0.5 - 6 °C. Within the category of non-green roofs, it is discernible that LCC roof tend to maintain slightly lower temperatures than concrete roof. This observation is consistent with the thermal conductivity values, wherein LCC demonstrates lower conductivity than concrete. Notably, the temperature contrast becomes particularly evident around midday, coinciding with peak outdoor temperatures, as room temperatures under LCC roofs consistently remain below those under concrete roofs. The maximum temperature divergence between concrete and LCC roofs is approximately 2 °C.

In contrast, when comparing different types of green roofs, it becomes evident that green roofs with a concrete base show slightly lower room temperatures compared to those with an LCC base. This can be indicated by the plastic drainage layer, which has a propensity to retain heat from the ground due to its plastic material. The maximum indoor temperature differential between green roofs with concrete and LCC bases is approximately 1 °C.

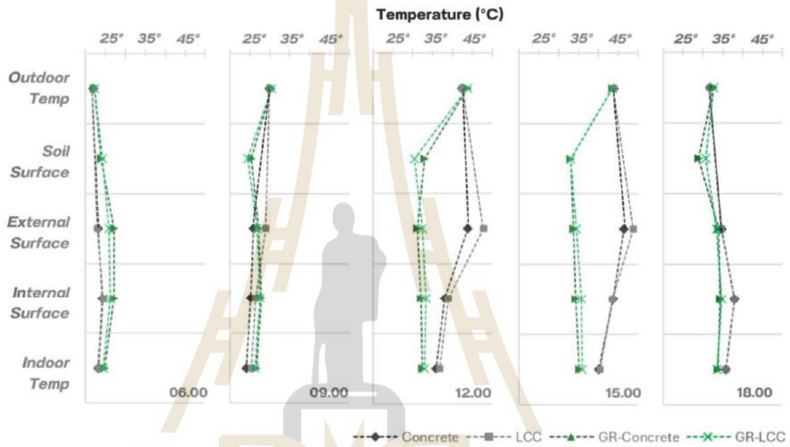

Figure 5. Indoor temperature in 3 days measurement compared to outdoor temperature.

Furthermore, Figure 5 above depicts the temperature gradients of four distinct roof types, delineated through measurements obtained from sensors embedded within each layer. These measurements are captured at 3-hour intervals, affording a comprehensive depiction of temperature fluctuations across various layers of the roofs under examination. The two models exhibit contrasting responses to varying environmental conditions. During the morning period, prior to direct exposure to sunlight, the temperature of the green roof system surpasses that of the non-green roof models. Subsequently, as direct solar heat is absorbed until noon, the indoor air temperature escalates, leading to heat transmission from the indoor air to the roof. Consequently, the internal surface temperature surpasses that of the external surface of the panel. In contrast, for the base model, temperature gradients at 12:00 and 16:00 signify the accumulation of heat traversing through the roof, resulting in the surface temperature reaching its zenith within daily temperature fluctuations. This observation further highlights that the majority of heat gain occurs through the roof rather than the wall. These findings underscore the efficacy of green roofs in mitigating the heat load attributable to solar radiation during daylight hours.

3.3 Cooling Load Estimation

Room temperature significantly influences electrical energy consumption, particularly in relation to cooling load. To standardize room temperature data for each roof type, adjustments will be made to maintain a consistent temperature of 24 °C. These calculations refer to Formula 3. An exemplification of the cooling load calculation for an LCC green roof is presented in Table 4.

Table 4. Cooling load calculation for GR-LCC

Time	U Value	Surface Area	Indoor Temp	Condition Temp	Temperature	Watt Hours Conversion	Cooling Load
	U (W/m^2K)	**A (m2)**	**To (°C)**	**Ti (°C)**	**ΔT (°C)**	**3 hours interval**	**Q (Wh)**
06.00 – 09.00	3.05	1	24.4	24	0.4	3	3.7
09.00 – 12.00	3.05	1	26.33	24	2.33	3	21.3
12.00 – 15.00	3.05	1	33.01	24	9.01	3	82.4
15.00 – 18.00	3.05	1	36.07	24	12.07	3	110.4
GR-LCC Cooling load over 12 hours daytime							217.9

*Wh = Watt hours

In the process of calculating cooling loads, disparities in material U Value and temperature deviations emerge as principal determinants. In the case of the LCC green roof calculation example, the morning temperature differential stands at a mere 0.4 °C, resulting in a minimal energy consumption of 3.7 Wh over a 3-hour interval. Conversely, during the period between 15:00 and 18:00, characterized by the highest temperature disparity peaking at 12.07 °C, the reference room, spanning an area of 1 m^3, consumes 110.4 Wh of electricity in the afternoon.

Table 5 shows the electricity consumption in room with various roof types at 3-hour intervals, over a 12-hour calculation period, offering insights into the efficacy of each roof type. Utilizing the LCC roof type demonstrates an energy-saving effectiveness of up to 58.35%, it caused by its low U Value, which impacts on energy conservation.

The maximum of savings potential is realized through the implementation of green roofs. Notably, the green roof concrete obtains the highest level of efficiency, with a 94.05% energy conservation rate compared to conventional concrete roofs. It slightly followed by the LCC green roof which achieves an efficiency level of 86.26%.

Table 5. Estimasi effisiensi cooling load

Time Consumption	Cooling Load (Wh)			
	Concrete Roof	LCC Roof	GR-Concrete	GR-LCC
06.00 - 09.00	0	0	4	4
09.00 - 12.00	10	29	11	21
12.00 - 15.00	667	275	34	82
15.00 - 18.00	909	356	46	110
Total cooling load / m^3	**1585**	**660**	**94**	**218**
Average colling per hours	**132**	**55**	**8**	**18**
Efficiency	**0.00%**	**58.35%**	**94.05%**	**86.26%**

*Wh = Watt hours

4. Conclusions

The proposed research approach help us in quantifying the efficiency energy by calculating the RTTV, measuring the temperature difference, and calculating the cooling load beetween non-green roof (Concrete roof, LCC roof) and green roof (GR-Concrete, GR-LCC).

As it is shown in results, green roofs have an effectiveness in reducing energy consumption. The research highlight the efficiency of the two green roof investigated, particularly GR-Concrete, which widely commercialized. Despite their efficiency, GR-Concrete face limited adoption in Thailand owing to factors such as high installation costs, the weight of materials, and challenging maintenance requirements.

In this context, GR-LCC emerges as a viable alternative, offering several advantages. Characterized by lighter materials and simplified installation procedures, GR-LCC not only reduces costs but also ensures ease of maintenance. Furthermore, while its efficiency is not quite different than the GR-LCC (94.05% and 86.26% respectively), making it a pragmatic choice for applying GR-LCC as a green roof alternatives in Thailand. Through this research, the author encourages to promotion of a green roof system combined with lightweight cellular concrete as a solution to building energy problems in Thailand.

Acknowledgements

This study is supported by research funds to extend knowledge from OROG Thailand Scholarship and SCG Roofing, Co. Ltd. The authors are grateful to Sustainable Innovative and Energy Efficient Construction Material (SIE-CON); and Infinity Concrete Technology, Co., Ltd. for leading this research.

References

Asadi, I., Shafigh, P., Abu Hassan, Z.F. Bin, Mahyuddin, N.B., (2018). Thermal conductivity of concrete – A review. J. Build. Eng. 20, pp 81–93.

Chapirom, A., Sinsiri, T., Jaturapitakkul, C., Chindaprasirt, P., (2019). Effect of speed rotation on the compressive strength of horizontal mixer for cellular lightweight concrete. Suranaree J. Sci. Technol. 26, pp 113–120.

Chica, L., Alzate, A., (2019). Cellular concrete review: New trends for application in construction. Constr. Build. Mater. 200, pp 637–647.

Chirarattananon, S., Chaiwiwatworakul, P., Hien, V.D., Rugkwamsuk, P., Kubaha, K., (2007). Revised Building Energy Code of Thailand - Potential Energy and Power Demand Savings. Proc. Jt. Int. Conf. Sustain. Energy Environ. 2, pp 1–10.

D'Orazio, M., DI PERNA, C., DI GIUSEPPE, E., (2012). Green Roofs as passive cooling strategies under Temperate Climates. Zemch 2012 pp 561–570.

Hashim, H.M., Sokolova, E., Derevianko, O., Solovev, D.B., (2018). Cooling Load Calculations. IOP Conf. Ser. Mater. Sci. Eng. pp 463.

Joshi, V. V., (2020). Heat transfer characterization of test rooms with six different roofs. Int. J. Heat Technol. 38, pp 131–136.

Kufeoglu, S., (2022). Sustainable cities and communities pp 48–49.

Losken, G., Ansel, W., Backhaus, T., Bartel, Y.-C., Bornholdt, H., Bott, P., Henze, M., Hokema, J., Kohler, M., Krupka, B., Mann, G., Munster, M., Neisser, H., Roth-Kleyer, S., Ruttensperger, S., Schenk, D., Sprenger, D., Upmeier, M., Westerholt, D., Fll, (2018). FFL: Guidelines for the Planning, Construction and Maintenance of Green Roofs.

Munir, A., Afifuddin, M., (2020). Thermal Performance of Precast Foam Concrete Integrated with Green Roofs System.

Parizotto, S., Lamberts, R., (2011). Investigation of green roof thermal performance in temperate climate: A case study of an experimental building in Florianópolis city, Southern Brazil. Energy Build. 43, 1712–1722.

Pratama, H.C., Sinsiri, T., Chapirom, A., (2022). Development of a Mixture of Lightweight Cell Crete for Green Roof Construction in Thailand pp 1–5.

Pratama, H.C., Sinsiri, T., Chapirom, A., (2023). Green Roof Development in ASEAN Countries: The Challenges and Perspectives. Sustain. 15.

Scape, U., (2019). Urbanscape Green Roof System..

Yaghoobian, N., Kleissl, J., Krayenhoff, E.S., (2010). Modeling the thermal effects of artificial turf on the urban environment. J. Appl. Meteorol. Climatol. 49, 332–345.

BIOGRAPHY

Hanny Chandra Pratama earned a Bachelor's degree in Architectural Engineering from the University of 17 Agustus 1945 Surabaya, Indonesia, where he developed a strong foundation in innovative building design. Following this, he pursued his Master's in Architecture at Khon Kaen University, Thailand, focusing on building technology and green design. During his doctoral studies, Pratama authored several research papers in national and international journals, contributing to advancements in research on Lightweight Cellular Concrete (LCC) and its application in building design to improve building performance. He also collaborated with several reputable public companies, such as SCG Roofing Co., Ltd., to develop the green roof LCC system, further expanding his expertise in green material design.

This dissertation represents the culmination of his academic journey and reflects a deep commitment to advancing knowledge in the development of green materials.